



**HAL**  
open science

# Optimization of energy integrated systems for vehicles applications

Zlatina Dimitrova

► **To cite this version:**

Zlatina Dimitrova. Optimization of energy integrated systems for vehicles applications. Engineering Sciences [physics]. CNAM Paris, 2020. tel-03140405

**HAL Id: tel-03140405**

**<https://hal.science/tel-03140405>**

Submitted on 12 Feb 2021

**HAL** is a multi-disciplinary open access archive for the deposit and dissemination of scientific research documents, whether they are published or not. The documents may come from teaching and research institutions in France or abroad, or from public or private research centers.

L'archive ouverte pluridisciplinaire **HAL**, est destinée au dépôt et à la diffusion de documents scientifiques de niveau recherche, publiés ou non, émanant des établissements d'enseignement et de recherche français ou étrangers, des laboratoires publics ou privés.



Distributed under a Creative Commons Attribution 4.0 International License

# Mémoire d'habilitation à diriger des recherches

Présenté par

**Dr. Zlatina Dimitrova**

Chef de projet en recherche et innovation

à la Direction de la Recherche et de l'Innovation de PSA Groupe

## Optimization of energy integrated systems for vehicles applications

12 Novembre 2020

Composition du jury:

**Rapporteurs:**

Madame Anna FONTCUBERTA I MORRAL, Professeur des universités, Ecole Polytechnique Fédérale de Lausanne

Monsieur Jean François HETET, Professeur des universités, Ecole centrale de Nantes

Monsieur François LANZETTA, Professeur des universités, Université de Franche-Comté

**Garant:**

Madame Christelle PERILHON, Maître de conférence HDR, Conservatoire national des arts et métiers

**Examineurs:**

Monsieur Sylvain ALLANO, Professeur des universités, Chief Scientific Officer de l'entreprise Flying Whales

Monsieur Miroslav DIMITROV, Maître de conférence HDR, Académie Militaire Nationale de la Bulgarie

Monsieur Sofiane KHELLADI, Professeur des universités, ENSAM Paris

Monsieur Plamen PUNOV, Maître de conférence HDR, Université technique de Sofia

**Invité:**

Monsieur Stéphane LEFEBVRE, Professeur des Universités, Conservatoire national des arts et métiers



# Acknowledgements

I would like to thank Professor Anna Fontcuberta i Morral, Professor Jean-François Hétet, Professor François Lanzetta, Professor Sofiane Khelladi, Associate Professor Plamen Punov, Associate Professor Miroslav Dimitrov, Professor Sylvain Allano and Professor Stéphane Lefebvre for their interest to participate in the jury and for their availability to evaluate this work. I would like to thank them to have accepted this mission. It is for me a pleasure and an honor to have proposed them as members of my habilitation jury. I would like to express my special gratitude to the reviewers of my work for the very constructive reports and appreciations of my work.

I would like to thank Associate Professor Christelle Périlhon for having given me the opportunity to write this manuscript and to present my application for habilitation in CNAM Paris. I would like to thank her for her support and her engagement to guide me through the habilitation application procedure. Her confidence, her motivation and her advices, were very helpful and stimulating during the preparation. I appreciate a lot our discussions, very helpful for my progress.

I would like to acknowledge Professor Jean-François Deü for the advices related to the habilitation process.

I further gratefully acknowledge the support of PSA Groupe and especially the support of the Research and Innovation Department. I would like to express my very great appreciation to Ms. Carla Gohin, Senior Vice President for Research, Innovation and Advanced Technologies of PSA Groupe for having given me the possibility to realize my habilitation project. I would like to acknowledge Mr. Ladimir Prince, Chief Scientific Officer and Vice President for Research, Innovation and Advanced Technologies of PSA Groupe for his support of my habilitation project, for his understanding and his assistance in the leading of the valuable research projects in PSA Groupe.

Many special thanks to General Major Dr. Grudi Angelov, Commandant of “Rakovski” National Defense College of Bulgaria for the assignment of my lectures in the Master Programs of “Rakovski” National Defense College. I am honored by the opportunity by the invitation to teach at this prestigious education institution. I would like to thank Colonel Associate Professor Miroslav Dimitrov, Commandant of the Logistics department of “Rakovski” National Defense College for the great welcome and the organization of my lectures in his department. Many special thanks as well to Colonel Professor Dimitar Nedialkov, member of the staff of “Rakovski” National Defense College and member of the Institute for Space Research of the Bulgarian Academy of Sciences for his support, his recommendation and his very high appreciation of my technical and research skills . I would like to thank all my colleagues and my students from “Rakovski” National Defense College of Bulgaria for their great welcome.

At this place, I would like to offer my special thanks to Mr. Guillaume Faury, Chief Executive Officer of Airbus Group for his permanent encouragement and the motivation during the habilitation. I am particularly grateful to Mr. Faury for his very first support of the idea of the habilitation project.

I would like to thank my very special friend “police man” for the interest on my research.

My very special thanks go also to Mr. Tomasz Kryszynski, Vice President for Research and Innovation at Airbus Helicopters for the unconditional support and for the excellent relation with PSA Groupe.

I would like to express my gratitude to all my colleagues from PSA Groupe, and our “OpenLabs”, for the collaboration on the research topics. I would like to thank my colleagues and my students for their

## Acknowledgements

---

contribution to the publications, the patents, the presentations and our participations to international scientific conferences and meetings.

I would like to thank Nicolas for his help, his support and for the technical discussions.

Finally, many thanks to my family, my parents Nadia and Kiril Dimitrovi, my brother Miroslav, my aunt Maria, for the permanent support, for the motivation and for their hope and their optimism.

*Versailles, 12 November 2020*

Z.D.

# Abstract

The main threads of the researches presented in this habilitation manuscript are the improvement of the energy efficiency of the vehicles energy systems, their emissions reduction, presenting competitive cost effective solutions of the energy storage and conversion technologies. The research considers energy efficiency, economic and environmental impact studies of innovative energy systems. In this manuscript the vehicles energy system evolves from autonomous on-board system to grid related system, with multi- energy vectors. Three main research topics are developed:

- Energy efficiency, storage and conversion on vehicles board

Internal combustion engines have limitation on efficiency due mainly to the heat losses. Processing an energy integration, it has been shown than an organic Rankine cycle can improve the overall powertrain efficiency by recovering the heat into electricity. In parallel, hybrid electric vehicles attractiveness increases as it enables important energy saving. The energy recovery potential of a single stage organic Rankine cycle for a thermal engine in combination with a mild hybrid electric powertrain is studied. The environomic methodology for design is applied on hybrid electric vehicles and electric vehicles, in order to explore the techno-economic and environmental trade-off for different hybridization level of the vehicles powertrains.

The variable engine valve trains are important for the gas exchanges and influence directly the effective efficiency of the internal combustion engine. This research presents an innovative application of an electromagnetic actuator for a future variable engine valve train. The design method is inversed to create a control law model. The control architecture is designed for a robust control of the actuator. The investigations show that very good dynamic performances of the controller are obtained.

The problems of the range and the energy storage of the vehicle on board are important and are introduced. Multi-objective optimization method is applied to estimate the optimal vehicles energy system designs for urban mobility and for long way electric mobility (> 500 km). Lithium-Ion battery systems become a major storage component in vehicle drivetrains. In this research, the investigation of the energy balance evolution for Li-Ion battery system is described. A method to determine the energy balance through experimental investigations and validate the model is also proposed.

- Extension of the vehicle energy systems, the vehicles as grid related systems

The recharging of the vehicles and their connection to the energy grid became an important question. The energy system is extended and includes the energy storage and conversion of vehicles and their connection to the grid. The extended energy system is modelled on vehicles flows on the highway and a single objective optimization is performed to define the optimal energy storage capacity of the vehicles and the optimal number of recharges of from the grid. The recharging time and the occupation rates of the chargers are as well evaluated. The optimality is researched for long way drives on electric mode.

An innovative mobile robot, equipped with energy power system, does the recharging of the high voltage batteries. The navigation function is central in the design of the mobile robot. The experimental results on a mobile robot platform show a distance error lower than 0.7% and an angle error less than 0.5%, promising for the acceptable accuracy of the system.

This research studies an innovative concept (SOFC-GT a Solid Oxide Fuel Cell with gas turbine module) for vehicle propulsion, considered to deliver mobility services and integrated energy services for a household. The major advantage of the energy integrated dual system is the reduction of the total global

warming potential (GWP) impact by around 30000 kg CO<sub>2</sub> eq. (60%) (from 50590 kg CO<sub>2</sub> eq. to 20338 kg CO<sub>2</sub>) in comparison to separate energy services for mobility and household needs.

- Energy storage and conversion systems for energy vectors; fuel cell electric vehicles, hydrogen and their ecosystem

This report researches the use of SOFC system powered by hydrogen produced through reforming of liquid fuel from renewable resources such as bioethanol. The SOFC installation has an integrated fuel reformer. Ni doped with a small amount of Pd as an active phase components is used for catalyst of the bio-ethanol steam reforming. The catalyst, which is used during the process, has an important role to achieve 100% conversion because it increases the rate of reaction in such a way that the system tends toward thermodynamic equilibrium.

To consider the impact of the different energy vectors, well-to-wheels balance on the energy efficiency and the CO<sub>2</sub> emissions is done and discussed for different vehicles propulsion systems.

## **Keywords:**

Energy storage, energy conversion, vehicles propulsion systems, energy grids and systems, multi-objective optimization

# Résumé

Le fil conducteur des recherches présentées dans ce manuscrit d'habilitation est l'amélioration de l'efficacité des systèmes énergétiques des véhicules, la réduction de leurs émissions, au travers de solutions compétitives et rentables de technologies de stockage et de conversion d'énergie. La recherche porte sur l'efficacité énergétique ainsi que sur les études d'impacts économiques et environnementaux des systèmes énergétiques innovants. Dans ce manuscrit, les systèmes énergétiques des véhicules évoluent des systèmes autonomes embarqués vers des systèmes liés au réseau, avec des vecteurs multi-énergies. Trois grands thèmes de recherche sont développés:

- Efficacité énergétique, stockage et conversion à bord des véhicules

Les moteurs à combustion interne ont une limitation de l'efficacité due principalement aux pertes thermique. En faisant une intégration énergétique, il a été démontré qu'un cycle de Rankine à fluide organique peut améliorer l'efficacité globale du groupe motopropulseur en récupérant la chaleur et en la transformant en électricité. Parallèlement, l'attractivité des véhicules électriques hybrides augmente car elle permet d'importantes économies d'énergie. Le potentiel de récupération d'énergie d'un cycle de Rankine à fluide organique pour un moteur thermique en combinaison avec une chaîne de traction à faible hybridation électrique est étudié. La méthodologie de conception « environomique » est appliquée aux véhicules hybrides électriques, afin d'explorer le compromis technico-économique et environnemental pour différents niveaux d'hybridation des groupes motopropulseurs des véhicules.

Les systèmes de distribution à levées de soupapes variables sont importants pour les échanges de gaz et influencent directement l'efficacité effective du moteur à combustion interne. Cette recherche présente une application innovante d'un actionneur électromagnétique pour un futur système de distribution variable. La méthode de conception est inversée pour créer un modèle de loi de contrôle. L'architecture de commande est conçue pour une commande robuste de l'actionneur. Les investigations démontrent de très bonnes performances dynamiques du contrôleur de l'actionneur.

Les problèmes d'autonomie et de stockage d'énergie à bord des véhicules électriques sont importants et sont introduits. Une méthode d'optimisation multi-objectifs est appliquée pour estimer les conceptions optimales de systèmes énergétiques des véhicules électriques pour la mobilité urbaine et pour la mobilité électrique à longue distance (> 500 km). Les systèmes de batterie au lithium-ion deviennent un élément de stockage majeur dans les systèmes de propulsion des véhicules. Dans cette recherche, l'étude de l'évaluation du bilan énergétique de la batterie Li-Ion est décrite. Une méthode pour déterminer le bilan énergétique par des investigations expérimentales et valider le modèle est également proposée.

- Extension des systèmes énergétiques des véhicules, les véhicules en tant que systèmes liés au réseau

La recharge des véhicules et leur connexion au réseau énergétique est devenue une question importante. Le système énergétique est étendu et comprend le stockage et la conversion d'énergie des véhicules et leur connexion au réseau. Le système énergétique étendu est modélisé par des flux de véhicules sur l'autoroute et une optimisation est réalisée pour définir la capacité optimale de stockage d'énergie des véhicules et le nombre optimal de recharges sur les trajets. Le temps et les taux d'occupation des chargeurs sont également évalués. L'optimalité est recherchée pour les longs trajets en mode électrique.

Un robot mobile innovant, équipé d'un système d'alimentation en énergie, recharge les batteries haute tension. La fonction de navigation est centrale dans la conception du robot mobile. Les résultats expérimentaux sur une plateforme de robot mobile montrent une erreur d'estimation de la distance

inférieure à 0,7% et une erreur d'estimation d'angle inférieure à 0,5%, promettant une précision acceptable du système de navigation.

Cette recherche étudie un concept innovant (SOFC-GT une pile à combustible à oxyde solide, couplé à une turbine à gaz) pour la propulsion des véhicules, considéré comme fournissant des services de mobilité, et des services énergétiques intégrés pour un ménage. Le principal avantage du système d'énergie intégrée combiné est la réduction de l'impact total du potentiel de réchauffement climatique (GWP) d'environ 30000 kg CO<sub>2</sub> éq. (60%) (de 50590 kg CO<sub>2</sub> éq. à 20338 kg CO<sub>2</sub> éq.) par rapport à des services énergétiques séparés pour la mobilité et les besoins des ménages.

- Systèmes de stockage et de conversion d'énergie pour les différents vecteurs énergétiques; véhicules électriques à pile à combustible, hydrogène et leur écosystème

Ce rapport étudie l'utilisation d'un système d'extension d'autonomie sur la base d'une pile à combustible à électrolyte solide (SOFC), alimenté par l'hydrogène produit par le reformage du carburant liquide à partir de ressources renouvelables telles que le bioéthanol. L'installation SOFC dispose d'un reformeur d'hydrogène intégré. Le Ni dopé avec une petite quantité de Pd est utilisé comme catalyseur du reformage du bioéthanol. Le catalyseur, qui est utilisé pendant le processus, a un rôle important pour atteindre une conversion de 100% du bioéthanol en hydrogène car il augmente la vitesse de réaction de telle manière que le système tend vers l'équilibre thermodynamique.

Pour prendre en compte l'impact des différents vecteurs énergétiques, le bilan du puits à la roue de l'efficacité énergétique et des émissions de CO<sub>2</sub> est réalisé et discuté pour différents systèmes de propulsion des véhicules.

## Mots clés:

Stockage d'énergie, conversion d'énergie, systèmes de propulsion des véhicules, systèmes et réseaux d'énergie, optimisation multi-objectifs

# Contents

<b>Acknowledgements</b> .....	<b>v</b>
<b>Abstract</b> .....	<b>vii</b>
<b>Keywords:</b> .....	<b>viii</b>
<b>Résumé</b> .....	<b>ix</b>
<b>Mots clés:</b> .....	<b>x</b>
<b>Contents</b> .....	<b>xi</b>
<b>Summary</b> .....	<b>xiii</b>
<b>Chapter 1 Introduction</b> .....	<b>1</b>
1.1 Context of the research .....	1
1.2 Main research questions and domains .....	3
1.3 Personal experiences and motivations .....	6
1.4 Outline and contribution of the present work .....	7
<b>Chapter 2 Literature review</b> .....	<b>9</b>
2.1 Energy efficiency, energy storage and conversion on vehicles board .....	9
2.2 Extension of the vehicle energy systems: the vehicles as grid related systems to the energy grids for optimal energy services for mobility.....	13
2.3 Fuel cell electric vehicles, energy vectors for hydrogen and their ecosystem .....	16
<b>Chapter 3 Energy efficiency, storage and conversion on vehicles board</b> .....	<b>21</b>
3.1 Energy efficiency .....	21
3.2 Energy converters on-board.....	26
3.3 Energy storage on-board – high voltage batteries.....	35
<b>Chapter 4 Extension of the vehicle energy systems: the vehicles as grid related systems to the energy grids for optimal energy services</b> .....	<b>51</b>
4.1 Design of electric vehicles grid related energy systems for optimal mobility service.....	51
4.2 Coordination interest for the optimization of electric vehicles long distance trips .....	57
4.3 Slow charging: Robotized charging of high voltage batteries for electric and hybrid electric vehicles .....	64
<b>Chapter 5 Energy storage and conversion systems for energy vectors: fuel cell electric vehicles, hydrogen and their ecosystem</b> .....	<b>73</b>
5.1 Energy balance of the production and the conversion of hydrogen in the fuel cells .....	76
5.2 Hydrogen from (bio)-ethanol steam reforming, selection of the catalysts: .....	78

5.3	A well-to-wheels balance of the different energy storage and conversion technologies for sustainable mobility solutions .....	90
<b>Chapter 6</b>	<b>Conclusions .....</b>	<b>95</b>
6.1	Energy efficiency, energy storage and conversion on vehicles board .....	95
6.2	Extension of the vehicle energy systems: the vehicles as grid related systems to the energy grids for optimal energy services for mobility .....	96
6.3	Energy storage and conversion systems for energy vectors: fuel cell electric vehicles, hydrogen and their ecosystem .....	97
6.4	General conclusion of the research work .....	98
<b>Chapter 7</b>	<b>Research perspectives.....</b>	<b>99</b>
7.1	Goals and philosophy .....	99
7.2	Research axes .....	99
7.3	From the method to the tool .....	100
7.4	Applications .....	101
<b>Appendix A</b>	<b>Methodology.....</b>	<b>103</b>
A.1.	Multi objective optimization and energy integration .....	103
A.2.	Economic models .....	107
A.3.	Environmental model: Life cycle assessment .....	109
<b>Appendix B</b>	<b>Models.....</b>	<b>111</b>
B.1.	Simulation models: EV, HEV, SOFC .....	111
<b>Appendix C</b>	<b>Energy efficiency, storage and conversion .....</b>	<b>123</b>
C.1.	Optimal designs for efficient mobility service for hybrid electric vehicles .....	124
C.2.	Optimal designs of electric vehicles for a long-range mobility .....	133
<b>Appendix D</b>	<b>Mobile Robotics .....</b>	<b>139</b>
D.1.	Perception.....	139
D.2.	Localization: SLAM .....	139
D.3.	Cognition: Mobile Robot Navigation Algorithms .....	140
<b>Appendix E</b>	<b>Extended energy systems .....</b>	<b>141</b>
E.1.	Integration of the environomic energy services for mobility and household using electric vehicle with a range extender of solid oxide fuel cell.....	141
<b>References</b> .....	<b>151</b>	
<b>Nomenclature</b> .....	<b>159</b>	
<b>List of Figures</b> .....	<b>171</b>	
<b>List of Tables</b> .....	<b>177</b>	
<b>Curriculum Vitae</b> .....	<b>179</b>	

# Summary

The main thread of the researches presented in this habilitation manuscript are the improvement of the energy efficiency of the vehicles energy systems, their emissions reduction, presenting competitive cost effective solutions of the energy storage and conversion technologies. There is a need of holistic design method for the future energy systems that considers on a simultaneous way the technical, economic and environmental challenges. For this reason, the research considers energy efficiency, economic and environmental impacts studies of innovative energy systems. In this manuscript the vehicles energy systems evolve from autonomous on-board systems to grid related system, with multi- energy vectors. This extended energy system considers the different energy grids (electricity, natural gas, hydrogen) and is integrated for large-scale improvement of the system efficiency, effective cost investment and environmental impacts reduction. The new integrated energy system has to deliver effective, affordable and sustainable energy services for mobility, electricity and heating. The manuscript is organized in 7 main chapters:

- Introduction
- Literature review
- Energy efficiency, storage and conversion on vehicles board
- Extension of the vehicle energy systems: the vehicles as grid related systems to the energy grids for optimal energy services for mobility
- Energy storage and conversion systems for energy vectors: fuel cell electric vehicles, hydrogen and their ecosystem
- Conclusions
- Research perspectives

## Energy efficiency, storage and conversion on vehicles board

In this chapter, the vehicle is considered as energetically autonomous system. This means that the energy system is limited on the storage and conversion on-board. The main energy services to be delivered by the onboard energy systems are the mobility and the cabin heating and cooling. The research domain considers three main domains: optimization of the global energy efficiency of the system (considering powertrain architectures), improvement of the efficiency of the main energy converters (for example internal combustions engines) and the optimization of the operating conditions of the high voltage batteries, which are the main storage system for the electric vehicles. This research category regroups from one side modelling, simulation and optimization works, and from the other one experimental tests and test benches design and realization. The research is realized in the period 2012-2020 and implements works on methodology development (Optimization of the energy efficiency) and technology development (Camless electromagnetic actuator and busbars for Li-Ion battery pack).

The following research items are included:

- Energy efficiency:
  - Waste heat recovery
  - Optimal design for efficient mobility service for hybrid electric vehicles
- Energy conversion:
  - Development of robust control of an electromagnetic actuator
- Energy storage:
  - Optimal designs for a long-range electric mobility
  - An energy balance evaluation in Li-Ion battery pack under high temperature operation

### Energy efficiency:

In this chapter, different technologies for energy recovery (kinetic and thermal) and their combination in different powertrain architectures are considered for improvement of the energy efficiency. The organic Rankine cycle is evaluated as waste heat recovery technology. The electrification of the ICE based powertrains brings different hybrid electric architectures, classified functionally according to their degree of hybridization and the size of the high voltage battery. The HEVs recover the kinetic energy during braking but are powered by ICEs, which present still thermal losses. The research question to investigate in this chapter is the efficiency improvement by the combination of two type energy recovery systems (HEV and ORC).

The optimal design of the hybrid electric vehicles for the kinetic energy recovery and the choice of the optimal battery size of the high voltage battery for HEV are as well investigated according to techno-economic and environmental criteria. This is a published article and is presented in Appendix C.

The research applies multi-objective and energy integration methodology.

To sum up, this research presents studies of the efficiency performance and the economic optimization for a middle class vehicle with a downsized gasoline engine. Two technological options are studied for the efficiency improvement of the baseline vehicle powertrain:

- Low degree electric hybridization technology – called Mild Hybrid electric powertrain
- Waste heat recovery system for two heat sources the engine water circuit and the exhaust gases, means an external thermodynamic cycle – ORC

The **main conclusion** coming from the driving cycles evaluation is the MHEV is an efficient technology for the drives with speed variations. The selected ORC design is efficient on the cycles using the charged area of the engine. The MHEV and the ORC are complementary technologies and their combination is especially efficient on the combined cycles containing urban and extra urban part. For the combined cycles and peri-urban the combination of ORC and MHEV bring the best fuel saving potential, superior to 35% in comparison with normal ICE vehicle.

The optimal environomic configurations for hybrid electric vehicles are researched by using multi objective optimization techniques. The optimization methodology is based on a genetic algorithm and is applied for defining the optimal set of decision variables for powertrain design. The analysis of the environomic Pareto curves on NEDC illustrates the relation between the economic and the environmental performances of the solutions. The life cycle inventory allows calculating the environmental performance of the optimal techno-economic solutions. The environmental and the economic trades-off are defined for the different impact categories. Their impact for the production phase and the use phase of the vehicle is studied. The sensitivity of the impacts categories on the electricity production mix is as well studied. The solutions in the lowest emissions zone show that the maximal powertrain efficiency on NEDC is limited on 45.2% and the minimal tank-to-wheel CO<sub>2</sub> emissions are 30 g CO<sub>2</sub> /km. They have the maximal cost – 75000 Euros. The increase of the electric part of the powertrain increases all environmental categories, because of the materials and the processes to produce the electric components.

**Energy conversion:**

In this part of the chapter, it is presented the development of an innovative electromagnetic actuator for engine valve train. This converter acts on the principle of linear electric machine, in bi-modes, converting electricity to force or force to electricity. The application of the designed innovative actuator is to replace the total mechanical engine valve train. This research contributes to improve the internal combustion engine (ICE) effective efficiency, by reducing the mechanical friction and by increasing the induced (thermodynamic) efficiency of the ICE.

The contribution of the presented research work is the use of an innovative concept of engine valve train based on Lorentz force electromagnetic actuator, which is characterized by performant and efficient magnetic circuit, lightweight moving part, direct driven by the current. This is an active actuator, which solves the problems highlighted in the previous researched – the control robustness and precision. A method for control, based on simulation and experimental steps is presented for the innovative actuator. The performances of the control are assessed. Test bench is built for the control research.

**To conclude**, the Lorentz force based electromagnetic actuator was developed and experiments are used to identify unknown model parameters for robust controller design. Simulations and experimental results show that a control law structure with a nonlinear feedforward and a plating strategy allow a real improvement of the convergence valve trajectory to a desired trajectory and make the actuator less sensitive to disturbances and parameter variations. The precision of the control law attests the controllability of the actuators technology and thus the good performances of the engine. The robust and precise controlling of the actuators on the intake side is especially important for the regulation of the airflow in the engine and this for gasoline engine concerns directly the regulation of the engine torque. The respect of the velocity during the valve landing requirements (at 6000 rpm 0,41 m/s measured for 0,5 m/s criterion for acceptability) is an important step and insures the respect of the noise criteria and the mechanical durability of the system.

**Energy storage:**

The compactness and the energy density are the main technology challenges in front of the energy storage in high voltage batteries for electric vehicles. The range of the electric vehicles and the range of electric mode for the electrified vehicles is the main challenge. This chapter investigates optimal design methods to increase the range of the electric vehicles. The trade-off of the electric vehicles is illustrated. The operational parameters and especially the temperature in the battery pack is an important parameter for the good performances of the batteries. Energy balance of the high voltage battery pack is investigated by experimental way in this chapter. The experimental data of the energy balance are used to design effective cooling strategies and technologies for batteries cooling. The experimental data allow as well modelling the thermal behavior of the batteries. The thermal models can be used to monitor the state of change and the state of health of the high voltage battery. Experimental test bench for the battery pack measurements was designed and operated to establish the energy balance.

**In conclusion**, this research presents a thermal energy balance of two types of the battery packs during the discharge process. One battery package was equipped with Al busbars while the other had Cu busbar. The investigated battery packages were made of sixteen cylindrical cells. The calculation of the energy balance allowed to calculate the amount of generated heat inside the battery packages which is key information from the operation safety point of view. The conducted calculations were validated by the measurements of real battery package. The difference between the calculated model and the measured values were 6% for the battery package with Cu busbar and 1% for the battery package with Al busbar. By replacing the Al with Cu busbar it is possible to reduce the generated heat  $Q_{GEN}$  by 10%. Cu- and Al-based busbars serves to the electrical connections in the battery pack, but as well serve as solution of passive cooling to evacuate the heat from the battery pack.

## Extension of the vehicle energy systems: the vehicles as grid related systems

The recharging of the vehicles and their connection to the energy grid became an important question.

This research contains the following items:

- Design of electric vehicles grid related energy systems for optimal mobility service
- Coordination interest for the optimization of electric vehicles for long- distance trips.
- Slow charging: robotized charging of high voltage batteries for electric and hybrid electric vehicles
- Integration of the environomic energy services for mobility and household using electric vehicle with a range extender of solid oxide fuel cell

The works are developed in the period 2017-2020 with the Robot charger project and the PhD thesis of my student Jean Hassler. The “Robot charger” is an experimental project with the development of a functional prototype and charging of the high voltage batteries of an electric vehicle with innovative wireless inductive technology for charging.

This chapter considers the recharging ecosystem and the design of the electric vehicles grid related energy systems for optimal mobility service. The question is to research recharging strategies that extend the autonomy of the electric vehicles and allow using electric vehicles for long range trips. The communication strategy and the coordination of the recharging plans of the vehicles reduce the waiting times on the recharging stations, increase the rate of use of the stations and optimize the number of chargers and so reduce the investment costs that are needed. The electric vehicles are considered as related to the electricity grid. The optimal recharging plan and the coordination of the recharging between the vehicles and the recharging infrastructure allow using electric vehicles for long distance trips. The rapid charging infrastructure is invested and deployed for the high ways. The domestic recharging systems are slow speed systems and the recharging operation at home is a frequent operation. An innovative robotized solution for recharging is investigated to do the recharging task at home. This innovation is called Robot Charger. The household is considered as cluster for energy integration where energy services for mobility and household needs such as electricity and heating are integrated. In this cluster integration the vehicle provides energy services to the household when is not used. The vehicle is equipped with highly efficient energy propulsion system based on electric vehicle with a range extender module of solid oxide fuel cell, using renewable fuel. The environomic multi-objective optimization is used for the energy services integration.

The **following conclusions** are coming out.

This research focused on the development of a smart cost and simple localization system for a robot , used for recharging of the batteries in an unknown environment. The localization in an environment is a fundamental capacity for a mobile robot. Smart cost platform means the use of low cost sensors and low cost hardware, thus the algorithm of localization has to run on low power computer and with simple sensors. The algorithm must respect three main constraints: computation efficiency, accuracy of the approximation of the position and ease of implementation. After implementing our platform on a three Omni wheels robot with a LIDAR and encoders, set up the communication protocols and set the parameters, a reference map was successfully build. According to the test’s results, the tracking performance is really good at moderate speeds (100 - 200 mm/s) as well as the localization accuracy with an error maximum of 2 cm. Thus, the SLAM is efficient enough to meet the requirements for the application.

The designs for different mobility services (urban and long ways distance electric mobility) of the electric vehicles are defined and the time interaction with the charging infrastructure is analyzed. Information and connectivity solutions that inform in real time the drivers for the availability and the location of the charging infrastructure, including the possibility to book and pay for charge points in different places is an important part of the solution. Combined with fast, i.e. high power charging capacities, pure electric vehicles would be able to serve long range needs. The analysis of the environmental Pareto curves on NEDC illustrates as well the relation between the economic and the environmental performances of the solutions.

This research presents the developed method and its modeling to find the optimal strategy for recharging on the highway for a flow of electric vehicles, in the case of long-range electric mobility. The flows are composed by different numbers of vehicles that have to travel long range distance on the highway. They have to stop and recharge their batteries on the chargers located on the stations. The waiting and recharging times are evaluated, considering the stops, the occupation rate, and the location of the chargers. In a first level simple optimization is performed by minimizing the waiting time for charging. The order of the vehicles stops their recharging strategy come out as results. Differential evolutionary genetic algorithm is used to solve the optimization problem. The initial population of the vehicles flows is generated randomly and the genetic algorithm operators (evaluation, selection and mutation) are used to converge to the solutions. The results from the study cases show that an additional number of chargers are needed to be installed to minimize the waiting time on the highway and to reduce the waiting and the recharging time on the highway stops. The investment cost of the chargers and the infrastructure has to be as well considered.

The vehicle is considered as grid related to the house and this means that its energy service of mobility and comfort is related to the energy services for the family house. The study contributes to consider in an integrated scale mobility and energy services for a household and introduces the use of the vehicle in dual mode. Solid oxide fuel cell coupled to gas turbine (SOFC-GT) module is introduced as a range extender of the autonomy of the electric vehicle. A base energy scenario for the house is also defined. The total yearly cost for the integrated system in dual mode stays still higher (1000 €/year) than the base case separately delivered energy services. This is due to the high investment cost of the equipment in the vehicle and the house. The major advantage of the energy integrated dual system is the reduction of the total GWP impact with around 30000 kg CO<sub>2</sub> eq. (60%). – from 50590 kg CO<sub>2</sub> eq. to 20338 kg CO<sub>2</sub> eq. This study illustrates large scale economic and environmental benefits opportunities by integration of the energy services for mobility and household.

## **Energy storage and conversion systems for energy vectors: fuel cell electric vehicles, hydrogen and their ecosystem**

This chapter presents the integration of the energy grids of electricity, natural gas and hydrogen. Renewable resources of energy are important for the production of clean hydrogen. The global well to wheels CO<sub>2</sub> emissions are reduced with the utilization of a green hydrogen. The hydrogen is an energy vector that can be used as energy storage of renewables energies in the energy grids.

The research is divided on three parts:

- Energy balance of the production and the conversion of hydrogen in the fuel cells
- Hydrogen production from (bio)-ethanol steam reforming, catalysts selection
- Well-to-wheels balance of the CO<sub>2</sub> emissions of the different energy storage and conversion technologies for sustainable mobility solutions

The research work is done in the period 2016-2020. The experimental works on the catalyst systems are done with the chemical department of the Lodz University of Technology (Poland). The global environmental impacts and comparisons of the different conversion and storage systems (well-to-wheels CO<sub>2</sub> emissions) are assessed in the frame of the workshops between PSA and Airbus.

This chapter presents innovative propulsion system with high efficiency, using fuel cells. Hydrogen is considered as clean energy, but several questions related to its production, its large-scale storage and distribution remains. The current state of the art of fuel cell vehicles is the use of pressurized hydrogen gas at 700 bar, stored on board the vehicles and converted into electricity by a proton-exchange membrane fuel cell (PEMFC). The storage and the distribution under 700 bar of hydrogen pressure present technical, economic and environmental problems. The idea of the research in this field is to propose a concept of energy storage under form of bioethanol and to convert bioethanol to hydrogen on board the vehicle by a solid oxide fuel cell (SOFC).

The hydrogen production is considered for different energy vectors and their ecosystem. This chapter presents the concept of electric vehicle with serial range extender to extend the vehicle autonomy. Fuel cell system powered by hydrogen produced through reforming of liquid fuel from renewable resources such as bioethanol is considered as a range extender module. The energy balance of the different types of fuel cells, powered by bio-ethanol is investigated. Three variants for ethanol conversion are investigated: variant 1: reforming of bio-ethanol in external reformer to hydrogen and its conversion in alkaline fuel cell, variant 2: reforming of bio-ethanol in external reformer to hydrogen and its conversion in a solid oxide fuel cell; variant 3: direct reforming of the bio-ethanol in the solid oxide fuel cell. The chemical processes for each variant are proposed and thermodynamic energy balance is calculated. The catalyst system for the bio-ethanol steam reforming is investigated on experimental way. It is needed a high active and selective catalytic system delivering 100% of bio-ethanol conversion to hydrogen. The total conversion of bio-ethanol to hydrogen is essential from the economic point of view. The catalyst which is used during the process has an important role to achieve 100% conversion. Typical catalytic systems used in steam ethanol reforming processes typically include precious metals Rh, Pd, Pt, Ru and Ir in monometallic formulations. Bimetallic systems are couple of precious metals with smaller amounts of transition e.g. Pd-Ni, Rh-Ni, Rh-Co and others. In view of the high price of noble metals, it is suggested to use higher concentrations of transition metals doped with small amounts of no noble metals eg. Ni doped with a small amount of Pd as an active phase components. The catalysts selection is done with laboratory experiments. While as a support it is suggested the usage of binary oxide system containing  $\text{Al}_2\text{O}_3$ , ZnO or  $\text{CeO}_2$  or  $\text{ZrO}_2$ . The main goal of this research is to select the most active and selective system which can be directly used in micro-reactor before the SOFC fuel cell. During the research tasks the most suitable liquid fuel will be selected and will be used as a substrate for hydrogen generation and finally to produce electricity using a SOFC fuel cell.

To consider the impact of the different energy vectors, well-to-wheels balance of the  $\text{CO}_2$  emissions is done for different vehicles propulsion systems. The impact on the energy efficiency and the emissions is discussed.

**To conclude**, in view of the high price of noble metals, it is suggested to use higher concentrations of transition metals doped with small amounts of no noble metals eg. Ni doped with a small amount of Pd as an active phase components. The catalysts selection is done with laboratory experiments. While as a support it is suggested the usage of binary oxide system containing  $\text{Al}_2\text{O}_3$ , ZnO or  $\text{CeO}_2$  or  $\text{ZrO}_2$ . After the investigations, the most optimal content of nickel for monometallic nickel supported catalyst is 5 % wt. of Ni. Further increase of the nickel content does not increase significantly the catalytic efficiency. All catalytic systems showed high activity and selectivity at high temperature of the reaction especially above  $500^\circ\text{C}$ . The main products obtained during the process were CO,  $\text{CO}_2$  and  $\text{H}_2$ . The high stability and high selectivity to hydrogen formation for mono and bimetallic systems was confirmed.

SOFC with integrated reformer of the bioethanol is the best fuel cell for the concept for a range extender unit. It presents the best energetic balance, from energy conversion point of view. In conclusion, it is proposed the working principle of the bio ethanol fuel cell for range extender unit for vehicle application with 15.15 MJ of electric energy output per kilogram of converted bio-ethanol.

As main conclusion, the well-to-wheels (WtW) CO<sub>2</sub> emissions depend of the efficiency of the conversion chain. They are strongly influenced by the electricity production mix. Fuel cell and electric powertrain technology help to reduce considerably the WtW CO<sub>2</sub> emissions, if we use low carbon electricity production mix and low carbon process for the hydrogen production. The production of electricity or hydrogen from renewable resources is a viable solution for low WtW CO<sub>2</sub> emissions. The use of renewable electricity for the electrolysis to produce hydrogen, is the best configuration for almost zero CO<sub>2</sub> emissions, 3 g CO<sub>2</sub>/km

## Research perspectives

This part presents the future works for the 4 coming years in the scientific department of PSA Groupe. The presented works on the technologies development will continue as innovations works to evaluate the technical and the economic maturity for the market.

In the context of the strong regulation of CO<sub>2</sub> emissions reduction, my research project is to implement the developed optimization method to a tool for the evaluation of energy integrated systems. The tool can be used for prospective research of solutions for affordable and sustainable mobility for the period 2030-2050.

### From the method to the tool

User platform can be created, implementing libraries related to the technologies, different energy resources and as well energy demand profiles. The optimization structure contains the simulation models and the optimizer based on genetic algorithm. As results the tools gives information about the sizing and the operation strategy of the technological equipment, distribution of the heat for city energy needs, mobility energy strategies for public and private transportation or consideration of the logistic strategy for goods, per rail or road.

The time horizon is for research is 2030 to 2050 and the temporary dynamic profiles could be considered, monthly or hourly. The solving algorithms are using mixed-integer nonlinear programming. The following characteristics can be noticed:

- decision variables,
- Parametrized assumptions & constraints
- Multiple indicators : Cost, CO<sub>2</sub>, primary Energy , Exergy, Employment, Waste
- Uncertainties, Monte-Carlo Simulation

### Applications:

The following applications can be developed:

- Evaluation of the services that electric vehicles could provide to the electric grid
- Evaluation of the strategies to use renewable energies in the mobility scenarios
- Evaluation of the scenarios of production and storage, distribution of clean hydrogen from biomass



# Chapter 1 Introduction

## 1.1 Context of the research

Automotive transport is governed by strict environmental regulations. They are local, national or international. The European regulation for CO<sub>2</sub> emissions requires the lowest levels of emissions per kilometer in comparison with other regions of the world. Figure 1-1 illustrates the CO<sub>2</sub> emissions forecast per regions. It is visible that there is a worldwide convergence for the reduction of the CO<sub>2</sub> emissions. The CO<sub>2</sub> emissions levels are very low in Europe going from 130 gCO<sub>2</sub>/km in 2015 to 95 gCO<sub>2</sub>/km in 2020. The next steps in Europe are to decrease the average value of emission per fleet to 75 gCO<sub>2</sub>/km in 2025. From 2025 the first time the European automotive market will be driven by the environmental regulations. The massive penetration of electric vehicles is expected from 2023, because the market is being prepared. The European carmakers are already being developing, industrializing and commercializing electric vehicles.

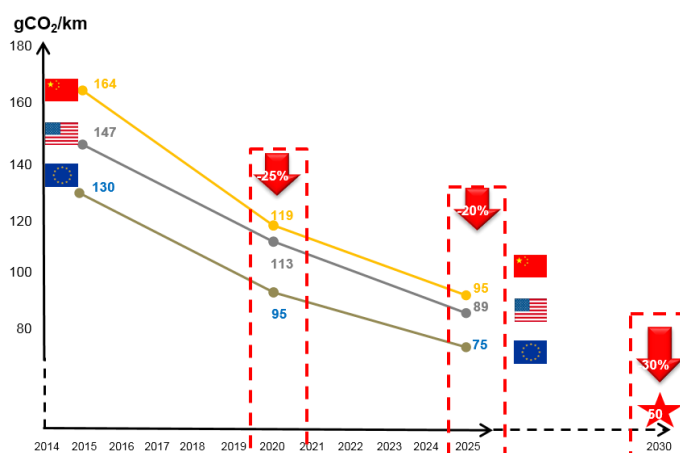


Figure 1-1: CO<sub>2</sub> emissions regulatory forecast per regions

By 2030 the CO<sub>2</sub> emissions have to be reduced to 50 gCO<sub>2</sub>/km, representing a slope of 30% reduction in comparison of the 2025 level. The target of 50 gCO<sub>2</sub>/km is ambitious and demands global investment in the energy technologies for vehicles. The regulation of the CO<sub>2</sub> emissions is given in a tank-to-wheels vision. This means that the regulation considers only the emissions during the use of the vehicles. The emissions for the production of the fuels are not considered. The global emissions from life cycle point of view, including well-to-wheels analysis and impact of the energy vectors production are not considered for the moment. The European parliament supports the targets of 32% for renewables in 2030 and minimum 14% of renewable energy in the transportation sector in 2030.

Decarbonisation and emission reduction from road transport are the main drivers for the electrification of vehicles, (xEV). The envisaged European CO<sub>2</sub> fleet emission limits for 2025 and 2030 already require a massive introduction of partially electrified vehicles (range extenders (REX), plugin hybrid electric vehicles (PHEV)) or full EV's (battery electric vehicles (BEV), fuel cell electric vehicles (FCEV)) [1] Further, local or regional air quality regulations such as potential zero emission zones will drive demand for these vehicles.

According to the ERTRAC[1] report the electrification of the road transport will significantly contribute to the improvement of air quality and the climate protection. To do that the electricity used has to be from low carbon / carbon neutral sources, (solar, wind, hydro, geo thermal). In the European electricity roadmap, it is assumed that electricity (or hydrogen) will be provided on an increasingly CO<sub>2</sub>-neutral basis.

The interest of the introduction of the electrification technologies in the automotive sector is explained in many researches [2], [3] and others. Today the state of the art considers that the technologies needed for the electrification of the vehicles gained in maturity and the largest deployment would allow decreasing the prices of the electrified vehicles. The users' expectations are the same as for the conventional fossil fuels vehicles:

- Prices as low as today's ICE driven vehicles or at least vehicles with total cost of ownership competitive to those as of today
- Range, reliability, durability and re-sale value of electrified vehicles similar to conventional vehicles
- Range adapted to specific use cases
- Usage comfort as good as the state of the art ICE-powered vehicles (availability, "re-fueling" time and possibilities, passenger comfort, transport volume)
- Safe parking and infrastructure also with direct connection to charging facilities

To meet the targets of sustainable development and greenhouse emission reduction of the future vehicles fleet, the automotive industry needs to deploy cost-competitive and efficient advanced energy conversion systems for the future commercial personal vehicles.

The challenges of the research work are to implement in the design action, the energy balance optimization for reducing the CO<sub>2</sub> and the environmental impacts. The design system has to satisfy the regulation of energy efficiency and the energy classes imposed on the future vehicle fleet and to consider the global energy vision. The design of the energy conversion systems for passengers' cars requires the consideration of the economical competitiveness, the highest conversion efficiency and the lowest environmental impacts. The approach in this work consists to choose adapted technology (technological options), give a cost vision and define environmentally optimal energy solutions for mobility. This work considers the energy system for mobility based on the energy storage and conversion systems on vehicle board and the energy and the conversion of the energy vectors for mobility.

The research questions are:

- How the design methods have to be modified to incorporate these competitiveness problems – energy efficiency, CO<sub>2</sub> and pollutant emissions, and cost, in the future vehicles and the energy service for mobility?
- Can one implement the environmental criteria in the design step of an efficient energy storage and conversion chain?
- Can we consider the vehicles as energy grid related systems, delivering optimal energy service for mobility?

This research proposes an evaluation method, based on multi-objective mathematical optimization, which can consider on a holistic way the objectives and proposes a structured vision on the possible decisions. The novelty of this research is to present the optimization method and to discuss possible applications and results, considering new technological options for energy conversion and storage of the energy. Energy balance of high voltage batteries is performed. The vehicles are considered related to the electrical grid. The energy grid is larger, combining interconnections between the electricity grid and others energy vectors, such as the hydrogen and the natural gas. The main research questions discussed in this manuscript are presented in paragraph 1.2.

## 1.2 Main research questions and domains

The research work can be summarized in 3 main categories:

- Energy efficiency, storage and conversion on vehicles board.
- Extension of the vehicle energy systems. The vehicles as grid related systems to the energy grids for optimal energy services for mobility.
- Energy storage and conversion systems for energy vectors. Fuel cell electric vehicles, hydrogen and their ecosystem.

The following paragraphs introduce the research topics developed in the manuscript.

### 1.2.1 Energy efficiency, storage and conversion on vehicles board

This research domain considers the vehicle as autonomous system from energy point of view. The vehicle has to deliver two main energy services: for mobility and for thermal comfort. The thermal comfort is related to the heating and the cooling of the cabin. The main target is to improve the energy efficiency of the system to reduce the energy consumption, the emissions and to increase the range. The efficiency improvement of the global on board energy system is investigated through waste heat recovery and electric hybridization on a system level. The components of the system such the converters and the stockers are as well investigated for efficiency improvement on components level.

#### **Waste heat recovery**

The efficiency gains of the energy systems for vehicles are directly related to the fuel saving and the emissions reductions. The development of efficient technologies for the driving profiles and the comfort demands is then needed. There comes the idea to define a vehicle energy system with integrated energy services for mobility and comfort. With the definition of the system we need a methodology for the integration of the energy services. This methodology is called an energy integration methodology. The energy flows are integrated into the energy system to increase the efficiency. The energy integration considers the energy demand profiles for mobility and comfort and uses technologies recovering waste energy into the energy system. Organic Rankine Cycle (ORC) is selected to recover the heat waste of the internal combustion engine (ICE). Waste heat recovery technologies and hybrid electric vehicles are briefly introduced in the following sections.

#### **Optimal designs for efficient mobility service for hybrid electric vehicles**

Hybrid electric vehicles designs are investigated according to technical, economic and environmental optimizations. The novelty of the present study is the application of the environomic optimization methodology for optimal design and operation parameters of the vehicle energy system. Methods, techniques to analyze, to improve and to optimize energy systems have to deal not only with the energy consumption and the economics, but also with the environmental impacts. The systematic consideration of the thermodynamics, the economic and the environmental impacts in the design and the operation of the energy system is called environomics.

#### **Development of robust control of an electromagnetic actuator**

The camless valvetrain is considered as a promising solution for improvement of the engine performance and its efficiency. Most of the camless valvetrains, based on reluctance force, suffer the problem of high impacts at valve seating, which induces noise and restricts its mass production.

The difficulty for the engine valves actuators in the case of full camless engine is to cover the large range of forces and dynamics, required for operating correctly all intake and all exhaust valves. Camless engine means that such electromagnetic valves are deployed to the complete intake and exhaust side. From previous studies and experiences with reluctance force based actuators, we know that main difficulties for the realization of camless engine valvetrain are:

- the precision of the actuators, where landing, the chock of the valves inducing noise
- the density of the delivered force
- the high electric consumption

The novelty of the presented research work is the use of an innovative concept of engine valve train based on Lorentz force electromagnetic actuator, which is characterized by performant and efficient magnetic circuit, lightweight moving part, direct driven by the current. This is an active actuator, which solves the problems highlighted in the previous researched – the control robustness and precision. A method for control, based on simulation and experimental steps is presented for the innovative actuator. The performances of the control are assessed.

The electrification of the vehicles induces the problem of their autonomy and their range. The on-board storage system impacts them directly.

### **Optimal designs of electric vehicles for a long-range mobility**

The problems of the range and the energy storage of the electric vehicle on board are important and are introduced. The energy system of electric vehicles is studied for different ranges and mobility usages. Multi-objective optimization method is applied to estimate the optimal vehicles energy system designs for urban mobility and for long way electric mobility (> 500 km). The optimal designs considering technical, economic and environmental criteria are presented. The trade-off between the autonomy of the electric vehicles and the energy densities of the high voltage batteries are illustrated.

### **An energy balance evaluation in Li-Ion battery packs under high temperature operation**

The high voltage batteries are one of the main components of the powertrain of electrified vehicles. Li-Ion batteries are the storage system for electricity in electric and hybrid electric vehicles.

The development of the battery system is related with many challenges. Some of them are the fast charging, the charging infrastructure, the fast evolution of technologies, and the management to keep the system in optimal operating conditions. In the thermal management system of the battery, the major challenge is to maintain the battery cells in the optimal range of temperature without ever exceeding limitations defined by cell manufacturers. This challenge grows with the needs of high power charging introduced to decrease of duration of the charge. To manage the thermal behavior of the battery one can use active systems such as cooling plate with liquid, fans or passive systems as the phase changes of the materials. The precise characterization of the energy balance of the high voltage battery pack is important for the design of different kind of thermal solutions. The energy balance of a battery pack is investigated experimentally to construct a thermal model for implementation in simulation tools for design.

## **1.2.2 Extension of the vehicle energy systems, the vehicles as grid related systems**

This research domain considers the electrified and the electric vehicles as connected to the electric grid and as a part of it. The vehicles became related to the energy grid and their can provide energy services for mobility but also for the households. New design methods have to consider the new limits of the extended energy system and the recharging systems became part of the optimization. The choice and the compromise between the size of the onboard storage and the frequency of the access of the vehicles to the recharging infrastructure are important to be defined. The recharging process takes time and the need of service for optimal recharging became visible. The vehicles have to be connected to the recharging infrastructure and domestic robotized solutions connected to the vehicles appear to bring recharging service. In a large scale energy services integration the vehicles can provide when not used

for mobility, energy services for the household. Significant reduction of the global CO<sub>2</sub> emissions is possible by the consideration of the larger energy system and the integration of the energy services for the expanded energy system.

### **Design of electric vehicles grid related energy systems for optimal mobility service**

The electrification of the vehicles and their connection to the electricity grid present the opportunity to consider the vehicle energy system as grid related. The autonomous energy system is enlarged and connected to the rest of energy grids. Thus the vehicles have to deliver as well the main energy service, which is the mobility but they can deliver or be part of the rest of the energy services that grid related systems can deliver: the electricity and the heat production. There is a need to consider the extension of the vehicle energy systems and to adapt the design of this enlarged system to deliver optimized energy services for all energy needs of the system.

### **Coordination interest for the optimization of electric vehicles long distance trips**

This research investigates the way to use the electric vehicles for long way trips, by extending in an intelligent way their intrinsic autonomy.

The drop in battery prices and the rise of their energy density has permitted the introduction of consumer cars with more than 400 km range, while improvements in high power charging point units (with a rate 100 kW and above) offer hundreds of kilometers range gain in 20 minutes. One risk remains: the travel time depends on the availability of charging stations, which can drop during rush hours, due to long queue, or grid power overload. These situations can highly affect user experience. Service for optimal recharging plan is studied.

### **Slow domestic charging: Robotized charging of high voltage batteries for electric and hybrid electric vehicles**

Users expectation for electric vehicles are the same as for the conventional vehicles: range adapted to specific use cases, usage comfort as good as the state of the art internal combustion engines -powered vehicles (availability, “re-fuelling” time and possibilities, passenger comfort...), and infrastructure also with direct connection to charging facilities. The management of the recharging of the batteries for the users is a central question. The domestic charging of the vehicles through robotized systems, which are innovative products and services, proposes users comfort and service.

### **Integration of the environomic energy services for mobility and household using electric vehicle with a range extender of solid oxide fuel cell**

The biggest part of the state of the art studies on energy conversion systems for vehicles are concentrated on the on-board energy storage and conversion systems during the phase where the vehicle is used, when this vehicle is driven. The holistic methods might be used to optimize not only the design and the energy systems of the vehicles, but are also enablers to evaluate new energy services of the vehicles propulsion systems, when the vehicles are not used for driving. They are related to the different energy grids- electricity and gas. In this system the vehicles are considered to be related to the energy grids. Their design is as well optimized for the additional energy services and functions in the enlarged energy integrated system.

The environomic optimization method is used in this research to explore the optimal design for vehicles with innovative propulsion system, considering the mobility and also the integrated energy service to the households. The environomic design of vehicles integrated energy systems consists in the systematic and holistic optimization for vehicle energy systems, according to technical, economic and environmental objectives. The method is developed for vehicles applications and is presented for electric vehicles in [2], for hybrid electric vehicles in [3] and for electric vehicles with innovative range extender module with SOFC in [4]. Solid oxyd fuel cells technologies are described in [5] and researched as range extenders for battery electric vehicles in [4] and [6].

### **1.2.3 Energy storage and conversion systems for energy vectors; fuel cell electric vehicles, hydrogen and their ecosystem**

#### **Fuel cell electric vehicles, energy vectors for hydrogen and their ecosystem**

Several solutions have been developed in order to improve the competitiveness of the electric vehicles. Technical work on advanced battery technologies, and economic aids related to environmental bonuses for the customer investment cost decrease are the most important. The range extender concept (serial hybrid) proposes an additional autonomy for the electric vehicles. However, internal combustion engines are known to have low efficiency 30-35% (for gasoline ICE used as a range extender) and still use fossil based fuels. They can also be operated with biofuels, but after the combustion the CO<sub>2</sub> emissions are released in the atmosphere but in this case we do not introduce additional amounts of CO<sub>2</sub> to the atmosphere.

The fuel cells with their high efficiency and electrochemical conversion of the fuel directly to electricity avoid the combustion and seems to be an excellent candidate to substitute the ICE in an optimal conversion chain. The proton- exchange membrane fuel cell (PEMFC) has been studied for most of the automotive applications. The advantages of the PEMFC are that they offer high safety, support well transients and operate on low temperature (80 °C). In 2005, the project FISYPAC built an electric vehicle powered by a 17 kW PEMFC coupled with a Li-Ion battery with capacity of 13 kWh. The vehicle was tested and reached autonomy of 500 km on NEDC with 1 kg/km of hydrogen (H<sub>2</sub>) consumption.

The weakness of the PEMFC is that they use hydrogen with high purity stored on the vehicle board. With the limited hydrogen distribution infrastructure, the use of PEMFC is also limited. The hydrogen has to be stored on 700 bars and this introduces some safety constraints. Additionally, it is important to emphasize that PEMFC must be powered by high quality pure hydrogen. Even a small amount of CO (about 10ppm) can deactivate the anode material used in fuel cell zone during the operation.

The main idea of this research axe is to study liquid fuels (for example bio-ethanol) as a source of hydrogen to avoid storage of compressed hydrogen under 700 bars on the vehicle board. An efficient conversion system for the bio-ethanol is researched based on a serial range extender vehicle architecture with fuel cells able to convert liquid fuel into electricity. A solid oxide fuel cell with integrated bio-ethanol reformer is proposed for converter in the range extender concept. The catalyst system for the ethanol steam reforming is investigated on experimental way. The performance of the catalyst system defines the conversion efficiency of the fuel cell system.

The well-to-wheels (WtW) CO<sub>2</sub> emissions balance, including the emissions for the production of the energy and the emissions during the use phase of the vehicle is performed. The well-to-wheels (WtW) CO<sub>2</sub> emissions balance illustrates the importance of the energy vectors for the global carbon dioxide emissions, the efficiency of the vehicles propulsion system.

## **1.3 Personal experiences and motivations**

The major part of my research work is for the Research and Innovation department of PSA, where I spent 14 years of professional experience. My research work is performed in the Research and Innovation Direction of PSA, where I am employed since 2006. I started my carrier as young engineer in the “Engines department” of the Research and Innovation Direction. My mission was to research innovation and technologies to improve the combustion process and thus the effective efficiency of the internal combustion engine. I was appointed to that position during 3 years (2006-2009). The core knowledge and skills are related to the thermodynamics, the mechanics and the internal aerodynamics.

From 2010 to 2012 I was employed in the department for vehicles development of PSA and engaged in the development and the industrialization of commercial vehicles. This was for me a large-scale industrial project, where I experienced the management of projects: human resources, budget, planning, engineering and quality management, industrial and time to market constraints. The production plant is located in Russia and I had the opportunity to visit the country and to practice the Russian language. I have managed R&D budget and industrial investments for the production plant.

I integrated the Research and Innovation Department in June 2012 and I was appointed to the research domain of vehicles propulsion systems. I started my Ph.D. thesis at Ecole Polytechnique Fédérale de Lausanne (EPFL), Switzerland in 2012 at the Laboratory of Industrial Energy Systems and Process Engineering (IPESE). I was doing my PhD work at the same time as my research activities in the PSA Research and Innovation Department. The duration of my Ph.D. thesis was 3 years and 3 months. I was affiliated to the doctoral school of Energy of EPFL where I followed and validated 12 ECTS credits. The topic of the Ph. D. research is entitled “Environomic design of vehicle integrated energy systems”. This topic is at the crossroad between Process and Mechanical Engineering. The research was motivated by the need of the automotive industry to meet the targets of sustainable development and greenhouse emission reduction of the future vehicles fleet.

Today I am a researcher in the Scientific Department of PSA. My research in related to the research and innovation projects in the domain of the energy and the vehicles propulsions systems. My nomination at this position is effective since January 2016. I am involved in the leading of the research activities, PhD thesis leading and partnerships with the academic research institutions (universities or research institutes) or with others industrials partners.

My professional project is to prepare my habilitation to direct research (HDR) and to continue to lead the research activities in the industry, for example in PSA. In the industry, we have considerable research resource – PhD Thesis, participation in research institutes in national and international level. For example, we have 80 PhD students in total and around 30 PhD new thesis are discussed every year for approval, with French Association Nationale de Recherche Technologique (ANRT) and the academic partners. My ambition is to transfer the knowledge and the good practice from the academia for research leading and to apply them from efficient and collaborative research in the industry, based on partnerships with the academia.

My main motivation is to increase and to transfer the knowledge and the interest of the research to the students and the professionals from the industrial sectors.

### **Practice and content of the teaching**

In 2019, I was invited as a guest lecturer to teach two disciplines in the Master Programs of the National Military Academy “Rakovski” of Bulgaria. The Academy has a unique contribution to the foundation of the Bulgarian Officers Corps, as well as to the establishment of the new Bulgarian State. Today it is a national institution for higher education, qualification, and scientific research on issues of national security and defense. The mission of Rakovski Defense and Staff Academy is to prepare military leaders and civilian personnel in all spheres.

For the Specialized Master Programs I proposed two new disciplines and they were selected in the chair of Logistics and Transportation. The interest of introduction of my lectures is the teaching of modern structured scientific and engineering methods deployed in the Research and Development sector of the automotive industry. They insure structured and systematic management of the technologies.

## **1.4 Outline and contribution of the present work**

The manuscript contains 7 Chapters and 5 Appendixes (A, B, C, D, E).

Chapter 1 introduces the motivations and the context of the research.

Chapter 2 introduces the prior art in the main research domains:

- Energy efficiency, storage and conversion on vehicles boards.
- Extension of the vehicle energy systems. The vehicles as grid related systems to the energy grids for optimal energy services for mobility.
- Energy storage and conversion systems for energy vectors. Fuel cell electric vehicles, hydrogen and their ecosystem.

Chapters 3, 4, 5, present the research results for the main research domains.

Chapter 3 presents the studies of the optimal designs of vehicles energy systems to increase the global energy efficiency onboard. Waste heat recovery and hybridization (electrification) of the vehicles are studied.

An electromagnetic actuator for engine valve train is presented. The purpose of the development of this technology is to increase the conversion efficiency of the internal combustion engine to reduce the fuel consumption and to reduce the CO<sub>2</sub> emissions through most efficient onboard energy converter – the internal combustion engine.

Chapter 3 studies the optimization of the on board energy storage system constituted from the high voltage batteries. The impact of the quantity of batteries to increase the vehicle range is studied. The recharging of the batteries is related with the heating of the batteries. Thus, the energy balance of the batteries is studied to obtain optimal performances on the battery storage.

Chapter 4 studies the connection of the vehicles to the energy grids. Technologies and strategies for recharging are studied for electric vehicles. A concept of integrated energy services for mobility and the household are researched. An innovative concept of electric vehicle with a highly efficient range extender module is presented to deliver optimal services for mobility and for heating and electricity generation for a household.

Chapter 5 studies the hydrogen as energy for fuel cell vehicles and the hydrogen ecosystem. The conversion of the bio-ethanol to hydrogen is studied. The optimal catalyst is selected to maximize the hydrogen yield obtained by bio-ethanol steam reforming. A Well-to-wheels CO<sub>2</sub> emissions balance of different energy storage and conversion technologies (different propulsion systems for vehicles) is presented. The impact of the energy vectors (fuels, electricity and hydrogen) for the sustainable mobility is estimated.

Chapter 6 draws the conclusions of the research work, estimating the contribution of the energy integration method.

Chapter 7 draws the perspectives of the research domains, related to the global integration of the energy grids for the different energy vector on a large scale. Thus, the energy grids can constitute large-scale energy conversion and storage system for the optimization of global energy services, for mobility, electricity production and cooling/ heating.

Appendix A presents the methodology for the optimization of energy integrated systems. This methodology is transferred and adapted for the study of extended and grids related vehicle energy systems.

Appendix B introduces the models of the technologies (the converters and the storage technologies), the possible powertrains architectures coming out from the combination of the energy technologies. The simulation models of the selected powertrain architectures are described. Appendix B contains also the description of the economic and the environmental models, used in the optimizations.

Appendix C contains the research results of the optimal designs for efficient mobility service for hybrid electric vehicles and the optimal designs of electric vehicles for a long-range mobility.

Appendix D contains basic definitions in the mobile robotics.

Appendix E contains the research results of the study “Integration of the environmental energy services for mobility and household using electric vehicle with a range extender made of solid oxide fuel cell”.

The Appendixes C and D include the results from recently published journals articles.

# Chapter 2 Literature review

## 2.1 Energy efficiency, energy storage and conversion on vehicles board

### Waste heat recovery

The vehicle is a dynamic system. The size and the efficiency of the converters depend on the dynamic driving profile. Energy integration is used to increase the energy efficiency of the vehicle energy system. An adapted methodology is proposed in [7] to select the best points for the integrated design of the system. The method clusterizes the dynamic profile on typical multi-periods where the vehicle is used. The design of the energy system is optimized for these main multi-periods. The energy integration is applied in [7] on hybrid electric vehicles. The potential of energy recovery of a single stage Organic Rankine Cycle is studied. The ORC is considered for a thermal engine in a hybrid electric powertrain. The contribution of the ORC is assessed for different drive cycles. After the process integration, a multi-objective optimization defines the design of a hybrid electric vehicle with an optimal waste heat recovery system. The energy balance of the internal combustion engine, for different operating points, is defined and analyzed in [8]. An energy integration methodology, based on process integration techniques is discussed in [8]. It is applied on the extended energy system of the vehicle. The possibilities of an ORC to recover waste heat from a 900 kW fast passenger ferry Diesel engine are investigated in [9]. The authors analyze in [10] the feasibility of an “on-board” innovative and patented ORC recovery system. The vehicle thermal source can be either a typical diesel engine (1400cc) or a small gas turbine set (15–30kW).

Hybrid vehicles can use energy storage systems to disconnect the engine from the driving wheels of the vehicle. This option enables the engine to be run closer to its optimum operating condition. Nevertheless fuel energy is still wasted as heat through the exhaust system. The article [11] presents the model of the engine of a diesel-electric hybrid bus, coupled with a hybrid powertrain. The performances of a hybrid vehicle over a drive-cycle are analyzed. This showed that including the waste heat recovery technology reduces the fuel consumption with 2.4% for a typical drive-cycle. The ORC has large applications such as agricultural biogas combined heat and power engines, biomass boilers, landfill biogas plants, small geothermal plants and concentrated solar thermal systems [12]. Most of the projects related to ORC systems, in the transport industry, discuss performance optimized solutions that include heat recovery in engine exhaust gas. The authors describe in [13] the development and exergetic assessment of a new hybrid vehicle incorporating gas turbine as powering option. A multiple heat source supercritical ORC (Organic Rankine Cycle) for vehicle waste heat recovery is studied in [14]. A vehicle energy-supplying system is proposed to satisfy energy demand of vehicle in every season in [15]. This system is based on an ORC. The authors modeled a hybrid electric heavy duty vehicle to assess energy recovery using a thermoelectric generator in [16].

**The literature describes** waste heat recovery of internal combustion engines or other converters, by external thermodynamic cycles, such as the Rankine cycle, with organic fluid. The organic fluid helps to evaporate to lowest temperature and so helps to valorize the low-grade heat. Few studies mentioned the waste heat recovery on hybrid electric vehicles and its potential for fuel consumption reduction.

### **Optimal designs for efficient mobility service for hybrid electric vehicles**

In the next decade, electric vehicles are expected to increase their market penetration. Main technologies for energy storage and conversion, the drive train components and the energy management will reach high maturity [1]. The industrialisation of those components on high scale and volume will reduce the cost of the electrification. The affordable cost will lead to the democratisation of electric vehicles on all vehicles segments. Hybrid electric vehicles with different levels of hybridization ratio are designed for urban and peri-urban drives. They allow zero emissions drives from thank-to-wheels view (25 km or 50 km range). The policy in the big cities is to support by incentives Hybrid electric vehicles with zero emission vehicles modes. The scarcity of not only fuel resources but also the adverse effects of the operation of energy intensive systems on the environment (pollution, degradation) have to be taken into consideration. Thus, the system can be properly designed and operated. The systematic consideration of thermodynamic, economic and environmental aspects for the design and the operation of an energy system is called environomics [17]. Environomic analysis is an extension of thermo-economics [18]. Environomic design of electric and hybrid electric vehicles are studies in [2], [19].

The automotive vehicles are increasingly restricted by environmental regulations. They have to reduce emissions of CO<sub>2</sub> and pollutants of exhaust gases of vehicles. The design choices of the vehicle powertrain become an important question. A simulation method of environmental impacts generated by the phase where the vehicles is used is proposed in [20]. Delogu et al. investigate in [21] the light weighted design and electrified powertrain as important strategies in the automotive industry to reduce fuel consumption and reduce emissions. Lightweighting of electric vehicles is considered a step to reduce forward the electric consumption of the vehicles. Alegre et al. showed in [22] a modelling of electric and parallel-hybrid electric vehicle with choice of type and size of the battery or weight. The tools allows observing the performance impact and the vehicles range. Through the use of a Geographic Information System combined with a mathematic algorithm (genetic algorithms) the planning of charging stations was obtained. The installation investment cost was minimized and the geographic distribution was optimized in order to increase the quality of the service. Electrified vehicles like hybrid electric vehicles, plug-in hybrid electric vehicles, battery electric vehicles, fuel cell electric vehicles and fuel cell hybrid electric vehicles are emerging as less polluting alternatives to internal combustion engines driven vehicles. It is important to assess the market penetration in the future of these categories of vehicles. A 'two-step' method is used in [23] to estimate the optimum market penetration of lightweight and electric-drive vehicles in the long-term and the impact on the light-duty vehicle fleet, focusing on Japan. The authors analyse in [24] different charging strategies for a fleet of electric vehicles. They test the value of a vehicle owner that can choose when and how to charge.

The authors analyse in [25] the scenario of development by the Danish Climate Commission. The results show that even with a limited short-term electric car fleet, these will have a significant effect on the energy system; the energy system's ability to integrated wind power and the demand for condensing power generation capacity in the system.

Alternative scenarios for energy planning are proposed for the transportation sector in [26]. The analysis of the projection of energy demand and greenhouse gas emission, in the form of CO<sub>2</sub>, NO<sub>x</sub>, and CH<sub>4</sub>, was conducted. The results show that by implementing an efficient vehicle scenario, global warming potential can be reduced by 15.80%.

**The literature shows** that emission policy considers hybrid electric vehicles as local emission reduction solution. Simulation models of fleets of HEV are used for energy planning activities. Few studies appear to consider on a holistic way the environomic scenario for the HEV use.

### **Development of robust control of an electromagnetic actuator**

The literature review highlights the problems and the research done on them. Liu and Chang focus in [27] on the valve seating performance of an electromagnetic valvetrain (EMVT) with moving coil linear actuator. The EMVT has inherent advantages to achieve low valve seating velocity. The seating performance of EMVT is evaluated by two indicators: seating velocity and holding force. Mercorelli studies in [28] a Lyapunov-based adaptive control law for an electromagnetic actuator: a direct adaptive non-linear control framework for a non-linear electromagnetic actuator is presented; the control strategy is an adaptive one in which the main parameter depends on the variable inductance of the actuator itself. Hoffmann and Stefanopoulou present in [29] the valve position tracking in electromechanical camless valvetrains (EMCV). One of the main problems in the EMCV actuator is the noise and wear associated with high contact velocities during the closing and opening of the valve. The contact velocity of the actuator and the valve can be reduced, and thus, noise and wear, by designing a tracking controller that consists of a linear feedback and an iterative learning controller. Peterson et al. describe [30] a nonlinear self-tuning control for soft landing of an electromechanical solenoid valve actuator (reluctance force actuator), which is a kind passive actuator with springs on the moving part. The authors studied low contact velocities or “soft landing” of the actuator on the solenoid faces and between the actuator and the valve is also necessary in order to maintain similar noise and wear levels with conventional camshaft-driven engines. Jang Liu et al present in [27] an electromechanical valve actuator (EMVA) using solenoid to actuate valve movement independently for the application of internal combustion engine. They proposed an EMVA structure by incorporating the hybrid magneto-motive force (MMF) implementation in which the magnetic flux is combined by the coil excitation and permanent magnets. This type is also a passive type of actuator. Making use of the dedicated flux arrangement, the proposed device can be used to fulfill the VVT features with reduced power source requirement and less electric device components. A dual flux channels EMVA is detailed and the design procedures are presented.

**The literature review illustrates** the technical problems related to the design and to the control that electromagnetic actuators for engine valve trains have. For this reason it is needed an innovative design and control of the actuators to solve all these technology problems stated in the prior art.

### **Optimal designs of electric vehicles for a long-range mobility**

Around 2030 electric vehicles are predicted to increase their market penetration and to bring evolution concerning the main technologies for energy storage and conversion, the powertrain components and the energy management [1]. The industrialization of those components on high scale and volume reduces the cost of the electrification and to its democratization on all vehicles segments. According to the ERTRAC Report [1] it is possible to distinguish two types of electric vehicles: user friendly affordable vehicles and high performance electric vehicles. The first category will develop in small and middle segments (A/B/C) and they represent a more optimized range/cost solution enabling a very big market penetration and then a considerable impact on greenhouse emissions reduction. The ranges of these vehicles are adapted to 200 km of drive and suit for urban and sub-urban use. The major challenge is to achieve significant cost reduction of the battery and the components of the propulsion system. The introduction of these vehicles is related to the support of the governmental policies (transportation energy taxes, city center driving), the infrastructure deployment and the cost of the electricity. The electric vehicles with high performances are deployed in the C/D/E segments. They will maximize the range in the performances offering at least 600 km of autonomy for a single charge of the battery. The cost of these vehicles is high because of the high battery capacity on board. The cell energy density needs to be improved to allow the deployment of these vehicles. The significant battery capacity can be rapidly recharged with high power chargers. These cars are designed for long distances use, on the highways and their deployment is related to the deployment of the infrastructure of high-speed chargers all along the highways.

The customers’ expectations and considerations for electrified vehicles are acceptable prices, range, reliability, durability and re-sale value similar to conventional vehicles. Some advantages may also be achievable through synergies of the electrification with the connectivity and the automation of the vehicles. This will provide benefits of the users by easy access to the charging infrastructure, optimization of the traffic and minimization of the energy consumption. Charging is a crucial topic for

the success of the electrification. Purely electric vehicles are pushed to compete with internal combustion engine vehicles one-on-one, where refilling takes place around once every week. With the right mix of infrastructure, electric vehicles could compete with vehicles powered by internal combustion engines, but with the added dimension of the refilling comfort. Daily e-charging would mean that drivers never have to stop at filling stations, except the rapid charging stations for the long way drives. Information and connectivity solutions that inform in real time the drivers for the availability and the distribution of the charging infrastructure, including the possibility to book and pay for charge points in different places is an important part of the solution. Combined with fast, i.e. high power charging capacities, pure electric vehicles would be able to serve long range needs.

Zengin and al. propose in [31] the waiting time in the queue of the customers for recharging their batteries. The model considers the stochastic recharging of the batteries capacities and the class of the vehicles. Furthermore, a charging strategy is proposed according to which the drivers are motivated to limit their energy demands. Karakitsios and al. introduce in [32] a methodology to analyze the impact of the fast inductive charging technologies to the grid. Levinson and al. explore the potential of public charging infrastructure to spur US battery electric vehicle [33]. They used market analysis and simulations. Zhang and al. develop in [34] a multi-period flow refueling location problem for electric vehicles (EVs) and charging infrastructure. The optimization model determines the optimal location of chargers for every station. Sun and al. explore in [35] the choice of the users to fast charging of the battery electric vehicles as a function of the available charging stations and the distance between them, in Japan. Wu and Sioshansi develop in [36] a model to optimize the location of public fast charging stations for electric vehicles (EVs). They use a stochastic flow-capturing location model to solve the uncertainty in where EV charging demands appear. Schroeder and Traber provide in [37] the business case of fast charging technology in a case study for Germany. They estimated that the Return on Investment (ROI) of a public fast charging station constitutes the main contribution. The general EV adoption rate is estimated to be the main risk factor for investment in public charging infrastructure.

**The literature review shows** that the success of the deployment of the electric vehicles is related to their access the recharging infrastructure. A global approach considering the vehicle as energy system related to the energy grid lacks.

### **An energy balance evaluation in LI-ION battery packs under high temperature operation**

Several researches have been done in the field of energy management in batteries. Energy and exergy analyses are conducted in [38] to investigate a new cooling system of hybrid electric vehicles (HEVs). A thermal energy storage system is integrated with a refrigeration cycle where octadecane is selected as the phase change material (PCM). The exergy destruction rate and the exergy of each component in a hybrid thermal management system are calculated. The findings of the exergy analysis reveal that the overall exergy of the system with PCM presence is 31%, having the largest rate of exergy destruction of 0.4 kW. In addition, the results of the parametric study show that an increase in PCM mass fraction results in an increase in exergy of the system.

A lithium-ion battery thermal management (BTM) system using the electric vehicle (EV) air conditioning refrigerant to cool the battery pack directly is investigated in [39]. In the system, basic finned-tube heat exchanger structure and a special aluminum frame are adopted to design the battery pack thermal management module with lithium-ion batteries of cylindrical shape. Experimental results show that the BTM system can control the battery pack's temperature in an appropriate preset value easily under extreme ambient temperature, as high as 40 °C. The temperature difference within the pack is less than 4 °C in the constant discharge rate of 0.5 C, 1 C, 1.5 C laboratory tests, and 1.5 °C in road drive tests.

Lithium-ion batteries are widely used in electric and hybrid electric vehicles due to their wide nominal range and high power densities. However, operating temperature, which has a pronounced effect on battery thermal and electrical performance, needs to be maintained within a specified range. In [41], a Li-ion battery pack has been tested under constant current discharge rates (e.g. 1C, 2C, 3C, 4C) and for a real drive cycle with liquid cooling. The experiments are performed using cold plates at 10°C, 20°C, 30°C, and 40°C coolant temperatures to obtain thermal and electrical parameters. For this, three 20Ah LiFePO<sub>4</sub> prismatic cells are connected in series and a battery thermal management system is designed

and developed for liquid cooling. To measure the temperature variation, 18 thermocouples are installed on the principal surface of all three cells. The results show that the battery pack temperature can be maintained within the required range at all four selected discharge rates with the coolant at 30°C. The discharge capacity of the battery pack increases with increasing coolant temperature and is found to achieve a maximum of 19.11 Ah at a 1C discharge rate with the coolant at 40°C.

Energy and exergy analysis are as well performed for PEM fuel cell [40]. This study presents the performance of a proton- exchange membrane (PEM) fuel cell in terms of its pressure and voltage parameters. The aim of this study is to improve the performance, efficiency and development of modeling and simulations of PEM fuel cells by experimental optimization. The energy and exergy efficiencies of the PEM fuel cell were found to be 47.6% and 50.4%, herein. Energy and exergy analysis can be performed for (PEM) fuel cell [41] or for the propulsion system for hybrid electric vehicles [7]. The literature review [42], [43], [44], [45], [46], [47], [48], [49], [50], [51], [52] and [53] show that the energy management of the batteries is the target of experimental and simulation works. Energy and exergy analysis are useful to evaluate the performances of the energy management systems for energy storage systems (batteries) or convertors (fuel cells) or complete propulsion system of vehicles. The energy and exergy balances are an excellent way to detect the energy waste in energy integrated systems.

**The literature review describes** the passive and active ways of cooling and the methods of design from the experiments to the design of the solution. Energy and exergy analysis are useful to evaluate the performances of the battery packs and need to be investigated.

## **2.2 Extension of the vehicle energy systems: the vehicles as grid related systems to the energy grids for optimal energy services for mobility**

### **Design of electric vehicles grid related energy systems for optimal mobility service**

The challenge is to integrate massively the electric vehicles in the energy grids. Several scenarios are researched through simulation and optimization to build viable energy planning for that. The authors present in [54] an optimization model for the planning of the infrastructure of chargers for electric vehicles. The model minimizes the overall (installation, maintenance, operation) placement costs of charging stations. The study illustrates results for the optimal charging stations placement layout and overall costs placement for different driving ranges and the required quality of service level by including a power system reliability check. The results are useful for the charging infrastructure investors and electric power system operators. The authors made in [55] the analysis of economic implications of innovative business models in networked environments for electro-mobility. Mainly the high investment cost for the EV and for the infrastructure are difficult points in the economic model. The research question that is investigated in [56] is where to install the charging stations to facilitate the long-distance travels and to meet the urban (local) demands considering both the existing stations and the installations are to be realized by legal regulations. The study in [57] introduces a multistage chance-constrained stochastic model for strategic planning of battery electric vehicle (BEV) inter-city fast charging infrastructure. A mixed integer programming model is developed to determine where and when charging stations are opened, and how many chargers are required for each station to meet the growing BEV inter-city demand. The optimization problem is solved by genetic algorithm. This study showed that investment in inter-city charging infrastructure is vital to alleviate the range anxiety. Other conclusion is that planning decisions depend on many factors, such as the design level of service and the vehicle range. The work in [58] established a mathematical model to optimize the layout of charging infrastructure based on the real-world driving data of 196 battery electric vehicles. The work has studied the connection of the number increase of charging points and retention rate. When the number of charging points increased from 60 to 220, the retention rate was 97% for slow charging and 95% for fast charging.

The authors developed a stochastic model in [59] that includes driving and charging behavior of BEV owners in Japan. The model is based on Monte Carlo methods and was implemented in MATLAB. They conducted simulations with this model to find out whether the existing infrastructure is adequate for the charging of a large number of BEVs.

**The literature review shows** that different simulation and optimization methods are used to optimize the energy planning and the resources and EV charging infrastructure distribution. The infrastructure for recharging of electric vehicles is characterized with high investment cost and high impacts on the electric grid. For this reason, an optimal techno-economic optimization for the planning of usage of the energy systems is needed.

### **Coordination interest for the optimization of electric vehicles long distance trips**

The authors in [60] offer a model that guarantees the confidentiality of users' data, in particular their vehicle condition and destination. It is based on reservations, transmitted by mobile networks, which allow charging stations to estimate their waiting times and vehicles to choose stations based on these data. The authors in [61] offer a solution that only requires local communications, including a cooperative exchange between vehicles to determine who should stop at the next charging station. They are based in particular on the work of [62], which shows that the optimal solution to this relaxed problem is achieved when the occupancy rate is constant, this means when the vehicles are equally distributed at the different charging points. The authors of [63], on the other hand, use game theory tools to allow users to optimize their travel costs and recharging stations to maximize their earnings, assuming that hourly prices are freely set: this results in a non-collaborative game. Overloading of the electricity grid is also considered. A cooperative approach to game theory is developed in [64], which makes it possible to gain in convergence speed and robustness. However, these papers only compare the performance of their solutions with theoretical solutions. This approach does not allow the evaluation of the remaining potential gain.

**We propose** a method to find an optimal recharging solution based on a differential evolution algorithm, as well as a communication schema, easy to deploy, that would permit to coordinate vehicles and reduce waiting time at charging stations, during long distance trips. The novelty of this research is the introduction of a communication system between the vehicles and the infrastructure to coordinate and to optimize the charging planning of the electric vehicles.

### **Slow charging: Robotized charging of high voltage batteries for electric and hybrid electric vehicles**

Battery electric vehicles (BEV) suffer from several disadvantages: the charging time of the battery, which is still much longer than refueling a liquid fuel tank and the lower autonomy, which creates range anxiety for the user. Accordingly, recent European market forecasts predict two possible scenarios: A sharp rise of EV sales that reach 60% of the market in 2030 due to a major technological breakthrough for EVs or a smoother increase in EV sales reaching 20% [64]. To support this mobility transformation and meet the growing stock of [1], the installation of associated equipment such as charging infrastructure for electric vehicles is necessary. In priorities, a deployment of charging stations to cover territories and thus compensate the lower autonomy of BEV [65] and a diversification of the technologies of charge. Today, the only technology available for EV users is the conductive charging by plug: domestic devices allow users to charge on the grid at home [66] and fast DC charging are available in most of the classical gas stations [67]. However, stakeholders are more and more interesting in wireless charging system (without plugs and cables) because it offers reliable, convenient and safe charging (No electric shock) for EV drivers [68]. The Wireless Electric Vehicles Charger (WEVC) is thus promising for EV charging and an alternative to the classic plug-in charger technology. The static WEVCS technology is used to charge the high voltage battery of a stationary EV. Generally, the transmitter pad is fixed on the ground of a parking place and the pick-up coil (induction plate) is on the underneath of the car [69] (Figure 2-1). Therefore, the power transfer has to be operational and efficient for a distance between 100 to 250 mm accordingly to the variety of ride height of passenger cars available on the market [70]. WEVC begins to enter the market of "charging technology for EV": Many actors (Companies or Research Groups) are developing stationary WEVCs for passenger cars. According to the literature, the current power range of existing prototypes is between 1 to 20 kW,

accepting an air gap of 100-300 mm with an efficiency between 71% and 93 % [69]. Furthermore, several charging pads just start to be sales, the performance of two technologies on sale are details in Table 2-1.

Table 2-1: Properties of stationary WEVCS on the market.

Corporation / R&D Institute	Vehicle type	Maturity	Cost (kUSD )	Air Gap distance (mm)	Operating Frequency (kHz)	Power Range (kW)	Efficiency (%)
Plugless Power (Evatran Group) [71], [72], [73]	Passenger car (Tesla Model S, BMW i3)	On sale	6-13	100	20	3.3 - 7.2 (240 V / 50 A)	84-90
WiTricity Corporation [74]	Passenger car / SUVs	On sale	N/A	100 - 250	85	3.6 - 11	90-93

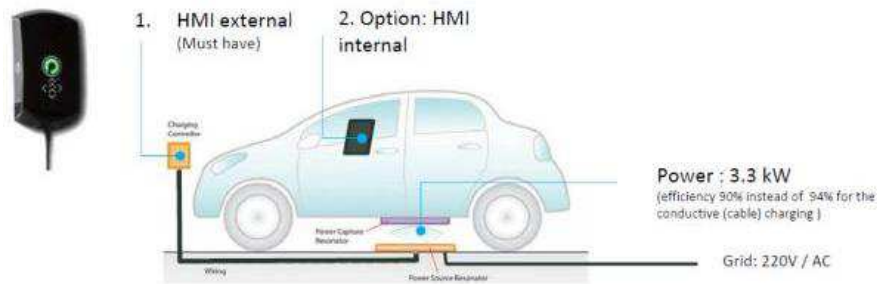


Figure 2-1: Static Wireless Electric Vehicles Charging System.

However, WEVCS suffer from electromagnetic emissions, the lack of equipment on current EV enabling the wireless power transfer, and the lower energy efficiency compare to the plug-in technology [69]. Indeed, this technology shows the limits: the efficiency of power transfer decreases drastically while the air gap or the misalignment between the two coils increase, due to leakage inductance [70]. Therefore, high power transfer is needed to charge an EV that implies great energy losses and important harmful electromagnetic emissions or at least incompatibility with implant medical devices [69]. The system requires a perfect alignment between the two coils in order to maximize the power transfer and avoid leakage fluxes [70]. Thus, this type of system is very restrictive for the driver: the average driver must do 3 to 4 maneuvers [74] to park correctly and even though the alignment is not always optimal. In existing applications, a display with an oversized primary plate helps the driver to position himself correctly [69] [75] [76] but that entails a higher cost.

**Thus, this research proposes** to redesign completely the classic WEVC system in order to solve this problem by robotic charging system [77]. A mobile robot equipped with the transmitter part of the WEVC will position itself with accuracy under the receiver coil to maximize the power transfer and to reduce the leakage of electromagnetic emissions. The mobile robot must respect several positioning specifications (an accuracy of  $\pm 2$  cm) while requiring inexpensive equipment and resilient algorithms.

**Integration of the environomic energy services for mobility and household using electric vehicle with a range extender of solid oxide fuel cell**

Vehicle-to-grid scenrios have been proposed in [78]. Prototypes installations prouved that the technological means to deliver many of the vehicle-to-grid services are available. Charging electric vehicles can, however, be added to planned demand side management schemes without the need for additional capital investment. Balancing power plants operated with gas serve as stabilizers of the grid in the case of high renewable and variable electricity penetration in power systems. The smart-grid including electric vehicles is playing a stabilization role for the grid [79]. The results show that even a small share of the fleet of electric vehicles providing load balancing to the grid could lead to important reductions in gas use and energy excess. The integration of renewable energy in the electricity sector

and as well the adoption of electric vehicles in the transportation sector have the potential to significantly reduce greenhouse gas emissions with Vehicle-to-Grid technology. The study [80] aims to evaluate the greenhouse gas emission reduction in case of intermittency coming from the introduction of wind power through. The researchers propose in [81] an optimal vehicle to grid planning and scheduling. According to [82], the strategy to reduce CO<sub>2</sub> emissions in the transportation sector is its renewable based electrification. However, the technical option vehicle-to-grid (V2G) requires the vehicle users to temporarily abstain from the usage of their batteries for V2G. 'Range anxiety' and the 'minimum range' are important for the acceptance of the users to participate in V2G.

**The literature review** illustrates separated optimizations of the vehicles use. The electric vehicles are considered as stabilizers for the fluctuations of the electric grid, generated by the electricity production by the intermittent energy sources (wind and solar energy).

## 2.3 Fuel cell electric vehicles, energy vectors for hydrogen and their ecosystem

### Hydrogen from ethanol steam reforming, catalysts selection

Catalytic ethanol steam reforming (ESR) is conducted at middle temperature or high-temperature ranges. The challenge is to develop catalyst working in the range of 723- 873 K. Few reports describe catalysts showing high activity, and durability at low temperatures, below 573 K.

Ethylene methane (or CH<sub>x</sub> species), and CO are regarded as coke precursors. Suppressing ethylene formation and methane formation and promoting water gas shift reaction (CO removal) helps to suppress coke deposition.

Four strategies for the suppression of coke deposition are reported in the literature [83].

- Use of basic support or promotor: Ethylene is usually formed by ethanol dehydration over an acidic site. Use of basic support results in decrease acidity and ethylene selectivity and so coke is suppressed.
- Use of redox active support or promotor. Redox active metal oxides such as CeO<sub>2</sub> with high oxygen mobility and oxygen storage capacity can contribute directly to oxidation of coke and/or adsorbed coke.
- Precise control of particle size and oxidation state of active metal. Highly dispersed small metal particles are suitable for the active site with coke resistance, because coke deposition mainly occurs over terrace site with high coordination number and the fraction of metal atom at terrace site decreased with decreasing metal particle size.
- Addition of second metal. Addition of Au, Cu or Co to Ni- based catalyst positively affects its stability and coke suppression, where Fe promotes steam gasification of deposited coke or adsorbed CH<sub>x</sub> species.

### Ni- based catalysts [84]

Various preparation methods, Ni precursors and supports have been actively investigated to obtain Ni catalysts with highly dispersed small Ni particles because the Ni- particle size is an important factor for controlling activity, selectivity and carbon deposition. For Ni catalyst, various supports have been investigated: Al<sub>2</sub>O<sub>3</sub>, M- Al<sub>2</sub>O<sub>3</sub>, Sn – La<sub>2</sub>O<sub>3</sub>, CeO<sub>2</sub> and etc.

As active metals, bi-metallic or tri-metallic catalysts such as Ni- Cu, Ni- Sn, Ni- Pt, Ni- R, Ni- Rh, Ni- Au and Ni- Cu- Fe have been used at 573- 973 K with 1.5- 9.0 of S/C ratio (steam/ carbon molar ratio).

Among Ni- based catalysts, Al<sub>2</sub>O<sub>3</sub> support has been applied widely to ESR because of its high surface area and stability. Al<sub>2</sub>O<sub>3</sub> support has an active site and promotes formation of ethylene, a coke precursor of coke deposition. Modification of Al<sub>2</sub>O<sub>3</sub> support by basic oxides (La<sub>2</sub>O<sub>3</sub> and ZrO<sub>2</sub>) neutralizes the acidic sites effectively and suppresses coke formation, although addition of excess amount of modifier decreases its specific surface area and activity.

Using  $\text{CeO}_2$  – based support for Ni- catalyst is reportedly one means of improving ESR. The reason is that it can prevent coke deposition by virtue of its oxygen storage capacity (OSC) and oxygen mobility at its surface. It is reported that addition of Au to Ni/  $\text{CeO}_2$  suppressed coke deposition, although is caused a slight decrease in OSC ability and ESR activity. Doping basic MgO or CaO or  $\text{CeO}_2$  is reported effective for carbon deposition suppression. Doping Zr, La, or Sm to  $\text{CeO}_2$  improved OSC ability and thereby increase activity and durability. Pizzolitto et al. described that 8wt%Ni5wt%La- $\text{CeO}_2$  shows ethanol conversion (> 90%) and hydrogen purity (>70%) even after 60h of reaction at 823 K. Reportedly, La- containing and Ni- containing perovskite oxide catalysts showed high activity and stability for ESR. In general, partial substitution of A and/or B site cations in  $\text{ABO}_3$  structure can control the redox properties of perovskite oxide. Partially substituted La- Ni- based perovskite oxides can produce highly dispersed metallic Ni sites and can prevent sintering of the metal active site. Therefore, the ESR can proceed with less coke formation.

### Hydrogen ecosystem and hydrogen economy

The automotive industry is challenged by very strict emissions regulation. The  $\text{CO}_2$  emissions levels tend to be drastically reduced to 50 g/ $\text{CO}_2$  km in 2030. The electrification of the vehicles is currently in progress in Europe, driven by the European  $\text{CO}_2$  emissions regulation and hydrogen is seen in the energy outlooks to be used as well for vehicular propulsion, and enabler to reach the  $\text{CO}_2$  emissions targets. The current  $\text{CO}_2$  emissions regulation considers the emissions from tank-to-wheel perspective and thus the electric and the fuel cell vehicles are accounted as zero emissions vehicles. The tank-to-wheel perspective means that only the emissions coming during the usage of the vehicles are considered. The emissions related to the production of the different fuels is not accounted. Introducing electricity and hydrogen as energy vectors for mobility depends on the global efficiency of the conversion chain, of the total energy resources to be used and the total  $\text{CO}_2$  emissions from well-to-wheels perspective.

Renewable energies increase their part in the energy mixes due to the energy transition needs. The sustainable energy system should become clean but as well reliable and affordable. The renewable energy production and energy demand are intermittent thus an integrated system approach is required considering energy conversion and storage. The authors propose in [85] a concept for a neighborhood where locally produced renewable energy is converted and stored in the form of heat and hydrogen, accompanied by rainwater collection, storage, purification and use. Hydrogen can be obtained from different sources of raw materials including water. Among many hydrogen production methods, high purity of hydrogen can be obtained by water electrolysis. In terms of sustainability and environmental impact, water electrolysis was considered as most promising techniques for high pure efficient hydrogen production from renewable energy sources. It emits only oxygen as byproduct without any carbon emissions [86]. Figure 2-2 shows the hydrogen production methods.

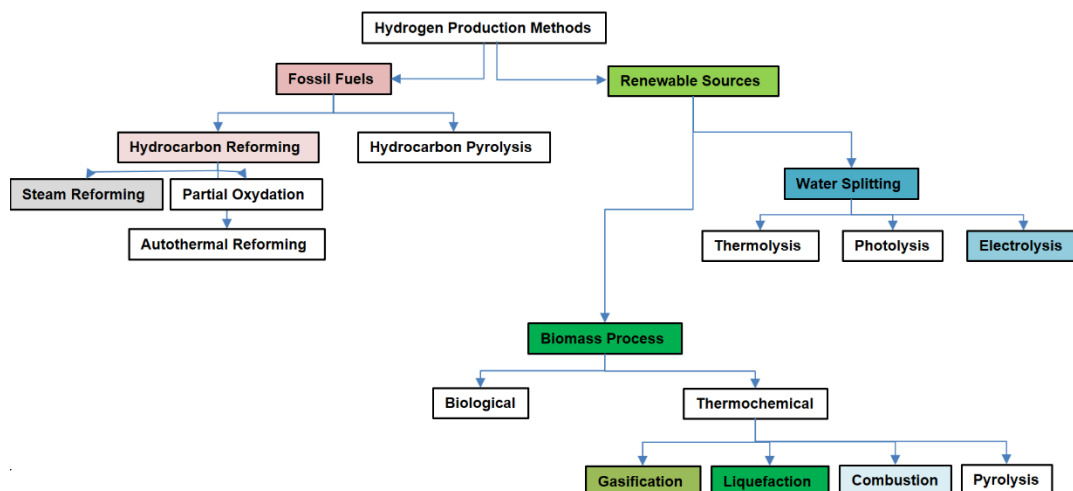


Figure 2-2: Hydrogen production methods

Biomass energy contributes a major portion in global renewable energy. Its share ever-grows in electricity production worldwide.  $H_2$  is considered as a clean energy fuel having with high energy density (122 kJ/g). This is three times higher than hydrocarbon fuels. Combustion of  $H_2$  fuels produces water and it does not contribute to greenhouse emissions. The authors present in [87] promising approaches applied to achieve biomass based hydrogen production by using microbes. This method is called bio-hydrogen fermentation using crops straws, agri-waste; industrial waste or naturally occurring organic rich biomasses (like molasses). The hydrogen is considered as carbon free fuel. Supply of low-carbon energy for heat, balancing of electricity at national grid and application in transportation sector preferred hydrogen over other carbon based gaseous biofuels. The fertilizers and the petroleum companies are considered to be at the largest users of  $H_2$  with respectively 50% and 37%. With the demand of the fuel cells the demand of hydrogen is increasing with 6 % the last five years.

There are some applications of  $H_2$ :

- $H_2$  is utilized for hydration of substantial oils for fuel production, foods hydration, and alkali hydration for fertilizers production.
- As  $H_2$  is the perfect electron donor, it is uses for diminishing nitrate, perchlorate, selenite, and a suite of other oxidized water contaminations.

Currently, the industrial application of hydrogen is equivalent to only 3% of the total energy consumption, and it is expected to grow significantly in the years to come [87].

The current hydrogen market is characterized with low demand. In this case, small-scale water electrolysis based hydrogen production is more cost-efficient than large-scale production. This is due to the potential to reach a high number of operating hours at rated capacity and high overall system utilization rate. The study in [88] shows that there is a relatively good business case for local water electrolysis and supply of hydrogen to captive fleets of trucks in Norway. The model is efficient if the size of the fleet is sufficiently large to justify the installation of a relatively large water electrolyze system.

Through the case study done for Spain, the authors prospectively assesses in [89] the techno-economic and environmental performance of a national hydrogen production mix by following a methodological framework based on energy systems modelling enriched with endogenous carbon footprint indicators [89]. The steam reforming of natural gas still arises as the key hydrogen production technology in the short term. The water electrolysis is the main technology in the medium and long term. In scenarios with very restrictive carbon footprint limits, the biomass gasification also appears as a key hydrogen production technology in the long term.

Metal hydrides are known as a potential efficient, low-risk option for high-density hydrogen storage [90]. In addition, based on the thermodynamic properties of metal hydrides, they give the opportunity to develop a new hydrogen compression technology. They allow the direct conversion from thermal energy into the compression of hydrogen gas without the need of any moving parts.

The amount of hydrogen released after high-pressure hydrogen loading in carbonate was evaluated in [91]. Calcium carbonate ( $CaCO_3$ ) and Mg-substituted  $CaCO_3$  were selected as adsorbents. Their crystal structures, specific surface areas (SBET), hydrogen content at high pressure, and the amount of hydrogen released in water were investigated.

Imbalance costs caused by forecasting errors are considerable for wind farms connected to the electricity grid. In order to reduce such costs, two onsite storage technologies, hydrogen production and lithium batteries are considered. Probability density distributions of wind forecasting errors and power level are first considered to quantify the imbalance and excess wind power. Then, robust optimal sizing of the onsite storage is performed under uncertainty to maximize wind-farm profit [92].

Among several candidates of hydrogen storage, liquid hydrogen, methylcyclohexane (MCH), and ammonia are considered as potential energy vectors with high hydrogen content, in terms of their characteristics, application feasibility, and economic performance [93]. In addition, as a main motor in the hydrogen introduction, Japan has focused and summarized the storage methods for hydrogen into these three methods. Liquid hydrogen needs a huge energy consumption during liquefaction and faces the boil-off phenomenon during storage. MCH has main obstacles in largely required energy in

dehydrogenation. Lastly, ammonia encounters high energy demand in both synthesis and decomposition (if required). In addition, from cost calculation, ammonia with direct utilization (without decomposition) is considered to have the highest feasibility for being massively adopted, as it shows the lowest cost (20–22 JPY/Nm<sup>3</sup>-H<sub>2</sub> in 2050).

The hydrogen industry currently faces the dilemma that they must meet certain measurement requirements (set by European legislation) but cannot do so due to a lack of available methods and standards. The authors outline in [94] the four biggest measurement challenges that are faced by the hydrogen industry including flow metering, quality assurance, quality control and sampling.

A detailed breakdown of the energy conversion chains from intermittent electricity to a vehicle, considering battery electric vehicles (BEVs) and fuel cell electric vehicles (FCEVs) is presented in [95]. The traditional well-to-wheel analysis is adapted to a grid to mobility approach.

**The recent literature review gives an overview** of the technologies for the hydrogen production, hydrogen storage, hydrogen transport and distribution and hydrogen conversion on vehicles or energy grid conversion. The main idea is to cover the whole “life cycle” of the hydrogen as energy vector.

From the literature review it comes out that, the hydrogen is seen as the energy carrier and the connector for different energy grids: electricity, natural gas and as a storage medium for renewable energies. The leading spots in term of hydrogen research are in North of Europe and in Japan. Recent studies from Nederland and Norway consider the hydrogen with production from renewable energy and highlight the economic benefit of stand-alone installations with small production capacity. The literature review summarizes the ways of hydrogen production and classifies them. The main need is to produce clean hydrogen. The current production of hydrogen is coming from the natural gas steam reforming. The water electrolysis and the biomass are seen as future ways (technologies) for the production of clean hydrogen. Other question concerning the hydrogen production is the sizing of the capacity of the installations. This question is directly related to the storage of the hydrogen. The hydrogen is very reactive molecule and its storage is a complex process. The literature review describes the compressions levels for the compressed gas hydrogen. The compression process presents important operating costs. The classification of the hydrogen storage ways is proposed. According to the classification, hydrogen can be stored in physical, adsorption or chemical forms. The physical forms of storage are the compressed gas and the liquefied hydrogen. They deliver pure hydrogen but present high operating costs related to the high-energy consumption to maintain them in their respective physical state. The chemical storage concerns the metal hydrides and the chemical hydrides. Metal hydrides present different opportunities for storage of hydrogen in a solid state. They need to be investigated to improve efficiency, storage capacity, to reduce cost and energy demand. The adsorption of hydrogen is done in porous materials: MOFs or carbon based materials (calcite). This way of storage is as well under scientific investigation. Japan has the leading position with the hydrogen storage in calcite. The chemical hydrides (for example ammonia) are the most promising way of hydrogen storage and transportation in liquid form, in the future. Ammonia is the best chemical hydride candidate, presenting the highest hydrogen content. A research direction related to the ammonia is how to convert it directly in adapted converters (fuel cells) without dehydrogenation process, which is costly, and need purification. Japan is as well leading in the ammonia research area. The literature review gives as well summary of the thermodynamic properties for all categories of hydrogen storage.

The research points out lack of regulation and difficulties by the distribution of the hydrogen at the tank stations to the customers. Main challenges are the measures of the quantities, the control of the quality and the sampling of the hydrogen for purity control. These difficulties are related to the lack of measure instruments for large utilization, calibrated to work at 700-900 bar pressure and the purity control capacity available locally.

Hydrogen is clearly seen as an energy carrier for extended energy grids, as stocker for renewable electricity and depending of the installation size can be competitive to Li-Ion stationary battery used for local storage in the electricity grid. Hydrogen production from renewables and Li-Ion stationary batteries demonstrate benefit to balance the global electricity grid and to reduce losses related to intermittence of the renewables.

**Energy planning for sustainable mobility for 2030: Energy storage and conversion technology options for the automotive sector**

Electric vehicles will not totally replace the conventional vehicles using internal combustion engines. The service of mobility will be adapted and different. The deployment of electric vehicles depends as well of the support of the governments to the customers' investments and the investment of the recharging infrastructure. The following literature review explains these points.

The authors analyze in [96] the factors supporting the transition to new forms of mobility, namely Electric Vehicles (EV). They analyzed EV, by dividing them into individual Battery Electric Vehicles (BEV), which are 100% electric, and Plug-in Hybrid Electric Vehicles (PHEV). Main conclusion is that policies should be tailored to each individual technology. Charging stations are drivers of electric mobility. As highlighted in [97], driven by the booming of electric vehicle (EV) market, the cost of lithium ion battery observes a remarkable decline. This fact could significantly improve the capability of EVs in coordinating with the power generation from distributed renewable energy. The smart charging is a cost-efficient electric vehicle – renewables energy coordination strategy. Vehicles to grid (V2G) could be more economically attractive in the long run due to its capacity to fully realize the potential of on-board EV batteries. Governments have implemented monetary and non-monetary policies to accelerate electric vehicle market diffusion [98]. The energy prices and financial incentives to influence EV adoption act positively. The authors identified in [99], 7 key elements which are significant risks in the supply for the electric vehicle industry: battery grade natural graphite, lithium and cobalt for electric vehicle batteries, and the rare earth elements dysprosium, terbium, praseodymium and neodymium for electric vehicle motors. The transition to electric mobility is accelerating, and, thus it is important to be able to anticipate and adapt future development of the electric vehicle-charging infrastructure [100]. Overall, the planning of electric vehicle charging infrastructure will support a successful transition to electric mobility. Electric vehicles can play a major role in the transition towards low-carbon energy systems [101]. Different energy scenarios are simulated with the help of planning software assuming a progressive increase in renewable energy sources capacity and electric vehicles penetration. Results show that, for the case study done for Germany, the additional electricity required leads to a reduction in CO<sub>2</sub> emissions only if renewable capacity for electricity production increases significantly. The Italian energy system benefits from the electrification of the transport even at low renewable capacity for electricity production. With assuming a complete electrification of private transportation where electric vehicles charging strategy is regulated to enhance renewable integration, CO<sub>2</sub> emissions can be reduced by 22% and 39% for Italy and Germany respectively.

**The literature review resumes** the main points of the development of the electrified vehicles PHEV, BEV or Fuel Cells vehicles. The problem is complex, with a high investment of time, financial and human resources. In this context, it is needed to plan the different stages and to give a clear strategic vision.

# Chapter 3 Energy efficiency, storage and conversion on vehicles board

This research domain contains three main parts: energy efficiency, energy conversion and energy storage on the board of the vehicles.

## 3.1 Energy efficiency

In the research and in the industry the main points for fuel (energy) consumption improvement are concentrated on the:

- Design parameters:
  - Improvement of the peak efficiency of the powertrain components (downsizing)
  - Improvement of the part-load efficiency of powertrain components
  - Possibility of energy recuperation (thermal, kinetic, pneumatic)
  - Optimization of the structure and the parameters of the propulsion system for the same vehicle
- Energy management parameters:
  - Energy efficient and control strategies offered from chosen propulsion system

In this chapter are considered different technologies for energy recovery (kinetic and thermal) and their combination in different powertrain architectures. The organic Rankine cycle is evaluated as waste heat recovery technology. The electrification of the ICE based powertrains brings different hybrid electric architectures, classified functionally according to their degree of hybridization and the size of the high voltage battery. The HEVs recover the kinetic energy during braking but are powered by ICE, which present still thermal losses. The research questions to investigate in this chapter are the efficiency improvement by the combination of two type energy recovery systems (HEV and ORC).

The optimal design of the hybrid electric vehicles for the kinetic energy recovery and the choice of the optimal size of the high voltage battery for HEV are as well investigated according to techno- economic and environmental criteria. This is a published article and is presented in Appendix A.

### 3.1.1 Performance and economic analysis of an organic Rankine Cycle for hybrid electric vehicles

Internal combustion engines have a main limitation on efficiency due mainly to the heat losses. Processing an energy integration, it has been shown than an Organic Rankine Cycle (ORC) can improve the overall powertrain efficiency by recovering the heat into electricity. In parallel, hybrid electric vehicles attractiveness increases as it enables important energy saving. The contribution of this research is to design highly efficient vehicles, using both Organic Rankine Cycle and hybrid electric technologies. An adapted methodology based on energy integration techniques is required to choose the best points for the integrated system design. This study applies a methodology on hybrid electric vehicles, so as to define the powertrain configuration of the vehicle that is energy integrated.

The energy recovery potential of a single stage Organic Rankine Cycle for a thermal engine in combination with a mild hybrid electric powertrain is studied. The assessment is done for different drive cycles. A study of economic feasibility and fuel consumption improvement is also done, in order to characterize the integrated energy system.

### 3.1.1.1 Waste heat recovery and hybrid electric vehicles

The target of this research is to illustrate the results from the multi-constrain optimization, which take into consideration performance and economic constrains, in order to achieve an efficient design of an ORC loop for recovery of the waste heat on a hybrid electric vehicle. The presented design is adapted and evaluated to operate on hybrid electric vehicles architecture. Once we perform the optimization, we should study if there is one design solution which is better than the other, or if there exists different solution which could correspond to different users' profiles. Finally, for the best design we should perform both a study on driving cycles, and an economic study, to determine if the Organic Rankine Cycle benefit is important enough to be implemented on those existing vehicles.

The contribution of this research is to apply energy integration methodology on mild hybrid electric vehicles for optimal powertrain design of hybrid electric vehicles. The research studies the impact of an energy recovery technology, such as the ORC on the mobility performances of HEV energy system. After integration of the energy services, a sensitivity analysis on the fuel benefits is done for different real drives representative driving cycles. The results are obtained by simulation, using vehicles models containing experimental engines and vehicles data. The ORC performances are obtained by simulation.

The energy integration and the multi-objective optimization methodology are presented in Appendix A. The models of the vehicle and the ORC are presented in Appendix B.

#### 3.1.1.1.1 Focus on the operating points

According to [7], [8], the best ORC we can implement on a car should use two streams from the vehicle for the evaporator: the water cooling system, and the exhaust gases. Moreover, the cycle has a much better efficiency if it reaches a superheating temperature.

Usually, hybridization methods are efficient at low power of the engine. These zones allow to use an additional electric motor or to recover energy from braking. However, the ORC is more efficient at full load operations, when the total quantity of heat to be recovered is higher. It seems interesting to add such a system to a hybrid vehicle, as the two ranges are different: an electric device work mainly during urban cycles, whereas an ORC works on national roads or highway. We want to emphasize this complementariness, we try to optimize the cycle for high-loaded operating points.

#### 3.1.1.1.2 Multi objective optimization settings

We want to perform an economic, environmental and technical performance optimization. To do that, we should decide what indicator to use.

- Economic: the ORC investment cost is considered as an indicator, defined by equation (A-11).
- Performance: The net output power, used as an objective for performance. The net power is the difference of the turbine power and the pump power for a given operating time in equation (3-1):

$$P_{\text{net}} = P_{\text{turbine}} - P_{\text{pump}}, \text{ kW} \quad (3-1)$$

The exergetic efficiency is verified for every solution.

We need to choose the variable of the ORC design. The system has two degrees of freedom. We choose to define two temperatures to launch the energy integration model:

- The evaporation temperature of the fluid. The interval of variation is defined between 330 °K and 360 °K in order to obtain correct exergetic efficiency.
- A difference of temperature,  $\Delta T_{min}$  [5], between the exhaust gas temperature and the superheat temperature of the cycle. The interval of variation is defined between 100 °K and 400 °K. This range is for second order for the results.

We use a simulation of a population with 200 individuals with a maximum number of evaluation of 10. The computing time is enough, and we get enough design to have a precise Pareto curve of the net output power depending on the investment cost.

### 3.1.1.1.3 Multi objective optimization results

#### Decision variables

We need to choose the variables for the ORC design:

- The evaporation temperature of the fluid  $T_{evap}$ . The interval of variation is defined between 330 °K and 360 °K. The criteria are to obtain good values of the exergetic efficiency.
- The superheat temperature  $T_{superheating}$  is defined between 700 °K and 1050 °K.

The function to be optimized for the ORC design is defined as:

$$\min(-\dot{P}_{net}(x), Cost_{ORC}(x)), \text{ with } x \in X(\text{decision\_Variables}) \quad (3-2)$$

#### Pareto-curves

The multi-objective optimization converges on the solutions presented on the Pareto curve (Figure 3-1). The trade-off between the ORC net power and the investment cost are illustrated to the Pareto curves. The best value of exergetic efficiency is reached at 25%. This is for investment cost interval between 350 and 700 Euros.

#### Method to get the ORC maps

As we want to get the ORC characteristics for each operating point, we should consider the new hot streams and cold streams, as defined in [7] and [8]. Firstly, we do the following assumption: the compressor power is the same for each operating point; we consider the flow rate to be the same. The heat cascades are defined in the energy integration method. By knowing the temperatures and the exchanged power, the energy integration module computes the power maps, the energy efficiency and the exergetic efficiency maps of the gasoline engine (Figure 3-2). The ORC map comes as a solution of the energy integration method.

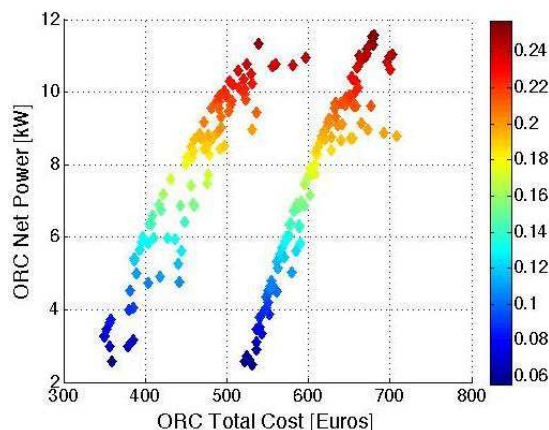


Figure 3-1: ORC Pareto curves: techno-economic trade-off, exergetic efficiency in [-], in the colorbar

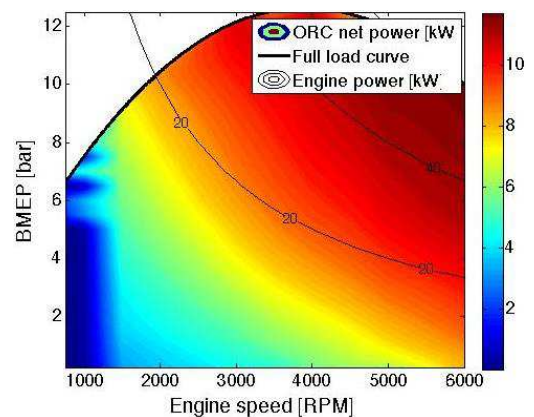


Figure 3-2: Map of the ORC power output, design after multi-objective optimization, ORC net power in [kW], in the colorbar

The maximum net power output is reached over the engine iso-line of 30 kW. This is the area of high rotation speeds and high loads. The optimal design of the ORC design is investigated for the loaded points. The high seeds and high loads zone is also the region with the most important heat losses. The selected design is extended on the engine operating field. One considers that the pump operates with permanent parameters.

### Simulation results on driving cycles

This study extends the methodology for design of vehicle energy systems on other drive cycles. The peri-urban cycle represents the home to work commuting. The holiday cycle is representative for long distances drives. The New European driving cycle (NEDC) is well known as reference and is as well considered. Table 3-1 summarizes their characteristics.

Table 3-1: Drive cycles characteristics

Cycle a	Distance, km	Duration, s	Average speed, km/h	Min acceleration, m/s <sup>2</sup>	Max acceleration, m/s <sup>2</sup>
NEDC	11.023	1180	32.26		
Peri-urban	39	2440	57	-2	2
Holiday	847	28800	105	-1.9	1.9

<sup>a</sup> The peri-urban and holiday cycles are based on the parts of the WLTP cycle.

### Comparison of different configurations

The gasoline engine in the hybrid electric powertrain obtains an additional flow of electrical power thanks to the heat recovery from the ORC. The studied architecture is a mild hybrid electric powertrain, as presented in Figure\_B-9. The hybrid electric powertrain has already an electric energy recovery system. This category of recovery system has an electric energy storage in the high voltage battery and is an effective solution for low speed drives, where the power delivered by the electric part of the powertrain is enough to drive the vehicles on purely electric drive. The fuel consumption is zero. The selected ORC design is optimized for the area characterized with high rotation speeds and high loads. This is a complementary zone, where the mild hybrid electric powertrain is not acting. The simulations results are displayed in the Table 3-2. The fuel consumption result on NEDC for the basic configuration of the vehicle is 4.6 l/100 km.

The Mild HEV is a low degree electrical hybridization of the vehicles powertrains, characterized with low capacity of the high voltage battery – between 1.2 kWh and 6 kWh. The efficiency improvement of the MHEV on the NEDC and the Peri-urban cycles is around 10 %, because these cycles except the urban part, have also a large extra urban part, which is more energy demanding and where the MHEV mode is not active. On the holiday cycle, the MHEV is not used. In conclusion the Mild HEV is an adapted technology for the city drive and can be consider as effective technology for urban drives.

The ORC design proposed for the net power map of the Figure 3-2 is optimal for high load and high speed engines operating points. For these points we have high temperature exhaust gases. Thus the waste heat recovery potential is important. The impact proposed ORC design is estimated on the different driving cycles. At first just the ORC impact is considered. From the results in Table 3-2 is visible that on the combined cycles (with urban part and extra urban part) – NEDC and peri-urban the efficiency improvement is 24% and respectively 34%. The ORC is well used in the charged part of the cycles. The fuel consumption reduction potential on holiday cycle is around 40%. The fuel consumption is below 4.5 l/ 100 km. The selected ORC design is an efficient equipment to recover the waste heat in the high speed demanding drives. In these zones the engine power demand is high.

It is as well interesting to analyze the aggregation of the MHEV and the ORC. For the combined cycles the combination of a MHEV and an ORC on a small downsized engine brings the best fuel saving potential – around 40%. The MHEV contributes to the efficiency improvement on the peri-urban drives and the ORC on the extra-urban drives. For the “holiday” long drive cycle, the ORC is the major contributor of the improvement.

The lowest consumption is obtained for NEDC cycle, because of its particularity to combine urban and highway drives at very smooth and progressive speed changing conditions. By their construction, based on WLTP, the peri-urban and the holiday cycles combine more transients and higher accelerations. In all configurations, their consumption is higher than the NEDC consumption.

In conclusion the mix of a low degree electric hybridization technology such as the Mild HEV and a technology for the waste heat recovery as the organic Rankine cycle is efficient for mixed usages of the vehicle. For the C-Segment vehicle the aggregation of the two energy recovery options is efficient. The powertrain efficiency increase for NEDC is of around 40%. The vehicle consumption is 3.32 l/100 km.

Table 3-2: Driving cycles and fuel consumption results on C-Segment Vehicle

Driving Cycle	Vehicle type	Fuel consumption, l/100 km	Powertrain efficiency gain, %
NEDC	C-Segment 1.2	4.72	-
	C-Segment 1.2 MHEV	4.16	10.8
	C-Segment 1.2 ORC	3.71	24
	C-Segment 1.2 ORC MHEV	3.32	38.4
Peri-urban	C-Segment 1.2	5.56	-
	C-Segment 1.2 MHEV	5.05	10
	C-Segment 1.2 ORC	4.14	34.2
	C-Segment 1.2 ORC MHEV	3.98	39.7
Holidays	C-Segment 1.2	5.94	-
	C-Segment 1.2 MHEV	5.86	1.3
	C-Segment 1.2 ORC	4.27	38.9
	C-Segment 1.2 ORC MHEV	4.35	36.2

The system is interesting to be realized and to be tested. The practical difficulty is related to the ORC installation. The Mild HEV architecture is well known in the state of the art and exists in serial production. The discussed ORC system presents challenges on the direct mechanical connexion between turbine and the electric generator, because of the high the rotation speed that they have to operate. The choice and the realization of the small size ORC components (pump and turbine) is as well challenging.

## Conclusions

This research presents a study of the efficiency performance and the economic optimization for a middle class vehicle with a downsized gasoline engine. Two technological options are studied for the efficiency improvement of the baseline vehicle powertrain:

- Low degree electric hybridization technology – called Mild Hybrid electric powertrain;
- Waste heat recovery system for two heat sources the engine water circuit and the exhaust gases, means an external thermodynamic cycle – ORC.

The ORC is designed on an optimal way for high load and high speed engine operating conditions. The design is optimized considering techno- economic performances indicators. For this evaluation a multi-objective optimization methodology is applied, including the energy integration. For this reason, the best fuel consumption improvement is obtained for the holiday cycle, characterized by long ways drives at high speed. For the combined cycles such as NEDC and peri-urban the combination of ORC and MHEV bring the best fuel saving potential, superior to 35% in comparison with normal ICE vehicle.

The main conclusion coming from the driving cycles evaluation is the MHEV is an efficient technology for the driving cycles with speed variations. The selected ORC design is efficient on the cycles using the charged area of the engine. For these operating points, the small gasoline engine is highly charged, due to the high power vehicle demands. The MHEV and the ORC are complementary technologies and their combination is especially efficient on the combined cycles containing urban and extra urban part.

The research of the optimal design of the hybrid electric vehicles (Appendix A) presents a powertrain design study on hybrid electric vehicles, considering different vehicle usages through adapted driving

profile – normalized cycle. The optimal environomic configurations are researched by using multi objective optimization techniques. The optimization methodology is based on a genetic algorithm and is applied for defining the optimal set of decision variables for powertrain design. The analysis of the environomic Pareto curves on NEDC illustrates the relation between the economic and the environmental performances of the solutions. The life cycle inventory allows calculating the environmental performance of the optimal techno-economic solutions. The environmental and the economic trades-off are defined for the different impact categories. Their impact for the production phase and the use phase of the vehicle is studied. The sensitivity of the impacts categories on the electricity production mix is as well studied.

In a second step the optimization is extended to a multi objective optimization with three objectives, integrating the environmental impacts as objective. The analysis of the evolution of the four impacts categories allows choosing one main environmental category, the GWP, to be minimized.

The analysis of the environomic Pareto curves on NEDC illustrates the relation between the economic and the environmental performances of the solutions. The optimization problem is then simplified from 3 objectives to 2 objectives optimization. The life cycle inventory allows calculating the environmental performance of the optimal techno-economic solutions.

The solutions in the lowest emissions zone show that the maximal powertrain efficiency on NEDC is limited on 45.2% and the minimal tank-to-wheel CO<sub>2</sub> emissions are 30 g CO<sub>2</sub> /km. They have the maximal cost – 75000 Euros.

The increase of the electric part of the powertrain increases all environmental categories, because of the materials and the processes to produce the electric components.

## **3.2 Energy converters on-board**

There are three main energy converters known on-board for automotive applications: internal combustion engines (ICE), electric machines (delivering torque by rotation) and fuel cells.

The ICE and the traction electric machines are well known and largely used in the industry for vehicular applications. They are combined in different architecture and constitute the main conversion components in the thermal, hybrid electric and electric vehicles. The fuel cell is a less applied technology for onboard energy conversion vehicular applications. The technology is mature but the main issues to be solved are related to the hydrogen availability and the cost of the technology that is still elevated. The main principles are shortly described in Appendix C. Chapter 5 studies a fuel cell application in vehicular energy system. Other type of fuel cell (converters) could be considered: alkaline fuel cell (AFC) or Proton-exchange membrane fuel cells (PEMFC), Solid Oxide Fuel Cell (SOFC).

In this part of the chapter, it is presented the development of an innovative electromagnetic actuator for an engine valve train. This converter acts on the principle of linear electric machine, in bi-modes, converting electricity to force or force to electricity. The application of the designed innovative actuator is to replace the total mechanical engine valve train. This research contributes to improve the ICE effective efficiency, by reducing the mechanical friction and the induced (thermodynamic) efficiency of the ICE. The linear electromagnetic actuator represents, as well the opportunity to replace the well know mechanical function of the engine camshafts by electric driven valve train. This chapter investigates an innovative technology improving the energy conversion efficiency of the internal combustion engine.

### 3.2.1 Development of robust control of an electromagnetic actuator

This research presents an innovative application of an electromagnetic actuator for a future camless engine valvetrain. The actuators are designed for a small gasoline engine. The design method is inversed to create a control-oriented model. The control architecture is designed for a robust control of the actuator. An experimental test bench is built for the correlation of the control model with experimental measures. Control strategies are developed and the performance indicators of the actuators are evaluated. The robust controller method uses CRONE system design methodology. The investigations show that the design of the innovative actuator and of its controller provides very good dynamic performances.

#### 3.2.1.1 System description: description of the innovative electromagnetic actuator

The Lorentz force based actuator module is designed for two valves, to act on an individual way each of the valves. The modules are equivalent for the intake or the exhaust side of the engine. The principle and the details of the actuator are described in [102].

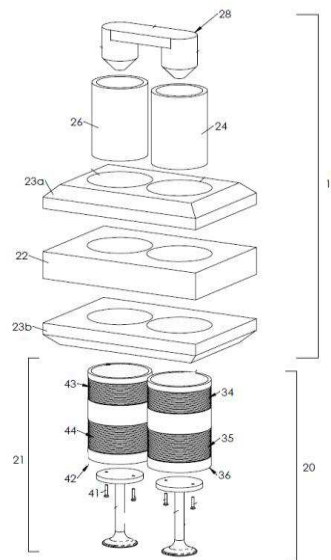


Figure 3-3: Schematic of the actuator

The valve module (Figure 3-3) is composed of one fixe part that forms the magnetic circuit, including one permanent magnet and ferromagnetic parts. The magnetic circuit is closed by using full ferromagnetic cylinders (26 and 24). The part 28 is also ferromagnetic and is used as cover to maintain fixed the cylinders (26 and 28). They are crossing the sandwich of the permanent magnet (22) and the two ferromagnetic parts (23a and 23b). The set of part indicated as (19) is fixed. The moving parts of the actuator are indicated as sets of parts (21) and (20). The actuator has one moving part for every valve. The moving part is composed of one carcass (42) and (36), which are concentric with the ferromagnetic cylinders (26) and (28). The carcass is wearing the wires (43, 44, 34, 35) and the valve is fixed on its bottom extremity of the carcasses (42) and (36). The material of the carcasses is chosen to be a composite. This allows enough good mechanical properties to pass the efforts for lightweight characteristics. The order of magnitude of the moving mass is around 36 grams, which insure low kinetic energy demand while moving. The composite is neutral for the electromagnetic field. The wires of every moving part are connected through flexible connections to the vehicle electric grid and can operate on different voltage levels. Other advantage of the innovative design is the small air gap in the magnetic circuit, important for the electric consumption of the actuator. The electric connection is independent for each valve, which insures an individual control and acting of the valves. The maximal valve lift is 7 mm. The size of the permanent magnet and the shape of the ferromagnetic parts that surround the permanent magnet are studied and optimized to deliver the target of the maximal force. The ferromagnetic cylinders close the magnetic circuit with a very small air gap, which is needed for good

efficiency of the actuator. The efficiency is directly related with the electricity consumption of the actuators, which has to be minimized. The discussed actuator design is innovative its magnetic circuit and lightweight moving part, including the valves and the carcasses, where the copper is wired.

The volume of the electromagnetic actuator module is compact. The dimensions are 50 mm\*80 mm\*55 mm. The actuator is delivering an electromagnetic force and is governed by:

$$F_{act}(I, Z) = B(Z) \cdot I \cdot L_{coil} \quad (3-3)$$

where  $F_{act}$  is the electromagnetic force delivered by the actuator in [N],  $B$  is the magnetic field in [T],  $I$  is the current amperage [A],  $L_{coil}$  is the length of the wire in [m] and  $Z$  is the valve position (m).

The size of the permanent magnet is related to the magnetic field and then to the electromagnetic force, delivered by the actuator and governed by equation (3-3). The relation between magnetic field, current and valve position has been modelled (Figure 3-4). This model has been obtained after simulation with Finite Elements Method Magnetics (FEMM), which contains Maxwell equations. The FEMM model of the actuator is validated with experimental results of the prototypes. As the current limit is 90A, the electromagnetic maximal force delivered by the actuator on each valve is 400 N. This level of force allows deploying the module also on the exhaust side, where the effort to open the combustion chamber under pressure is important. The actuator does not contain a mechanical spring with an energy storage function. Its structure is active, without a passive mass/spring system and present main advantages for the controlling of the actuator. The active principle of the controlling avoids the passive resonance modes, which are difficult to control and provoke vibrations and noise during when the valve lands on the valve seat.

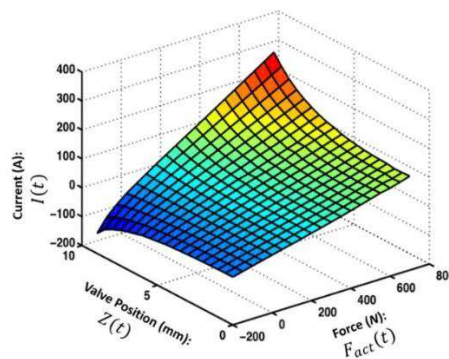


Figure 3-4: Electromagnetic modelling of the actuator

The introduced actuator has an efficient magnetic circuit. Due to its design the actuator is directly driven by the current and belongs to the so-called family of active actuators. This fact introduces the novelty of the study and also presents an advantage for the active control of the actuator and thus the precision obtained by the control of the actuator. The method used for the control of the active actuator presents interest for the state of the technology. The implementation and the experimental results are as well useful.

The actuator nonlinear model is described in Appendix B

### 3.2.1.2 Design of the control system

In order to make the EMA a reliable solution to perform variable valve timing operation in Camless engines, an extremely delicate stage to be addressed is the design of the Control System ([103], [104], [105], [106]). The main function of the CS is to move the valve from the closed to the opened position (and vice versa) while satisfying robust tracking of the reference position valve (Figure\_ B-11) [107],

low energy consumption requirements and avoiding high intensity impacts [108] (ex: impacting velocity less than 0.4 (m/s) at 6000 rpm).

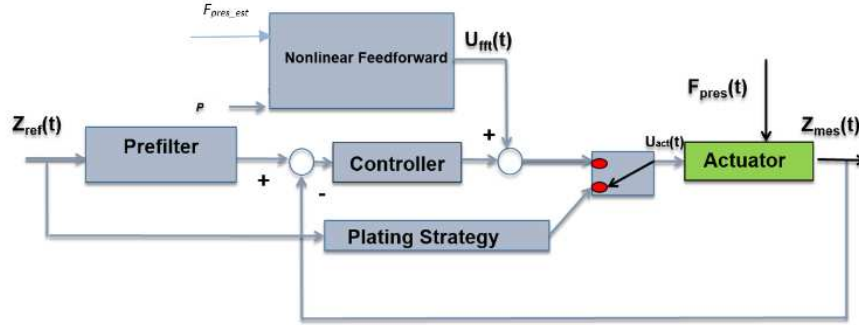


Figure 3-5: Structure of the control system architecture

For this purpose, a control system architecture presented by Figure 3-5 is proposed. It consists mainly of a robust controller designed with the CRONE methodology allowing a control by feedback position provided by a sensor system and a complementary feedforward control.

#### Frequency domain system identification of the actuator

The global model of the actuator is highly nonlinear, and because of the natural integral behavior, the limits of displacement, the variable friction force and the very high speed of the actuator, it is difficult to achieve an open loop and time-domain classical system identification of its dynamical behavior. Thus, for the design of the feedback controller with the frequency-domain based CRONE methodology, a frequency-domain system identification of the linear behavior of the actuator around an operating point close to the middle valve position is achieved.

First, for the local stabilization of the valve position around 3mm, a very simple PID controller is designed from the gain and phase of the system roughly measured in open loop at 1000 rad/s. The mean value of  $U_{act}$  and its sine variation amplitude have been defined by a trial and error process. The PID controller ensures a 1000 rad/s open-loop gain crossover frequency and a  $40^\circ$  phase margin. Using this PID feedback controller, the frequency response of the system is measured in closed-loop: the reference valve position  $Z_{ef}$  is defined by a mean value of 3mm and a sine variation with a frequency successively from 1000rad/s to 10000rad/s, no feedforward ( $U_{FF} = 0$ ) and filter effects are used. The experimental gain and phase measures are obtained by comparing the sine part of  $Z_{mes}$  to that of  $U_{act}$ . Then, the parameters of a black-box model defined by (3-4) are optimally tuned to fit the measured frequency response of the experimental actuator. The optimization provides the nominal values of the linear model parameters.

$$G(s) = \frac{Z_{mes}(s)}{U_{act}(s)} = \frac{K \left(1 + \frac{s}{\omega_p}\right)}{s \left(1 + \frac{2\xi_1 s}{\omega_{n1}} + \left(\frac{s}{\omega_{n1}}\right)^2\right) \left(1 + \frac{2\xi_2 s}{\omega_{n2}} + \left(\frac{s}{\omega_{n2}}\right)^2\right)} \quad (3-4)$$

Optimized parameters:

$$\begin{aligned} K_0 &= 276; \omega_{p0} = 9000 \text{ rad/s}; \\ \omega_{n10} &= 1597 \text{ rad/s}; \xi_{10} = 0.8446; \\ \omega_{n20} &= 9840 \text{ rad/s}; \xi_{20} = 0.1069. \end{aligned} \quad (3-5)$$

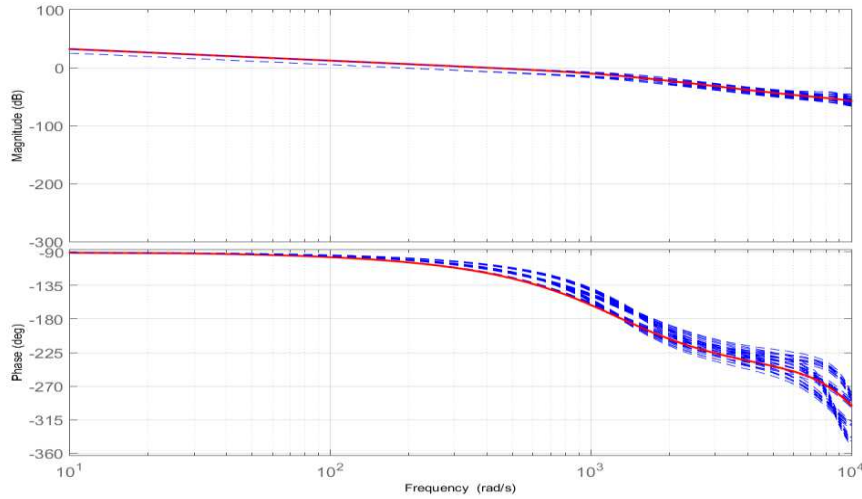


Figure 3-6: Bode diagram of nominal plant frequency response (—) and set of frequency responses of  $G(s)$  (---)

The nominal black-box model (3-4) and its parameters defined by (3-5) are derived to define an uncertain plant model that will be used for a robust controller design. Uncertainty ranges are defined by:

$$\begin{aligned}
 K &\in \left[ \frac{K_0}{1.5}, K_0 * 1.5 \right]; \quad \omega_p \in \left[ \frac{\omega_{p0}}{1.1}, \omega_{p0} * 1.1 \right]; \\
 \omega_{n1} &\in \left[ \frac{\omega_{n10}}{1.1}, \omega_{n10} * 1.1 \right]; \quad \xi_1 \in [\xi_{10} - 0.1, \xi_{10} + 0.1]; \\
 \omega_{n2} &\in \left[ \frac{\omega_{n20}}{1.1}, \omega_{n20} * 1.1 \right]; \quad \xi_2 \in [\xi_{20} - 0.05, \xi_{20} + 0.05].
 \end{aligned} \tag{3-6}$$

Figure 3-6 presents the set of frequency responses of  $G$  that defines the uncertain plant. It shows significant uncertainties both on the gain and on the phase of the plant.

### Tuning of the parameters of the nonlinear model of the actuator

Even if the linear model of the uncertain plant is useful to design a controller whose robustness could be verified by using the experimental system, the nonlinear model presented by Figure\_B-10 is needed to assess the control system (feedback and feedforward controller) for more realistic working cases, for instance when pressure forces are taken into account as disturbances. Thus, the mechanical, electrical and electromechanical parameters of the nonlinear model described by section 3 are tuned by minimizing the difference between the gains and phases of its numerically linearized model (obtained with the *linmod* Matlab-Simulink function) and the experimental gains and phase used in section 3.1. The optimized mechanical and electrical parameter values are:

$$\begin{aligned}
 L_{bob} &= 95.067 \mu\text{H}; \quad R_{init} = 0.03050 \Omega \\
 m &= 0.0676 \text{ kg}; \quad L_{coil} = 7.4409 \text{ m}; \quad K_{visc} = 1.5 \text{ Ns/m}
 \end{aligned} \tag{3-7}$$

Figure 3-7 permits the comparison between experimental closed time responses (for an engine speed of 6000 rpm) and those of the simulated nonlinear model. The agreement of these responses validates the proposed model.

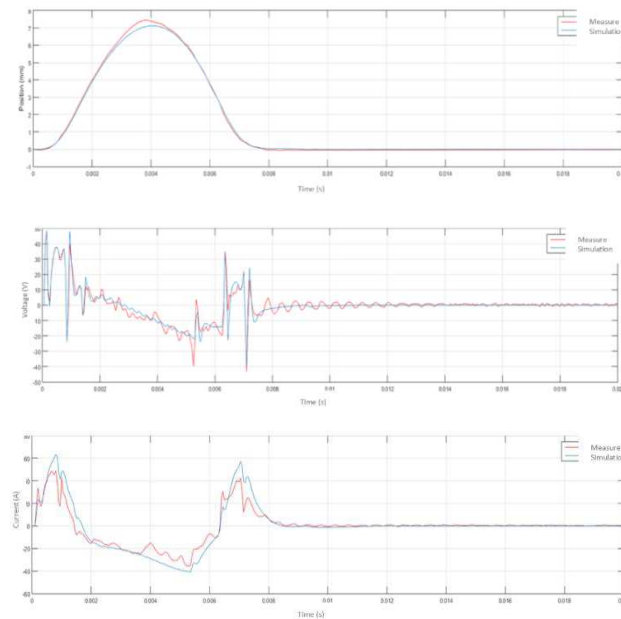


Figure 3-7: Experimental time responses (—) and nonlinear model time responses (—): position; voltage; current

#### CRONE design of a robust feedback controller

The CRONE CSD methodology is a frequency-domain approach developed since the eighties ([109], [110], [111], [112], [113], [114]). It is based on the common unity-feedback configuration presented by Figure 3-5. Three CRONE CSD generations have been developed, successively extending the application field. The controller or the open-loop transfer function is defined using fractional order integro-differentiation. They enable to design, simply and methodologically, LTI robust control-systems. Using frequency uncertainty domains (for instance provided by a perturbed black-box model), the uncertainties (or perturbation) are taken into account in a fully-structured form without overestimation, thus leading to control-systems that are as less conservative and thus as high performing as possible [115]. The first two generations are based on real fractional order differentiator or integrator and provide robust feedback controller for plants with gain variations. The third generation should be used for any kind of plant perturbation model: around open loop gain crossover frequency or closed loop resonant frequency, the nominal open loop  $\beta_0(s)$  (for the nominal plant  $G_0(s)$ ) is defined by a set of band-limited complex fractional order integrators. Integer order proportional integrator and low-pass filter define  $\beta_0(s)$  respectively at low and high frequencies. Right half plane or underdamped poles and zeros of the nominal model of  $G_0(s)$  are included in  $\beta_0(s)$  for closed-loop internal stability and damping. After some high-level parameters of  $\beta_0(s)$  being optimized for a robust and high performing closed-loop, the feedback controller  $C$  is finally defined from the ratio  $C_R(s) = \beta_0(s)/G_0(s)$ .

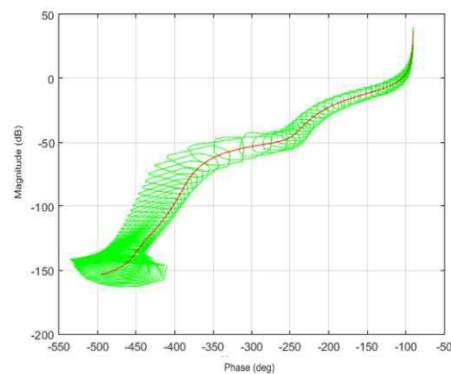


Figure 3-8: Nichols plot  $G$ : nominal frequency response (—); uncertainty domains (—)

When the designed controller has to be discrete-time for an implementation purpose, in order to take into account the effect of time-discretization, the initial digital control system design problem with the sample period  $T_s$  is transformed into a pseudo-continuous problem by:

- taking into account the transfer function of a zero-order hold on the plant input;
- computing the Z-transform of the continuous-time set {plant and holder};
- achieving a bilinear variable change, for instance  $z^{-1} = (1-w)/(1+w)$ .

The controller  $C(w)$  can then be designed using the CRONE frequency-domain method knowing that  $G(w)$  (with  $w = j\nu$  and the normalized pseudo-frequency  $\nu = \tan(\omega T_s/2)$ ) is the exact frequency response of  $G(z)$  (with  $z = e^{j\omega T_s}$ ). Figure 3-9 shows the Nichols plot of  $G(w)$  whose uncertainty domains take into account the uncertain parameters (4) of the plant model.

To track reference valve position for engine speed up to 6000 rpm, the desired closed-loop bandwidth should be at least more or less 900 rad/s, the corresponding pseudo-frequency is 0.02. The required nominal resonant peak of complementary sensitivity  $T$  is 1 dB, the resonant peak limitation ( $T$ ) is 4.5dB, the sensitivity function limitation ( $S$ ) is 6dB and the plant input sensitivity function limitation ( $SG$ ) is 3 dB. Taking into account the measurement noise, the limitation of the control effort sensitivity function ( $CS$ ) is 48 dB. A controller with a high static gain (without integrator) is enough to ensure a good tracking of a steady state reference signal with a good rejection of the effect of disturbance on the plant input. Three right half plane zeroes of  $G_0(w)$  are included in  $\beta_0(w)$ . The high frequency order of  $\beta_0(w)$  is defined to limit the control effort sensitivity at high frequency and to obtain a strictly proper controller. The nominal open loop transfer function to be tuned is thus defined by:

$$\beta_0(w) = K_\beta \left( \frac{\nu_0}{w} + 1 \right)^1 \left( \frac{1+w/\nu_1}{1+w/\nu_0} \right)^{a_0} \left( \Re e_i \left\{ \left( \alpha_0 \frac{1+w/\nu_1}{1+w/\nu_0} \right)^{i b_0} \right\} \right)^{-q_0 \text{sign}(b_0)} \frac{\left( 1 - \frac{w}{1} \right) \left( 1 - \frac{w}{1.22} \right) \left( 1 - \frac{w}{95} \right)}{\left( \frac{w}{\nu_1} + 1 \right)^4} \quad (3-8)$$

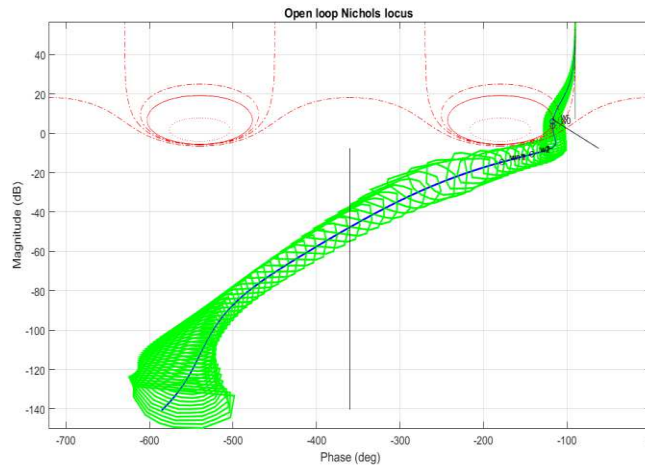


Figure 3-9: Nichols plot of  $\beta_0$  nominal frequency response (—); uncertainty domains (—); 1 dB M-contour (—)

By taking into account the frequency domain uncertainty, 4 parameters of  $\beta_0(w)$  are optimized in order to minimized the variations of the peak value of  $T$  and to fulfil performance frequency domain constraints on sensitivity functions  $T$ ,  $S$ ,  $SG$  and  $CS$ . Optimized parameter values are:  $Y_r = |\beta_0(j\nu_r)| = 6$  dB;  $\nu_r = 0.015$  (resonant frequency);  $\nu_0 = 0.018$ ;  $\nu_1 = 0.1$ . Thus,  $a_0 = 0.99$ ,  $b_0 = 0.81$ ,  $q_0 = 3$  and  $K_\beta = 2.28$ . Figure 3-9 presents the Nichols plot of the optimized open loop frequency response. All sensitivity constraints are met: the greatest values of the resonant peaks of  $T$ ,  $S$ ,  $SG$  and  $CS$  are respectively 2.07dB, 5dB, -10dB and 47dB. This last value is very close to the 48dB limit which shows that a larger bandwidth

cannot be obtained: depending on the parametric state of the system, the closed loop bandwidth is more or less between 1000 rad/s and 5000 rad/s. Then, the frequency response of the fractional version  $C_F(w)$  of the controller is fitted by an order 7 rational transfer function  $C_R(w)$ . Finally, the digital controller  $C(z)$  is obtained by achieving the inverse variable change  $w = (1-z^{-1})/(1+z^{-1})$ .

### Nonlinear Feedforward and plating strategy

To ensure performance for high engine speeds and to reduce the effect of the cylinder internal pressure on the output of the exhaust camless valve actuator, since the controlled system has a notable nonlinear behavior, a nonlinear feedforward control is necessary. It is based on the inversion of the dynamic model of the actuator in order to obtain at each moment a balance of the forces having an influence on the movement of the valve. The resultant  $F_{act}$  of the forces acting on the actuator given by (B-15) (which also includes the friction force) is used by the online calculation (in real time) of the corresponding current  $I$  using the order 5 polynomial equation that approximates the electromagnetic model of the actuator depicted by Figure 3-4. No hysteresis phenomenon has been taken into account. A recorded estimation of the pressure force  $F_{pres\ est}$  is used into the  $F_{act}$  calculation. Using a strictly-proper inverse model of the electrical part of the model, it is easy then to deduce the necessary feedforward control voltage that should ensure the valve position reference tracking and the rejection of the effect of the internal pressure in the cylinder. Furthermore, a plating strategy is added in order to maintain the valve closed especially at the end of the intake cycle. This strategy consists in applying a constant and non-zero control signal outside the opening phases of the valve, outside these phases, the control signal remains that of the valve position reference tracking.

### 3.2.1.3 Experimental and simulation assessments

Figure 3-11- Figure 3-14 present the simulation results for exhaust valve control at 6000 rpm. It should be noted that the peak pressure force is observed after the exhaust valve closing and the actuator is able to overcome the pressure force at the opening valve. Figure 3-13 Figure 3-14 Figure 3-10 show the obtained experimental results valve at 6000 rpm. This test is only significant of the intake phases as the experimental testing bench is not able to apply a resistant force close to the pressure forces observed for exhaust phases. We observe that the robust feedback and nonlinear feedforward control system ensures a good valve position tracking, Finally, in order to validate the proposed control-system, experimental valve seating velocities are shown on Table 3-3 for various engine speeds. It is demonstrated that, except for the low engine speed (<2000 rpm) where the speed estimations are very noisy, the obtained seating velocities fulfill the imposed limitations for a smooth valve seating, which ensure a “soft-touch” behavior. All these simulations and experimental tests mean that the designed controller ensures a good level of precision to drive the actuators under realistic conditions.

Table 3-3: Seating valve velocity (m/s) at various engine speeds

Engine speed (rpm)	Experimental velocity (m/s)	Limitation criteria, Mechanical system velocity (m/s)
1000	0.18	0.05
2000	0.3	0.1
3000	0.11	0.2
4000	0.17	0.3
5000	0.32	0.4
6000	0.41	0.5

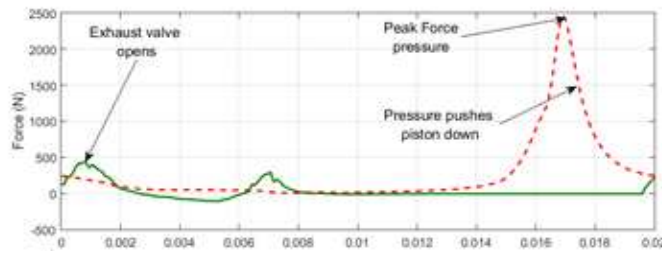


Figure 3-10: Pressure force (---) and force generated by the exhaust valve actuator (—) at 6000 rpm

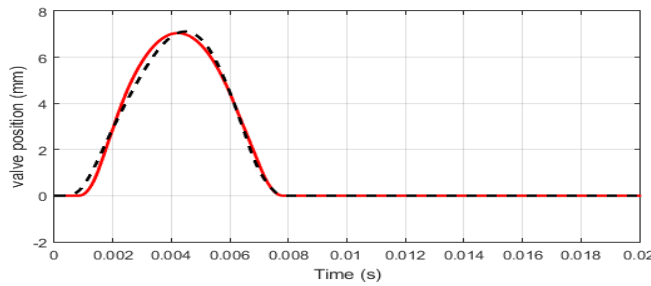


Figure 3-11: Opening and closing of the exhaust valve at 6000 rpm: reference signal (—); simulation response (---)

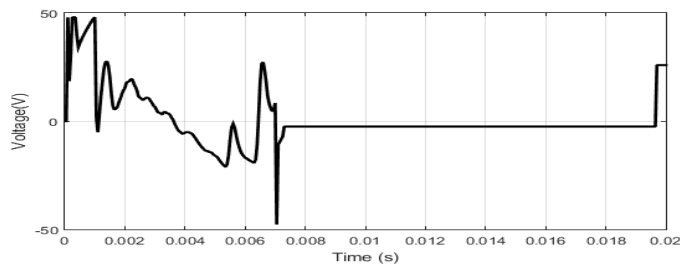


Figure 3-12: Control voltage at 6000 rpm (exhaust simulation)

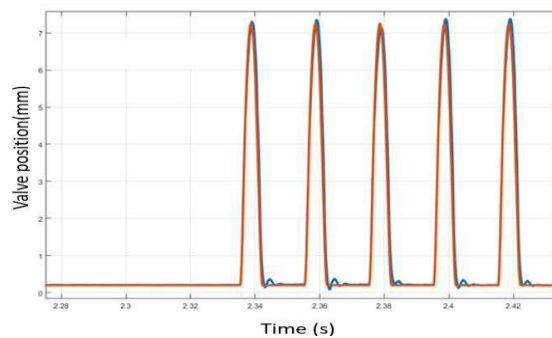


Figure 3-13: Opening and closing of the intake valve at 6000 rpm: reference signal (—); experimental response (---).

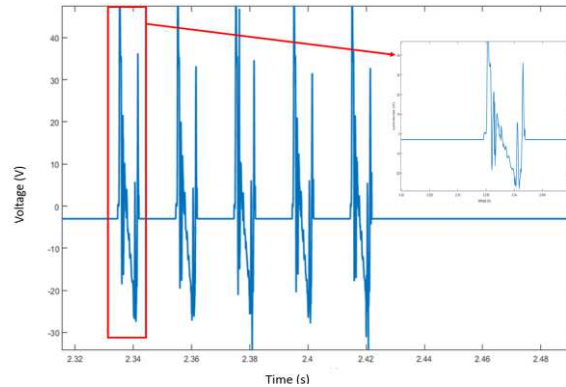


Figure 3-14: Control voltage at 6000 rpm

### Conclusions

The precision of the developed actuator and the robustness of the designed control system are important parameters for the integration of the actuators in the engine cylinder head. This electromagnetic actuator gives the possibility to manage the engine gas exchange on a very performant way. The precision provided by the control system attests the controllability of the actuators technology and thus the good performances of the engine. The robust and precise controlling of the actuators on the intake side is especially important for the regulation of the airflow in the engine and this for gasoline engine concerns directly the regulation of the engine torque. The respect of the velocity requirements during the valve landing is an important step and insures the respect of the noise criteria and the mechanical durability of the system.

These results are promising for the development of the engine control system that manages the gas exchanges of the engine. Future steps of the work could be the integration of the actuators in the engine cylinder head, the integration of the electronics and the development of the control strategies for full camless engine.

## 3.3 Energy storage on-board – high voltage batteries

This part of the chapter introduces and states the art of the current technologies for energy storage on board for electric and electrified vehicles that are the high voltage batteries. The compactness and the energy density are the main technology challenges in front of the energy storage. The process in this domain is discussed and the innovative technology of solid state batteries is introduced. The range of the electric vehicles and the range of electric mode for the electrified vehicles is the main challenge. This chapter investigates optimal design methods to increase the range of the electric vehicles. The operational parameters and especially the temperature in the battery pack is an important parameter for the good performances of the batteries. Energy balance of the high voltage battery pack is investigated by experimental way in this chapter. The experimental data of the energy balance are used to design effective cooling strategies and technologies for batteries cooling. The experimental data allow as well modelling the thermal behavior of the batteries. The thermal models can be used to monitor the state of change and the state of health of the high voltage battery.

### 3.3.1 The progress of the compactness and the energy density: the hope of the Solid State batteries.

Electrochemical batteries are key components of the electric vehicles and the hybrid electric vehicles. Batteries are devices that transfer chemical energy into electrical energy and vice-versa. They represent a reversible electrical energy storage system. Traction batteries are characterized in terms of power, which has to match the power of the electric path and nominal capacity, which has to match the desired driving range specification. The nominal capacity is usually expressed in Ah, which is the temporal

integral of the current that could be delivered by a full battery when it is completely discharged under certain conditions. A dimensionless parameter is the state of charge (SoC), which describes the capacity remaining in the battery expressed as a percentage of its nominal capacity. Desirable attributes of traction batteries for EV and HEV applications are:

- High specific energy
- High specific power
- Long lifecycle time
- Low initial and replacement costs
- High reliability
- Wide range of operating temperatures
- High robustness

Figure 3-15 illustrates the schematic of a battery cell.

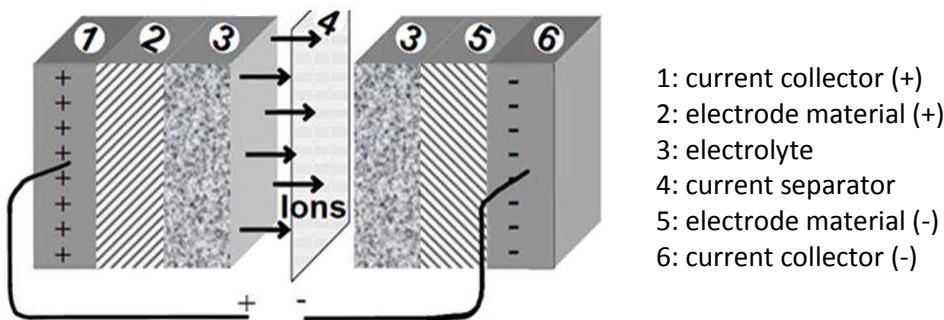


Figure 3-15: Battery cell components and principle

The specific energy is the amount of useful energy that can be stored in the battery per unit mass, typically expressed in Wh/kg. This parameter takes into account the fact that not the whole capacity can be actually used. In fact, the battery operation is typically defined by a certain SoC window, whose limits are the minimum SoC that can be attained during discharging and the maximum SoC that can be reached during charging. The charging and discharging phase of a Li-Ion cell are presented in Figure 3-16.

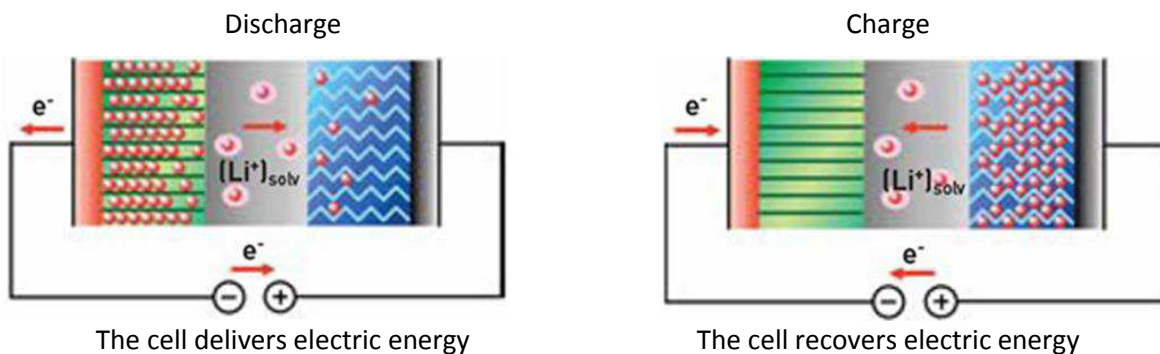


Figure 3-16: Discharging and charging phases of a Li-Ion cell

The specific energy of a battery is important for the range of a purely electric vehicle. For hybrid electric vehicles, possibly more important is the specific power, typically expressed in W/kg, which determines the acceleration and top speed that the vehicle has to reach.

A panoramic vision of the battery types and their applications is given in Figure 3-17. The energy densities of the batteries cells applied in the serial hybrid electric and electric vehicles are between 90 and 150 Wh/kg. The electric vehicles that are currently under development with a range target over 200 km can obtain Li-Ion batteries with 200 Wh/kg of cells density. The cells energy density is important

for the development of the electric vehicles and the research is working on future generation of batteries with the target to increase their energy density.

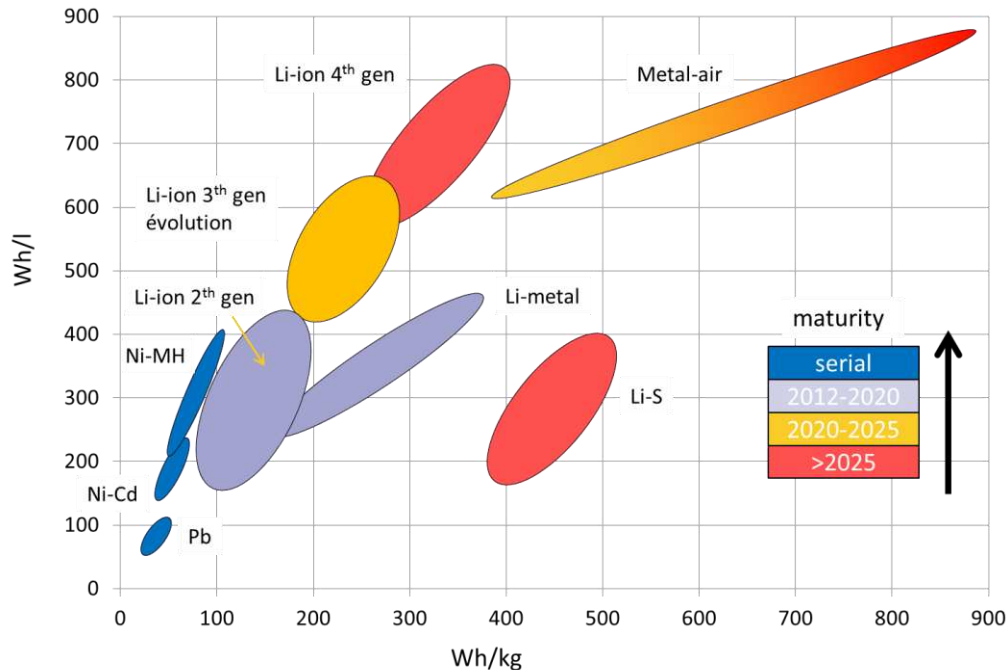


Figure 3-17: Cells technologies – evolutions of the technologies and their maturity [116]

Batteries are composed of a number of individual cells in which the main components are present: two electrodes, where half reaction takes place, resulting in a circulation of electrons through an external load, and a medium that provides the ions transport mechanism between the positive and negative electrodes. The cathode is the electrode where reduction (gain of electrons) takes place. It is the positive electrode during discharging and negative electrode during charging. Contrary, the anode is the electrode where oxidation (loss of electrons) takes place. It is the negative electrode during discharging, the positive during charging.

Recent research shows that batteries with solid electrolyte can present advantages to compactness and stability, in comparison of the current technologies of Li-Ion batteries, with liquid electrolyte. The main claims of the solid-state batteries are:

- Improved safety (no leakage, volatilization, flammability)
- Improved electrochemical performances (higher energy density for increased EV autonomy, capacity and voltage output)
- Lower specific cost (€/ kWh)(packaging opportunity because of the downsizing and the compactness if the technology, materials use and manufacturing)

Figure 3-18 presents the evolutions stages between the conventional Li-Ion battery with liquid electrolyte and the all solid-state components, which is convenient for bipolar cell concepts, inducing downsizing of the battery packs. The hybrid electrolyte (Jellify Polymer) is an intermediate technology.

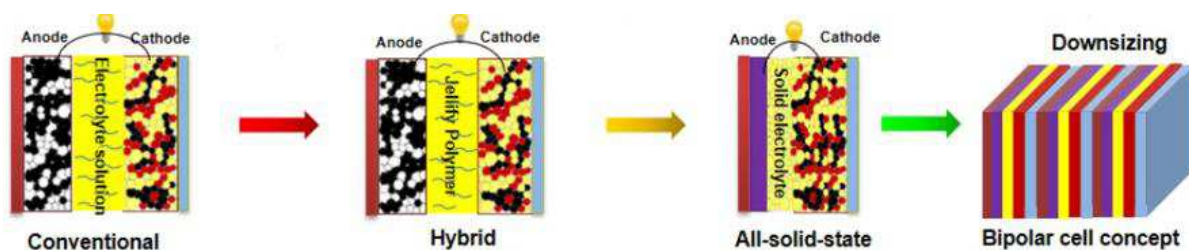


Figure 3-18: Evolution of the batteries technology: opportunities for compactness

The main gain of compactness is done by reduction of the dimensions of the anode and the electrolyte separator. The solid state batteries have Li Metal Anode with high specific current of 3860 mAh/g. As the electrolyte is solid none separator is needed for the electrolyte. Figure 3-19 displays the comparisons of the dimensions of the battery types.

	Disassembly liquid electrolyte cell	Hybrid cell	All-Solid cell
↓	 Cu current collector	9μm	9μm
↑	 C Anode $C_{th} = 372 \text{ mAh/g}$	45μm	< 1μm Li Metal Anode; $C_{th} = 3860 \text{ mAh/g}$
↑	 Electrolyte Separator	25μm	20μm No Separator
↑	 NMC cathode	50μm	50μm
↓	 Al current collector	15μm	15μm

$A = 0,0504 \text{ m}^2$   
 $L \times l = 24\text{cm} \times 21\text{cm}$

Figure 3-19: Comparison of the dimensions for different battery types

There are still a lot of challenges, fundamentals, and production and integration points, remaining to bring the solid-state battery technology to the market. The most important fundamental problems to be solves are (Figure 3-20):

- Ionic conductivity of the electrolyte,
- Improvement of the solid- solid interface (resistive Solid-Electrolyte Interphase (SEI) between Li and the electrolyte, the life span, grains boundaries lead to increased resistance of the cell)
- Dendrite growth: inhomogeneous Li deposition
- Stability: solid electrolyte react with active materials and need to be protected

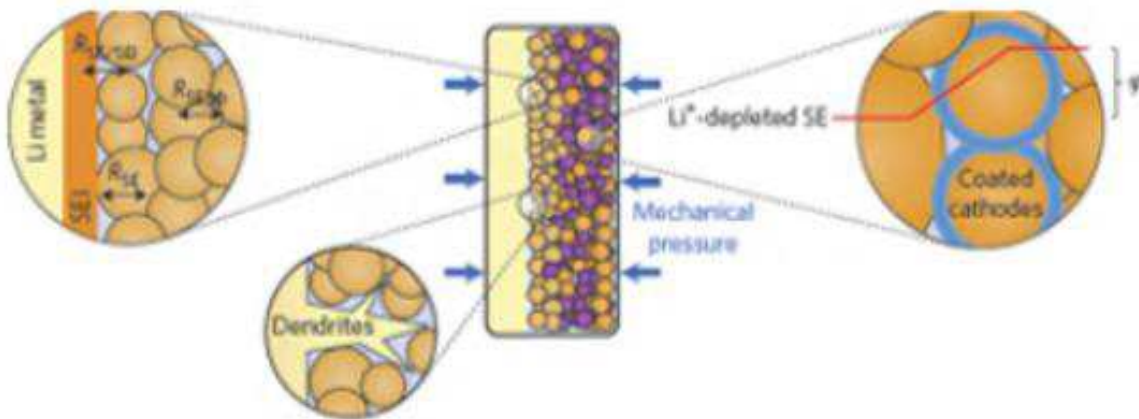


Figure 3-20: Fundamentals issues of the solid-state batteries

There are three main families of solid electrolytes, presented in Figure 3-21: solid polymer electrolyte, ceramic electrolyte and hybrid composite. The liquid electrolyte (Li salt in organic solvents) is given for comparison.

Liquid electrolyte (Lithium salt in organic solvents)	Solid polymer electrolyte	Ceramic electrolyte	Hybrid & composite
Carbonates: EC, DEC, PC, DMC Ethers: DOL, DME... Fluorinated carbonates: F-EC, F-VC, F-EPE.....	Poly ethylene oxide (PEO) based solid polymer Single ion conducting SPEs Polyacrylonitrile PAN	<b>Oxide-based</b> Lithium phosphorus oxynitride (LIPON) Perovskite: $\text{Li}_{0.34}\text{La}_{0.51}\text{TiO}_{2.94}$ Alumina $\alpha$ - $\beta$ -alumina; Garnet: $\text{Li}_7\text{La}_3\text{Zr}_2\text{O}_{12}$ (LLZO) LISICON: $\text{Li}_{2.2}\text{Zn}_{1-x}\text{GeO}_4$ NASICON: $\text{Na}_{3.7}\text{Zr}_{1.7}\text{La}_{0.3}\text{Si}_2\text{PO}_{12}$  <b>Sulfide Glass and Glass-Ceramic</b> Thio-LISICON: $\text{Li}_{2.5}\text{Si}_{0.5}\text{P}_{0.5}\text{O}_4$ , $\text{Li}_{0.54}\text{Si}_{1.74}\text{P}_{1.44}\text{S}_{11.7}\text{Cl}_{0.3}$ Argyrodit: $\text{Li}_6\text{PS}_2\text{Cl}$ Glasses: $\text{Li}_2\text{S-P}_2\text{S}_5$ , $\text{Li}_{10}\text{GeP}_2\text{S}_{12}$ Oxy-sulfides: $(100-x)(0.6\text{Li}_2\text{S}-0.4\text{SiS}_2)-x\text{LiMO}_x$	- Gel polymer + inorganic/organic fillers or plasticizers - SPEs with inorganic fillers - High salt: $(\text{Li}(\text{BH}_4)_{1-x}(\text{NH}_2)_x)$ - IL-nanoparticle hybrid - Polymer-nanoparticle hybrid - Polymer-ceramic composite: $\text{Li}_7\text{P}_3\text{S}_{11}$ wrapped PEO-LiClO <sub>4</sub> - Li-Polymer Matrix electrolyte: salt/Polymer/Solvent-Plasticizer

Figure 3-21: Classification of the solid electrolyte types

The solid-state battery technology is promising but it is still far from market maturity. In the near future the Li-Ion battery technology with liquid electrolyte is remaining the main technology for the electrification of the vehicles and it needs still to be improved and well managed when integrated in the vehicles (packaging, electric connections, thermal cooling and controlling (Battery System Management)).

### Conclusions of the study “Optimal designs of electric vehicles for a long-range mobility”

The relations between the battery capacity, the battery energy density and the range of the electric vehicles are investigated in Appendix C.2. The designs for different mobility services (urban and long ways distance electric mobility) of the electric vehicles are defined and the time interaction with the charging infrastructure is analyzed. Information and connectivity solutions that inform in real time the drivers for the availability and the location of the charging infrastructure, including the possibility to book and pay for charge points in different places is an important part of the solution. Combined with fast, i.e. high power charging capacities, pure electric vehicles would be able to serve long range needs. The analysis of the environomic Pareto curves on NEDC illustrates as well the relation between the economic and the environmental performances of the solutions. Electric vehicles can be used for long way mobility (>400 km), if they have a consequent quantity of battery on board (between 100 and 150 kWh). The density of the battery is also important for the autonomy of the electric vehicles. The important capacity of the batteries induces the need of the high power chargers to allow the fast charging of the batteries. The pick power demands induce to investigate adequate links for such electric vehicles with the electricity grid. The multi-objective optimization can be used in an enlarged energy system, including the electric vehicles and the electric grid.

### 3.3.2 An energy balance evaluation in LI-Ion battery packs under high temperature operation

Electric vehicles and hybrid electric vehicles are expected to increase their market penetration and to bring evolution concerning the main technologies for energy storage and conversion, the drive train components and the energy management. Lithium battery systems become a major component in vehicle drivetrains. In this research, the investigation of the energy balance evolution for Li-Ion battery system is described. The accessory environment of lithium battery systems is important for an accurate thermal and electrical management and the respect of the performances. A method to determine the energy balance through experimental investigations is proposed. Different configurations of Al and Cu busbars were used during the research. The evaluation of the energy balance is related to the energy dissipated and the exergy available in the battery system. The influence of different configurations of interconnections on the energy balance is shown.

In this study the energy balance of a battery package made from 18650 type cylindrical cells is investigated. The energy balance was calculated for a discharge process to avoid the influence of a power supply on heat transport during the charge process. The calculation and measurements were conducted for a realistic scenario. The maximum discharge current 2C-3C was used in order to keep the

temperature of the cells below 650°C. Battery modules were equipped with aluminum (Al) busbar or copper (Cu) busbar. The calculation of the energy balance was made with the proposed electro-thermal model of a battery module. The validation of the calculation was made through the measurements.

The first part of the study gives a proposal of a method to evaluate the quantity of energy produced under the effect of discharge process. An energy balance was built for the system characterization. This energy was evaluated for different types of materials of the busbars. The second part is dedicated to the experimental tests. In this part different configurations of busbars are evaluated.

### 3.3.2.1 Energy balance in Li-ion battery system

Li-ion battery systems are a very attractive technology for energy storage systems (ESS) for EVs and HEVs. They provide very high energy density and they enable the storage of high capacity in relatively compact cells. Based on the prediction, the market demand for the battery will rise very quickly. Based on the cylindrical cell it is possible to build modular systems of the battery packages. These battery packages can be easily connected in order to build big ESS. However, the operating temperature needs to be maintained within a specified range. This is needed to keep the electrical performance in a nominal range and to slow down the aging process of the cells.

In order to determine the energy balance, the amount of energy in the battery package has to be determined. The formula for the amount of total energy  $E_{tot}$  in a battery pack with  $b$  cells is shown in equation (3-9):

$$E_{tot} = b \cdot V_n \cdot C \quad (3-9)$$

where,  $b$  – number of the cells in a battery pack,  $V_n$  – nominal voltage of the Li-ion cell,  $C$  – capacity of the Li-ion cell.

However, this theoretical amount of energy is not available in normal conditions. To obtain the total energy the cell must be fully discharged, which leads to the destruction of the Li-ion battery.

The total accumulated energy  $E_{tot}$  can be divided into six parts of energy as shown in Figure 3-22.

The first two parts are:

- heat  $Q_{cell}$ , which is generated in the cells due to the internal resistance of cells  $R_{wc}$  and the chemical reactions in these cells,
- heat  $Q_{cab}$  generated in all cables and metallic connections due to their resistance  $R_c$  and  $R_{con}$  used to connect the battery package with the load,
- the  $Q_{dis}$  is the dissipated heat due to convection from the cells and the busbars,
- the fourth part is the  $Q_{bus}$ , and this is a Joules heat generated in the busbar,
- the fifth part in an energy  $EL$  that is delivered and effectively used by the load,
- the last part is the  $E_{BMS}$ , which is an energy delivered to Battery Management System (BMS).

First four parts are frequently considered as the lost energy, which reduces the efficiency of energy conversion in a battery pack, and limit the total amount of the exergy. In addition, these energies make the whole package warm up which is usually a highly undesired effect. The heat dissipated to ambient form metallic connections and cables is very small and it can be neglected.

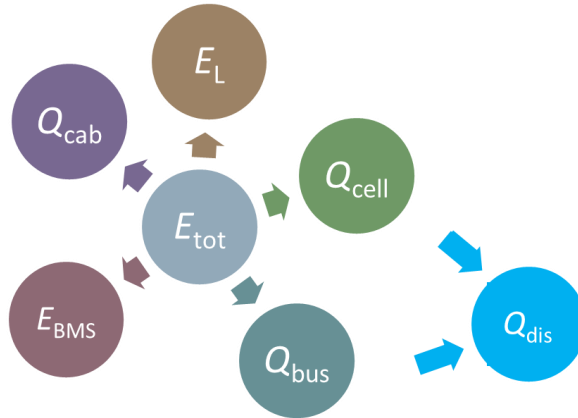


Figure 3-22: Energy distribution in the energy storage system

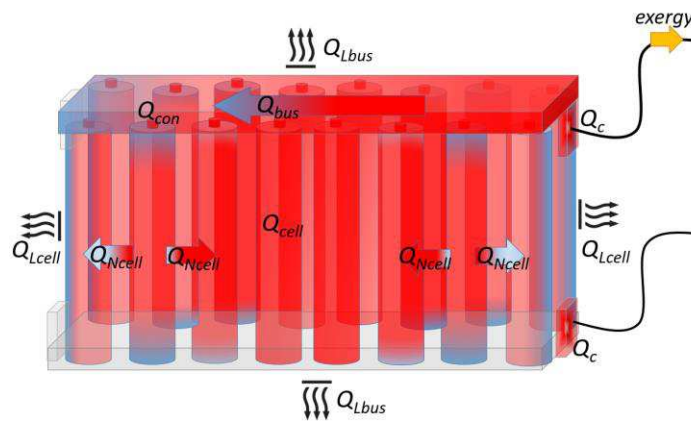


Figure 3-23: Energy flow in a battery pack

The heat  $Q_{cell}$  is generated in every cell of the battery pack. The Joules heat is generated in the busbars, cables and metallic connections between the cell and busbar as shown in Figure 3-23. Some of that heat is dissipated from the cells and busbars to ambient. The cells inside the battery package have a different condition for heat dissipation hence the cells inside the battery package can exchange the heat  $Q_{Ncell}$  between themselves.

The equation (3-10) for heat generation inside the battery was proposed by Bernardi [117]:

$$\begin{aligned}
 \dot{Q}_{cell} = & -IV - \sum_l I_l T^2 \frac{d \frac{U_{L,OCV}}{T}}{dT} + \\
 & + \sum_l \frac{d}{dt} \left[ \int_{v_j} \sum_i c_{i,j} RT^2 \frac{\partial}{\partial T} \ln \left( \frac{\gamma_{i,j}}{\gamma_{i,j}^{avg}} \right) dv_j \right] + \\
 & + \sum_{j,j \neq m} \sum_i \left[ \left( \Delta H_{i,j \rightarrow m}^0 - RT^2 \frac{d}{dT} \ln \frac{\gamma_{i,m}^{avg}}{\gamma_{i,j}^{avg}} \right) \frac{dn_{i,j}}{dt} \right]
 \end{aligned} \tag{3-10}$$

The first term in equation (3-10) is the electrical power produced in the battery, the second term is the sum of producible reversible work and entropic heating from the reaction. The third term is the heat produced from mixing, and the last term is the heat from material phase change.

This formula can be simplified to the form of equation (3-11) when the enthalpy-of-mixing and phase change terms are not considered [117] [118].

$$\dot{Q}_{cell} = IV - \sum_l I_l \left[ U_{l,ocv} - T \partial \frac{U_{l,ocv}}{\partial T} \right] + M_c c_{pc} \frac{\partial T}{\partial t} \quad (3-11)$$

Recently, a new proposal of equation (3-11) has been presented [119] into the following equation (3-12):

$$\dot{Q}_{cell} = R_{wc} i_{cell}^2 - i_{cell} T \frac{\Delta S}{n_e F} \quad (3-12)$$

where  $R_{wc}$ ,  $i_{cell}$ ,  $n_e$ ,  $F$  and  $\Delta S$  denote internal resistance of a cell, current of a single cell, number of electrons participating in the reaction, Faraday constant and entropy change. The values of  $\Delta S$  and  $R_{wc}$  for cylindrical batteries SONY-US18650G3 was estimated by Inui et al., [120].

In the battery package the heat is not only generated in the cells. The Joules heat generation occurs in busbars and also in all metallic connections and wires. The Joules heat in a battery pack can be calculated with equation (3-13):

$$\dot{Q}_{bus} + \dot{Q}_{cab} = i_{BP} \cdot V_{BP} = i_{BP}^2 \cdot (R_{bus} + R_c) \quad (3-13)$$

where  $\dot{Q}_{bus}$  is the Joules heat generated in the busbars and  $\dot{Q}_{cab}$  is sum of the Joules heat generated in cables  $\dot{Q}_c$  and metallic connections  $\dot{Q}_{con}$ ,  $i_{BP}$  is a current in battery pack,  $V_{BP}$  is a voltage of a battery pack,  $R_c$  is a resistance of cables and metallic connections in a battery package.

In a battery package some part of  $E_{tot}$  will be lost. This energy, called  $\dot{Q}_{dis}$  is a heat dissipation to the ambient from the cells and the busbars and it can be described with equation (3-14):

$$\dot{Q}_{dis} = \dot{Q}_{Lcell} + \dot{Q}_{Lbus} \quad (3-14)$$

where  $\dot{Q}_{Lcell}$  and  $\dot{Q}_{Lbus}$  are the heats dissipated from the cells and the busbars.

One of the most important parameters of a battery is the energy efficiency which is often [40] defined as the ratio of a provided electrical energy  $E_L + E_{BMS}$  to the  $E_{tot}$  of the fully-charged battery as presented in equation (3-15).

$$\eta_{cell} = \frac{E_L + E_{BMS}}{E_{tot}} = \frac{\int (R_{load} + R_{BMS}) \cdot i_{cell}^2(t) dt}{V_n \cdot C} \quad (3-15)$$

where  $R_{load}$  is the resistance of a load.

The amount of energy required for the BMS is hard to predict, since different constructions of the BMS consume different amount of electric energy. In further investigation presented this energy will be neglected.

### 3.3.2.2 Electro-thermal model of a single cell in a battery pack

#### Model formulation

The heat change  $\dot{Q}$  of a battery package with  $b$  cells can be calculated with a proposed heat accumulation model described by equation (3-16):

$$\dot{Q} = b\dot{Q}_{cell} + \dot{Q}_{bus} + \dot{Q}_{cab} - (b\dot{Q}_{Lcell} + \dot{Q}_{Lbus}) \quad (3-16)$$

If the temperature of all cells in the battery package is uniform the equation (3-11) and equation (3-16) can be transferred to another form (3-17) to easier designate the terms conducted with the heat accumulation in a cell. The first term on the right side of equation (3-17) is related to the heat generated in battery package  $\dot{Q}_{GEN}$ . The second term is related to the heat dissipation from the cells and busbars to the air.

$$\frac{\dot{Q}}{S_{BP}} = \frac{\dot{Q}_{GEN}}{S_{BP}} - [h_c(T_c - T_A) + h_b(T_b - T_A)] \quad (3-17)$$

where,  $S_{BP}$  is a surface of a battery package,  $h_c$  is the heat transfer coefficient of a cell,  $h_b$  is the heat transfer coefficient of a busbar,  $T_c$  and  $T_A$  are the cell and ambient temperature.

The heat generation takes place in three elements of the battery pack: in the cells, in the busbars and in the metallic connections and cables. Therefore  $\dot{Q}_{GEN}$  in a battery pack can be expressed with equation (3-18):

$$\dot{Q}_{GEN} = \dot{Q}_{cell} + \dot{Q}_{bus} + \dot{Q}_{cab} \quad (3-18)$$

It is known [121], [122], [123] that heat generation in a single cell is a sum of the reversible heat of the electrodes  $\dot{Q}_{rev}$  due to entropy change, the irreversible heat  $\dot{Q}_{irr}$  which corresponds to all types of heat generated in the cell as a result of the electrochemical reaction  $\dot{Q}_r$  and ohmic heating  $\dot{Q}_{ohmic}$ , as shown in equation (3-19).

$$\dot{Q}_{cell} = \dot{Q}_{irr} + \dot{Q}_{rev} = \dot{Q}_r + \dot{Q}_{ohmic} + i_{cell}T \frac{\partial U_{OCV}}{\partial T} \quad (3-19)$$

From equation (3-13), equation (3-18) and equation (3-20) the total heat generation in a battery package can be calculated:

$$\dot{Q}_{GEN} = b(\dot{Q}_r + \dot{Q}_{ohmic}) + i_{BP}T \frac{\partial U_{OCV}}{\partial T} + i_{BP}^2 R_c + i_{BP}^2 R_{bus} \quad (3-20)$$

The  $\dot{Q}_{irr}$  can be also presented in the following form [118], [121], [124]:

$$\dot{Q}_{irr} = i_{BP}(U_{OCV} - V) \quad (3-21)$$

where,  $V$  is the terminal voltage of the cells.

Based on equation (3-17), equation (3-20) and equation (3-21) the heat accumulated in a battery package can be calculated according to equation (3-22):

$$\dot{Q} = i_{BP}(U_{ocv} - V) + i_{BP}T \frac{\partial U_{ocv}}{\partial T} + i_{BP}^2(R_c + R_{bus}) - [h_c S_c (T_c - T_A) + h_b S_b (T_b - T_A)] \quad (3-22)$$

It can be assumed that the heat accumulation of the battery package is the heat accumulation of all cells  $b \cdot \dot{Q}_{Acell}$  and heat accumulation of busbars  $\dot{Q}_{Abus}$  as shown in equation (3-23) hence the heat accumulation of a battery package can be calculated from equation (3-24).

$$\dot{Q} = b\dot{Q}_{Acell} + \dot{Q}_{Abus} = \frac{bM_c c_{pc}}{\partial t} (T_c - T_A) + \frac{M_b c_{pb}}{\partial t} (T_b - T_A) \quad (3-23)$$

$$\begin{aligned} \frac{bM_c c_{pc}}{\partial t} (T_c - T_A) = & \\ = & \left( i_{BP}(U_{ocv} - V) + i_{BP}T \frac{\partial U_{ocv}}{\partial T} \right) + i_{BP}^2(R_c + R_{bus}) \\ & - \left[ h_c (T_c - T_A) S_c + h_b (T_b - T_A) S_b + \frac{M_b c_{pb}}{\partial t} (T_b - T_A) \right] \end{aligned} \quad (3-24)$$

### Model assumptions and calculation

To calculate the electro-thermal model the following constants had to be assumed: heat transfer coefficient of the side walls of the cells  $h_c$ , heat transfer coefficient of copper busbar  $h_{b\_Cu}$ , heat transfer coefficient of aluminum busbar  $h_{b\_Al}$ , specific heat of li-ion cells  $c_{pc}$  and busbar  $c_{pb}$ . Based on the literature the following values were assumed:  $h_c = 7.9 \text{ W/m}^2\text{K}$  [120], [125], [126],  $c_{pc} = 800 \text{ J/kgK}$  [127], [128],  $h_{b\_Al} = 20 \text{ W/m}^2\text{K}$  [129], [130],  $h_{b\_Cu} = 15 \text{ W/m}^2\text{K}$  [130], [131], specific heat of Al busbars  $c_{pb\_Al} = 900 \text{ J/kgK}$  [129] and specific heat of Cu busbar  $c_{pb\_Cu} = 385 \text{ J/kgK}$  [129].

Enthalpy-of-mixing and phase change terms are not considered. In addition, all cells were carefully selected before the tests and they had designated capacity and internal resistance. The difference of cells SoC level was less than 1%. Moreover, the nominal voltage of the whole battery package was measured just before the test to obtain the same conditions during measurements.

For the calculations the battery package made of sixteen 18650 type cylindrical cells connected in parallel was assumed. The cells are connected with two busbars made of Al or Cu placed on top and bottom of the cells.

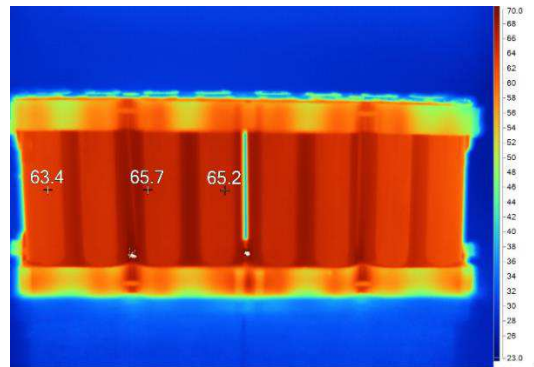


Figure 3-24: Temperature inside the battery package, in °C

The temperature inside the battery package is uniform and there is no heat exchange between the cells as shown in Figure 3-24, only natural convection via side walls of the cells and surfaces of the busbars

was taken into account. The temperatures of the busbars are the same as the cell temperature. It was decided not to separate  $R_{load}$  and  $R_c$ , because in real conditions the cells must still be connected with the load by cables. The heat flow in battery package is shown in Figure 3-25. The heat is dissipated via natural convection from the busbars and cells. Joules heat is generated in busbars, cables and metallic connection between cells and busbars. Each cell generates the same amount of heat  $Q_{cell}$ .

The symmetry of a battery package is taken into account and therefore only half of the battery package is shown.

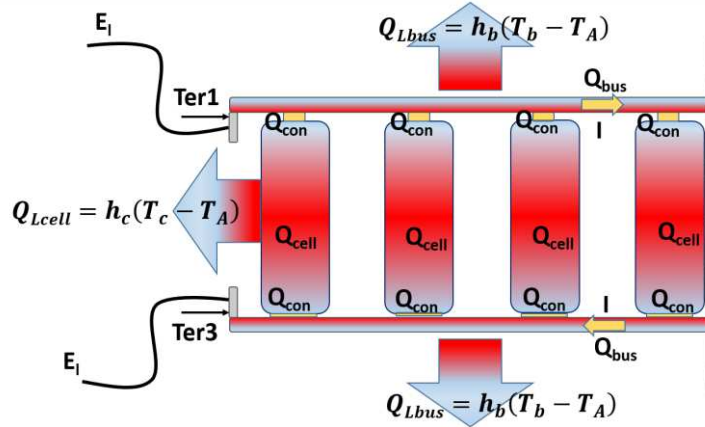


Figure 3-25: Heat flow in a battery package

To calculate the  $Q_{bus}$  in the symmetry of the busbar (Figure 3-25) was taken into account as shown in equation (3-25).

$$Q_{bus} = 2 \int_0^{t_{off}} ((2i_{cell}(t))^2 0.5R_{bus} + (4i_{cell}(t))^2 0.375R_{bus} + (6i_{cell}(t))^2 0.25R_{bus} + (8i_{cell}(t))^2 0.125R_{bus}) dt \quad (3-25)$$

where  $t_{off}$  is the time of discharge process of the battery package.

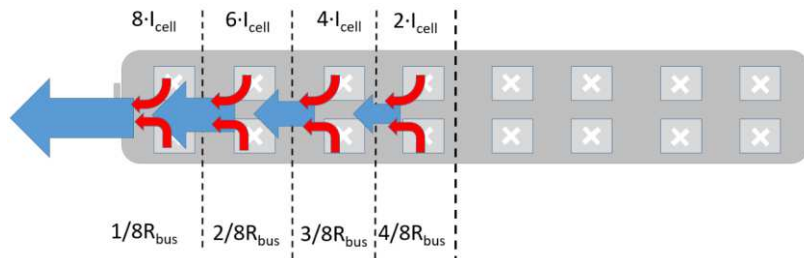


Figure 3-26: Symmetry of the busbar

Equation (3-26) can be used to determine the sum of energy  $E_L$  and  $Q_{cab}$ .

$$E_L = \int_0^{t_{off}} R_{load} \cdot i_{BP}^2(t) dt \quad (3-26)$$

For the model calculation the temperature gradient between the cells and the ambient as well as between the busbars and the ambient were taken as presented in Figure 3-27.

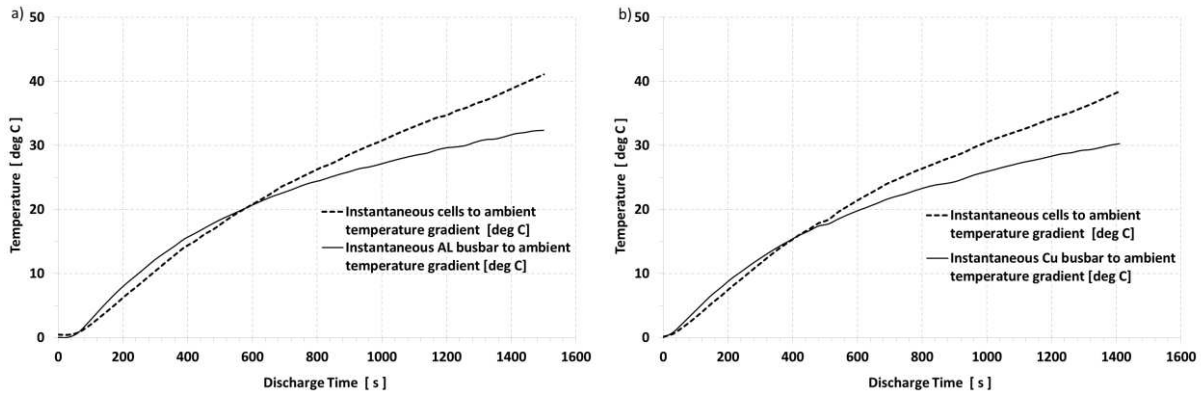


Figure 3-27: Temperature gradient in battery pack with Al busbar a), Cu busbar b)

Based on (3-25), (3-36) and characteristic shown in Figure 3-27 the energy balance for battery package was calculated. The obtained results are presented in Table 3-4.

Table 3-4: Energy balance calculation for the battery pack

Energy type	Cu Busbar	Al Busbar
$16 \cdot Q_{\text{Accell}}$ [kJ]	23.6	25.1
$Q_{\text{Abus}}$ [kJ]	0.6	1.6
$16 \cdot Q_{\text{Lcell}}$ [kJ]	17.5	20.5
$Q_{\text{Lbus}}$ [kJ]	4.3	6.5
$Q_{\text{GEN}}$ [kJ]	46.0	53.7

Based on the model calculation it can be stated that in the battery package with Cu busbar 46 kJ of heat will be generated, while in the battery package with Al busbar  $Q_{\text{GEN}} = 53.7$  kJ. The battery package with the Cu busbar will accumulate almost 53% of this heat and the rest will be dissipated. In the battery package with Al busbar around 50% of  $Q_{\text{GEN}}$  will be accumulated. The different values of  $Q_{\text{GEN}}$  result from lower resistance of copper busbars.

### 3.3.2.3 Electro-thermal model validation

#### Measurement setup and procedure

The proposed electro-thermal model was validated with the real measurements. For the evaluation of the discharging parameters of Li-Ion cells in battery modules, the SONY-US18650G3 cylindrical cells with nominal capacity of  $C = 3120$  mAh, rated voltage  $U_{\text{ocv}} = 4.20$  V, rated internal resistance  $R_{\text{wc}} = 13$  mOhm and average mass of  $M_c = 46.6$  g were used. A module of 16 batteries connected in parallel (16P1S) was adopted for the tests. The cells were placed in a 2x8 package with an air gap of 2 mm. Thus the heat exchange conditions with the surroundings are similar for all cells. The configuration dedicated for the tests has been equipped with 4 connection terminals as shown in Figure 3-28.

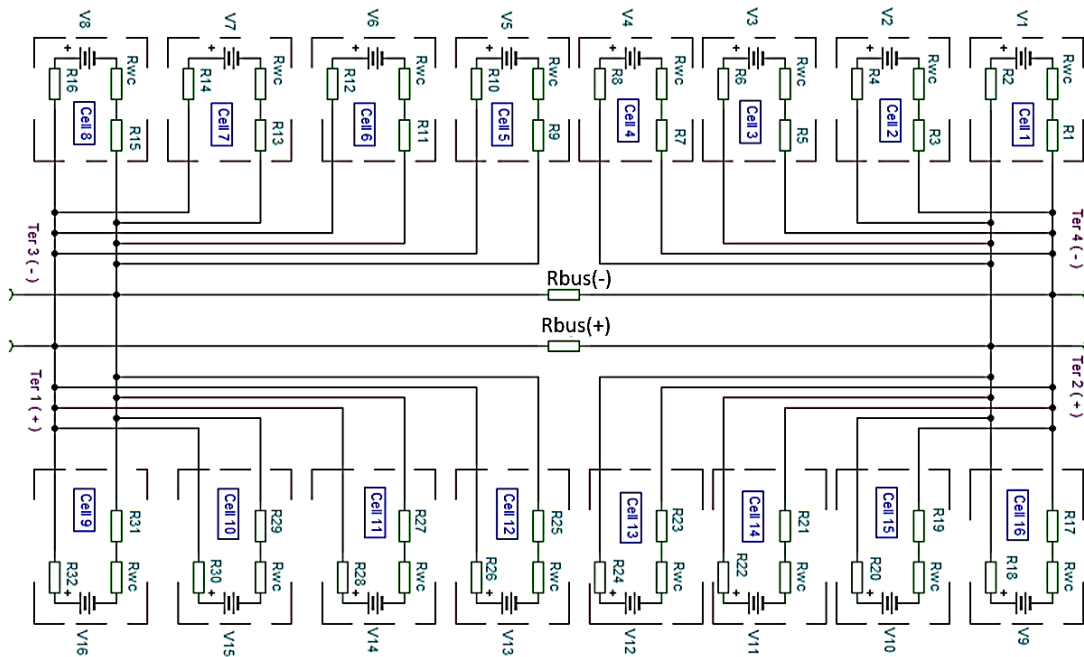


Figure 3-28: The electrical circuit of the battery module with the parasitic resistances in steady-state operation conditions

In Figure 3-28 the cell potentials have been marked as V1-V16, internal cell resistances as  $R_{wc}$ , resistances of welded cell-busbar connections as  $R_1 \div R_{32}$  and resistance of busbars  $R_{bus}$  measured as terminal-to-terminal (T1-T2, T3-T4) connection.

The electrical connections of the cells in the 16S1P system were made using hybrid busbars made of copper and aluminium, respectively, equipped with nickel pads dedicated to welded connections as shown in Figure 3-29. Table 3-5 lists the busbar parameters.

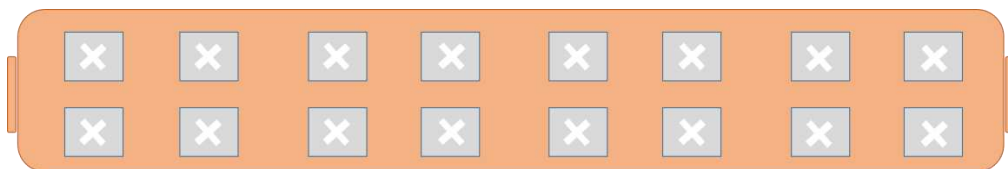


Figure 3-29: Front view of the Cu busbar with 16 welding spots

All cells used to make the module were selected so the electrical parameters  $R_{wc}$  and  $X_{wc}$  were from a range  $1.02 \text{ m}\Omega < R_{wc} < 1.12 \text{ m}\Omega$ ,  $0.45 \text{ m}\Omega < X_{wc} < 0.55 \text{ m}\Omega$ . Before the tests, the cells in the battery package were charged to a voltage of 4.20 V with the current 3.0 A (constant current/constant voltage – CC/CV) at room temperature 23°C and they were discharged in the same way till the voltage 2.60 V with the Chroma BTS 17011. Charge and discharge procedures were repeated three times in order to prepare the cells for the tests.

Table 3-5: Parameters of busbars applied for the tests

Parameter	Copper Busbar	Aluminium Busbar
Thickness [mm]	0.50	1.50
Width [mm]	32.25	32.15
Length [mm]	150.50	158.50
Resistance Terminal-to-Terminal [mΩ]	0.492	0.677
Number of welding spots	16	16
Total mass of busbar[ kg ]	0.028	0.027

Dissipation parameters and thermal dependencies were determined during the discharging of the battery package. Cell discharging was carried out with the measurement system based on Keysight 34972A multi-channel scanning multimeter with 34901A scanning module. The temperature profiles were measured during the discharge process with the discharge current 2C-3C. The load resistance has been selected to prevent the load current exceeding 3C value and in the absence of forced cooling system and to keep the temperature of the battery module below 65°C. During the discharge tests, temperature measurements of the cells and the busbars were carried out. In Figure 3-30 the points of temperature measurement has been presented.

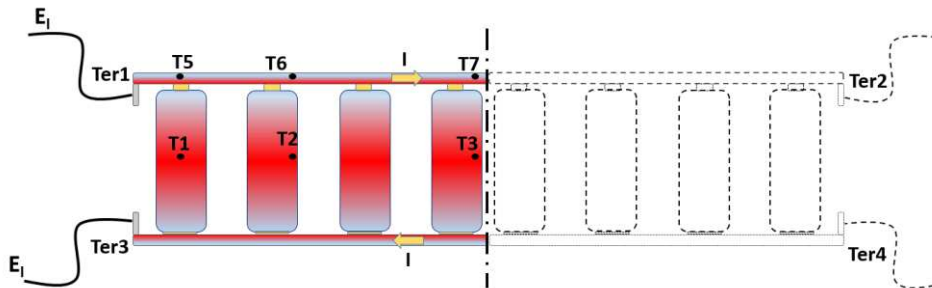


Figure 3-30: Distribution of temperature measurement points on the battery package

The distribution of the measurement points resulted from the symmetry of the packet relative to X and Y axis. The ambient temperature  $T_0$ , the temperature of the T1, T2 and T3 cells and the temperature of the T5, T6 and T7 busbar were recorded simultaneously with the measurements of electrical parameters. For temperature measurement, Keysight K-type thermocouples and the Keysight 34972A multi-channel scanning multimeter with 34901A scanning module were used.

Discharge tests were carried out in an explosion proof chamber with the 0.25m<sup>3</sup> volume without air exchange and forced cooling. Discharge test procedures were performed with battery charge monitoring up to the voltage  $U_{ocv} = 4.18 \pm 1\%$  load cut-off system at  $V_{cutoff} = 2.60V \pm 1\%$ . Temperature measurements at  $T_0 \div T_7$  points,  $V_{BP}$  voltage and  $I_{BP}$  current were carried out synchronously with the frequency of 2 samples per minute until  $V > V_{cutoff}$ .

### 3.3.2.4 Results and discussion

Temperature as a function of time of the discharge process is shown in Figure 3-31. For the battery package with Al busbar (Figure 3-31a) during the initial phase of discharge busbar near the terminal was getting hot the fastest. It was caused by the highest current density in this place. At the end of the discharge the temperature of the cells was around 5°C bigger than for the busbars and it can be explained as better heat dissipation from the busbars. The Al busbar can be treated as thermal bridge for the cells and therefore the temperature inside the battery package is almost uniform.

At the beginning of the discharge of the battery pack with Cu busbar temperature measured in point T1 also raised quicker. However lower resistance of Cu busbar in comparison of Al busbar caused that finally busbar had lower maximal temperature during the discharge, as shown in Figure 3-31b. It is also the reason why the cells in battery pack had lower temperature.

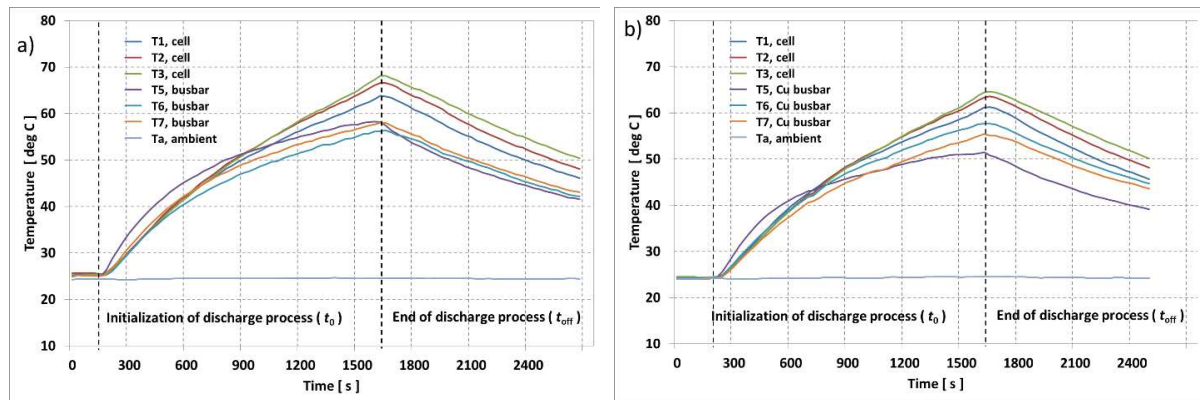


Figure 3-31: Characteristics  $T(t)$  measured for the battery pack with Al busbar a), with Cu busbar b)

Table 3-6 shows the measured energy balance for both types of the battery packs. In both cases they had the same initial value of  $E_{tot}$ . The battery package with Cu busbar allowed 5.5kJ more of electric energy to be delivered to the load than the battery package with Al busbar. The  $Q_{GEN}$  in the battery package with Cu busbar was more than 10% lower in comparison to  $Q_{GEN}$  in the battery package with Al busbar.

Table 3-6: Balance of energy in battery system

Type of busbar	$E_{tot}$ [kJ]	$E_l$ [kJ]	$Q_{GEN}$ [kJ]
Copper	647.0	598.4	48.6
Aluminium	647.0	592.9	54.1

The measurement validates the developed model of a battery package. The difference between the calculated and the measured  $Q_{GEN}$  is less than 6% for the battery package with Cu busbar and 1% for the battery package with Al busbar. The small difference between the calculated and measured values of  $Q_{GEN}$  is caused by the inaccurate assumption. The theoretical values of the coefficient taken for model calculation can be slightly different than realistic values. As shown in Figure 3-31 the temperatures of the cells and the busbars are not the same and that caused different heat dissipation from cells and busbars.

Table 3-7: Balance of energy in battery system

Type of busbar	$Q_{GEN}$ [kJ] from exp.	$Q_{GEN}$ [kJ] from model
Copper	48.6	46.0
Aluminium	54.1	53.7

## Conclusions

The cylindrical batteries allow to build a very wide range of different battery package. Such battery package can be further connected in a modular systems e.g. for the big energy storage systems. The investigation of a heat generation in modular system is very important. This research presents a thermal energy balance of two types of the battery packs during the discharge process. One battery package was equipped with Al busbars while the other had Cu busbar. The investigated battery packages were made of sixteen 18650 type cylindrical cells. The calculation of the energy balance allowed to calculate the amount of generated heat inside the battery packages which is key information from the operation safety point of view. The conducted calculations were validated by the measurements of real battery package. The difference between the calculated model and the measured values were 6% for the battery package with Cu busbar and 1% for the battery package with Al busbar. By replacing the Al with the Cu busbar it is possible to reduce  $Q_{GEN}$  by 10%.

# **Chapter 4 Extension of the vehicle energy systems: the vehicles as grid related systems to the energy grids for optimal energy services**

The recharging of the vehicles and their connection to the energy grid became an important question. This chapter considers the recharging ecosystem and the design of the electric vehicles grid related energy systems for optimal mobility service. The idea is to research recharging strategies that extend the autonomy of the electric vehicles. The electric vehicles can be used for long-range trips. The communication strategy and the coordination of the recharging plans of the vehicles reduce the waiting times on the recharging stations, increase the rate of use of the stations, optimize the number of chargers, and so reduce the investment costs that are needed. The electric vehicles are considered as vehicles related to the electricity grid. The optimal recharging plan and the coordination of the recharging between the vehicles and the recharging infrastructure allow using electric vehicles for long distance trips. The rapid charging infrastructure is invested and deployed for the high ways. The domestic recharging systems are slow speed systems. The recharging operation at home is a frequent operation. An innovative robotized solution for recharging is investigated for the recharging task at home. This innovation is called the “robot charger”. The household is considered as the cluster for energy integration where energy services for mobility and household needs (electricity providing and heating) are integrated. In this cluster integration the vehicle provides energy services to the household when is not used. The vehicle is equipped with highly efficient energy propulsion system based on electric vehicle with a range extender module of solid oxide fuel cell using renewable fuel. The environomic multi-objective optimization is used for the energy services integration. The results show a large-scale reduction of emissions and efficiency improvement of the energy integrated system in comparison of the conventional system, where energy for mobility and household are provided on a separate way.

## **4.1 Design of electric vehicles grid related energy systems for optimal mobility service**

In this research, the energy system is extended and includes in its boundaries the energy storage and conversion of vehicles and their connections to the energy grid. The extended energy system is modelled on vehicles flows on the highway and a single objective optimization is performed to define the optimal energy storage capacity of the vehicles and the optimal number of recharges of from the grid.

The recharging systems are classified according to their power. Figure 4-1 defines the charging systems as slow and fast charging systems. The power determines the time to charging of the battery. The time and the occupation rates of the chargers are as well evaluated. The optimality is researched for long trip drives on electric mode. The results illustrate a method to rethink the usage and the energy management on the vehicle during the driving. As well it is researched how to adapt the recharging capacities and their location on the grid, by using a holistic approach. The target is to propose a high quality service for the electric mobility for long way drives.



Figure 4-1: Definition of the recharging systems

The novelty of the present study is the modelling and the optimization of the design and the operation parameters of the extended vehicle energy system. This system includes the vehicles and their interactions with the electricity grid. The optimization manages the minimization of the vehicles waiting time on the charging stations. On that way the relation to the energy grid, is considered, as well. Methods, techniques to analyse, improvement and optimizations of energy systems have to deal with not only the energy consumption and economics of the electric vehicles, but also with the availability and the distribution of the charging infrastructure. The target is to propose strategies to manage the recharging plans of the electric vehicles for long way trips.

### 4.1.1 Minimization of the waiting time

The model of the recharging is described in Appendix B.

#### Problem definition

The vehicle is considered as a part of the electric grid, when is it connect to charge its high voltage battery. For an optimal operation, the battery state of charge is considered variable between 30% and 80% of the total battery capacity. In some cases the vehicle should fulfill the entire battery, in some other cases a given percentage of the battery. The problem of the energy demand and supply of the electric vehicles on the highway has to be modelled and optimized. Figure 4-2 introduces the graphical representation of the highway and the recharging infrastructure.

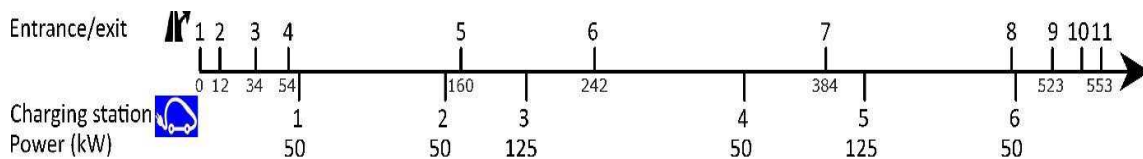


Figure 4-2: Highway with charging stations installations

The charging stations characteristics located on the road are given in Table 4-1:

Table 4-1: Initial charging stations characteristics

Localization of the station (km)	Power output (kW)	Number of chargers
60	50	1
150	50	1
200	125	1
334	50	1
408	125	1
501	50	1

The charging stations are located on different spots and the distance between them is not equivalent. The electric vehicles have different battery capacities stored on board (100 kWh, 60 kWh and 41 kWh). These capacities correspond to future electric vehicles deployed on the markets. The recharge of the vehicles on the highway is considered to occur between 15% and 80 % of the State of charge (SoC) of the high voltage battery. The battery can be fully recharged in the home installation, which is with charging powers lower than 50 kW. The vehicles have to quit the highway with at least 20% of the state of charge (SoC). To recover this condition of minimum SoC when leaving the highway, the vehicles have to stop on the closest recharging station.

The flows of the electric vehicles entering on the highway are characterized with the following types, described in Table 4-2.

We assumed in this research that the vehicles speed and energy consumption are constant during the drive. Those assumptions are not too strong, as the related approximations (few minutes) are negligible compared to waiting times (around half an hour).

Even if batteries charging power are given as constants, these powers depend on many factors, such as the battery temperature, state of charge and state of health, but also availability of the grid power. The charging profile can then be very complex and not reproducible, but some characteristics remain:

- Charging power is almost constant and equal to the max until the SoC reaches 80%
- It is easier to charge a battery when its SoC is low

This charging power model is applicable for SoC between 0 to 80%. For all cars, the charging power, when the SoC is 0%, is equal to the maximum charging power. It then slowly and linearly decreases when the SoC increases. The slope depends on the vehicle. We will also assume that users will recharge only up to 80% of SoC.

Table 4-2: Vehicles types for the flows constitution

Parameters	Vehicle type 1	Vehicle type 2	Vehicle type 3
Battery capacity [kWh]	100	60	41
Minimal SoC [-]	15	15	15
Maximal SoC [-]	80	80	80
Power of charge	125	350	44
Electric consumption [kWh/100km]	18	15	15
Max speed [km/h]	130	130	110
Final SoC required (Quitting the highway) [-]	20	20	20

The decision variables for the powertrain design are defined in Table 4-3:

Table 4-3: Decision variables for powertrain design

Decision variables for design	Range
Number of charging stations [-]	[1-6]
Number of chargers per charging station [kW]	[1-150]
Charged Power [kW]	[0-350]
SoC per vehicle [%]	[20-80]

## 4.1.2 Results of the optimization

The optimization of the waiting time is performed for a flow of 10 electric vehicles, driving on the highway (4-1):

$$\min(\text{Time}_{\text{waiting}}(x)), x \in X_{\text{decision\_variables}}, 10\_Vehicles \quad (4-1)$$

The flow is composed of 10 vehicles. The random function of Matlab is used to distribute the vehicles, their battery capacity and state of charge, the numbers of in-/out-comes from the highway and the time of their entrance. The random generated traffic configuration is summarized in Table 4-4. The highway disposes with 6 chargers, disposed according to Figure 4-2.

Table 4-4: Electric vehicles flow on the high way – 10 vehicles

Vehicles number	Battery capacity	Number of the Incomes [-]	Number of the Outcomes [-]	Initial SoC (entering to the highway)	Time of entering (h)
1	100	7	10	70	6,49
2	60	1	10	96	7,50
3	41	3	10	90	8,15
4	41	2	9	100	8,62
5	60	1	3	82	9,10
6	100	3	4	58	10,19
7	41	1	5	58	11,19
8	41	2	10	80	11,23
9	60	5	7	96	11,75
10	100	1	10	64	11,90

The results of the minimization of the waiting times of the vehicles are given in Figure 4-3. For this configuration of the traffic with 10 vehicles and 6 chargers on the road, the vehicles do not need to wait to recharge their batteries. The available charging infrastructure is enough to cover the recharging needs. Figure 4-3a represents the evolution of the State of charge (SoC) of each vehicle as a function of the time on the highway. When the vehicles are traveling, the SoC decreases. The charging periods of the highway stay are marked by the increasing of the SoC of the vehicles. The charging periods have different time durations, and deferent slopes. That is directly related to the battery capacity (Table 4-2) and the power of the charger (Table 4-1). There are different cases of trips. The trips represented on the Figure 4-3a are all optimal. They present minimal waiting time, minimal number of stops and minimal charged energy from the grid. According to the trip that they have to do, and their initial SoC, some vehicles enter, drive and quit the highway without any stops. This is the case of vehicle 1 and vehicle 9. The slope of discharge of their batteries is deferent, because the different capacity of the batteries on board. Both of the vehicles drive at 130 km/h of speed. The vehicle 1 has 70 kWh of energy in the battery when enters on the highway and quits it with 40 kWh. There is no need to stop and recharge the batteries on the highway. The vehicle 9 enters with 57 kWh of energy in the battery and quits it with 24 kWh of battery, which represents 40% of the battery capacity. Thus, in the case of vehicle 9, there is no need as well to stop and recharge on the highway. The vehicles have to stop in average 2 or 3 times to recharge, according to their battery capacity and the long distance trip that they have to perform. Figure 4-3a shows as well that the random flow of 10 vehicles stays on the highway for a total time of 11 hours. From illustrations on the Figure 4-3b one can see that none of the vehicles wait for an available charger. They arrive and can start to recharge without having queue length. Figure 4-3c shows that the queue length is zero for all the chargers on the highway.

The time spent on the highway for each vehicle depends on the trip time, the waiting time to access the charger and the recharging time. Figure 4-3d illustrates the ratio between the stops time to the trip time for every vehicles. The ratio is defined by (4-2):

$$r = \frac{Time_{waiting} + Time_{charging}}{Time_{trip}} \quad [-] \quad (4-2)$$

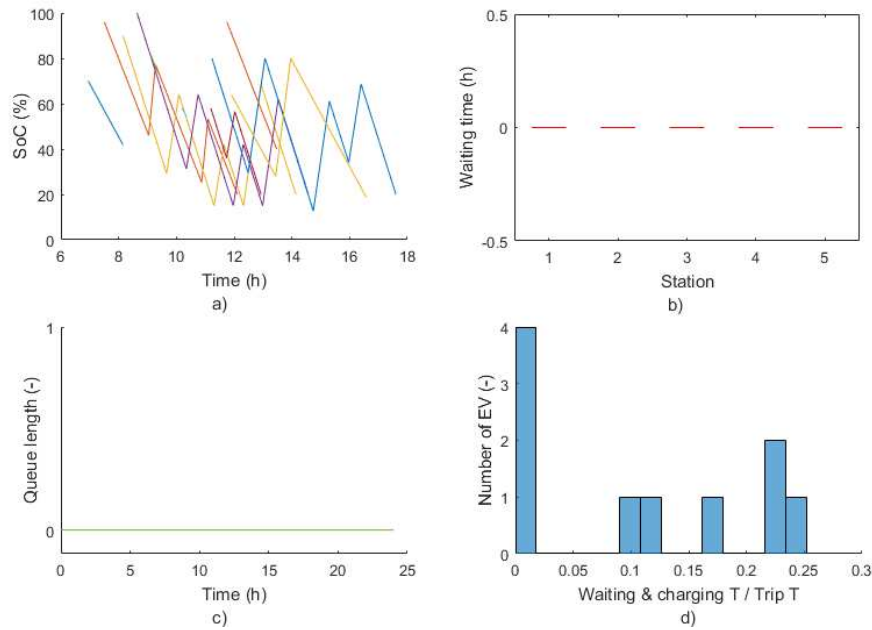


Figure 4-3: Results from the optimization: flow of 10 vehicles, minimization of the waiting time

Figure 4-3d shows that four vehicles are characterized by zero waiting and charging time. One vehicle waits 10% of its trip time to recharge. Other two vehicles are waiting 20% of their trip time for recharging. The maximum of the ratio is reached for one vehicle that spends 25% of its trip time to recharge. This vehicle has battery capacity of 40 kWh and stays for 500 km on the highway and has to stop for recharge at least 3 times.

In order to test the performances of the optimization method the number of the vehicles in the highway flow is increased to 30. Optimization of the waiting time is performed for a flow of 30 electric vehicles, driving on the highway (4-3):

$$\min(\text{Time}_{\text{waiting}}(x)), x \in X_{\text{decision\_variables}}, 30\_Vehicles \quad (4-3)$$

The flow is composed of 30 vehicles. The random function of Matlab is used to distribute the vehicles, their battery capacity and state of charge, the numbers of in-/out-comes from the highway and the time of their entrance. The random generated traffic configuration is applied. The highway disposes with 6 chargers, disposed according to the Figure 4-1. The results of the optimization converge on the results, illustrated in Figure 4-4. The vehicles stay 12 hours on the highway. Their batteries are recharged between 20% and 80% of SoC on the highway, with the high power chargers. Some of the vehicles enter on the highway with fully recharged batteries, for that reason their SoC is superior to 80%. In the case of a flow of 30 vehicles and 6 chargers, some of the vehicles have to wait for available chargers when they stop to the charging infrastructure. The waiting times are illustrated with the flat curves in Figure 4-4a. For better visibility of the optimization results, the descriptive statistics are used in the Figure 4-4b. The box plot diagrams of the vehicles waiting times are used for every charger station. The box plot diagram in descriptive statistic is a standardized way of displaying the distribution of data based on the five-number summary: minimum, first quartile, median, third quartile, and maximum. In the simplest box plot the central rectangle spans the first quartile to the third quartile (the interquartile range or IQR). A segment inside the rectangle shows the median and "whiskers" above and below the box show the locations of the minimum and maximum (Station 1 and Station 4, (Figure 4-4 b)). When the "whiskers" are absent means that the interval of data is important and the minimum and maximum are plotted with markers (Station 2, Station 3 and Station 6). From Figure 4-4 b one can see the maximal waiting times for every station. For example for the maximal waiting time on the charger on the station 1 is 0,62 h, the maximal waiting time on the charger on the station 2 is 0,9 h (which also the maximal time for the entire flow) and 0,62 h for the charger on Station 4.

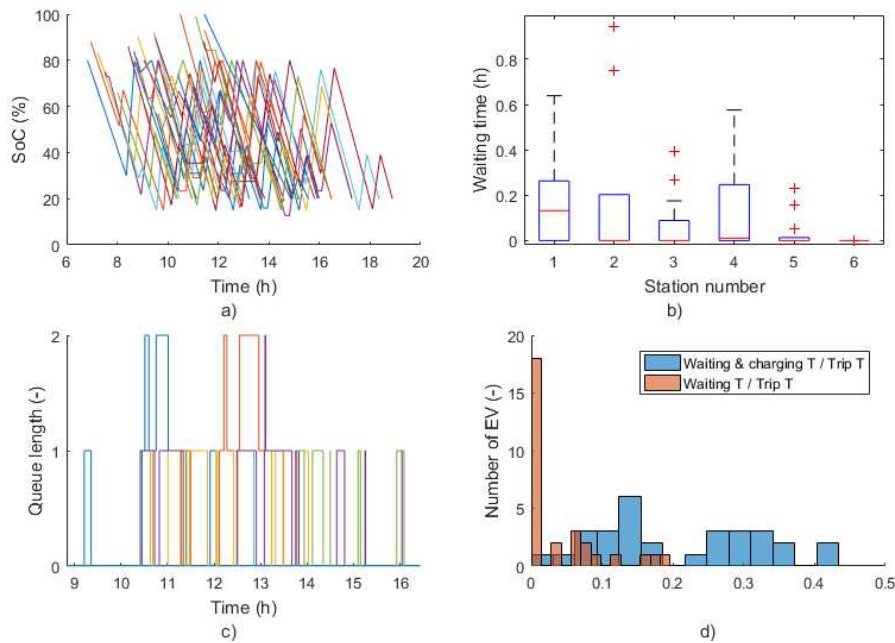


Figure 4-4: Results from the optimization: flow of 30 vehicles, minimization of the waiting time

The repartition of the maximal waiting time can be explained by the fact that the chargers on Station 1, Station 2 and Station 4 had the lowest power of 50 kW. They are as well located in the beginning and the middle of the highway, and the number of vehicles is important on that section. The charger 6 has as well the same power of 50 kW but is located at the end of the highway, so the vehicle flow is not important to cause important queue of vehicles. The chargers on Station 3 and 5 have the power of 125 kW and allow charging the batteries on a rapid way.

The queue length as a function of the time is presented in Figure 4-4c. One can see that the maximal queue length is composed of 2 vehicles. The waiting times on the chargers are different because the different vehicles have different capacities of the batteries.

Figure 4-4d illustrates the time repartition from the vehicles point of view. The ratio of the waiting time to the trip time and the ratio of the waiting and charging time to the trip time is illustrated per number of vehicles. One can notice that the maximal ratio of waiting time to the trip time is 0,2. The largest number of vehicles 18, never stops to recharge. The rest of the vehicles waiting are one or two, according as well to the representation in Figure 4-4d. The histograms represented in blue include as well the recharging time to the waiting time. The maximal ratio is noted to 0,4. This means that two vehicles spend 40% of their trip time to wait and recharge. The rest of the values are divided between 0 and 0,4 , with maximal number of vehicles 7, sending 15% of their trip time to wait on the queue and recharge their batteries.

**Conclusions**

The discussed study cases of the vehicles flows (10 and 30 vehicles), illustrates the method and the simulation model, proposed to investigate the long-range mobility with electric vehicles. The results of the study cases show on a didactic way the impact of the vehicles flow density and the consideration of the model of the number of vehicles, the queue lengths to access the chargers on the stations and the time to recharge the batteries of the vehicles. The method allows identifying the frequency of recharging and the usage of the chargers. This analysis is useful to reduce the waiting times and recharging times of the vehicles. The placement of additional chargers can be tested. The investment cost of the charging stations can be considered in the decision criteria. The localization of the chargers has to be minimal from investment cost point of view. Techno-economic multi-objective optimization can be introduced to show the trade-off between the optimal number of chargers that have to be introduced to reduce the waiting times, and the total investment cost of the infrastructure.

## 4.2 Coordination interest for the optimization of electric vehicles long distance trips

This research presents a method to coordinate electric vehicles recharging during long distance trips. It relies on communications between vehicles and infrastructures. The communications are called V2X. The objective is to enhance the use of the infrastructure by improving the distribution of vehicles between the different charging stations. The objective is to reduce the waiting time. The performance of this system is compared to an uncoordinated situation and a situation with optimal vehicle distribution. A case study on a 550 km highway is conducted. The results show a 10% reduction in the time spent in stations thanks to the communication. This situation is tested for a heavy traffic.

In this research, we are motivated by the means that must be implemented in order to coordinate the choices of EVs quick charge, especially during long distance trips. By allowing electric vehicle drivers to avoid queues, it shows great potential timesaving for users and better use of the charging infrastructure, limiting consequently the necessary investments. However, these means must be designed in such a way that they can be easily implemented.

In the following sections, the deployed method is firstly presented including the model and the assumptions. The algorithm used for the optimal solution research is detailed. Thereafter the proposed communication scenarios are described, with its structure and its calibration. The model is applied to a simulation of the vehicles flow on a 550 kilometers highway.

### 4.2.1 Minimization of the waiting time

$$T_{Trip,n} = T_{Driving,n} + \sum_{j=1}^N T_{Station j,n} \quad (4-4)$$

$$T_{Station j,n} = T_{Wait j,n} + T_{Charge j,n} + T_{Other j,n}$$

Where:

$T_{Wait j,n}$  = Waiting time for an available charging point, when the station is full (in minutes)

$T_{Charge j,n}$  = Time required to store the intended amount of energy (in minutes)

$T_{Other j,n}$  = Constant representing time needed for all other operation: decelerating, accessing the station, launching the charging session (here set to 5 min)

We sum up the optimization definition by:

$$\begin{aligned} \min_x \quad & f(x, y) \\ \text{u.c.} \quad & \forall t, \forall n, SoC_{min,n} \leq SoC_n(t) \\ & \forall n, SoC_n \leq SoC_{max,n} \text{ after recharge} \\ & \forall n, SoC_{exit,n} \leq SoC_{exit required,n} \end{aligned} \quad (4-5)$$

We want to minimize  $f$  as a function of the decision variables  $x$ , as defined in (4-5) under constraints of State of Charge (SoC). Variables  $x$  are the scheduled energy stored  $(E_{n,j})_{\forall n,j}$ .  $SoC_n(t)$ ,  $SoC_{min,n}$  and  $SoC_{max,n}$  respectively represents state of charge of vehicle  $n$  at time  $t$ , minimum and maximum.  $SoC_{exit,n}$  and  $SoC_{exit required,n}$  represent respectively the SoC at highway exit obtained and required. The variables  $x$  of this function are continuous.

For the optimum to be reached, it is necessary to have, for each electric vehicle:

$$\sum_i^N E_{n,i} = E_{Required,n} \tag{4-6}$$

In general, it is preferable to minimize the number of stops, it saves  $T_{other}$ . However, it may sometimes be useful for an EV to make an additional stop to avoid a queue.

## 4.2.2 Electric vehicles communication scenarios

### Communication issues

The quality of a communication system depends not only on its performance but also on its ability to be easily deployed. Figure 4-5 presents all the constraints that are considered.

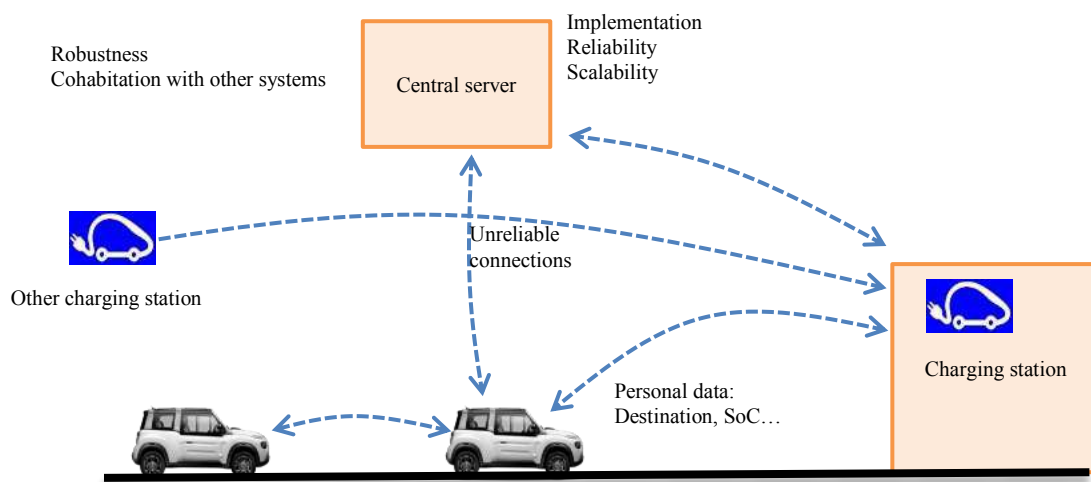


Figure 4-5: Overview of possible communication flow and related constraints

Firstly, such a system relies on wireless connections between vehicles, charging stations and a central server. This communication is called V2X. These connections can be based on mobile network or WLAN. The first technology operate for long distances and the second one for local communication (less than few kilometers). The risk of dead zones and the latency of these communications make us eliminate solutions requiring continuous or rapid exchanges.

A centralized server gathering the requests of all users could make it possible to find optimal solutions. However, its implementation, reliability and required computing power can be significant hurdle, especially if the system deployment achieves a large scale. A distributed system, without a centralized server, eliminates this problem.

Users can be also reluctant to share their personal data, such as destination, average speed or state of the vehicle. Finally, constraints of robustness and cohabitation must also be considered.

Figure 4-6 displays the communication flow chart.

### Proposed communication schema

Considering all constraints mentioned in the previous paragraph, Figure 4-5 describes the innovative communication schema that is proposed. Communications between EVs and charging stations use mobile networks. This process, from the vehicle point of view, follows five steps:

1. The electric vehicle (EV) calculates several possible combinations of stops, with different stations and amounts of energy to store that permit to reach its destination. Local CPU resources do this computation.
2. The electric vehicle (EV) requests the scheduled waiting time at charging stations at a specific arrival time, for all combinations.
3. The EV sends a notification to selected stations, containing arrival time and estimated charging time.
4. The vehicle starts again the cycle composed of the steps 2 and 3, every period  $T$ .

The vehicle will first do this cycle when starting the trip, before entering the highway. It will then refresh according to a period  $T$ . It is noted  $T_{adv,n}$  the time between the beginning of the trip and the moment when the vehicle enters the highway. Stations will compute expected waiting times using notifications sent by all the vehicles.

From the station point of view, the system is composed of a device that must receive request of waiting time estimation and notification of recharge, and compute scheduled waiting times.

### Used algorithms

Different algorithms are used in this system. First, on the vehicle side, it is used the previous differential evolution algorithm to find a recharging combination that minimizes travel time. Other recharging combinations are evaluated. The combinations to be evaluated that have the same number of stops and the same amount of charged energy as the previous solution are chosen. These potential solutions are selected if they result in an increase in total travel time of less than 10%. Then on the station side, the calculation simply consists in keeping an updated list of scheduled recharges. This list contains arriving times and estimated charging times. The station can then evaluate the queue throughout the day and deduce waiting times.

The proposed system is easily feasible. First, the required computing power is not a problem. On the vehicle side, the complexity of the calculation is similar to the navigation technologies. It is therefore possible to use the same computer resources as those of the navigation system. On the station side, the amount of calculation to be performed depends on the number of vehicles on the road. However, as these calculations are not very complex, they can be performed by an affordable computer system. Secondly, it is a distributed system. This allows it to be deployed over large territories, such as a country or Europe, and to many vehicles, without the risk of saturating a central server. Finally, this solution does not require the share of personal data.

## 4.2.3 Results and cases studies

### Case study

The generated data represents the situation of a highway during a day with 100 electric vehicles. The road has one way, 11 entrances and exits and is 553 km long. It includes six charging stations, each with three charging points of 50, 100 or 125 kW maximum available power. Figure 4-1 displays their implantation. There are three types of vehicles in this simulation: urban, sedan and luxury.

Table 4-5 gives their respective characteristics.

The model is based on daily highway flow modelling on the data found in [132].

Figure 4-7 shows the average daily flow of vehicles entering the French A6 motorway in the Ile de France region during the year 2017. These are the data of highway entrances equipped with counting loops. It indicates that the flow is almost constant between 8 a.m. to 9 p.m. It is to be noticed that the traffic during the night is more than three times lower than during the day.

As we want to study crowded situations, we will focus on the situation during the day. Therefore, the flow is modeled with a uniform distribution of departure time over a period, between 8 a.m. to 9 p.m.. Randomly entry and exits number of vehicles are chosen, while imposing a minimum distance of 250 km. It is also used a uniform distribution for the SoC at departure, in the range 50%-100%. SoC at arrival (when the car exits the highway) is required to be above 30%, and SoC when entering a charging station to be above 15%. Electric vehicles are charged to a maximum of 80% or below.

Table 4-5: Studied vehicles characteristics

Car Type	Urban	Sedan	Luxury
Battery (kW.h)	50	60	100
Maximum charging power (kW)	50	100	125
Consumption (kW.h/km)	0.15	0.18	0.18
Driving Speed (km/h)	110	130	130
Generation probability	0.3	0.6	0.1

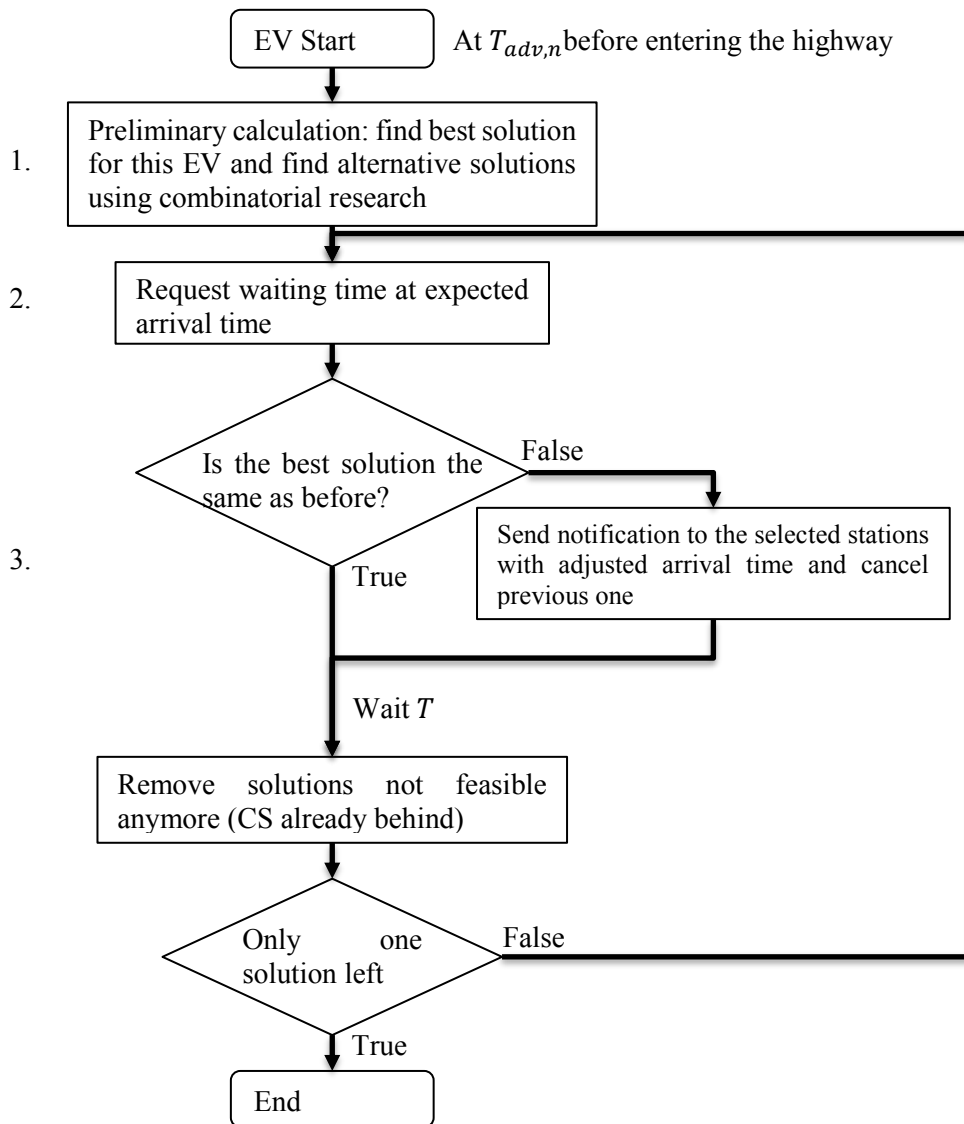


Figure 4-6: Communication flow chart

## Trips characteristics

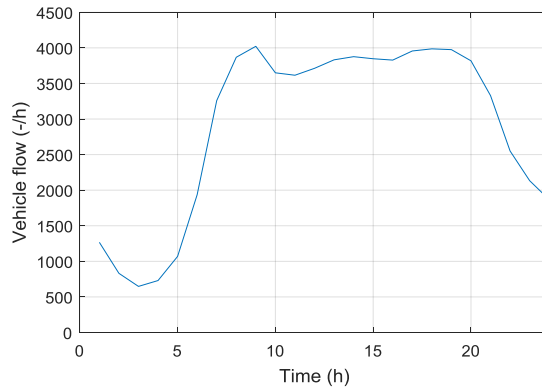


Figure 4-7: Average daily incoming vehicle flow

The following figures present the characteristics of the EV trips generated by the assumptions presented in the previous paragraph. In order to illustrate only the driver's needs, we do not consider waiting times at the stations in this section. Figure 4-8 shows two histograms: the distribution of trip distances and trip times, considering recharge times. It shows the diversity of the routes studied and the fact that they are mainly between 400 and 550 km.

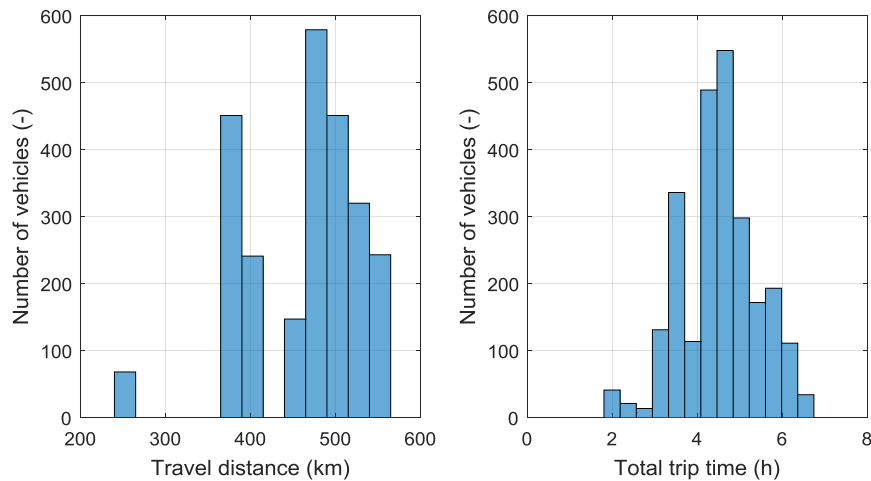


Figure 4-8: Generated vehicles trip characteristics

Figure 4-8 shows the histogram of the charging time over total trip time ratios for the different vehicles studied, according to their type. It also shows the impact of vehicle characteristics on their ability to make long journeys. It is interesting to note that the size of the battery does not affect the previous formula. However, it comes into play when the charge level is different between entrance and exit, which explains the dispersion of EVs in the histogram: those starting with a full battery will have less need to charge during the trip.

### First study case

We performed these first simulations with 100 vehicles during one day. Three situations are compared:

- Without coordination: EV drivers have no information about choices made by other EVs. Each driver optimizes his charging schedules separately, reproducing the choices that a driver can make when only knowing the charging stations position and power.
- Communication: Strategy defined in the previous section, in the case where all vehicles use the system. We set the time period  $T$  and  $T_{adv}$  at 10 minutes.
- Global optimization: Situation in which all information is centralized and choices are made in an optimal way, considering waiting times when making choices. This vehicle repartition is close to the optimal one.

Figure 4-9 shows the average waiting time at the different stations for the three situations. The communication and even more the global optimization can reduce average waiting times. This is made possible by a better distribution of vehicles between stations. It is to be noted that the decrease in waiting time at station 3, the busiest station, does not result in an increase in waiting time at the other stations. The charging infrastructure is therefore better used.

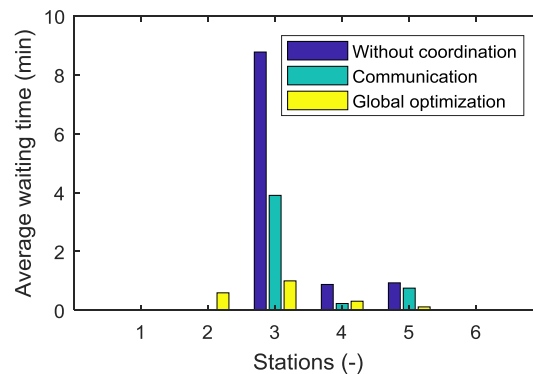


Figure 4-9: Average waiting time comparison

### Conclusions

The simulations were performed with 100 vehicles a day and averaged them over 15 days. In order to qualify a situation as satisfactory for users, a quality criterion was defined. The infrastructure is considered as sufficient if it meets the following quality criterion:

- 90% of EVs entering a charging station will have less than 5 minutes to wait.
- All waiting times are less than half an hour.

The following figures show the results of the comparison between the three scenarios. Figure 4-10 shows the cumulative distributions function of waiting times at the different stations for the three scenarios. The dotted line represents the quality criterion defined above. The communication and even more the global optimization can reduce waiting times for all drivers entering charging stations. Thus, for station 3, the busiest, there is a decrease in the maximum waiting time from 74 to 40 and then 20 minutes (respectively for the three scenarios) and an increase in the proportion of refills for which the waiting time is zero from 41% to 60% and then 81%. It can be also noticed the balancing of waiting times between stations.

Table 4-6 shows the average waiting and charging times for the three scenarios. There is a slight increase in recharging time and a decrease in waiting times. This shows the choices made by some people to recharge at lower power to reduce their waiting time. This represents a total saving of around 9% of the total time spent in stations thanks to communication, out of a potential decrease of 13% with overall optimization.

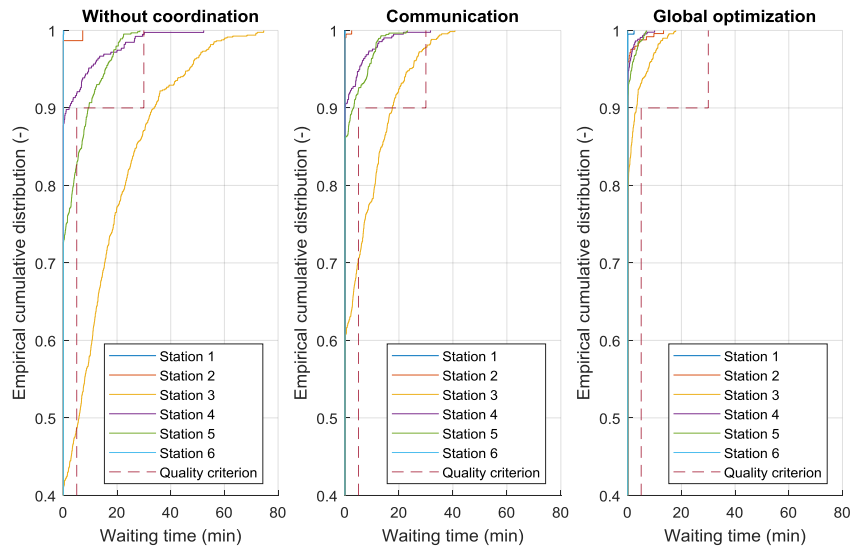


Figure 4-10: Waiting times at charging station, 3 charging points per station

Table 4-6: Average charging and waiting time for the three scenarios

	No coordination	Communication	Global optimization
Average charging time (min)	46.0	47.3	47.7
Average waiting time (min)	15.6	8.8	5.8
Total (min)	61.6	56.1	53.5
Saving compared to No C.	-	9%	13%

Figure 4-11 shows the same comparison in a more crowded situation. There are the same number of cars per day, but only two charging points per station. The decrease in the area above the curves is even more pronounced than in the previous situation, particularly for charging station number 3. The time spent in stations is then reduced by 46% and 55% respectively with communication and overall optimization, compared to the uncoordinated scenario.

In conclusion, we can note two things about the performance of the proposed communication solution: the good distribution of vehicles, reducing the time spent in stations to a level close to the ideal distribution, as well as the increased efficiency in the event of high traffic.

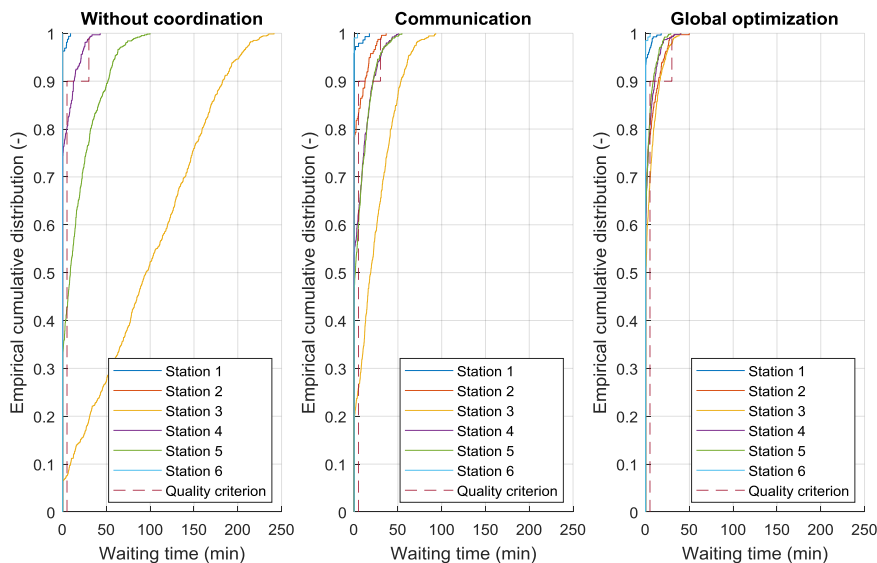


Figure 4-11: Waiting times at charging station, 2 charging points

A comparison of its performance against an uncoordinated situation and one with overall optimization shows a 9% gain in time spent in stations out of a potential of 13%. In addition, the system is ever more useful in crowded situations, with a time gain of 46% out of a potential of 55%. In the future, it will be interesting to study the robustness of such a system when not all travelers use it.

### 4.3 Slow charging: Robotized charging of high voltage batteries for electric and hybrid electric vehicles

This research presents an innovative recharging service for the high voltage batteries of the electrified vehicles, provided by a robot. An innovative mobile robot, equipped with energy power system, does the recharging task. The navigation function is central in the design of the mobile robot. The navigation system must create a safe path planning to the vehicle and then ensure an accurate positioning of the mobile robot and safe navigation in its environment. The Localization and Mapping are the fundamental keys to provide the mobile robot with autonomous capabilities. The research presents a recent development and its experimental validation, in the Simultaneous Localization and Mapping method to serve the robot navigation, coupled with an advanced cognitive system. The proposed navigation system uses advances in Mobile Robot Localization and Mapping methods and a LiDAR sensor. The cognition uses deterministic algorithms to fulfil the positioning accuracy, the smart cost of the equipment, and easy implementation requirements for industrialization. The experimental results on a mobile robot platform show a distance error lower than 0.7% and an angle error less than 0.5%, promising for the acceptable accuracy of the system.

#### 4.3.1 Mobile robot for recharging

##### 4.3.1.1 Why a mobile robot?

Currently, mobile robot applications go through a tremendous increase due to the miniaturization of computer devices, the progress in the information treatment and algorithms. Mobile robot can perform autonomous task and evolve in a dynamic and unknown environment, which make it flexible and performing. In our case, the robot presented in Figure 4-12 has to deal with different goals: it must be able to reach and serve several parking spaces. To complete its mission, the robot has to detect the car, localized the receiver underneath the car, create and follow a safe path to reach the coil, positioning itself precisely and then start the power transfer after having compensated the air gap. The most important ability of a mobile robot is the navigation.

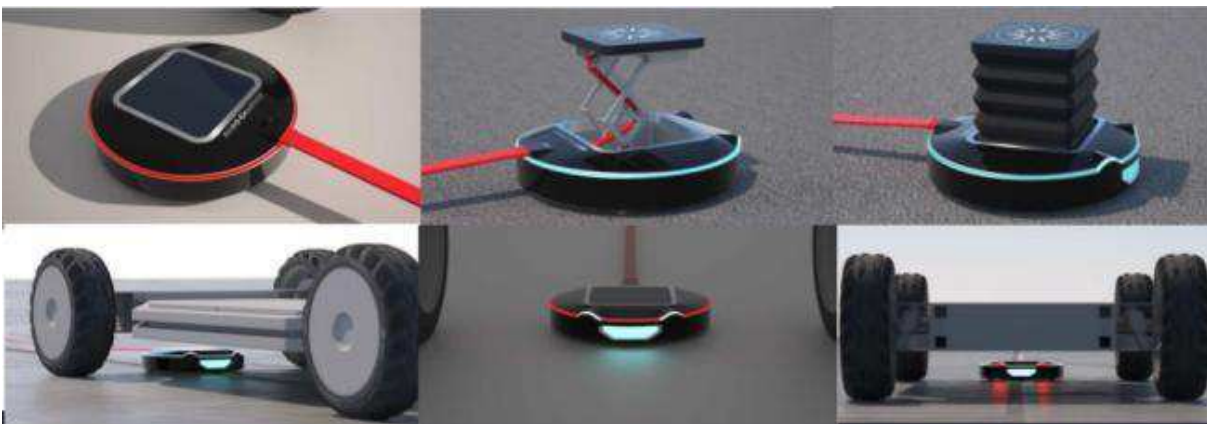


Figure 4-12: Numerical model of the mobile robot

The robot navigation includes three specific faculties [77]:

- Be able to perceive, integrate and evolve in the environment by avoiding obstacles
- Self-localization
- Be able to reach goal locations

To do so the navigation system of the mobile robot must include a robot positioning system, path planning and map building [77]. Four different steps allow the navigation of the robot inspired of the human behavior: Perception, Localization, Cognition and Motion.

The objective of the research is to make the functional definition of the navigation system of the mobile robot in a simple and reliable way, to ensure the proper functioning of the robot and the realization of its service. The presented literature review helped to define mobile robotics, to identify important concepts and scope on the relevant techniques and methods to apply for the “Robot Charger” case. The research done will be useful for several reasons:

- It introduces several algorithms of different type with relevant simulations and experiences in mobile robot navigation in localization and cognition. It gives open source modules that can be used in the Robot Charger system.
- Several challenges for the development emerged from this study:
- The Localization should rely more on the LiDAR than on Dead-reckoning sensors (Exploration of SLAM or alternative techniques).
- Parking places usually do not have special geometry that would be detected by the LiDAR. In addition, the environment change every time since the car will not park in the same way or, in the case of several parking spaces; there will be an irregular presence of cars.

This research contributes to design a cost effective localization platform respecting the requirements of the “Robot Charger” in terms of accuracy and detection of obstacles. This platform will be integrated into the Smart Cost Navigation System.

## **4.3.2 Research work**

### **4.3.2.1 Design of a cost effective navigation system for a mobile robot**

A multitude of Navigation system has been studied in the literature and each of them shows good results. Even though, it is an evidence that the quality of the result depends mainly on the mathematical tools combined with the computing power that is granted as well as the quality of the sensors used. In our case, we want a cost effective navigation system. The navigation system is required to work with low cost materials and sensors. Accordingly, one of our main constraints for the design is an available low computational power and sensors with enough good performance. Even though, the navigation system must be efficient enough to allow the robot to fulfil its tasks.

#### **Perception with lidar and encoders**

From the literature review, we know there are two types of positioning systems called relative and absolute. In addition, each positioning system can be realized using different sensor families and give specific properties. The combination of one of each type is necessary to get a good tracking performance. Indeed, relative positioning systems offer good accuracy in the short term, but tend to drift while absolute position system that refers to the environment can correct the drift. For the relative positioning system we use the robot’s encoders, it gives the speed and the sense of rotation of each wheel. Combined with the dynamic models of the robot, the distance travelled and the direction can be computed. For the absolute positioning system, the choice of a "map matching" system comes from the fact that the environment of the robot is unknown and there will be no landmarks. Furthermore, this system works well with the method SLAM. The use of the camera or LIDAR to build this system is common, but even if the device is not expensive the disadvantages of the camera is the computing power needed to process the images. On the contrary, the LIDAR is a range finder sensor.

The process of the data is simpler. Furthermore, a high performance LIDAR is very affordable today. For the following, we use the low cost 360-degree laser range scanner RPLIDAR A2 M8. It can measure a distance up to 12 meters (accuracy~1%), which is fitting with the requirement in the precision and the size of the environment. Moreover, thanks to the 360° measurement, the robot will have a total vision of its environment and will be able to navigate safely in every direction.

### SLAM: Different approaches

After the perception comes the localization. The robot has to evolve in an unknown environment. Thus, the use of the method “Simultaneous Localization and Mapping” is necessary: the robot will be localized while it builds the map gradually. Several types of SLAM have already been developed using different combination of mathematical tools from the Iterative Closest Point to the particle filter, and use different representations such as grid-based or feature-based map. All these parameters influence the performance of the SLAM and the computational cost that is an important criterion in our case. We tested several open-source SLAM such as MRPT project [133], DP SLAM [134] and BreezySLAM and CoreSLAM [135]. All these different methods are able to locate the robot with enough accuracy to reach its goal. However, the outcome of our research is to design a smart cost platform and simple code to be understandable. Then, we choose to run our SLAM on a single board computer because the price of the component needed to run the program must be as low as possible. The Breezy SLAM seems to be the most adapted solution to reach our objectives. Furthermore, the simplicity of the code will make easier possible modifications and tuning of the parameters.

## 4.3.3 Implementation of a smart cost localization system

### 4.3.3.1 The prototype platform of the mobile robot

The Breezy SLAM has a LIDAR mode, an odometry mode and a LIDAR + odometry mode. The interface to set the parameters is in python language and the parts of the algorithm that need high computational speed are in language C. Furthermore, Map-building and the Particle filter are two different parts that can be modified without create interference; adding a new particle filter without compromising the mapping part of the code is possible. We implemented the breezy SLAM on Nitrogen 6X to test the Lidar mode . The Nitrogen 6X is a single board computer from the brand boundary device with four CPU cores and a CPU Clock of 2 GHz with Linux OS. We run several tests to set the parameters and get the optimum result. Robotic platform used is a three omnidirectional wheel mobile robot. We tested on it the mode Odometry + Lidar. The mobile robot equipped with the Lidar is controlled directly from an Android application. An Arduino commands and controls the three motors, it receives the order from the user via Wi-Fi thanks to a Wi-Fi Shield. The Nitrogen is running the SLAM program while receiving sensor data from the Lidar and from the encoders. The map and the tracking of the robot is displayed on an internet server (Figure 4-13).

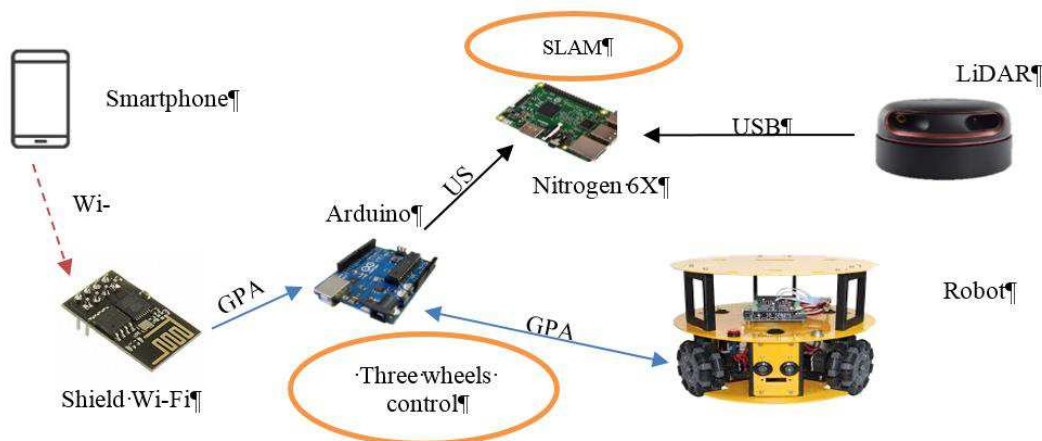


Figure 4-13: Structure and communication of the mobile robot with SLAM

## Algorithm

The CoreSLAM is a simple method that can deal with ambiguous situations and is able to integrate the odometry since we can implement a non-linear error model. The basic operation of the CoreSLAM is based on a method called Incremental Maximum Likelihood (IML), at every moment the algorithm research the best likelihood match between the current observation and the current map. The IML is not a really a “simultaneous” method and build a single map incrementally without keeping another version compare to SLAM studied before. At the same time, the IML is simpler than other methods. The steps are the following (Figure 4-14):

- (a), (b) The robot start to create a first mapping of its environment
- The robot moves, but the map stays unchanged. Via the odometer’s data and its previous position, the algorithm calculates the velocity to make a first estimation of the new position (c).
- The particle filter (Monte Carlo algorithm) creates several hypothetic positions around the first estimation and then calculates for each one a “score” of likelihood (score explain below) between the map and the current scan. The RMHC algorithm finds the particle with the lowest score, which correspond to the real position of the robot (d).
- The new position is updated on the map and then the map is updated (e), (f).

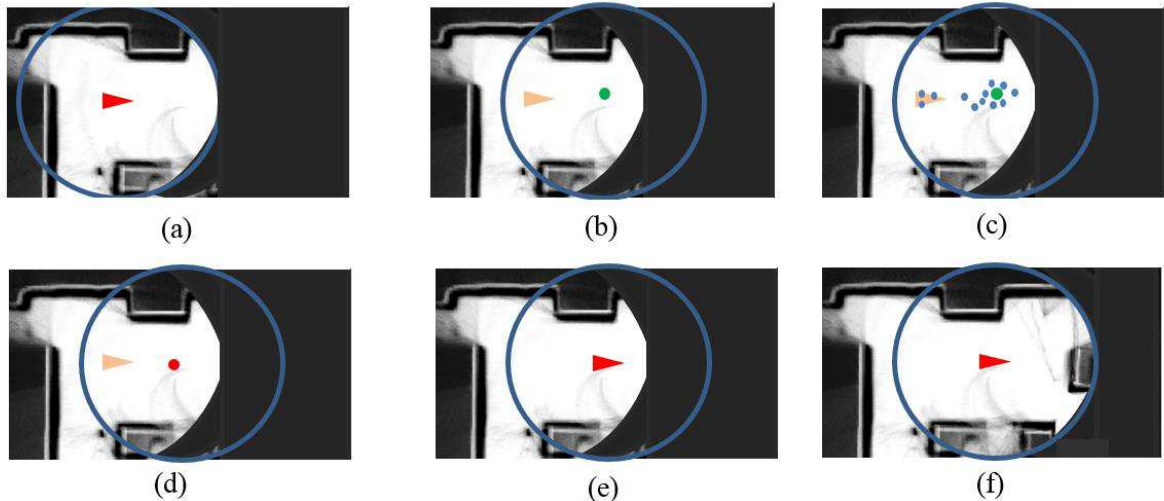


Figure 4-14: Representation of the different steps of the algorithm

The Monte Carlo algorithm generates the hypothesis (particle), its ease of implementation makes it a very used algorithm. The accuracy of the position and the computation load increases with the size of the particle set used. The setup of the particle set is also an advantage because it gives flexibility on the computational resource compared to other algorithms.

The score system is a simple operation that is executed thousands of times for one localization. It uses the value of pixels in grey-level to attribute a score, it goes from 0 (black pixel) to 255 (white pixel). Each hit point from the current laser scan is compared to the latest map accordingly to the frame of a particle then a sum of all the values determine the score of this hypothesis pose. A high score means that a lot of hit point land in a white part of the map thus the hypothetical position is unlikely to be the correct position. On the contrary a hypothesis with low score means that the scan fit well the map thus it is more likely the real position of the robot. The Random Mutation Hill Climbing (RMHC) is a local search algorithm; it helps to find the hypothesis particle with the best likelihood. Most of the code is in Python, except three functions with a high computational time that are in C language: the function “Distance Scan to Map” that determine the likelihood of a given position, “Map Laser Ray” that integrate a new scan to the map and the RMCH algorithm.

## Parameters

As explained previously, several parameters can be set in order to optimize the SLAM according to the components used, here a recap and details of each one:

- **Samples:** It corresponds to the minimum number of samples that delivers the LIDAR in one scan. It goes from zero to 250 samples per scan. It influences the positioning accuracy. More measurement means more precision. Ideally, we will set the parameters to 250, but the more samples per scan the more the computational cost is high. Thus, a high rate could give an unchanging position or an empty map.
- **Quality:** It is the integration speed of the scan on the map; it can be tuned from zero to 255. It can influence the localization capabilities because its influence the quality of the map on the display.
- **Size of the map:** This parameter is important because it defines the maximum size of the map that can be discovered by the robot. The program does not re-scale the map. The size to enter is in meters and, in the original code. The robot first position is in the middle of this map. To define this parameter, we must take into account the area to be mapped by the robot.
- **Pixels of the map:** Define the number of pixels on the map, its influence the quality of the resulting map. This parameter must be set accordingly to the computation power. Too many pixels are computationally expensive; on the contrary, fewer pixels can degrade the position estimation.
- **Resolution of the map:** It is the ratio between the size of the map by the number of pixels, it defines the quality of the map but also the quality of the positioning. A low resolution (high size of the map and a low number of pixels) gives poorer results as well as for the resulting map than for the quality of the positioning
- **Number of iterations:** This parameter is linked to the RMHC algorithm. It sets the number of solutions that will be explored. A higher number will significantly increase the accuracy of the position and the computational time.
- **Alpha:** Correspond to the slippage probability of the robot in the non-linear error model of the particle filter.

## Maps

To represent the surrounding environment of the robot, the CoreSLAM uses a grey-level map (Grid based map) containing three types of data:

- **Obstacles:** the value of the pixels is 0 (black)
- **Navigable area:** the value of the pixels is 255 (white)
- **Undiscovered area:** the value of the pixels is 128 (grey)

For the integration of the laser ray on the map, it uses a Bresenham algorithm to draw the laser ray as a straight line on the map with the pixels. One particularity of the map is the representation of obstacles: Indeed obstacles are represented as digging holes with a fixed width with the lower point corresponding to the position of the obstacle whereas most of mapping techniques use a single point. The “hole” corresponds directly to the peakiness of the likelihood function and it leads to a better efficiency of the particle filter. Then the map can be interpreted as a surface with attractive holes (Figure 4-15). The default robot position is in the middle of the map, while the robot is moving the map is progressively built. The obstacles are clearly identifiable on the map above, the SLAM adds to the map every object detected as a wall with a fixed thickness corresponding to the likelihood function. Notice that the “noise” in the lower part of the map is due to the low number of samples (100) and scan integration speed to high.

### 4.3.3.2 Qualification of the performance

To qualify the performance of our localisation system, we performed several tests to determine its behaviour in narrow/wide environment, how it handles dynamic obstacles, but also the accuracy in

detecting movement (tracking). The maximum of iteration has been set to 1000. Beyond this number, intermediate tests show that there is no longer noticeable improvement. The slippage probability has been set to 10 %, thus 10 % of the particles will stay at the initial position while the others will move accordingly to the data from the odometry. We test it by simulating a slippery: we raise the robot so that the wheels cannot touch the ground and give the order to go forward, the odometry inform the robot that it is moving while the robot is motionless: The position on the map of the robot remains fixed.

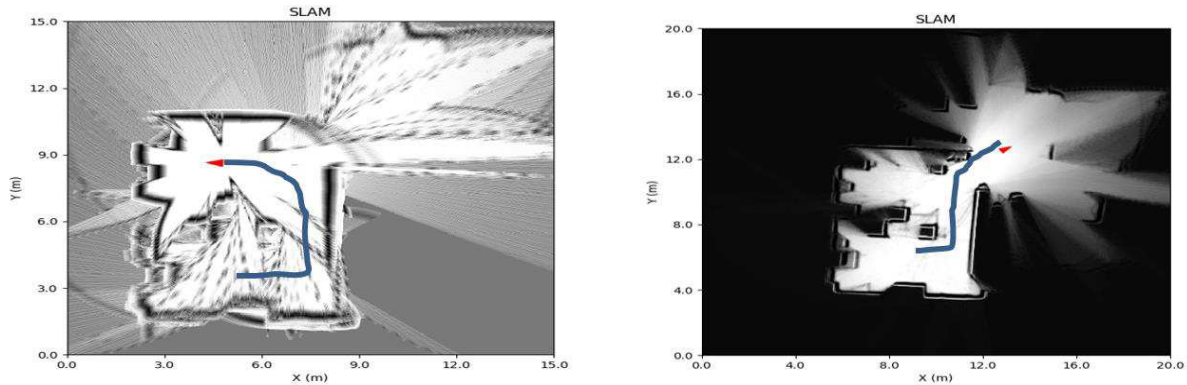


Figure 4-15: Mapping of the mechanical labotary. a) Quality: 50 / Size: 15 b) Quality: 1 / Size: 20

The parameter “hole width” is set to 300 mm, then every obstacle will have a larger of 0.3 m on the map. Finally, after several tests we set the integration speed of the scan (quality) to the minimum (1 out of 255). The resulting map is clean and stable. This is the optimal setting to build a map. We succeed to map the mechanical laboratory at PSA (Figure 4-15).

On the second map (Figure 4-15b), we observe clearly the obstacles (Black line with white line on both sides) and the obstacle-free area compare to the first map (Figure 4-15a). The drawback to the low integration speed is that building the map takes longer and the integration on the map of fine obstacles take more time. Even though, we see that BreezySLAM supports every movement of the robot and keep the map stable even during the rotation of robot which is the most tricky movement in SLAM. In addition, the algorithm treats moving obstacles. If the obstacle moves, its representation on the map moves also. We also highlighted some weakness of our system during these tests. The LIDAR can send wrong information of depth depending on which surface it reaches and with which angle. Sometimes the laser ray can go through the material as for a glass or semi-opaque glass material. Also in environment with no obstacle in the scope of the LIDAR or an environment with a specific pattern as a corridor, the robot has a tendency to lose its position. The algorithm will not detect any change in the environment and will therefore believe in a slippage. In order to qualify the accuracy of the localization, we perform these tests: tracking accuracy at different speeds, calculation of the distance and angle errors in the localization. The first test consists of move the robot at different speeds over the same distance. It will highlight the influence of the speed of movement on the tracking of the robot’s position. The test runs as follows: Two parallel lines are installed on the ground three meters apart. The robot will travel this distance at three different speeds: 100 mm/s, 200 mm/s, 400 mm/s. When the robot reaches the last line, the position calculate by the breezy slam is saved. Then we can compare the estimation of the position at the time  $t$  (the moment when the robot reaches 3 meters) (Table 4-7).

Table 4-7: Tracking of the robot

Speed (mm/s)	100	200	400
Estimation of the position (mm)	2881	2959	1777
Difference with actual value at time $t$ (mm)	119	41	223

As, we observed the SLAM is more reactive on the tracking at a good speed (200 mm/s), it is coming from the latency: at low speed, it needs more scans to detect the movement. At the speed 400 mm/s, the robot does not have enough time to build the map correctly, thus the SLAM loses the tracking of the robot. The second test will show the distance and angle errors after a different kind of displacements. We will compare the real position of the robot (distance and angle) with the estimated position of the SLAM. The robot will make the following moves (with a speed of 100 mm/s):

- Combination Rotation / Translation: Move 4 meters, rotation of 90 degrees, move 2 meters.
- 2 types of translation: Move 3 meters. Move 50 mm.
- Rotation: Rotation of 450 degrees.

Table 4-8: Localization errors

Type	Combination	Translation (3m)	Translation (50 mm)	Rotation	400
Distance Error (mm)	22.4	19,88 mm	5,75 mm	-	1777
Distance Error (%)	0.5 %	0,7 %	11,5 %	-	223
Angle Error (°)	0.5	-	-	4°	

## Conclusions

The SLAM is stable when the robot is motionless. The position remains at 0 most of the time, with occasionally a derivation up to around 6 mm in X or/and Y. Furthermore, even with two mobile obstacles (Humans) around the robot, the position does not vary. According to Table 4-8, the localization error remains stable around or below 2 cm. This meets the requirements. The orientation of the robot that the SLAM calculates is also really close to the real orientation. Map was built gradually during each runs. Thus, when the robot performs three rotations while building the map, this increases the errors of localization because the data from the LIDAR during a rotation is more difficult to compute than during a translation. Thus, the BreezySLAM is powerful enough for our needs, it could be used for the “Robot Charger”.

Smart cost platform means the use of low cost sensors and low cost hardware, thus the algorithm of localization has to run on low power computer and with simple sensors. The algorithm must respect three main constraints: computation efficiency, accuracy of the approximation of the position and ease of implementation. After implementing our platform on a three Omni wheels robot with a LIDAR and encoders, set up the communication protocols and set the parameters, we successfully build a reference map of an area (Figure 4-16). In addition, the drawbacks of this platform are highlighted: Errors in the map when the ray of the LIDAR reaches a glass or semi opaque glass, not detecting thin obstacle and can be lost when there is a lack of obstacles (reference) up to 10 meters around the robot or when there is a long pattern (corridors). Even though, according to our test’s results, the tracking performance is really good at moderate speeds (100 - 200 mm/s) as well as the localization accuracy with an error maximum of 2 cm. Thus, the SLAM is efficient enough to meet the requirements for the application.

The steps to use this localization system in a real application could be done. First, the robot charger performs a first recognition in the new environment to build a reference map. Then, the map becomes a reference map for the localization of the robot during its operation. It will continue scanning the environment to detect new obstacles. The next step is to implement a cognitive system in order to navigate in the environment according to the map.

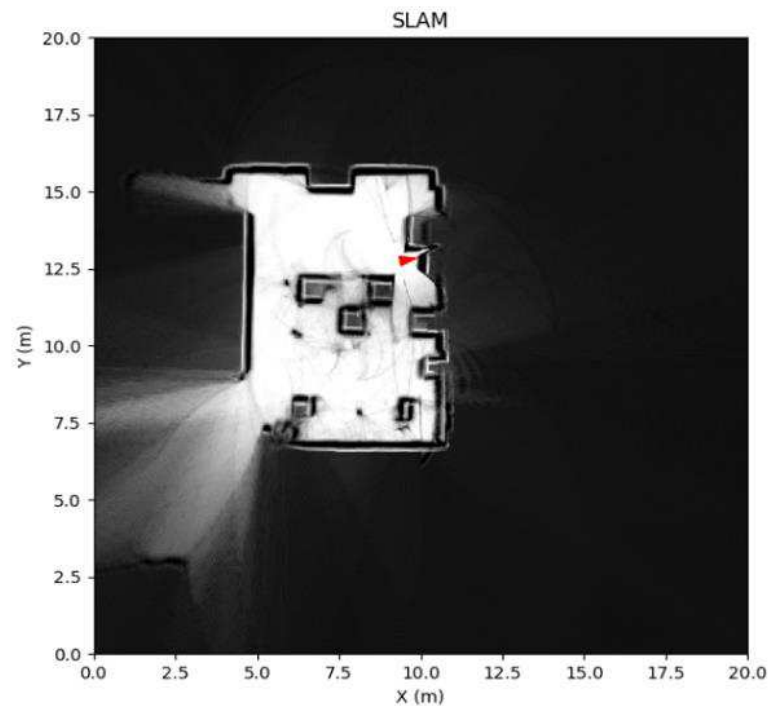


Figure 4-16: Reference map of the robot

#### **Integration of the environomic energy services for mobility and household using electric vehicle with a range extender of solid oxide fuel cell**

This study is a published article and is presented in Appendix D. The conclusions are bellow.

The total GWP impact of the base case scenario is estimated to 50590 kg CO<sub>2</sub> eq. The multi-objective optimization for environomic design of the new vehicle- house system is performed for the definition of the environomic design of the driving and the residential mode. In the case of the energy supplied in France the optimization sizes the SOFC-GT module for the mobility needs. The rest of the energy needs of the house are covered by the grid supply. Optimal design of the range extender vehicle in dual mode is proposed for 200 km of autonomy, investment cost of 28430 € and 3808 €/year of total driving yearly cost. The base case scenario has lower investment (20900 €) and total driving yearly cost (3229 €/year).

The total yearly cost for the integrated system in dual mode stays still higher (1000 €/year) than the base case separately delivered energy services. This is due to the high investment cost of the equipment in the vehicle and the house. The major advantage of the energy integrated dual system is the reduction of the total GWP impact with around 30000 kg CO<sub>2</sub> eq. (60%). – from 50590 kg CO<sub>2</sub> eq. to 20338 kg CO<sub>2</sub> eq. This study illustrates large scale economic and environmental benefits opportunities by integration of the energy services for mobility and household.



# Chapter 5 Energy storage and conversion systems for energy vectors: fuel cell electric vehicles, hydrogen and their ecosystem

This chapter presents an innovative propulsion system with high efficiency, using fuel cells. The hydrogen production is considered for different energy vectors and their ecosystem.

Hydrogen is considered as clean energy, but several questions related to its production, its large-scale storage and distribution remain. The current state of the art of fuel cell vehicles is the use of pressurized hydrogen gas at 700 bar, stored on the board of the vehicles and converted into electricity by a membrane fuel cell (PEM) technology. Storage and distribution under 700 bar of hydrogen pressure present technical, economic and environmental problems. The idea of the research in this field is to propose a concept of energy storage under the form of bioethanol and to convert the bioethanol to hydrogen on the board the vehicle by using a solid oxide fuel cell (SOFC).

This chapter presents the concept of electric vehicle equipped with serial range extender to extend the vehicle autonomy. The fuel cell system powered by hydrogen produced through reforming of liquid fuel from renewable resources such as bioethanol is considered as a range extender module. An alkaline fuel cell and a solid oxide fuel cell are investigated for the use of a variety of liquid fuels instead of traditionally used hydrogen in others types of fuel cells. The energy balance of the different types of fuel cells powered by bio-ethanol is investigated. Three variants for the ethanol conversion are investigated: variant 1: reforming of bio-ethanol in external reformer to hydrogen and its conversion in alkaline fuel cell, variant 2: reforming of bio-ethanol in external reformer to hydrogen and its conversion in a solid oxide fuel cell; variant 3: direct reforming of the bio-ethanol in the solid oxide fuel cell. The chemical processes for each variant are proposed and thermodynamic energy balance is calculated. From the results it is visible that the most efficient configuration is the variant 3 and concerns the direct reforming of the bio-ethanol by the solid oxide fuel cell. The variant 3 delivers 15.15 MJ of electric energy output per kilogram of bio-ethanol, used in the fuel cell.

The catalyst system for the bio-ethanol steam reforming is investigated on experimental way. It is needed a high active and selective catalytic system requiring 100% of bio-ethanol conversion to hydrogen. The total conversion of bio-ethanol to hydrogen is essential from the economic point of view. The catalyst which is used during the process has an important role to achieve 100% of conversion. Typical catalytic systems used in steam ethanol reforming processes typically include precious metals Rh, Pd, Pt, Ru and Ir in monometallic formulations. Bimetallic systems exist couple precious metals with smaller amounts of transition e.g. Pd-Ni, Rh-Ni, Rh-Co and others. In view of the high price of noble metals, it is suggested to use higher concentrations of transition metals doped with small amounts of no noble metals eg. Ni doped with a small amount of Pd as an active phase components. The catalysts selection is done with laboratory experiments. While as a support it is suggested the usage of binary oxide system containing  $\text{Al}_2\text{O}_3$ ,  $\text{ZnO}$  or  $\text{CeO}_2$  or  $\text{ZrO}_2$ . The main goal of this research is to select the most active and selective system which can be directly used in micro-reactor before the SOFC fuel cell. During the research tasks the most suitable liquid fuel will be selected and will be used as a substrate for hydrogen generation and finally to produce electricity using a SOFC fuel cell. To consider the impact of the

different energy vectors a well-to-wheels balance on the energy efficiency and the CO<sub>2</sub> emissions is done. The balance concerns different vehicles propulsion systems. The impact on the energy efficiency and the emissions is discussed.

The investigated concept presents the advantage to extend the vehicle basic electric range thanks to this highly efficient converter. A second advantage is the reforming of a liquid fuel on board which avoids the storage of hydrogen under elevated pressure. This proposal suggests the use of SOFC system powered by hydrogen produced through reforming of liquid fuel from renewable resources such as bioethanol. The SOFC installation has an integrated fuel reformer. The SOFC operates at high temperature (800 °C to 1000 °C). Figure 5-1 presents the overall layout system based on SOFC. This kind of fuel cell can use a variety of fuels instead of traditionally used hydrogen in others types of fuel cells. It can be powered by CH<sub>4</sub>, C<sub>2</sub>H<sub>5</sub>OH, CO or others fossil fuels. This is very advantageous from the application point of view of such fuel cells on board of automobiles. In this case we have not any problems with the purity of the produced hydrogen which is strongly required to power PEMC stack system. That is why we need a high active and selective catalytic system requiring 100% of fuel conversion. This system will be applied in the micro reactor directly before the SOFC fuel cells stack system (Figure 5-1).

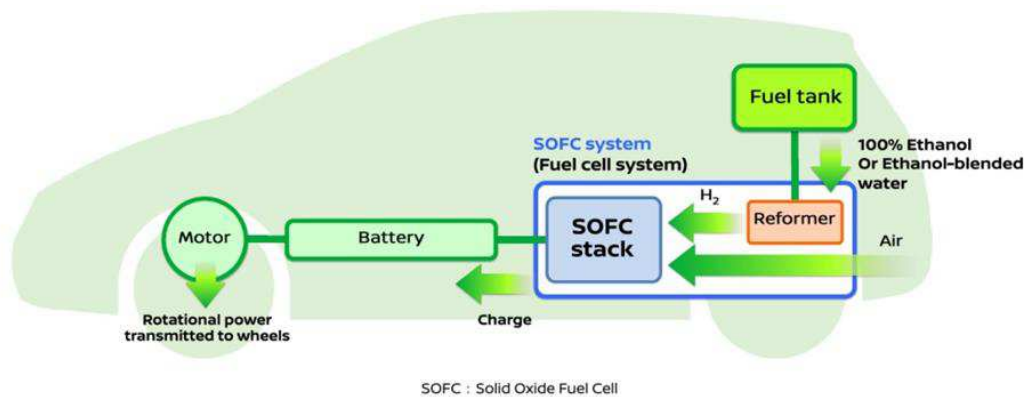


Figure 5-1: Vehicle propulsion system with an innovative range extender system [136]

The total conversion of C<sub>2</sub>H<sub>5</sub>OH is essential from the economic point of view. The catalyst which is used during the process has an important role to achieve 100% conversion because it increases the rate of reaction in such a way that the system tends toward thermodynamic equilibrium. Figure 5-2 presents the possible reaction which takes place during the steam reforming of ethanol reaction. As we can easily observed the selection of the best catalyst to this process is important to obtain the final product mixture (CO<sub>2</sub> and H<sub>2</sub>).

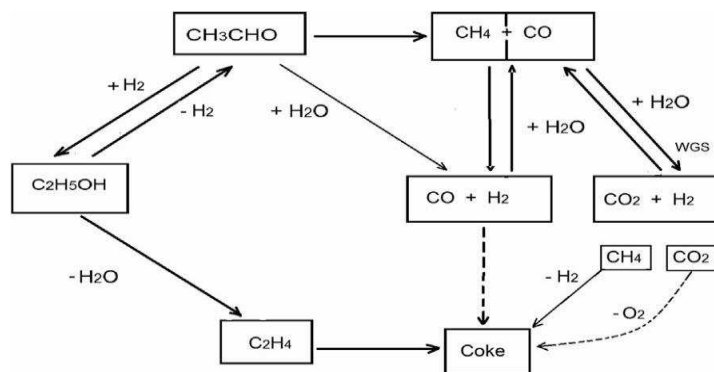


Figure 5-2: Reactions involved in the ethanol steam reforming.

One of the best candidates is the ethanol. The ethanol can be obtained from sugar beet, sugar cane and other plants. Ethanol and especially bio-ethanol is convenient for reforming in the reactor before the fuel cell and has the advantage to be a renewable fuel, produced from biomass, as illustrated from Figure

5-3. The main advantage of the concept is to obtain a long range, with easily supply of liquid fuel that it has a carbon neutral life cycle.

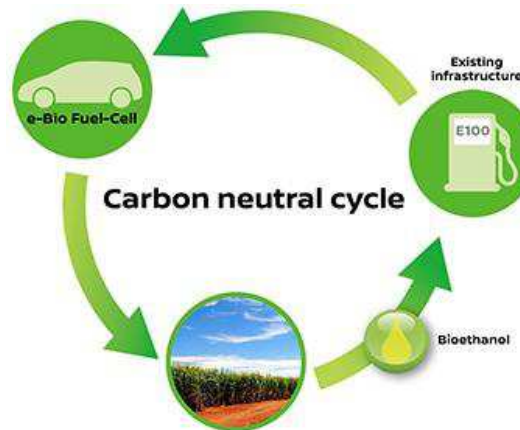


Figure 5-3: Carbon neutral cycle of the e-Bio Fuel Cell vehicle

Figure 5-4 presents the working principle of the e-Bio Fuel Cell system. The system produces hydrogen from ethanol- blended water through reformer. The main reaction is  $C_2H_5OH + 3H_2O \rightarrow 6H_2 + 2CO_2$ . The  $H_2$  produced in the reformer reacts with the oxygen from the air in the SOFC and then produces electricity and heat. The electricity is used to charge the high voltage battery of the vehicle. The heat is reused in the reformer to help the reforming of bio-ethanol to water. Thus, the system has a high efficiency of 65%.

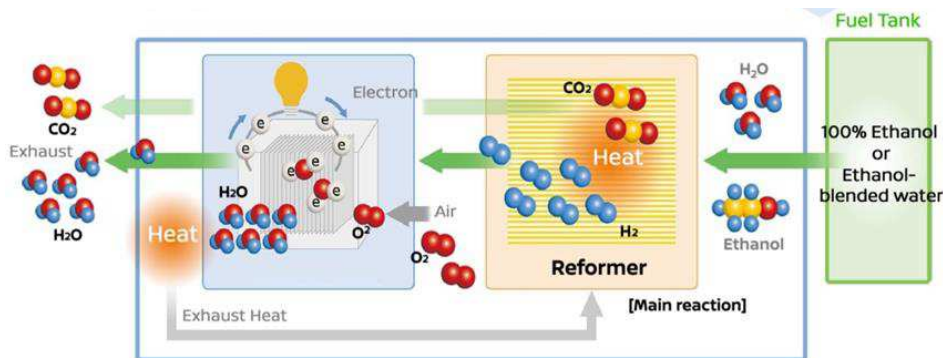


Figure 5-4: Working principle of the e-Bio Fuel Cell system

The SOFC is the best fuel cell for the concept. It presents the following advantages to be used to power electric vehicles:

- Long lifetime
- Low - costs of the electrodes
- Gases produced in SRE process can directly be used to power fuel cell stack
- High fuel efficiency
- Various compounds could be used to power fuel stack even natural gas
- Chemical stability of the solid electrolyte
- Low cost of raw materials for the electrolyte production

The disadvantages of using SOFC to power electric vehicles are:

- High operating temperature
- Long start-up
- Mechanical and chemical compatibility issues

## 5.1 Energy balance of the production and the conversion of hydrogen in the fuel cells

The results in part 5.1 and 5.2 are coming from the research collaboration between PSA and the Chemical department of the Lodz University of Technology (Poland).

The choice of bio- ethanol is favorable by the fact that it is non- toxic compared to methanol. It is easily available. It is easily converted under atmospheric pressure and there is a large possibility to obtain it from biomass. Bioethanol has the property to be stored easily in liquid form, and to be safely used. Bio ethanol is as well a renewable energy source.

It is possible to obtain different configurations of energy vectors (fuels) and types of fuel cell. The alkaline fuel (AFC) cell is powered by hydrogen. The solid oxide fuel cell (SOFC) can use liquid fuels, directly or by reforming the fuels in an integrated reformer. According of the type of fuel, the processes that the fuels pass through are different (Figure 5-5).

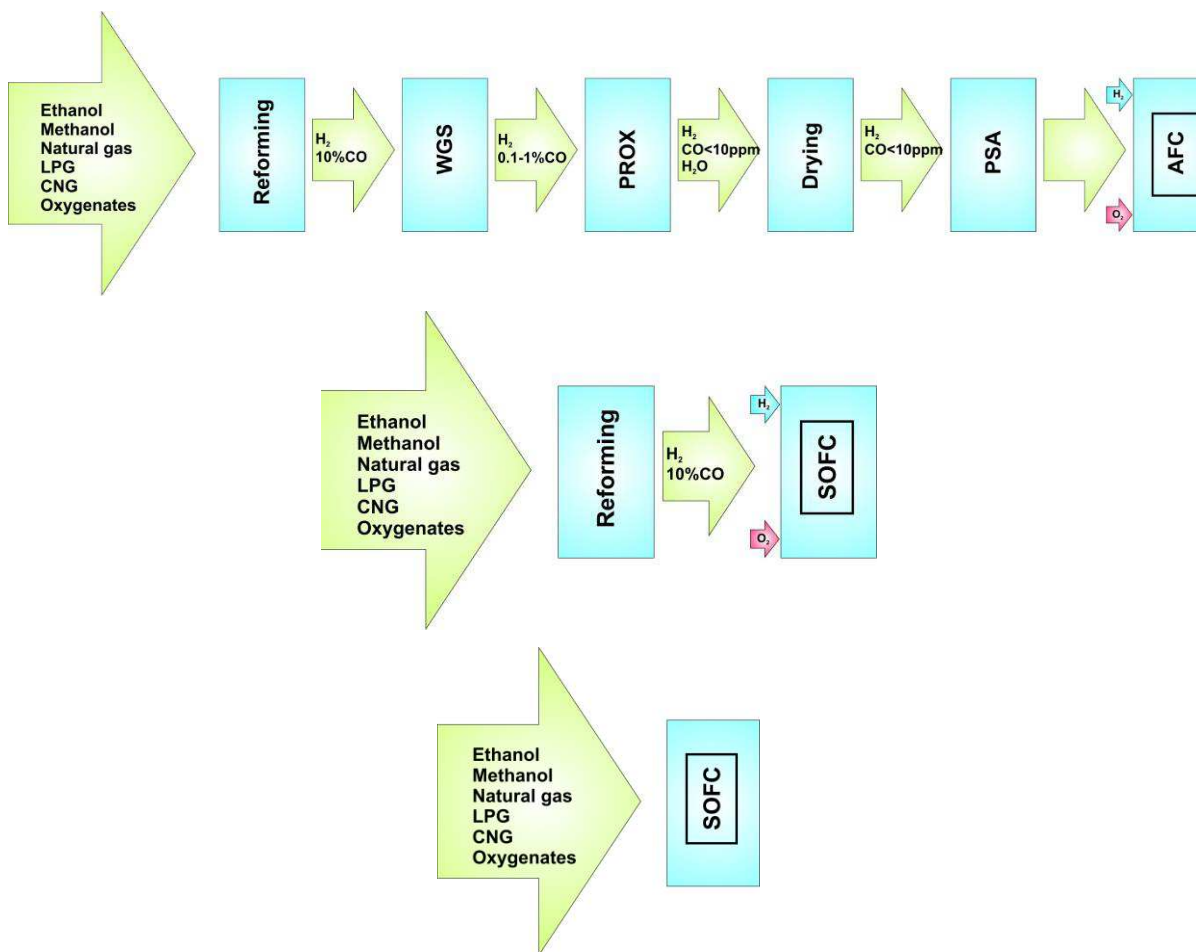


Figure 5-5: Schematic diagram of the various type of fuel cell powered by various feedstocks

One can observe from Figure 5-5 that to use the fuels for the alkaline fuel cell the fuels have to pass through different steps in order to reduce the content of CO after the reforming stage. The alkaline fuel cell needs pure hydrogen, because of the risk of contamination of the electrodes by CO. The SOFC has the advantage to accept the hydrogen from after the reforming or to be directly power by the different fuels, without any transformation of the fuels. Figure 5-5 defines three different energy systems between fuels and converters. The energy balance of the three systems, with different chemical processes of the fuel adaptation, will be investigated to understand and to compare the efficiency of conversion of the fuel adaptation steps of the three scenarios. This balance concerns the chemical energy available after the chain of chemical processes needed to adapt the fuels (vaporization, reforming, drying, PSA and H<sub>2</sub> generation) for the fuel cells inputs. For the calculation of energy balance, the thermodynamics of the processes and the chemical reactions are used. The efficiency of the different types of fuel cell is considered. The energy output of 1 kg of ethanol is after that available for conversion in the fuel cell to obtain electricity. Table 5-1 presents the comparisons of the values of the energy balance for the different configurations (variants) presented in Figure 5-5. From the results is the visible that variant 3 presents the configuration with the highest efficiency. This concerns the direct reforming of the bio-ethanol by the SOFC.

Table 5-1: Comparison of the values of the energy balance for the different configurations

	Vaporiser kJ/mol fuel	Reformer kJ/mol	Dryer kJ/mol	PSA (CO <sub>2</sub> separation) kJ/mol	Process of H <sub>2</sub> generation MJ/kg	Fuel cell Input MJ/ kg <sub>EtOH</sub> (chemical)	Fuel cell efficiency %	Fuel Cell output MJ/kg <sub>EtOH</sub> (electric)
Variant 1 (C <sub>2</sub> H <sub>5</sub> OH+H <sub>2</sub> O )	-466.45	-337.98	39.31	-21.85	-7.78	20.06 (AFC)	60% (AFC)	12.04 (AFC)
Variant 2 (C <sub>2</sub> H <sub>5</sub> OH +H <sub>2</sub> O)	-466.45	-342.10	----- -	-----	-8.08	20.10 (SOFC)	65% (SOFC)	13.06 (SOFC)
Variant 3 (C <sub>2</sub> H <sub>5</sub> OH+ O <sub>2</sub> )	----- ---	----- ---	----- ----	----- -----	0.00	23.30 (SOFC)	65% (SOFC)	15.15 (SOFC)

Table 5-2 summarizes the advantages and the disadvantages of the different conversion configuration, presented in Figure 5-5.

Table 5-2: Advantages and disadvantages of the different configurations (variants)

	<b>Advantages</b>	<b>Disadvantages</b>
Variant 1	Low cost fuel cell. Compatible to all types of fuel cells.	The lowest overall system efficiency. Multiple chemical processes. Three catalytic converters (at least one of them contain Pt catalyst). System load can not be adjusted on-line. Overall large dimensions difficult to use in a small size vehicles.
Variant 2	Overall system efficiency is slightly higher in comparison to multistep process. System load can be adjusted on-line in the limited range. It is not necessary to remove CO from the H <sub>2</sub> stream. Only one catalytic reactor is used. Low requirements on the type of fuel.	Only SOFC cell could be used. Limited number of start/stop cycles. Limited lifetime of SOFC system.

Variant 3	<p>The highest overall system efficiency.</p> <p>The most compact configuration.</p> <p>System load can be adjusted on-line in the limited range.</p> <p>It is not necessary to remove CO from the H<sub>2</sub> stream.</p> <p>Only one catalytic reactor is used.</p> <p>Low requirements on the type of fuel.</p>	<p>Only SOFC cell could be used.</p> <p>Limited number of start/stop cycles.</p> <p>Limited lifetime of SOFC system.</p>
-----------	----------------------------------------------------------------------------------------------------------------------------------------------------------------------------------------------------------------------------------------------------------------------------------------------------------------------	--------------------------------------------------------------------------------------------------------------------------

The variant 3, which presents the direct reforming of bio-ethanol, is the most efficient combination. In conclusion, it is proposed the working principle of the bio ethanol fuel cell for range extender unit for vehicle application. This unit delivers 23.3 MJ of chemical energy per kilogram of bio-ethanol. After conversion of the bio-ethanol in the SOFC fuel cell module 15.15 MJ of electric energy per kilogram of bio-ethanol is obtained.

The SOFC with integrated reformer of the bioethanol is the best fuel cell for the concept for a range extender unit. It presents the best energetic balance, from energy conversion point of view.

It presents the following advantages to be used to power electric vehicles:

- Long lifetime
- Low - costs of the electrodes
- Gases produced in SRE process can directly be used to power fuel cell stack
- High fuel efficiency
- Various compounds could be used to power fuel stack even natural gas
- Chemical stable of the solid electrolyte
- Low cost of raw materials for the electrolyte production

The disadvantages of using SOFC to power electric vehicles are:

- High operating temperature
- Long start-up
- Mechanical and chemical compatibility issues

The next part investigates the best catalyst system to integrate to the reformer to maximize the hydrogen yield and the stability of the conversion reaction from bioethanol to hydrogen.

## 5.2 Hydrogen from (bio)-ethanol steam reforming, selection of the catalysts:

For future carbon- neutral hydrogen production, the catalytic ethanol steam reforming (ESR) using bioethanol is seen as a promising solution. Ni- based and Co- based catalysts have been studied as a cost attractive solution for large-scale hydrogen production. However these non-noble transition metals catalysts present several difficulties including deactivation and activity by formation of coke and methane. Minimizing coke and methane formation requires an appropriate promoter or second metal, in addition to precise control of particle size and oxidation state of the active metal and acid-base and redox properties of support by changing the composition. Highly dispersed small metal particles are suitable for the active site with coke resistance, which can be prepared using an appropriate preparation method and/or support with good metal-support interaction. For example for Co catalyst, the oxidation state and redox properties of the supported Co strongly affect catalytic activity and durability. The oxidation-redox properties should be controlled by allowing or modification by promoter and/or support. Ethylene, regarded as a coke precursor, is formed mainly over the acid site of support. Therefore, basic support is effective for coke suppression. Redox active supports with oxygen storage capacity and oxygen mobility contribute to removal of deposited coke, change in metal oxidation state, and thereby improve coke resistance.

The main target of the research is to obtain a high active, selective and stable catalytic system for steam reforming of ethanol (ESR). The research is experimental and contains the following steps and durations:

- Preparation of the support material
- Preparation of mono and bimetallic catalysts by wet impregnation method
- Determination of the optimal process conditions
- Optimization of the catalysts composition and reaction conditions
- Determination of the susceptibility for carbon deposition
- Specific surface area measurements. Selective surface area measurements

The purpose is to obtain the highest possible yields of H<sub>2</sub>, using ethanol steam reforming and adapted catalyst for the reactions. The mechanism of ethanol steam reforming is displayed in Figure 5-6 and the main reactions included in the ESR are described by equations (5-1) to (5-13).

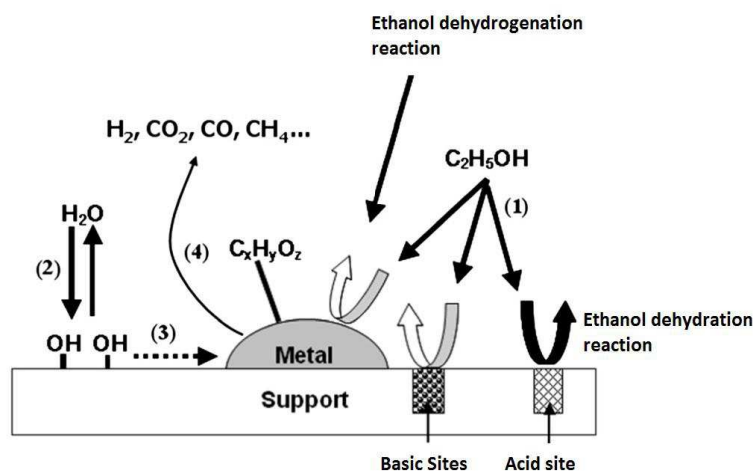
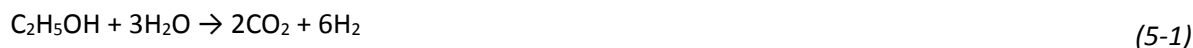


Figure 5-6: Mechanism of ethanol steam reforming [137]



#### Thermal decomposition



#### Ethanol dehydrogenation reaction



#### Ethanol dehydration



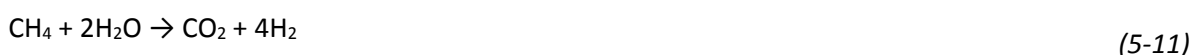
#### Acetaldehyde decarbonylation



#### Ethylene hydrogenation



#### Coke formation

**C<sub>2</sub>H<sub>4</sub> polymerization****Methane pyrolysis****Boudouard reaction****CO<sub>2</sub> formation**

The selected research conditions are at P – atmospheric pressure and T – 400-600°C.

The typical catalytic systems are composed from metal catalyst and supports:

- Metal catalysts: Co, Ni, Pd, Pt, Rh, and Ru
- Supports: (SiO<sub>2</sub>, Al<sub>2</sub>O<sub>3</sub>, CeO<sub>2</sub>, ZrO<sub>2</sub>, MgO, SiO<sub>2</sub>-Al<sub>2</sub>O<sub>3</sub>, SiO<sub>2</sub>-MgO, AC)

There are noble and non-noble metals catalyzing the reactions and the reactions and their efficiency depends on the operating conditions as temperature and pressure.

From the operating conditions for ethanol steam reforming (ESR) for noble and non-noble catalysts data reported in the tables in the literature, it is visible that the reactions conditions are different. Noble catalysts need lowest temperatures for reactions conditions. On the other side, the conversion efficiency depends as well from the different types of catalysts. They have as well different selectivity properties for reactions products as CH<sub>4</sub>, CO, CO<sub>2</sub>, C<sub>2</sub>H<sub>4</sub> and liquid. As result, the final H<sub>2</sub> yield of the ESR is different and it depends of catalyst choice.

From the data reported, catalytic performance appears to be influenced not only by the operational conditions employed, but also the nature of the metal phase and support used. Noble metal-based catalysts frequently exhibit better activity when compared to non-noble metal catalysts; however, these catalysts are very expensive. As a less expensive alternative, cobalt-based catalysts have been shown to have high activity and selectivity toward hydrogen, due to their capacity for CeC bond cleavage. Generally, acidic supports, such as Al<sub>2</sub>O<sub>3</sub>, are known to favor the dehydration reactions to ethylene and diethyl ether, followed by polymerization of ethylene to form coke. Basic supports, such as MgO, favor dehydrogenation and condensation reactions producing acetaldehyde and acetone.

The presence of these undesirable products, generated from these reactions, hinders the overall hydrogen production reducing the catalyst selectivity towards H<sub>2</sub>. However, better catalytic performance with good stability and high hydrogen selectivity can be expected over supports with redox properties, such as CeO<sub>2</sub>. This oxide has been commonly used as catalyst or catalyst support, as well as an effective promoter for catalysts, in the ethanol steam reforming process. This oxide has high oxygen mobility and storage capacity, and can act as a local source or sink for oxygen involved in reactions taking place on its surface. Notably, cerium oxide is known to enhance the reducibility, stability and the dispersion of the supported metal.

It is not obvious to select the best catalyst. This is question of compromise, between the main indicators of performance of the catalytic systems. A radar of the generic performances of the catalytic system is

displayed in Figure 5-7. It is very important to master the process of production of the catalyst to respect the below shown performances.

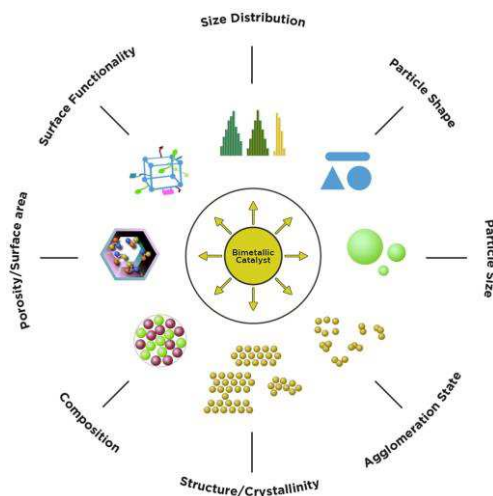


Figure 5-7: Main performances of the catalysts (bimetallic catalyst)

The main goal of the present research is to optimize the conditions of the chemical process (temperature, the composition of the gas mixture, stability test) and to select the composition of the catalyst for the ethanol steam reforming (ESR) and the hydrogen production for SOFC application. The ESR is integrated to the SOFC System and the heat operating conditions are between 600- 1000°C.

As catalytic systems are selected:

- Monometallic Ni- based catalysts
- bimetallic Pd-Ni catalysts

supported on  $\text{Al}_2\text{O}_3$ ,  $\text{ZnO-Al}_2\text{O}_3$ ,  $\text{CeO}_2\text{-Al}_2\text{O}_3$

The catalysts are produced according to a production process in laboratory conditions. They are tested as well in laboratory conditions. The following part describes the experimental work conduct for a research work for one-year period.

### 5.2.1 Experimental work

The applied investigation methods are Brunauer–Emmett–Teller (BET) theory - specific surface area, chemisorption method, and catalytic activity measurements. BET theory aims to explain the physical adsorption of gas molecules on a solid surface and serves as the basis for an important analysis technique for the measurement of the specific surface area of materials. The BET theory applies to systems of multilayer adsorption and usually utilizes probing gases that do not chemically react with material surfaces as adsorbates to quantify specific surface area. Nitrogen is the most commonly employed gaseous adsorbate used for surface probing by BET methods.

#### **N<sub>2</sub> adsorption-desorption**

Nitrogen adsorption isotherms of catalyst and supports were obtained at – 196 °C using a Sorptomatic 1900 (Carlo Erba Instruments Figure 5-8). The samples were previously outgassed at 300 °C and equilibrated under vacuum for at least 4 h before measuring the adsorption-desorption isotherm. Specific surface areas were evaluated from the measured monolayer capacity (Brunauer–Emmett–Teller method) using the range of relative pressure from ~ 0.05 to 0.33 and the value for nitrogen cross-section 0.162 nm<sup>2</sup>. The pore size distribution was calculated by the Dollimore and Heal (DH) method from the desorption branch of the isotherm.



Figure 5-8: Photo of 1900 Sorptomatic apparatus 51

### 5.2.1.1 Preparation of the catalysts

Firstly the support is prepared according to the steps presented in Figure 5-9. After that, the steps in Figure 5-10 are applied to prepare the monometallic catalyst.

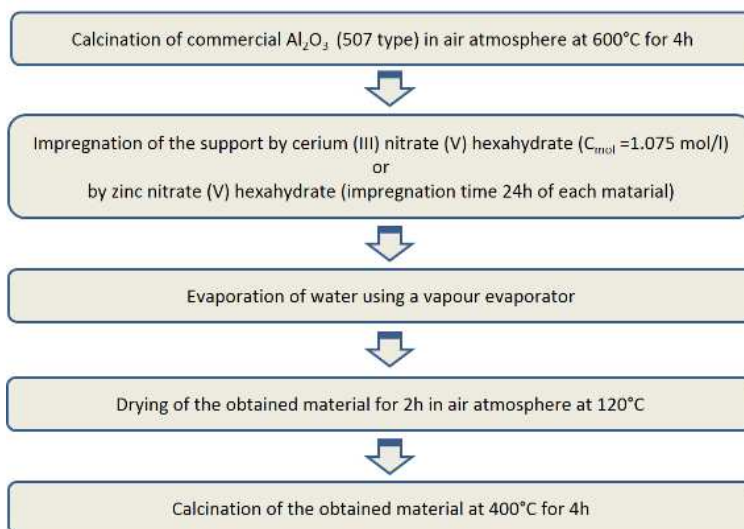


Figure 5-9: Catalyst support preparation scheme

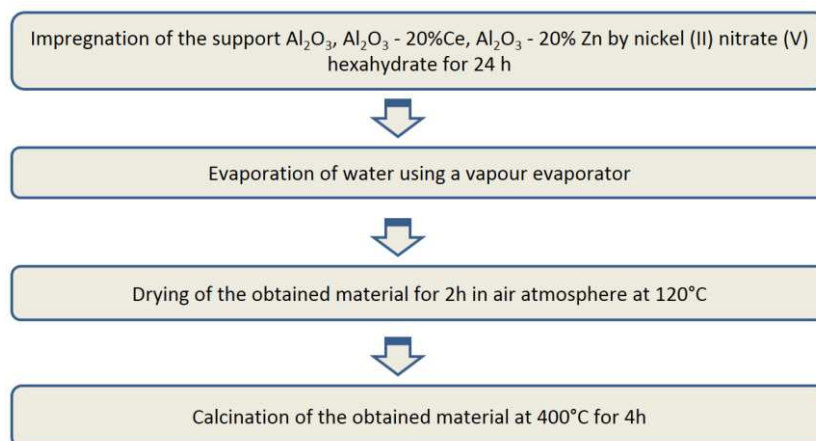


Figure 5-10: Monometallic supported catalysts preparation scheme

Catalysts were prepared using a wet impregnation method. The  $\text{Al}_2\text{O}_3$  monoxide was prepared by precipitation method from an aqueous solution of  $\text{Al}(\text{NO}_3)_3 \cdot 9\text{H}_2\text{O}$  and using a concentrated ammonia solution as a precipitating agent. The obtained precipitate was filtered off under vacuum, washed with deionized water until the filtrate became neutral, dried at  $120^\circ\text{C}$  for overnight, and calcined at  $400^\circ\text{C}$  for 4 h under air. As a carrier a commercial Alumina Fluka 507 C was used. In the first step on alumina surface the  $\text{CeO}_2$  or  $\text{ZnO}$  was deposited by impregnation method from appropriate nitrates (Ce or Zn). The loading of Zn (Ce) was 20%wt. Samples were dried and finally calcined in air atmosphere. To obtain oxidic form of carrier samples were dried and finally calcined in air at  $400^\circ\text{C}$ . After that Ni was deposited by wet impregnation method from nickel nitrate water solution. In the next step the catalysts precursors were dried and calcined at  $400^\circ\text{C}$ . Prior to process catalysts were reduced in hydrogen stream at  $400^\circ\text{C}$  to transform nickel oxide to metallic nickel. The nominal nickel loadings were 5 and 20%.

### 5.2.1.2 Characterization

The materials were characterized by BET surface area measurements to measure the specific surface area and porosity of the prepared supports:  $\text{Al}_2\text{O}_3$ ,  $\text{Al}_2\text{O}_3$ -20%Ce,  $\text{Al}_2\text{O}_3$ -20%Zn. The selected catalysts were determined by the BET method based on low temperature ( $-196^\circ\text{C}$ ) nitrogen adsorption method in a Sorptomatic 1900 Carlo-Erba apparatus (Figure 5-8). Samples before the measurements were degassed at  $350^\circ\text{C}$ .

Table 5-3 shows the results of the surface area measurements and the average pore radius of the prepared supports and catalysts.

Table 5-3: Characterization of the samples (supports and catalysts) with BET analysis

Support	BET surface area [ $\text{m}^2/\text{g}$ ]	Average pore radius [nm]
$\text{Al}_2\text{O}_3$	100	2.79
$\text{Al}_2\text{O}_3$ - 20%Ce	76	2.64
$\text{Al}_2\text{O}_3$ - 20%Zn	67	2.56
5%Ni/ $\text{Al}_2\text{O}_3$	99	2.91
20%Ni/ $\text{Al}_2\text{O}_3$	66	2.59
5%Ni/ $\text{Al}_2\text{O}_3$ - 20%Zn	55	2.63
20%Ni/ $\text{Al}_2\text{O}_3$ - 20%Zn	40	2.65
5%Ni/ $\text{Al}_2\text{O}_3$ - 20%Ce	68	2.67
20%Ni/ $\text{Al}_2\text{O}_3$ - 20%Ce	54	2.72

Table 5-3 shows that the adding of 20% of Ce and Zn (in oxidic form) on the  $\text{Al}_2\text{O}_3$  support reduces the surface area of the catalyst support. On the other hand, adding Ni on the  $\text{Al}_2\text{O}_3$  support to 5% or 20% decreases as well the specific surface area. The introduction of 5% of Ni increases the average pore radius of the  $\text{Al}_2\text{O}_3$  support to 2.91 nm for almost the same specific surface area of  $99 \text{ m}^2/\text{g}$ . The addition of 20% of Ni to the  $\text{Al}_2\text{O}_3$  support decreases the specific surface area more than the 5% Ni to  $66 \text{ m}^2/\text{g}$  and the average pore radius to 2.59 nm. All other combinations of bimetallic supports and Ni introduction lead to small specific surface area and average pore radius in comparison of the initial  $\text{Al}_2\text{O}_3$  support. The lowest specific surface area was observed for the catalyst systems containing the highest amount of nickel oxide (20 wt%). Such result can be due to the blockage of support pores by the deposited metal particles.

Figure 5-11 represents the evolution of the specific surface to the average pore radius for the different catalysts and catalyst supports combination. One observes the same tendency as in Table 5-3.

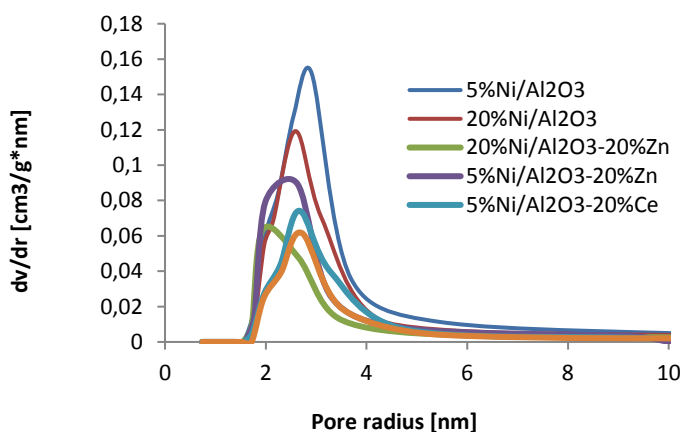


Figure 5-11: BET measurements

### 5.2.1.3 Activity evaluation

A test of the activity of the catalysts is done. A sample **20%Ni/Al<sub>2</sub>O<sub>3</sub>** is selected and tested in two configurations. The formation of  $\text{H}_2$ , CO and  $\text{CO}_2$  is investigated in the interval of temperature from  $50^\circ\text{C}$  to  $700^\circ\text{C}$ .

**Configuration 1:** 20%Ni/Al<sub>2</sub>O<sub>3</sub> p = 1Bar, C<sub>2</sub>H<sub>5</sub>OH: H<sub>2</sub>O = 1:4.5, T = 50 - 700°C, after red. at 500°C catalyst mass  $m_{\text{kat}} = 0.2 \text{ g}$

Before activity tests the catalyst was reduced in hydrogen stream at  $500^\circ\text{C}$  for 3 hours (the reduction temperature was chosen on the base of literature studies). During the process, the reduction of NiO take place according the scheme:  $\text{NiO} + \text{H}_2 \rightarrow \text{Ni} + \text{H}_2\text{O}$

**Configuration 2:** 20%Ni/Al<sub>2</sub>O<sub>3</sub> p = 1Bar, C<sub>2</sub>H<sub>5</sub>OH: H<sub>2</sub>O = 1:4.5, T = 50 - 700°C, calcined at  $400^\circ\text{C}$  catalyst mass  $m_{\text{kat}} = 0.2 \text{ g}$

For preliminary activity tests experiments (Figure 5-12, Figure 5-13) respectively were done using MS-spectrometer as a detector with the heating ramp rate  $10^\circ\text{C}/\text{min}$ . Based on above mentioned experiment the optimal temperature range for activity measurements were chosen, and we decided to study activity in the temperature range  $250\text{--}600^\circ\text{C}$ .

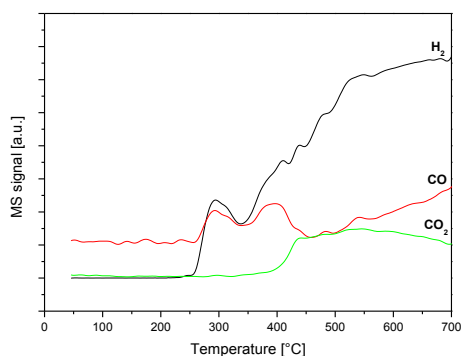


Figure 5-12: Activity test of 20%Ni/Al<sub>2</sub>O<sub>3</sub>, configuration 1

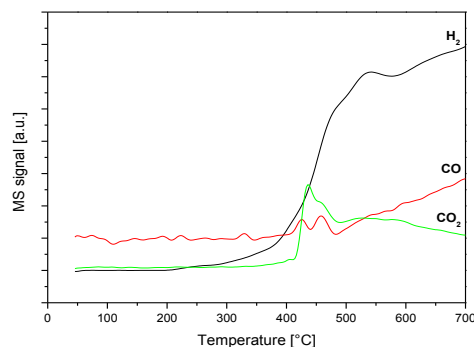


Figure 5-13: Activity test of 20%Ni/Al<sub>2</sub>O<sub>3</sub>, configuration 2

One can observe from Figure 5-12 and Figure 5-13 that the activation of the catalyst occurs from early for the configuration 1 at 250°C. The activation of the catalyst in the second configuration occurs for higher temperature: 400 °C.

In the next step is investigated the influence of the reaction mixture on the ethanol conversion value at 300°C and 350°C for the catalyst in configuration 1. The catalyst is redoxed at 300°C or 500 °C. The water to ethanol proportion varies and is investigated the way this impacts the conversion of the ethanol water mixture as a function of the temperature:

20%Ni/Al<sub>2</sub>O<sub>3</sub> p = 1Bar, C<sub>2</sub>H<sub>5</sub>OH: H<sub>2</sub>O = 1 : 3, 1 : 4.5, 1 : 6, T = 300, 350°C, after reduction, performed at 300 or 500°C, catalyst mass m<sub>kat</sub> = 0.2 g

The conversion ratio of ethanol and the H<sub>2</sub> selectivity of the catalyst, for different ethanol to water ratio are shown in Figure 5-14 and Figure 5-15.

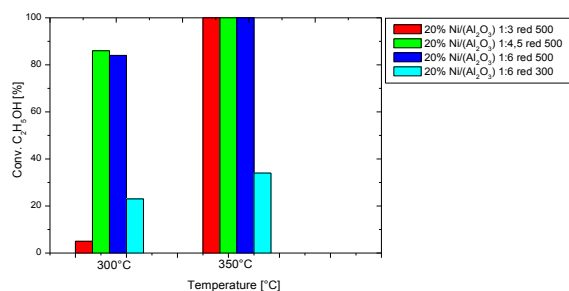


Figure 5-14: Ethanol conversion ratio

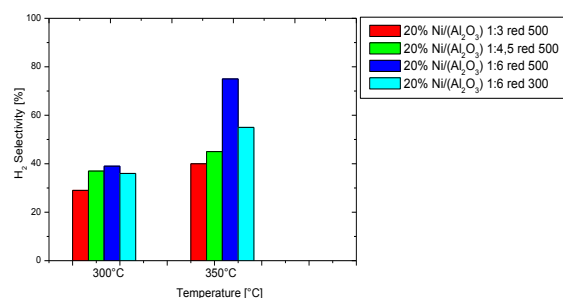


Figure 5-15: Hydrogen selectivity for the catalyst

The total 100% conversion ratio of ethanol is reached for 350°C, for catalyst reduced at 500 °C and for all ethanol to water ratios. At 300°C the conversion ratio of the lower water content and the lower temperature reduction, are low due to incomplete reduction of NiO at 300°C or partial oxidation of active phase during process by water vapor.

Figure 5-15 shows that the best selectivity of H<sub>2</sub> is obtained at 350°C and for 1:6 ethanol to water ratio. According to expectations, increase of water content shifts balance of the reaction to hydrogen and carbon dioxide.

Further is investigated the influence of the reaction temperature and Ni concentration in ethanol steam reforming (ESR).

The conditions of the tests are the following:

$p = 1\text{ bar}$ ,  $\text{C}_2\text{H}_5\text{OH} : \text{H}_2\text{O} = 1:4.5$ ,  $T = 280 - 600^\circ\text{C}$ , after reduction  $500^\circ\text{C}$ , catalyst mass  $m_{\text{kat}} = 0.2\text{ g}$

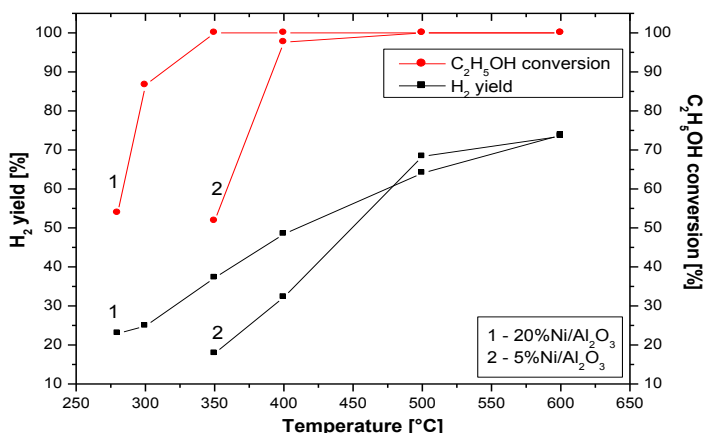


Figure 5-16: influence of the reaction temperature and Ni concentration in ethanol steam reforming (ESR) process

In Figure 5-16 the effect of nickel loading on the catalyst efficiency is shown. One can conclude that Ni increases the catalysts efficiency significantly. At the same process conditions, a significant increase in activity is observed after increasing metal content in the catalysts, for 20% of Ni.

### 5.2.1.4 Influence of the Ni concentration and Zn addition in ESR process

The conditions of the tests are the following:

$p = 1\text{ bar}$ ,  $\text{C}_2\text{H}_5\text{OH} : \text{H}_2\text{O} = 1:4.5$ ,  $T = 350 - 600^\circ\text{C}$ , after reduction  $500^\circ\text{C}$ , catalyst mass  $m_{\text{kat}} = 0.2\text{ g}$

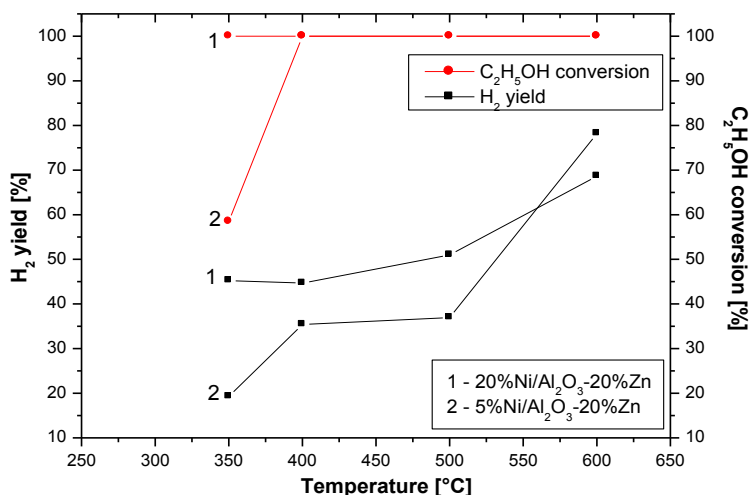


Figure 5-17: Influence of the Ni concentration and Zn addition in ethanol steam reforming (ESR) process

From Figure 5-17 we can conclude that the highest content of Ni allow to obtain higher ethanol conversion ratio and higher  $\text{H}_2$  yield at low temperatures from  $250^\circ\text{C}$ , for 20%Ni/ $\text{Al}_2\text{O}_3$ . The catalyst with 5% of Ni activates at  $350^\circ\text{C}$ . At  $500^\circ\text{C}$  the performances of the both catalyst are equivalent. From the analysis of Figure 5-17 is visible that addition of 20 % of Zn contributes to the improvement of the ethanol conversion and the  $\text{H}_2$  selectivity for the temperatures  $300^\circ\text{C}$  to  $500^\circ\text{C}$ . For temperature of  $500^\circ\text{C}$  the selectivity of  $\text{H}_2$  decreases for the both Ni catalyst, with the addition of Zn in the  $\text{Al}_2\text{O}_3$  substrate.

The influence of the Ni concentration and Zn addition on the H<sub>2</sub> selectivity in ESR process for different temperatures is displayed in Figure 5-18.

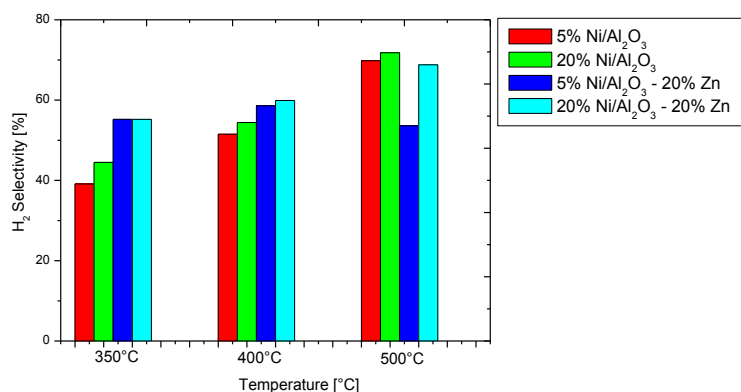


Figure 5-18: The influence of the Ni concentration and Zn addition on the H<sub>2</sub> selectivity in ethanol steam reforming (ESR) process

It is visible that at 500°C the 5%Ni Al<sub>2</sub>O<sub>3</sub> catalyst loses in hydrogen selectivity. To improve this the Cerium Ce is tested as substitute of the Zn.

The Influence of the Ni concentration and Ce addition in SRE process are shown in Figure 5-19. The conditions of the test are the following:

$p = 1\text{Bar}$ ,  $\text{C}_2\text{H}_5\text{OH} : \text{H}_2\text{O} = 1:4.5$ ,  $T = 350 - 600^\circ\text{C}$ , after reduction  $500^\circ\text{C}$ , catalyst mass  $m_{\text{kat}} = 0.2\text{ g}$

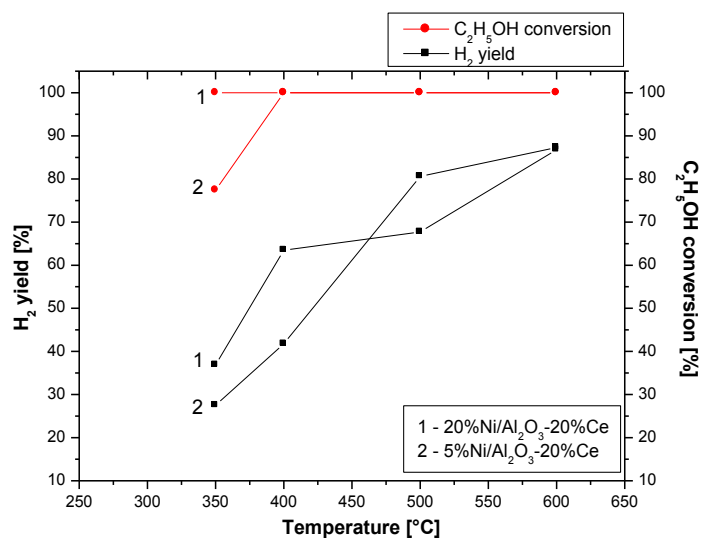


Figure 5-19: Influence of the Ni concentration and Ce addition in SRE process in ethanol steam reforming (ESR) process

The addition of Ce activates the catalyst at higher temperature from 350°C, to reach 100% ethanol conversion, but present the advantage to increase the hydrogen selectivity, especially for temperatures 500°C – 600°C.

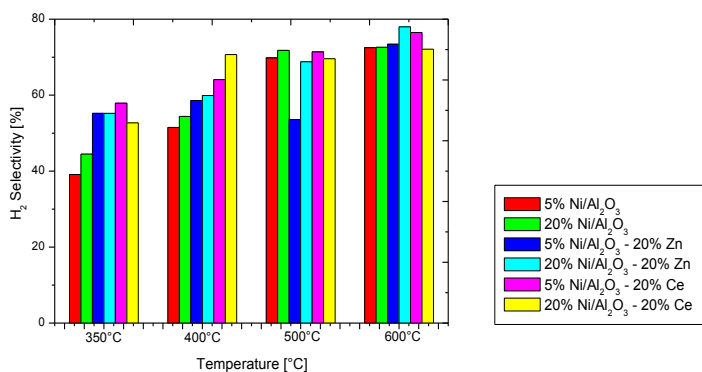


Figure 5-20: H<sub>2</sub> selectivity for monometallic Ni catalyst for ESR process

Figure 5-20 shows the Ce additive improves H<sub>2</sub> selectivity for temperatures higher than 350°. At 400 °C, the H<sub>2</sub> selectivity is sensitive to additives of the substrate. At 400°C, the highest concentration of Ni and the Ce additive in the catalyst combination 20Ni%Al<sub>2</sub>O<sub>3</sub>20%Ce shows the highest hydrogen selectivity of 70%. At 500° the 5%NiAl<sub>2</sub>O<sub>3</sub>20%Zn losses hydrogen selectivity performance. The substitution of the Zn by Ce for the low concentration of 5% Ni catalyst improves H<sub>2</sub> selectivity until 70%. At 600°C, the all catalyst variants including the low Ni 5% concentration obtain high H<sub>2</sub> selectivity, over 70%. Low concentration 5% Ni catalyst with Ce additive in the Al<sub>2</sub>O<sub>3</sub> support covers the needs of bio-ethanol conversion and hydrogen selectivity for temperatures up to 400°C.

**Bimetallic catalysts help to :**

- Determination of the promotion effect of Pd on the catalytic activity
- Optimization of the palladium content in the investigated systems
- Determination the content of carbon deposit which was formed during ESR process

Palladium is introduced to the low concentration Ni catalyst with Ce additive to the Al<sub>2</sub>O<sub>3</sub> support. Two low concentrations of palladium are used: 0.1% and 1%. The catalysts are evaluated and the results presented in Figure 5-21.

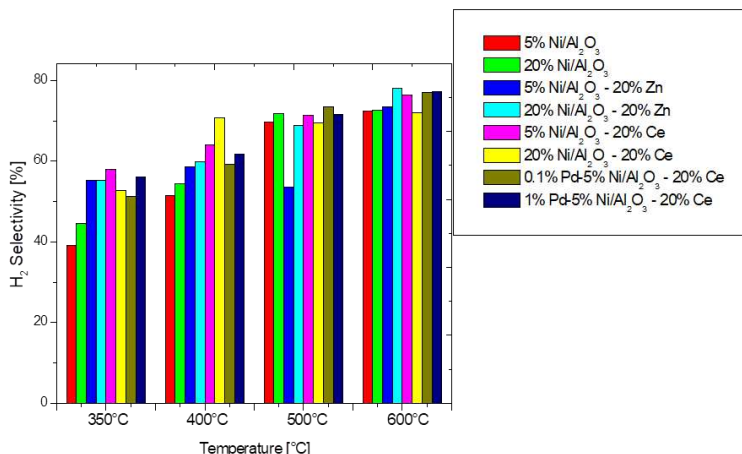


Figure 5-21: influence of the catalyst composition on the H<sub>2</sub> selectivity in ESR process – monometallic and bimetallic catalysts

The introduction of small concentration of palladium to the Ni based catalysts improves the H<sub>2</sub> selectivity. For 300°C and 400°C the highest concentration of 1% of palladium presents highest selectivity, but stays lower to the 20% Ni catalyst concentration. For 500°C, 0.1% Pd bimetallic catalyst presents the highest selectivity value. At 600°C, the bimetallic catalysts present excellent selectivity values. They are in the same range as the 20% Ni with Zn additive. Finally, for 600°C the palladium brings stability of H<sub>2</sub> selectivity for high temperature, as shown by the stability tests results at 600°C (Figure 5-22 and Figure 5-23).

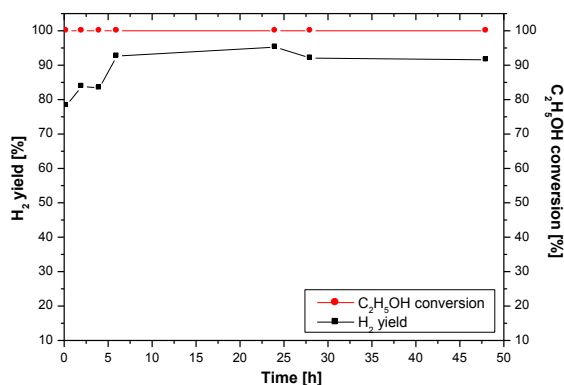


Figure 5-22: Stability test in ESR process,  $p = 1\text{Bar}$ ,  $\text{C}_2\text{H}_5\text{OH}:\text{H}_2\text{O} = 1:4.5$ ,  $T = 600^\circ\text{C}$ , after red.  $500^\circ\text{C}$ ,  $m_{\text{kat}} = 0.2\text{ g}$  5%Ni/Al<sub>2</sub>O<sub>3</sub>-20%Ce

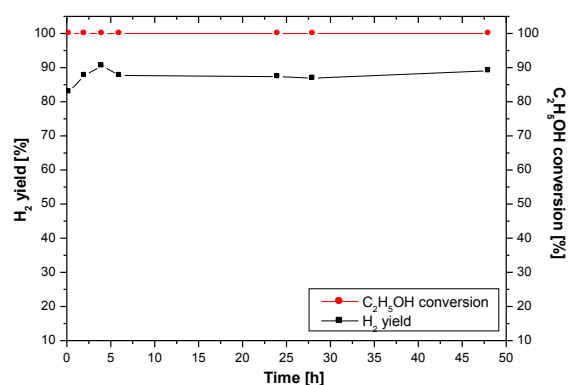


Figure 5-23: Stability test in ESR process,  $p = 1\text{Bar}$ ,  $\text{C}_2\text{H}_5\text{OH}:\text{H}_2\text{O} = 1:4.5$ ,  $T = 600^\circ\text{C}$ , after red.  $500^\circ\text{C}$ ,  $m_{\text{kat}} = 0.2\text{ g}$ , 0,1%-Pd-5%Ni/Al<sub>2</sub>O<sub>3</sub>-20%Ce

The lowest concentration of 0.1% of palladium in the bimetallic 5% Ni catalyst is sufficient to bring optimal H<sub>2</sub> selectivity. The CO selectivity curve for the two selected catalysts is presented on Figure 5-24.

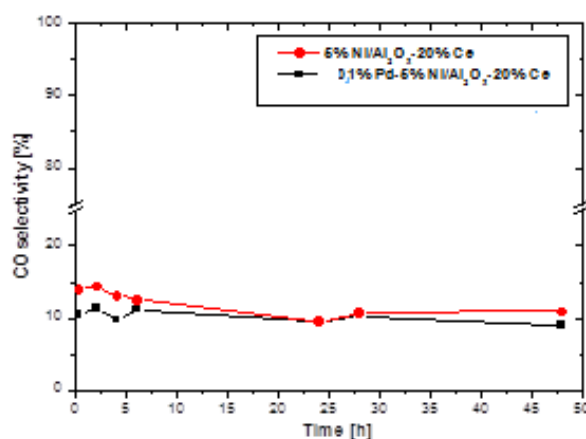


Figure 5-24: CO selectivity of 5%Ni/Al<sub>2</sub>O<sub>3</sub>-20%Ce and 0,1%-Pd-5%Ni/Al<sub>2</sub>O<sub>3</sub>-20%Ce catalysts

**The following conclusions can be drawn:**

- The most optimal content of nickel for monometallic nickel supported catalyst is 5 % wt. of Ni. Further increase of the nickel content does not increase significantly the catalytic efficiency.
- All catalytic systems showed high activity and selectivity at high temperature of the reaction especially above  $500^\circ\text{C}$ . The main products obtained during the process are CO, CO<sub>2</sub> and H<sub>2</sub>.
- The highest selectivity to hydrogen formation are observed at both 500 and  $600^\circ\text{C}$ .
- The optimal ratio between ethanol and H<sub>2</sub>O is 1:4.5. The increase of the molar ratio between these two components does not cause the increase of the ethanol conversion and hydrogen yield. The mixture ratio is closed to the stoichiometric.
- The activation of the catalytic systems in reductive mixture result in increase of their catalytic activity in ethanol reforming process.
- The high stability and high selectivity to hydrogen formation for mono and bimetallic systems was confirmed.
- Promotion effect of palladium on hydrogen selectivity in ESR process at high temperature range ( $500\text{-}600^\circ\text{C}$ ) was confirmed. The same effect was observed in low temperature process.

## **5.3 A well-to-wheels balance of the different energy storage and conversion technologies for sustainable mobility solutions**

### **5.3.1 Emissions and energy efficiency**

The most important driver for electric mobility (beyond climate protection) is the ability to operate locally emissions free, contributing to the air quality in cities, and with less noise. Although it should be reminded that noise reduction benefits from electrified vehicles are limited to up to 30 km/h, according to the ERTAC report [1]. Electric and electrified vehicles are particularly attractive since they represent vehicles that offer the most efficient use of regenerative energy. Although electric vehicles are more efficient, the CO<sub>2</sub> emissions are strongly dependent on the electric mix, used for the battery charging and the electricity production. This balance is prepared in the frame of the PSA- Airbus workshops, where advanced energy technologies are discussed.

The evolution of the well-to-wheels CO<sub>2</sub> emissions of battery electric vehicles (BEV), Fuel Cell Electric Vehicles (FCEV) in comparison with the conventional powertrains is shown in Figure 5-25 and in Figure 5-27 and described in much detail in the energy mix tables.

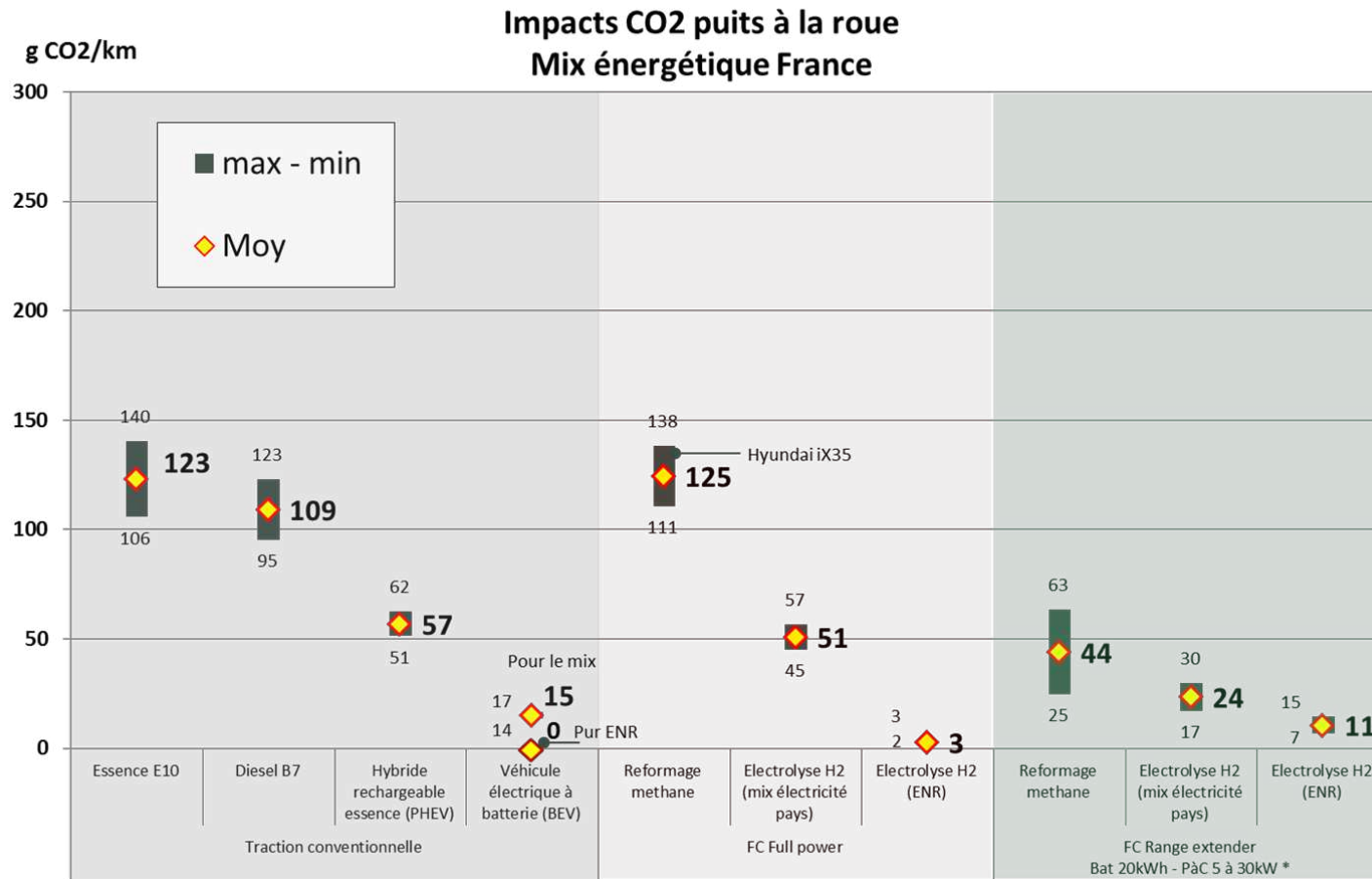


Figure 5-25: W-t-W total CO<sub>2</sub> emissions for different powertrain solutions for vehicles

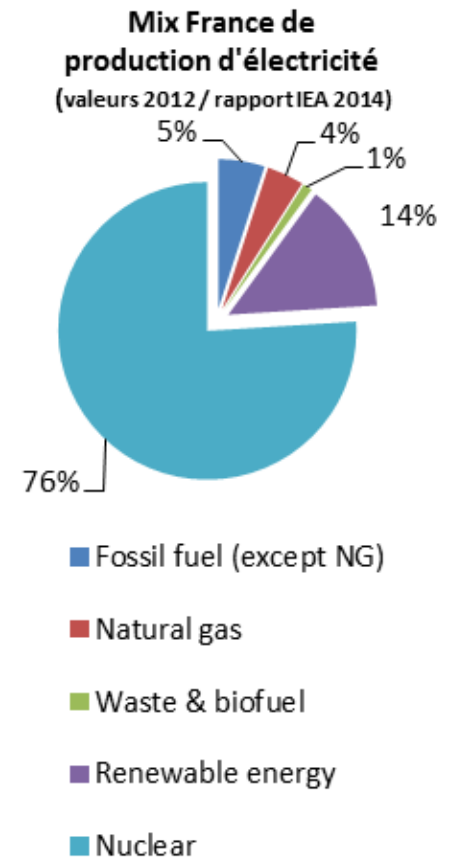


Figure 5-26: Energy mix of France for LCA analysis

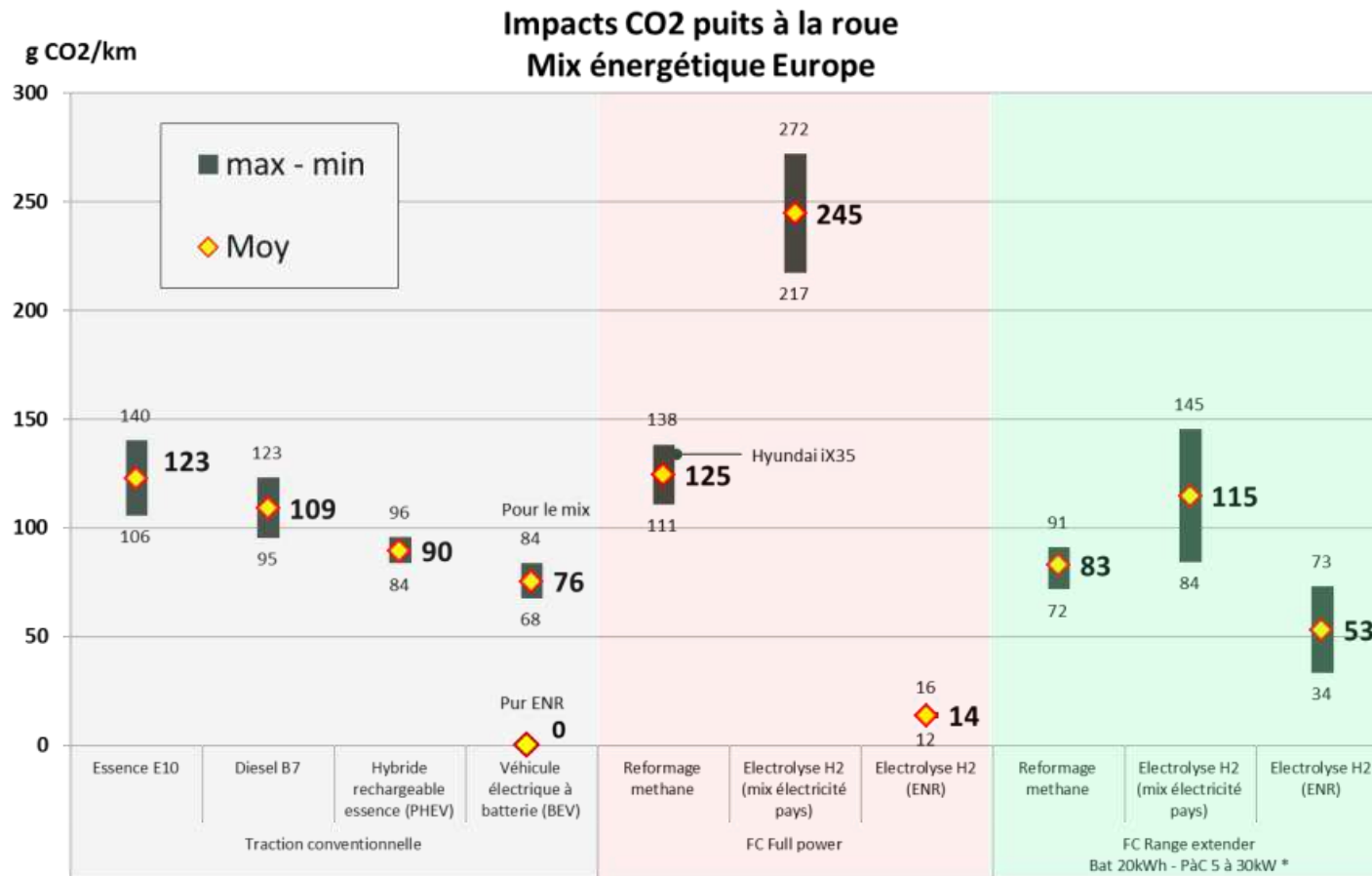


Figure 5-27: W-t-W total CO<sub>2</sub> emissions for different powertrain solutions for vehicles

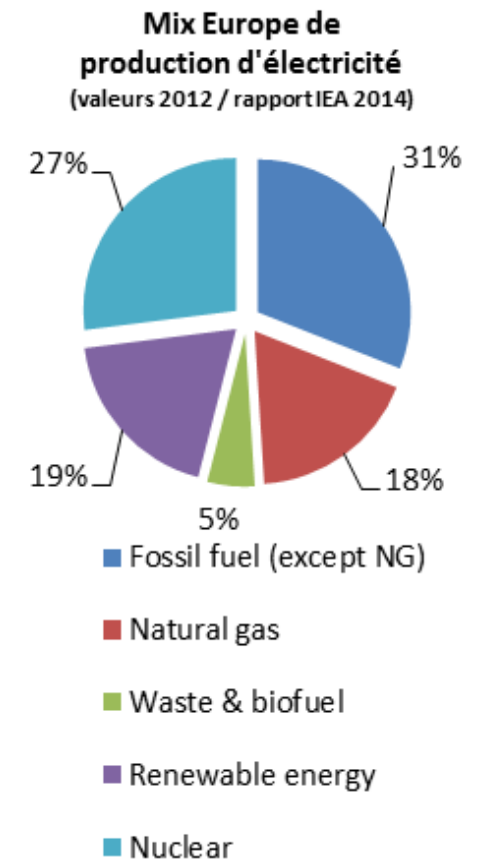


Figure 5-28: Energy mix of Europe for LCA analysis

Figure 5-25 shows the CO<sub>2</sub> emissions in well-to-wheels perspective and for different powertrains configurations: ICE powered vehicles, different types of hybrid electric vehicles, electric vehicles, and as well fuel cell electric vehicles. As it is a well-to-wheel CO<sub>2</sub> emissions perspective it is necessary to consider the electricity production mix and the way of production of hydrogen. Figure 5-26 shows the considered electricity production mix, which considers the French case, with electricity produced from nuclear at 76%. This electricity mix presents low CO<sub>2</sub> emissions. Two different configurations of fuel cell vehicles is as well considered: full power fuel cell vehicles and fuel cell as a range extender in the case of serial hybrid electric vehicle. One can see that the hydrogen production way is as well considered in the analysis: methane steam reforming, water electrolysis with the electricity from the grid, considering the electricity production mix and H<sub>2</sub> production with electrolysis, using renewable energy from the grid. A sensitivity analysis is given in the Figure 5-27, where the powertrain configurations are considered with different electricity mix – The average European electricity production mix. Figure 5-28 presents the average European production mix (2014). This mix contains different energy vectors (coal, natural gas, renewable energy, nuclear, etc.), with the repartition shown in Figure 5-28.

The evolution of the total well-to-wheel (WtW) CO<sub>2</sub> emissions is given as a function of the different powertrains (on board energy storage and conversion) configurations. There are min and max values, because of the variation of the efficiency of the onboard energy storage and conversion technologies combinations. The average value represents the average technology for each category.

In terms of WtW CO<sub>2</sub> emissions (Figure 5-25 and Figure 5-26), gasoline internal combustion engine (ICE) vehicles are evaluated to 123 g CO<sub>2</sub>/km. As the Diesel internal combustion engine (ICE) presents better onboard conversion efficiency than the gasoline ICE, the Diesel engine vehicles are evaluated to 109 g CO<sub>2</sub>/km. The ICE vehicles are not related to the electricity grid. The introduction of Plug-In hybrid electric (PHEV) technology connects the vehicles to the electricity grid. The WtW CO<sub>2</sub> emissions of those vehicles are dependent of the electricity production mix. For the case of low carbon electricity production mix (Figure 5-25 Figure 5-26), the PHEV reduce their WtW CO<sub>2</sub> emissions twice in comparison with the gasoline ICEV to 57 g CO<sub>2</sub>/km. This is due to the improvement of the Tank-to-Wheel (TtW) efficiency of the energy storage and conversion due to the hybrid electric technology. At the same time the use of the PHEV with the European electricity mix (EU Mix) shows 90 g CO<sub>2</sub>/ km. The last value is higher than 57 g CO<sub>2</sub>/km. The same trend of electricity mix dependence is observed for the battery electric (BEV). The composition of the electricity production mix reflects directly the WtW CO<sub>2</sub> emissions. Used with low carbon electricity (Figure 5-25) the electric vehicles emit 15 g CO<sub>2</sub>/km and 0 g CO<sub>2</sub>/km is electricity from renewables is used. If the BEV are used with the average EU mix, the emissions are 76 g CO<sub>2</sub>/km. This value is 5 times higher in comparison to the BEV emissions in the French contexts (Figure 5-25) and is it as well higher in comparison of the PHEV used in the low carbon electricity production mix. The emissions of the battery electric vehicles (BEV) vehicles remain lower than the internal combustion engine (ICE) vehicles. In the case of full power FCEV (130 kW of PEM fuel cell as prime mover), the production of hydrogen from methane steam reforming is not carbon free. Thus, the emissions of full power fuel cell electric vehicles (FCEV), powered with H<sub>2</sub> from methane steam reforming (MSR) are 125 g CO<sub>2</sub>/km. This value is equivalent to the CO<sub>2</sub> emissions of the ICE vehicles. The way to produce hydrogen impacts strongly the WtW emissions. The hydrogen produced from water electrolysis, powered with low carbon electricity (French mix, Figure 5-25) reduces the CO<sub>2</sub> WtW emissions with more than 50% to 51 g CO<sub>2</sub>/km. The use of renewable electricity for the electrolysis is the best configuration for almost zero CO<sub>2</sub> emissions, 3 gCO<sub>2</sub>/km. On the other hand, if the hydrogen (H<sub>2</sub>) is produced from water electrolysis but powered with European electricity production mix (EU Mix) (Figure 5-28), the emissions are higher - 245 gCO<sub>2</sub>/km. This value is twice higher than the use of H<sub>2</sub> produced from methane steam reforming and respectively higher than the ICE vehicles. The clean production of H<sub>2</sub> is important for the reduction of the WtW CO<sub>2</sub> emissions. The introduction of the fuel cell as a range extender for the electric vehicles (5-30 kW of fuel cell and 20 kWh of Li-Ion battery) leads to reduction of the size of the fuel cell and respectively the consumption of the hydrogen. This has as well a benefit for the total cost reduction. The fuel cell technology remains an expensive technology and the implementation of fuel cell module as a serial range extender for electric vehicles allows maintaining a good range of performances and acceptable cost.

The lower H<sub>2</sub> consumption in this configuration of range extender explains the lower CO<sub>2</sub> emissions, for the hydrogen obtained from methane steam reforming (MSR) and from water electrolysis. The electricity to charge the high voltage battery is as well considered. BEV with range extender of fuel cell emits 44 gCO<sub>2</sub>/km and 24 gCO<sub>2</sub>/km if the hydrogen is produced from water electrolysis. The part of electricity to charge the battery of the electric vehicles is accounting and the WtW emissions are 11 gCO<sub>2</sub>/km. The impact of the electricity production mix in this case is very strong. This is visible especially for the hydrogen produced by water electrolysis. For the hydrogen produced from water electrolysis using European electricity, and used in a range extender fuel cell vehicle where we obtain 115 gCO<sub>2</sub>/km. This is in the same order of magnitude that the ICE vehicles. For a fuel cell range extender vehicle using hydrogen produced from the water electrolysis and French electricity mix we obtain 24 gCO<sub>2</sub>/km.

### **Conclusions**

As main conclusion, the emissions depend of the efficiency of the conversion chain. The total WtW CO<sub>2</sub> are strongly influenced by the electricity production mix. Fuel cell and electric powertrains technologies help to reduce considerably the WtW CO<sub>2</sub> emissions, if we use low carbon electricity production mix and low carbon process for the hydrogen production. The production of electricity or hydrogen from renewable resources is a viable solution for the global WtW CO<sub>2</sub> efficient solution.

# Chapter 6 Conclusions

This report presents my research, related to the field of energy storage and conversion, with applications in the vehicles energy systems. The research is based on modeling, optimization but also experiments. The work is organized around three main research domains. The conclusions are organized according to the main research domains, followed by general conclusion, opening the perspectives of the research.

## 6.1 Energy efficiency, energy storage and conversion on vehicles board

This research presents studies of the efficiency performance and the economic optimization for a middle class vehicle with a downsized gasoline engine. Two technological options are studied for the efficiency improvement of the baseline vehicle powertrain:

- Low degree electric hybridization technology – called Mild Hybrid electric powertrain;
- Waste heat recovery system for two heat sources the engine water circuit and the exhaust gases, means an external thermodynamic cycle – organic Rankine cycle (ORC).

The main conclusion coming from the driving cycles evaluation is that the MHEV is an efficient technology for the drives with speed variations. The selected ORC design is efficient on the cycles using the charged area of the engine. The MHEV and the ORC are complementary technologies and their combination is especially efficient on the combined cycles containing urban and extra urban part.

The optimal environomic configurations for hybrid electric vehicles are researched by using multi objective optimization techniques. The optimization methodology is based on a genetic algorithm and is applied for defining the optimal set of decision variables for powertrain design. The analysis of the environomic Pareto curves on NEDC illustrates the relation between the economic and the environmental performances of the solutions. The life cycle inventory allows calculating the environmental performance of the optimal techno-economic solutions. The environmental and the economic trades-off are defined for the different impact categories. Their impact for the production phase and the use phase of the vehicle is studied. The sensitivity of the impacts categories on the electricity production mix is as well studied. The solutions in the lowest emissions zone show that the maximal powertrain efficiency on NEDC is limited on 45.2% and the minimal tank-to-wheel CO<sub>2</sub> emissions are 30 g CO<sub>2</sub>/km. They have the maximal cost – 75000 Euros. The increase of the electric part of the powertrain increases all environmental categories, because of the materials and the processes to produce the electric components.

A Lorentz force based electromagnetic actuator was developed and experiments are used to identify unknown model parameters for robust controller design. Simulations and experimental results show that a control law structure with a nonlinear feedforward and a plating strategy allow a real improvement of the convergence valve trajectory to a desired trajectory and make the actuator less sensitive to disturbances and parameter variations. The precision of the actuators and the robustness of the control law are important parameters for the integration of the actuators in the engine cylinder head. The electromagnetic actuators give the possibility to manage the engine gas exchange on a very performant way. The precision of the control law attests the controllability of the actuators technology and thus the good performances of the engine. The robust and precise controlling of the actuators on the intake side is especially important for the regulation of the airflow in the engine and this for gasoline engine

concerns directly the regulation of the engine torque. The respect of the velocity requirements during the valve landing is an important step and insures the respect of the noise criteria and the mechanical durability of the system.

The cylindrical batteries allow to build a very wide range of different battery package. Such battery package can be further connected in a modular systems e.g. for the big energy storage systems. The investigation of a heat generation in modular system is very important. This research presents a thermal energy balance of two types of the battery packs during the discharge process. One battery package was equipped with Al busbars while the other had Cu busbar. The investigated battery packages were made of sixteen 18650 type cylindrical cells. The calculation of the energy balance allowed to calculate the amount of generated heat inside the battery packages which is key information from the operation safety point of view. The conducted calculations were validated by the measurements of real battery package. The difference between the calculated model and the measured values were 6% for the battery package with Cu busbar and 1% for the battery package with Al busbar. By replacing the Al with Cu busbar it is possible to reduce the generated heat  $Q_{GEN}$  by 10%. Cu- and Al- based busbars serves to the electrical connections in the battery pack, but as well serve as solution of passive cooling to evacuate the heat from the battery pack.

## **6.2 Extension of the vehicle energy systems: the vehicles as grid related systems to the energy grids for optimal energy services for mobility**

This research focused on the development of a smart cost and simple localization system for a robot, used for recharging of the batteries in an unknown environment. The localization in an environment is a fundamental capacity for a mobile robot. Smart cost platform means the use of low cost sensors and low cost hardware, thus the algorithm of localization has to run on low power computer and with simple sensors. The algorithm must respect three main constraints: computation efficiency, accuracy of the approximation of the position and ease of implementation. After implementing our platform on a three Omni wheels robot with a LIDAR and encoders, set up the communication protocols and set the parameters, a reference map was successfully build. According to the tests results, the tracking performance is good at moderate speeds (100 - 200 mm/s) as well as the localization accuracy with an error maximum of 2 cm. Thus, the SLAM is efficient enough to meet the requirements for the application.

The designs for different mobility services (urban and long ways distance electric mobility) of the electric vehicles are defined and the time interaction with the charging infrastructure is analyzed. Information and connectivity solutions that inform in real time the drivers for the availability and the location of the charging infrastructure, including the possibility to book and pay for charge points in different places is an important part of the solution. Combined with fast, i.e. high power charging capacities, pure electric vehicles would be able to serve long range needs. The analysis of the environomic Pareto curves on NEDC illustrates as well the relation between the economic and the environmental performances of the solutions.

This research presents the developed method and its modeling to find the optimal strategy for recharging on the highway for a flow of electric vehicles, in the case of long-range electric mobility. The flows are composed by different numbers of vehicles that have to travel long range distance on the highway. They have to stop and recharge their batteries on the chargers located on the stations. The waiting and recharging times are evaluated, considering the stops, the occupation rate, and the location of the chargers. In a first level simple optimization is performed by minimizing the waiting time for charging. The order of the vehicles stops their recharging strategy come out as results. Differential evolutionary genetic algorithm is used to solve the optimization problem. The initial population of the vehicles flows is generated randomly and the genetic algorithm operators (evaluation, selection and mutation) are used to converge to the solutions. The results from the study cases show that an additional number of chargers are needed to be installed to minimize the waiting time on the highway and to reduce the waiting and

the recharging time on the highway stops. The investment cost of the chargers and the infrastructure has to be as well considered.

The vehicle is considered as grid related to the house and this means that its energy service of mobility and comfort is related to the energy services for the family house. The study contributes to consider in an integrated scale mobility and energy services for a household and introduces the use of the vehicle in dual mode. SOFC-GT module is introduced as a range extender of the autonomy of the electric vehicle. A base energy scenario for the house is also defined. The total yearly cost for the integrated system in dual mode stays still higher (1000 €/year) than the base case separately delivered energy services. This is due to the high investment cost of the equipment in the vehicle and the house. The major advantage of the energy integrated dual system is the reduction of the total GWP impact with around 30000 kg CO<sub>2</sub> eq. (60%). – from 50590 kg CO<sub>2</sub> eq. to 20338 kg CO<sub>2</sub> eq. This study illustrates large scale economic and environmental benefits opportunities by integration of the energy services for mobility and household.

## 6.3 Energy storage and conversion systems for energy vectors: fuel cell electric vehicles, hydrogen and their ecosystem

Optimal conditions and catalysts are researched for hydrogen production from bio-ethanol using ethanol steam reforming mechanism. In the studied concept the ethanol steam reforming is integrated in a SOFC in a serial hybrid architecture.

In view of the high price of noble metals, it is suggested to use higher concentrations of transition metals doped with small amounts of no noble metals eg. Ni doped with a small amount of Pd as an active phase components. The catalysts selection is done with laboratory experiments. While as a support it is suggested the usage of binary oxide system containing Al<sub>2</sub>O<sub>3</sub>, ZnO or CeO<sub>2</sub> or ZrO<sub>2</sub>. After the investigations, the most optimal content of nickel for monometallic nickel supported catalyst is 5 % wt. of Ni. Further increase of the nickel content does not increase significantly the catalytic efficiency. All catalytic systems showed high activity and selectivity at high temperature of the reaction especially above 500°C. The main products obtained during the process were CO, CO<sub>2</sub> and H<sub>2</sub>. The high stability and high selectivity to hydrogen formation for mono and bimetallic systems was confirmed.

The SOFC with integrated reformer of the bioethanol is the best fuel cell for the concept for a range extender unit. It presents the best energetic balance, from energy conversion point of view. This unit delivers 23.3 MJ of chemical energy per kilogram of bio-ethanol. In conclusion, it is proposed the working principle of the bio ethanol fuel cell for range extender unit for vehicle application with 15.15 MJ of electric energy output per kilogram of converted bio-ethanol.

It presents the following advantages to be used to power electric vehicles:

- Long lifetime
- Low costs of the electrodes
- Gases produced in SRE process can directly be used to power fuel cell stack
- High fuel efficiency
- Various compounds could be used to power fuel stack even natural gas
- Chemical stable of the solid electrolyte
- Low cost of raw materials for the electrolyte production

Disadvantages of using SOFC to power electric vehicles:

- High operating temperature
- Long start-up
- Mechanical and chemical compatibility issues

Well-to-Wheel (WtW) CO<sub>2</sub> emissions depend of the efficiency of the conversion chain, but they are strongly influenced by the electricity production mix. Fuel cell and electric powertrain technology help

to reduce considerably the WtW CO<sub>2</sub> emissions, if we use low carbon electricity production mix and low carbon process for hydrogen production. The production of electricity or hydrogen from renewable resource is a viable solution for the WtW CO<sub>2</sub> efficient solution.

## 6.4 General conclusion of the research work

The design of efficient energy systems for vehicles is complex and presents a challenge for the engineers. This task requires the development of design tools taking into account energetic, economic and environmental aspects simultaneously. The target for the automotive engineers is to assess the potential of the different technology options for vehicle energy systems and to propose to the decision makers the solutions presenting interest for future research and development. The main interest is to include this systematic approach in the early design stage of the vehicles development process and thus to optimize the financial efforts in terms of R&D and industrial investment. The vehicles are part of the global energy system and deliver energy services. The new extended limits of the system have to be considered in the method.

The generic method for environomic design of vehicle grid related energy systems is summarized in Figure 6-1.

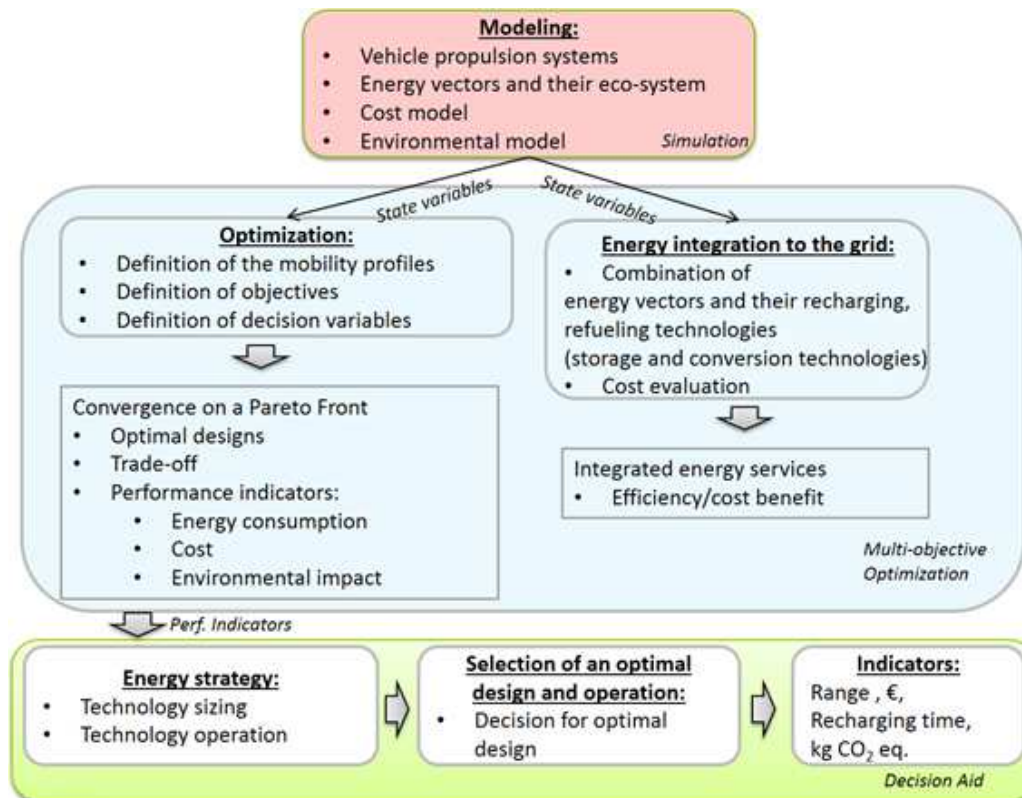


Figure 6-1: method for environomic design of vehicle grid related energy systems

The future technologies for sustainable mobility are the electrified vehicles (electric and hybrid electric vehicles) and fuel cell propulsion vehicles. The fuel cell vehicles have to use green hydrogen or liquid fuels that are rich to hydrogen such as the bioethanol. The electricity used for mobility needs has to be green and produced from renewables. Hydrogen is as well used as energy storage for renewable intermittent energies. The methanation permits to link the natural gas grid and the hydrogen grid. The enlarged energy grids are the stockers for the intermittent energies. The electric machines and the fuel cell are the converters on vehicle onboard to move the vehicles on a sustainable way. For that, it is needed to apply systematic method for evaluation. The research perspectives set the future axes of the research.

# Chapter 7 Research perspectives

## 7.1 Goals and philosophy

The general goals of the research program are based on energy, processes and environment core science and defined as an investigation of integrated processes and energy conversion systems that integrate renewable energy resources for urban environments. The integrated energy systems supply multiple energy services and are a key issue for our energy future. New materials are also needed for the energy harvesting, conversion, storage, efficiency, as well for the environmental protection and reparation. The development of advanced computer aided methodologies combining thermodynamics and optimization techniques help engineers in the development of more efficient and more sustainable processes and energy conversion systems that allow important energy and emissions savings. The research field of “Energy, processes and environment”, applied to urban energy systems, combines process integration techniques, exergy analysis, process modelling and thermo-economic optimization. Process synthesis methodologies are also used, as an application and development of computer aided process engineering methods: data treatment, simulation, process integration, mixed integer linear and nonlinear programming, and multi-objective optimization. The research field of urban energy systems combines multiple disciplines, on the current state of energy related research including impacts of energy use and conversion on critical resources such as water, or on climate change. Life cycle assessment methods are used for the environment impacts estimations.

The research program is proposed to be established on the described field of “Energy, processes and Environment” by developing concepts and solutions for energy integration in the urban, industrial and also the transportation sectors. Experimental tests on the advanced technologies for energy integration can be performed in the laboratories for the validation of the models. Energy planning activities can be also generated and developed as an additional axis in the research program.

## 7.2 Research axes

An application example is the energy integration in the urban systems. The activities in the field of urban systems concern large-scale integration of energy systems using networks (heating, cooling, hydrogen, water, CO<sub>2</sub>), considering simultaneously the available (renewable) energy resources, the industrial processes and the buildings requirements. The system boundary extension is a natural evolution of the process system design application

Another example of application of the energy integration is the transportation sector.

The research focuses on a smart, green and responsible transportation for sustainable mobility. The mobility is important for the economic and social development of the population, but also has to respect the environment. The challenge for the future is to imagine and develop sustainable mobility in smart clusters. The transport means can be considered as autonomous or grid related. The energy grids are as well related. Figure 7-1 illustrates the integration of the energy grids of electricity, hydrogen and natural gas. For example, for the last 20 years the cities have been challenging the mobility paradigm, generated around cars as principle mode of transport. Many efforts from the research and the industry came to improve the efficiency of the vehicles (all types), their comfort and security. The modern vehicles are characterized by low emissions and diversification of the powertrain for the energy integration

adaptation. Today the vehicle paradigm is also being challenged by climate change and current natural resources deployment.

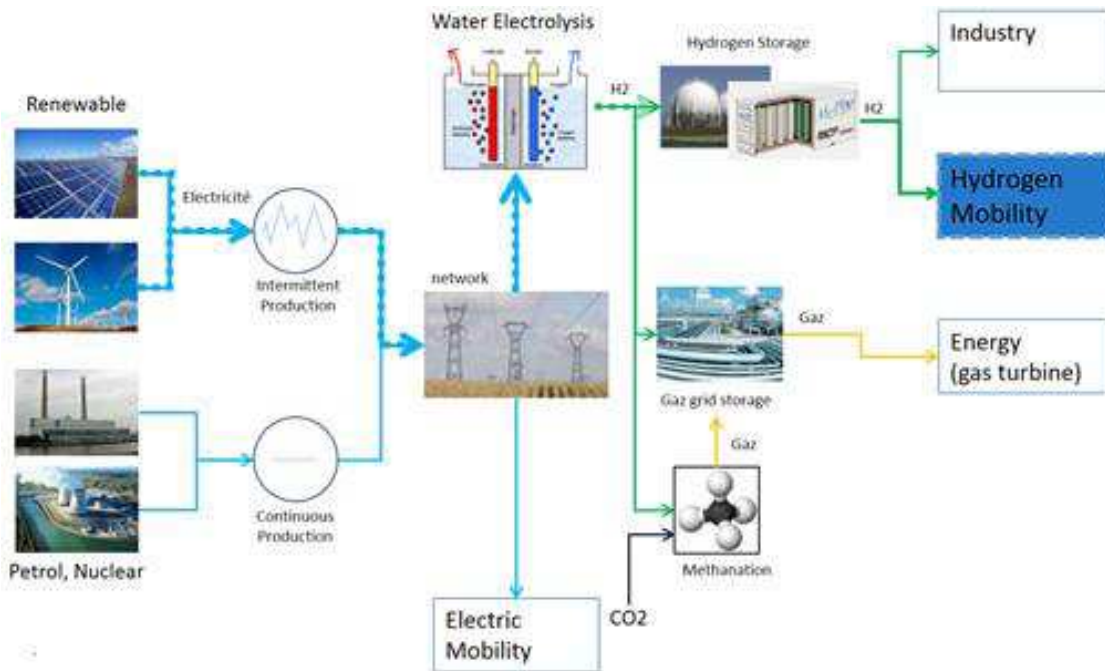


Figure 7-1: Technologies for storage and conversion of hydrogen between energy grids. Integration of energy grids and services.

The energy grids of the different energy vectors are connected and integrated on a large-scale energy system, with different production, storage and distribution capacities (Figure 7-1).

The number of electric vehicles and hybrid electric vehicles increase in the mobility market. The range and the energy storage of the vehicle on board are important. The recharging of the vehicles and their relation to the energy grid became an important question. The energy system boundary can be extended to the vehicles and the grid system, including the chargers and it needs to be optimized. There is a wide spread use of new information and communication technologies for all means of transport. The real time information and the on demand transportation know rapid development. There is a change of focus from the development of the products –vehicles to development of infrastructures, related with the improvement and the integration of the management of the mobility services. Electric and hybrid electric vehicles and other advanced powertrain vehicles are promoted for usages in the cities and the extension of the charging points network is needed. The environmental and economic sustainability of the services is also required. The wish of the clusters to integrate sustainable mobility is clear and as conclusion the development and use of electric and hybrid electric vehicles especially for city mobility are recommended. However a real business model does not exist. Due to the high investment expenditure, new approaches to solve the problem are needed.

The research in the field of transportation engineering and transportation systems could be focused on the development of integrated approaches and testing of business models for the local production and distribution of energy (fuels, electricity, hydrogen) to create conditions for market take-up in urban and sub-urban areas, infrastructure deployment and adequate vehicles equipment. The approaches will conclude the system integration of the infrastructure with a large vehicle fleet.

### 7.3 From the method to the tool

The prospective method can serve to evaluate different options for the vehicles and the recharging (refueling) technologies related to the density of the recharging installation and the investment capacities. The connections with other industrial sectors are as well presented.

The optimization and simulation tool has to fulfill the following requirements:

- Enough flexible to simulate a wide range of conversion technologies with different level of detail
- Integrate a dynamic profile simulation and estimation of the system performances and resistance efforts
- Possibility to include fuels options, as energy vectors
- Define the size of the equipment
- Include economic models to deduce the cost of the equipment
- Include environmental life cycle assessment (LCA) based models to deduce the environmental impacts
- Give operation strategies possibilities

The tool can be used for scenario generation to research affordable and sustainable solutions for mobility.

User platform can be created, implementing libraries related to the technologies, different energy resources and as well energy demand profiles. The optimization structure contains the simulation models and the optimizer based on genetic algorithm. As results the tools gives information about the sizing and the operation strategy of the technological equipment, distribution of the heat for city energy needs, mobility energy strategies for public and private transportation or consideration of the logistic strategy for goods, per rail or road.

The temporary dynamic profiles could be considered, monthly or hourly. The solving algorithms are using mixed-integer nonlinear programming. The following characteristics can be noticed:

- decision variables,
- Parametrized assumptions & constraints
- Multiple indicators : Cost, CO<sub>2</sub>, primary Energy , Exergy, Employment, Waste
- Uncertainties, Monte-Carlo Simulation

## 7.4 Applications

The methodology is applicable in large domains of industrial fields: energy efficiency, process system design and energy systems design. The transportation category is related to all those categories.

The following applications can be developed:

- Assessment of the services that electric vehicles could provide to the electricity network
- Assessment of the strategies for the use of renewable energies in sustainable and profitable mobility scenarios.
- Assessment of the scenarios for the production, storage and distribution of clean hydrogen from biomass

The biomass is one of the main energy vectors for the production of clean hydrogen. The experimental research on the discussed concept of serial range extender with SOFC with integrated steam reformer can be continued. The main axes are presented below.

Bio-ethanol and conversion of the hydrogen:

- The future researches for the SOFC with integrated bio-ethanol steam reformer are:
  - determination of the conditions of usage ethanol as a fuel for a SOFC fuel cell,
  - developing new material for a SOFC dedicated for ethanol oxidation,
  - testing SOFC materials (activity, stability etc.)
  - testing the SOFC efficiency in the case of use ethanol as a fuel

The energy resources and the metal resources are scarce. A global optimization of the energy and the material demand is needed. The circular economy describes the usage, the recycling and the recirculation of the materials. The main question that the automotive industry has to solve is the development of adapted clean technologies. The automotive industry has to propose sustainable products and sustainable services for mobility. The automotive industry focuses on the development of multiple technologies, convenient for the different local markets and regulations. There is the need to plan and to develop key technologies and key activities.

In conclusion, globalization, urbanization, digitalization, scarcity of resources, renewable energies, and the growing demand for affordable mobility are leading to changed, much more dynamic market requirements and new business models.

# Appendix A Methodology

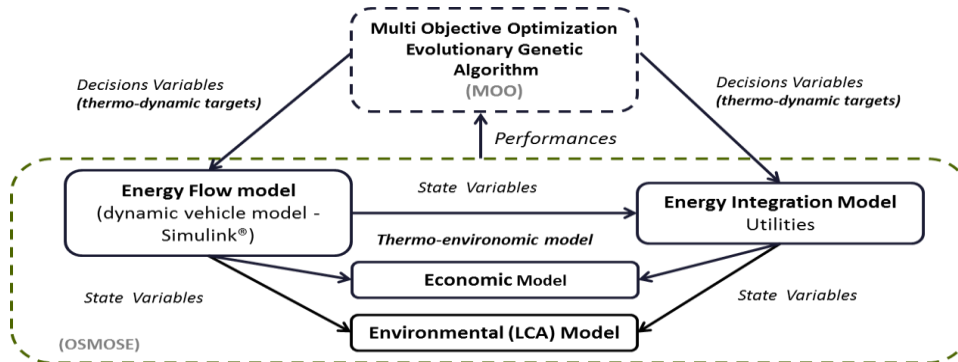
## A.1. Multi objective optimization and energy integration

### A.1.1. Multi-objective optimization

The optimization and simulation tool to be used in this thesis work has to fulfill the following requirements:

- Enough flexible to simulate a wide range of conversion technologies with different level of detail
- Integrate a dynamic profile simulation and estimation of the system performances and resistance efforts
- Possibility to include alternative fuels options
- Define the size of the equipment
- Include economic models to deduce the cost of the equipment
- Include environmental LCA based models to deduce the environmental impacts
- Give an operation strategies possibilities

The general computational framework of the environomic optimization (Figure\_ A-1) has already been done and described in [116].



Figure\_ A-1: Computational framework of environomic optimization.

The computational platform combines the energy flow models and process/ design integration techniques to model the interactions between unit operations. The energy is exchanged between the unitary processes or design units. In a first time, the energy flow model calculates the energy transformations in the process/ design unit for a specific configuration and operating conditions. The resulting mass and energy flows are used to generate the energy integration model, with optimization of the heat and power production, by minimizing the total exergy and operating cost.

The thermodynamic states and flow rates of the energy-flow and energy integration models are used in a post- calculation phase to size the equipment, to estimate the cost and to evaluate the performance of the process or design configuration. The performance indicators can be used in the frame of multi-objective optimization framework, in which an evolutionary algorithm is implemented.

A set of decision variables addressing technology choices and operating conditions of the process or design units and utility system can be provided for this.

The environmental model consists in a life cycle inventory of the processes or design units. For each thermo-economic configuration of the system the life cycle impacts are evaluated. The life cycle impact can be also used as objective function for the optimization.

The basic methodology has for objective to implement systematically the vehicle LCA model to show the environmental life cycle performance and the economic models will be used to estimate the cost and the investments. The objectives are conflicting and can be considered in its multi-objective, environmental (i.e. energetic, environmental and economic) optimization.

A superstructure including the optional technological solutions and the potential resources is built and the thermo-economic models of these components are developed. First the three different sub-systems composing a vehicle system have to be simulated separately. These include:

- The mobility profiles and the energy services for the vehicle
- The energy resources
- The conversion technologies

Each model of the resource and of the technologies has to be included in the superstructure.

These sub-systems are then integrated using process integration techniques to build the complete energy conversion system. The process integration model is solved as a Mixed Integer Linear Programming (MILP) sub-problem, which decision variables are the utilization rates of the technologies in the superstructure during the different operating conditions.

The thermo-economic performances and Life Cycle Impact Assessment (LCIA) of the integrated system are calculated, based on the process operating conditions and on the system design.

The multi-objective Mixed Integer Non-Linear Programming (MINLP) problem is then solved using an evolutionary algorithm.

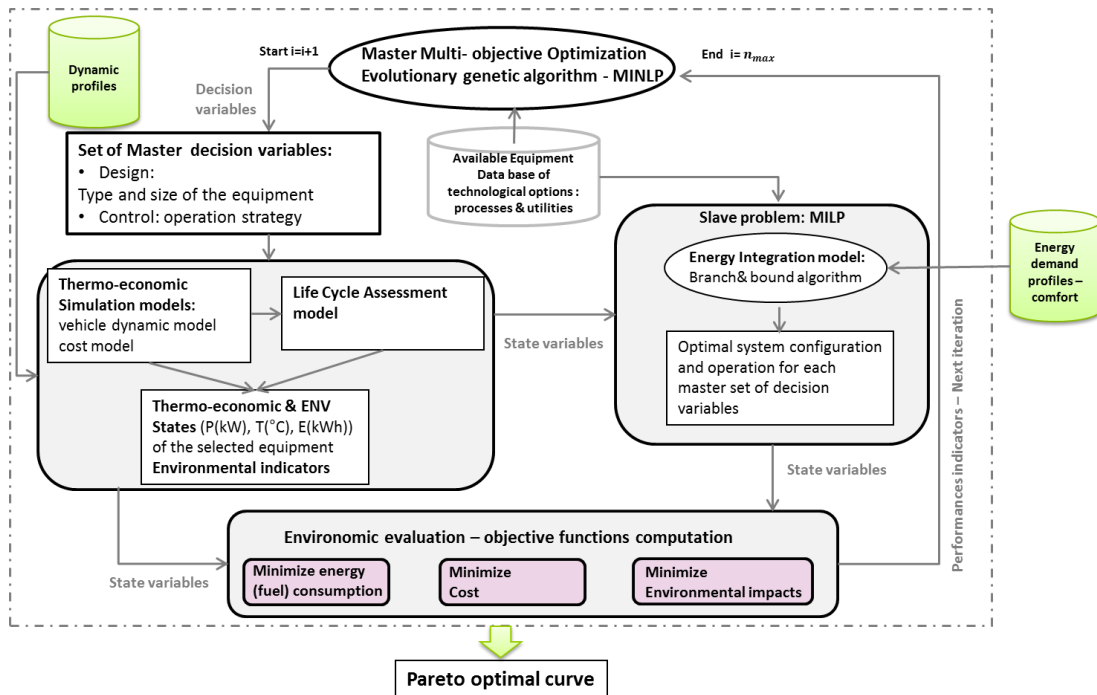
The general computational framework has already been adapted for vehicle applications in [2] and [3]. The superstructure contains a vehicle simulation models, validated with experiments. The models contain dynamic and thermal layouts. The cost equations are integrated in the economic model. The energy integration model uses the results from the dynamic and thermal flows calculations. The optimizer in OSMOSE is based on a genetic algorithm. This optimization technique is multi-modal and gives local optimums. The organic Rankine cycle (ORC) is considered as a utility for the energy integration. The ORC design is optimized according to techno-economic objectives. The optimization consists in four major parts – a master multi objective optimization (MOO), a thermo economic simulation (TES), a slave optimization (energy integration - EI). The techno-economic evaluation (TEE) is the last part. The life cycle impact assessment (LCIA) indicators are used as optimization objectives. They are implemented in the master optimization, according environmental optimization.

**Master Optimization:** The types and the size of the equipment are defined in the decision variables. An evolutionary algorithm (EMOO) solves the master optimization with 3 objectives: minimization of the fuel consumption, minimization of the investment cost and minimization the environmental impacts (Figure\_ A-2).

**Thermo-economic simulation:** This simulation occurs in a second step. The thermodynamic and economic state of the selected equipment is calculated.

**Economic evaluation:** The techno-economic evaluation (TEE) uses the selected superstructure in the master level and the result of the slave optimization phase, to calculate objective functions of the master optimization – cost, and CO<sub>2</sub> emission.

The results of multi-objective optimization converge to the Pareto frontier curve.



Figure\_ A-2: Structure for multi-objective optimization

**Slave optimization:** The energy integration calculates the best operating strategy of selected equipment by solving a mixed integer linear model (MILP). The aim is to minimize the total cost under the energy balance and the heat and power cascade constraints. The input data used in the energy integration includes the values of the master decision variables, the resources, the power dynamic profile and the comfort profile.

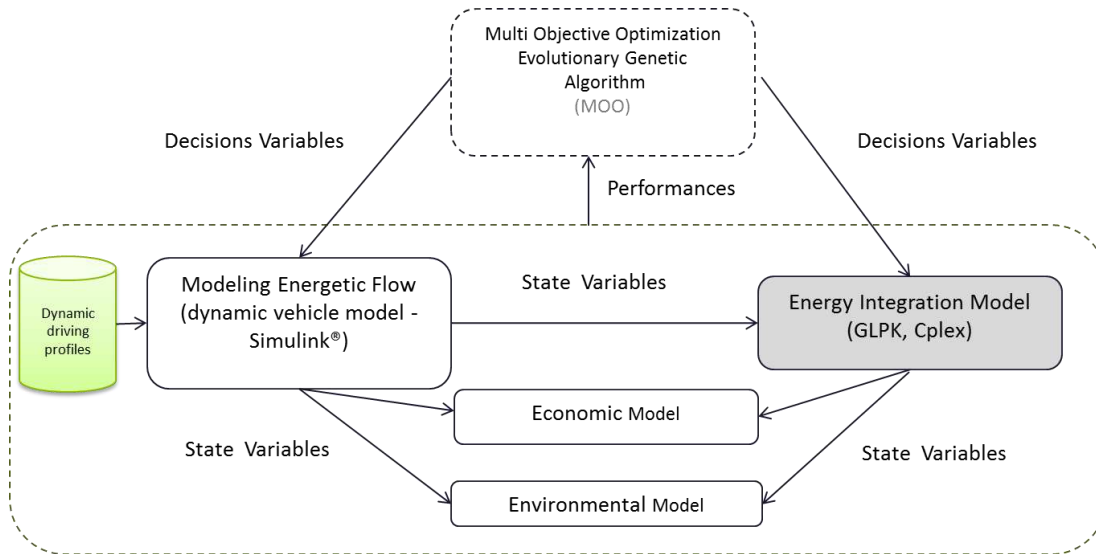
The energy integration is done in the second stage of the approach and this is a slave optimization based on mixed integer linear programming. The energy integration defines the potential of heat recovery and deduces the choice and the sizing of the adapted utilities. In the energy integration problem the engine and the vehicle cabin are defined as processes “cold” and “hot” streams between which a heat exchange has to occur. The minimum energy requirement of the system is then estimated and a utility is used to close the energy balance and estimate the energy recovery potential.

The utility system pertinent for energy recovery – for example the organic Rankine cycle (ORC) is defined in the energy integration module. In the EI the level of temperatures (evaporation and superheating) of the ORC are optimized to obtain the maximal net power output. The optimization is done for each operating point and each working fluid and comfort demand. The outcomes of this optimization are the ORC loop sizing (working fluid flow, sizes of the turbo machines and exchanged heat in the evaporation and the condensation) the efficiency and the net power output. The solutions converge on a Pareto curve. The number of the solution is identified by an ID number. Different ID of solutions of the Pareto curves are detailed in the chapters of results.

### A.1.2. Energy integration

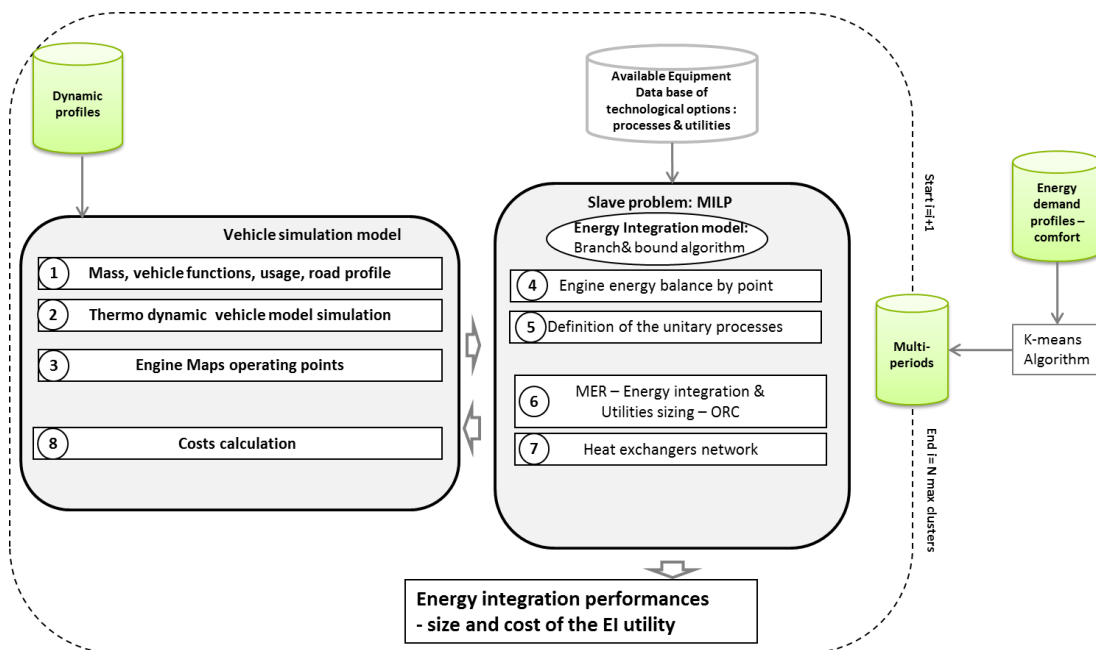
The process optimization proposes a structured methodology to identify, characterize and quantify the waste heat of a system. The process integration (PI) methodology dates back to the 1970s and the first developments are in the heat integration.

The methodology is adapted and explained for vehicle and illustrated in Figure\_ A-3.



Figure\_ A-3: Architecture of the multi-objective optimization tool for vehicle applications

The energy integration is the slave optimization part of the OSMOSE Superstructure. The energy integration calculates the best operating strategy of selected equipment by solving a mixed integer linear model (MILP) (Figure\_ A-4). The aim is to minimize the total cost under the energy balance and the heat and power cascade constraints. The input data used in the energy integration includes the values of the master decision variables, the resources, the power dynamic profile and the comfort profile. To do the energy integration optimization a multi-periods representation of the operating profile is needed, reducing the number of variables and the calculation time. Figure\_ A-4 illustrates the energy integration steps for vehicle energy system.



Figure\_ A-4: Energy integration and multi-periods model

## A.2. Economic models

### A.2.1. Vehicles economic model:

The cost of the vehicle is evaluated for every iteration as a function of the size and the efficiency of the energy converters and energy storage technologies. The cost of the equipment is directly related to the size of the components. In this study the efficiency improvement of the hybrid electric vehicle powertrain through PI is researched. The energy integration methodology is based on the heat integration, which targets the maximum heat recovery in the energy system. The approach consists in mapping all hot and cold streams in the system and displays the heat composite curve. The methodology gives the advantage to provide a global picture of the heat exchanges in the system. It also provides the MER – minimum energy requirement. MER is the minimum amount to be introduced or extracted from the system by means of cold or hot utilities. As a result, the utilities are selected and sized. Process integration techniques and energy analysis are used to measure the useful potential of the waste heat

The Table\_ A-1 summarizes the cost equations.

Table\_ A-1: Equations for the economic model [116]

Components	Costs [€]	
Converters		
Electric motor	$30 \text{ [€/kW]} * P_{EM} \text{ [kW]}$	(1)
Thermal engine	$15 \text{ [€/kW]} * P_{TE} \text{ [kW]}$	(2)
Fuel cell	$1500 \text{ [€/kW]} * P_{FC} \text{ [kW]}$	(3)
Hybrid pneumatic system	6000 [€]	(4)
Storage system		
Battery	$600 * \text{[€/kWh]} * q_{bat}^{0.2477 * \log(\text{bat}_{\text{specifmass}}(\text{battpe}) + 0.5126)} \text{ [kWh]}$	(5)
Supercapacitor	$15 \text{ [€/kW]} * P_{SC} \text{ [kW]}$	(6)
Body		
Nominal cost (car shell)	$17.3 * \text{car\_shell\_mass [kg]} - 3905.4 \text{ [€]}$	(7)
Vehicle use in France 2013		
Electricity household	0.14269 [€TTC/kWh]	
Electricity industry	0.07768 [€TTC/kWh]	
Gasoline	1.645 [€/L]	
Diesel	1.451 [€/L]	
Emissions		
CO2 emissions	Taxes system bonus/malus	

The cost of the electric motor considers the cost of the power unit. The battery cost depends on the battery type and the energy storage capability of the material. The fuel cell cost considers the cost of its adaptation in the powertrain. The price of the hybrid pneumatic system is considered to be 6000 euros and this value is including the hybrid air system adaptation in the vehicle and the powertrain and is based on the industrial experience on the hybrid propulsion systems and their adaptation in the vehicle.

The nominal cost represents the vehicle shell cost. The vehicle shell is the completely equipped vehicle without the powertrain components. This linear correlation (7), (Table\_ A-1) takes into account the price of the parts and the manufacturing cost of the vehicle shell. The margin of the carmaker is included in the price. The correlation is obtained by official commercial vehicles prices for customers for different vehicle classes. This correlation illustrates the link between the increasing cost and the increasing size and mass of the vehicle. For each calculation, a new vehicle mass is calculated and updated with the mass of the defined powertrain.

A simplified vehicle objective cost function is constructed, composed of the vehicle powertrain cost and the vehicle body cost during the production phase.

The economic indicators are defined by the following equations:

### Investment cost – CAPEX (Capital Expenditure)

This is corresponding to the investment price that the customer has to pay for a given vehicle definition. For low CO<sub>2</sub> emission, the environmental bonus is deduced from the investment cost of the customer. The investment cost is given and named below as  $Cost_{vehicle}$  in €.

$$Cost_{vehicle} = Cost_{powertrain} + Cost_{car\_shell} - Bonus_{CO_2} \quad (A-1)$$

in €

### Operating cost – OPEX

The operating cost is calculated based on 150000 kilometers on the different driving cycles.

$$Cost_{operating} = Cost_{energy} * Energy_{consumption} * \frac{150000}{100} \quad (A-2)$$

in €,  $Energy_{consumption}$  in kWh/100 km

### Total mobility cost

The total mobility cost is composed from the investment and operating costs.

$$Total_{cost\_mobility} = CAPEX + OPEX \text{ in €} \quad (A-3)$$

### Actualized yearly cost

The actualization of the cost is defined on 10 years investment basis using an actualization rate of 4%. Then the yearly actualized cost (YAC) is computed for different vehicles according to the following formula.

$$YAC = \frac{OPEX}{n} + CAPEX * \square \quad \text{in €} \quad (A-4)$$

$$\square = \frac{i * (1+i)^n}{(1+i)^n - 1}, i = 0.04, n = 10$$

With OPEX- operating cost, CAPEX the investment price, i the actualization rate (4%, n the investment time (10 years).

### Economic model for waste heat recovery

As economic indicator, the total price of the ORC is defined. Here just the investment cost is considered. This cost is a linear function to consider the parts produced on large units' volume. The investment cost is the sum of the following equations (A-5) to (A-11):

$$Cost_{evaporator} = 18.84 Area_{evaporator} + 14.49, \text{ Euro, area in m}^2 \quad (A-5)$$

$$Cost_{condenser} = 4.01 Area_{condenser} + 4.96, \text{ Euro, area in m}^2 \quad (A-6)$$

$$Cost_{pump} = 0.083 flowrate + 165, \text{ in Euro, flowrate in kg.s}^{-1} \quad (A-7)$$

$$Cost_{turbine} = 0.015 Power_{turbine} - 30, \text{ in Euro, power in kW} \quad (A-8)$$

$$Cost_{pipe} = 26, \text{ Euro} \quad (A-9)$$

$$Cost_{fluid} = 10, \text{ Euro} \quad (A-10)$$

$$Cost_{ORC} = Cost_{evaporator} + Cost_{condenser} + Cost_{pump} + Cost_{turbine} + Cost_{pipe} + Cost_{fluid}, \text{ Euro} \quad (A-11)$$

## A.3. Environmental model: Life cycle assessment

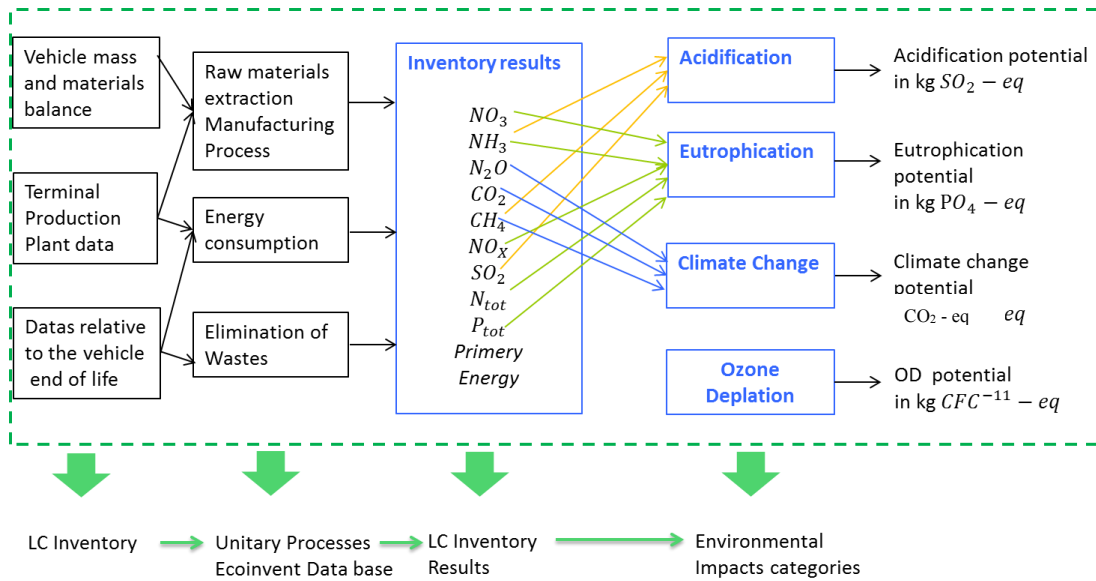
The LCA method is applied as an indicator for the vehicle energy system design. The results of LCA are used to communicate on ecological labels and to demonstrate the CO<sub>2</sub> print improvement due to the introduction of new technologies like the electrified powertrains. The literature shows that the functional unit for LCA vehicle study is to transport persons on 150000 km for 10 years [116] and this functional unit is also used for the study.

This study refers to the 3 main indicators, used from the most part of the automotive industry, and applied by PSA – the GWP 100 years, the eutrophication, the acidification. The CML01\_short indicator is selected in the OSMOSE LCA model. The ozone depletion is also part of the CML01\_short indicator, which has 4 categories. They are summarized in the Table\_A-2.

Table\_A-2: Listing of impact categories implemented in cml01\_short

Category	Definition	Unit
Acidification potential, average European	H <sub>2</sub> CO <sub>3</sub> formation in oceans and on land by dissolving CO <sub>2</sub> in water	kg SO <sub>2</sub> -eq
Climate change, GWP 100a	Significant and lasting change in the statistical distribution of weather patterns over an extended period of time (100 years)	kg CO <sub>2</sub> -eq
Eutrophication potential, generic	Environmental response to addition of nitrates and phosphates. (CML01) -Mass of algae, phytoplankton ↗ -Biodiversity desirable fish species ↘	kg PO <sub>4</sub> -eq
Stratospheric ozone depletion, ODP steady state	Ozone depletion	kg CFC <sup>-11</sup> -eq

The study is based on the life cycle assessment methodology steps, detailed largely in [138]. The methodology applied in the LCA module of OSMOSE is summarized in Figure\_ A-5.

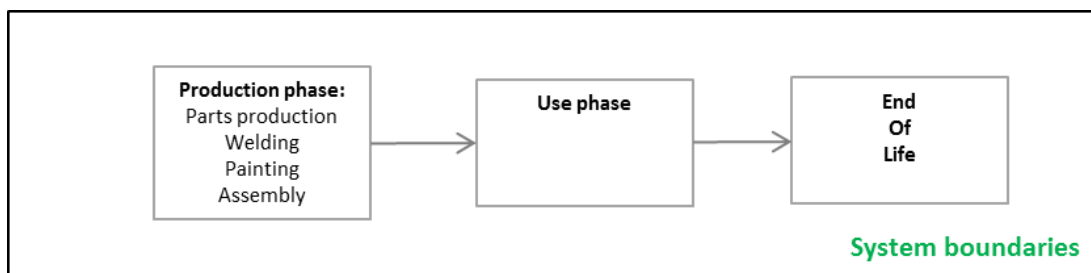


Figure\_ A-5: Steps of the life cycle analysis, selection of the environmental impacts and categories

The EcoInvent processes, equivalent to processes used by PSA with Gabby, for a vehicle with equivalent mass and composition to 3008 HY4 D-Segment serial vehicle, are identified.

The life cycle of a product, a system or a service contains three distinct successive phases: the production phase, the use phase and the end-of-life phase. The unitary processes and flow diagram for vehicles are defined in Figure\_ A-6.

The functional unit for the LCA is the total distance driven throughout the vehicle’s lifetime - 150000 km [139].



Figure\_ A-6: Vehicle unitary processes flow chart – system definition

The inventory in the production phase is composed of:

- the mass and material balance for each part of the vehicle sub-systems
- the corresponding manufacturing process in the Eco Invent® database
- the data about the manufacturing processes in the vehicle production plant (welding, painting, assembly)

The Eco Invent® database is used for sourcing of the the unitary processes and the raw materials for the production of the parts. Seven substructures constitute the vehicle, on the way to identify the powertrain components: electric machine, low voltage battery, high voltage battery, power unit, thermal engine, gearbox, vehicle body (car shell).

# Appendix B Models

## B.1. Simulation models: EV, HEV, SOFC

The model components are modeled using differential equations. The links between the energy storage and conversion technologies constitute the powertrain architecture. The energy flow is computed from the wheels to the energy sources. This is called the backwards method to estimate the energy consumption (Figure\_B-1).



Figure\_B-1: Generic backwards simulation model

**Driving cycle:** a predefined time - speed profile is the input of the model. Along the cycle, the profile defines the gear to be engaged.

**Vehicle model:** the vehicle model computes the traction force at the wheels  $F_t$  at every time step of the speed profile. The power demand is so defined. The vehicle model takes into account the rolling resistance and the aerodynamic resistance. The uphill force is considered in case of driving a slope.

$$m * \frac{dv}{dt}(t) = F_t(t) - F_{resistance}(t) \quad \text{in N} \quad (B-1)$$

The resistance force can be divided on four sub-forces:

The tire friction:

$$F_r = m * g * c_r \quad \text{in N} \quad (B-2)$$

Where  $g$  is the Earth's gravitational constant in  $m/s^2$ ,  $m$  is the mass of the vehicle and in kg  $c_r$  is the rolling friction coefficient.

The wheel bearing friction

$$F_{bearing} = m * g * \mu * \frac{d}{D} \quad \text{in N} \quad (B-3)$$

Where  $\mu$  the bearing coefficient,  $D$  the wheel diameter in m is and the  $d$  the bearing bore diameter in m.

The aerodynamic losses

$$F_a = \frac{1}{2} * \rho_a * C_a * A * (v + v_{wind})^2 \text{ in N} \quad (B-4)$$

Where  $\rho_a$  is the air density in  $\text{kg/m}^3$ ,  $C_a$  is the aerodynamic drag coefficient in [-], A is the vehicle front area in  $\text{m}^2$ , v is the vehicle speed and in  $\text{m/s}$ ,  $v_{wind}$  is the frontal wind speed in  $\text{m/s}$ .

The uphill force

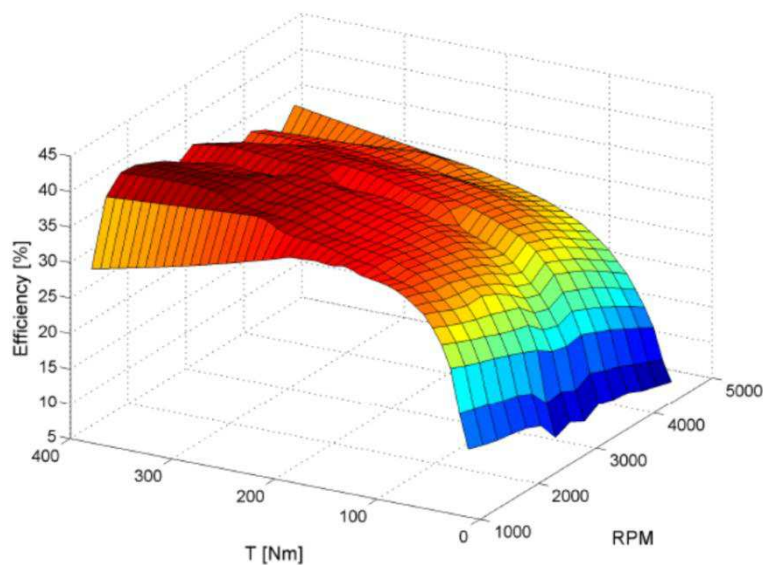
$$F_{uphill} = m * g * \sin(\alpha) \text{ in N} \quad (B-5)$$

Where  $\alpha$  is the slope in rad.

Using the vehicle speed  $v$ , the traction force  $F_t$  and the wheel radius one can compute the wheel torque and rotation speed and then determine the power required to move the vehicle.

**Transmission model:** A transmission is used between the wheels and the energy converter to adapt the speed and the torque levels. The major part of the vehicle transmissions are 5 and 6 speed manual gear boxes. The gear ratio is imposed just in the NEDC. More complex transmission such as continuously variable transmission (CVT) is also modeled. The advantage of the CVT is to choose the optimal fuel consumption gear ratio for every given drive profile. This is very suitable for customer's drives profiles.

**Energy converters:** The energy converter transforms the energy (chemical or electrical) from the energy storage unit into mechanical power. As the dynamics of these converters can be complex the modelling is simplified using efficiency maps. These maps are obtained by measurement on test bench and usually represent the conversion efficiency as a function of the load and the speed demand of the primary shaft. An example is given in Figure\_ B-2:

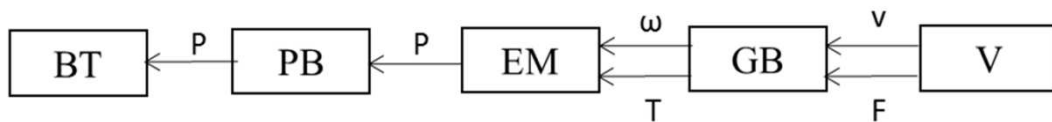


Figure\_ B-2: Efficiency map of a diesel engine

Thus given that the speed and the torque of the primary shaft are known, the power that the energy storage unit has to provide is computed by a simple interpolation in the efficiency map.

### B.1.1. Electric vehicle model

Electric vehicles are characterized by an electric energy conversion chain upstream of the drivetrain. This energy conversion chain consists of a battery (or another electricity storage system) and the electric motor with its controller. The autonomy of the electric vehicle is directly related to the density and the size of the high voltage battery. The time required for charging is usually not negligible and surely it is larger than the typical refueling time of ICE based vehicles. Recently introduced passenger cars mostly use permanent magnets synchronous machines as traction motor, with peak power ranges from 50 to 80 kW. Lithium-ion battery energy typically ranges from 15 to 25 kWh. For combined driving cycles, the top speed and range of such cars now comfortably reach 135 km/h and 160 km autonomy. The electric consumption is typically measured in kWh/100 km or Wh/km. This depends on the efficiency of the powertrain components, mainly of the electric machine, the battery and the transmission. The electric machine acts in motor and generator mode and during braking the kinetic energy is recovered and stored in the high voltage battery as electricity. Typical values of the energy consumption of modern electric cars are 10-15 kWh/100 km for combined driving cycles. The electric vehicle is modeled with the quasi-static approach. While in ICE-based powertrains the power flows are mechanical and thermal in electric vehicle, the electric flow plays a fundamental role. The constituents (“power factors”) of electric power are voltage and current. Since the former can only have positive values, it plays an analogous role to that of speed in mechanical power. The current can switch direction to represent both power flows from (positive current) or to the storage system (negative current). The negative current occurs during the regenerative braking. Thus current is the electric analogue of torque and force. The causality of power factors of an EV is listed in Figure\_ B-3.



Figure\_ B-3: Electric vehicle quasi-static model – BT- battery, PB – power link, EM- electric machine, GB- gear box, V- vehicle.

The main characteristics of the electric vehicle model are given in Table\_ B-1:

Table\_ B-1: Electric vehicle main characteristics [116]

Sub-System	Characteristics	Value
Vehicle	Nominal mass [kg]	1195
Gear box	IVT efficiency [-]	0.9
Energy	Electricity	
Electric motor	$P_{EM}$ [kW]	125
Battery	Type	Li-ion
	Capacity [kWh]	19

### B.1.2. Hybrid electric vehicle dynamic model

The model is based on mechanical and electrical flows, modelled in SIMULINK. The temperature maps of the internal combustion engine are constructed from engine test bench measurement maps. The level of the model is quasi-static. The vehicle follows dynamic profiles. Time- speed driving profiles are generated from a library of driving cycles. The model has a loop control structure. The control is done on the required mechanical power needed to follow the dynamic cycle.

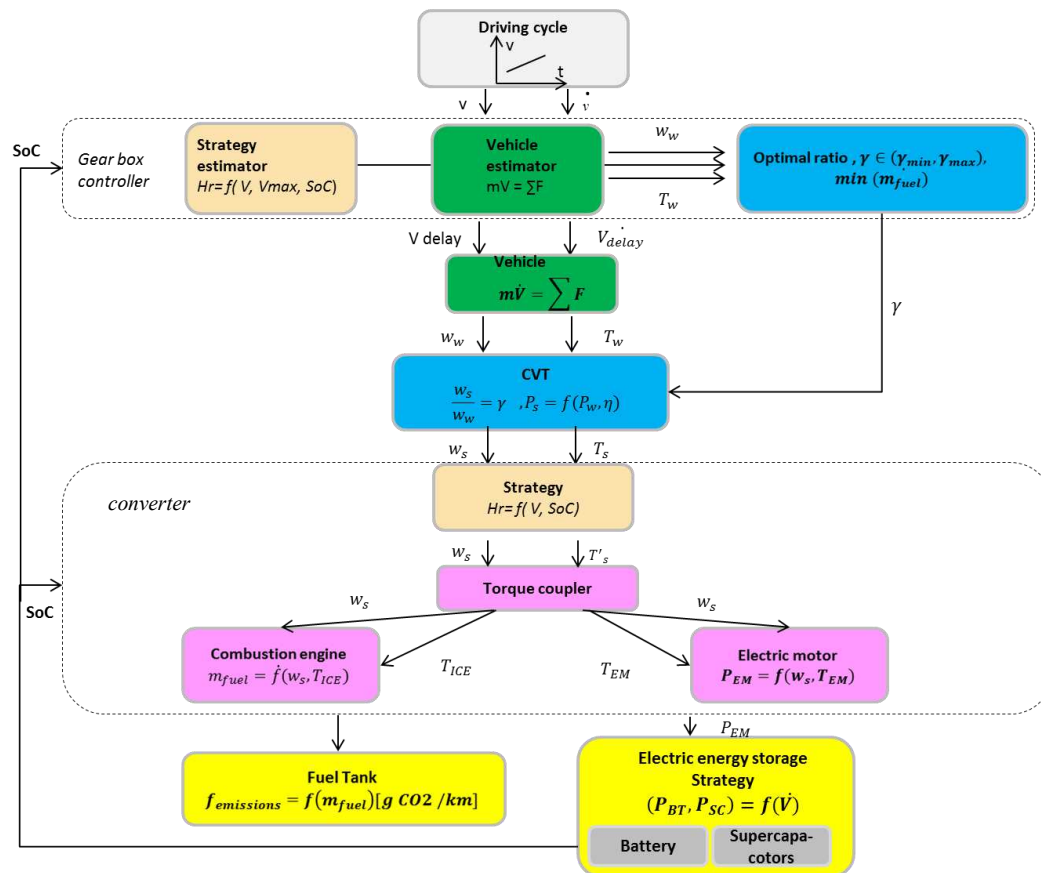
The main characteristics of the hybrid electric simulation model are given in Table\_ B-2.

Table\_B-2: D- Class hybrid electric vehicle characteristics [116]

Sub-System	Characteristics	Value
Vehicle	Nominal mass [kg]	1660
Gear box	CVT efficiency [-][91]	0.84
	MGB efficiency [-]	0.95
	6 gears	
Engine	Displacement [l]	2.2
	Number of cylinder	4
	Rated power [kW]	120
	Max. speed [rpm]	4500
	Max. Torque [Nm]	380
	Idle speed [rpm]	800
	Idle fuel consumption [l/h]	0.33
	Deceleration Fuel cut- off	Yes
Fuel	Type	Diesel
	Density [kg/l]	0.84
	Lower heating value [MJ/kg]	42.5
Electric motor	Power [kW]	27
Battery	Type	Ni MH
	Capacity [kWh]	1.2

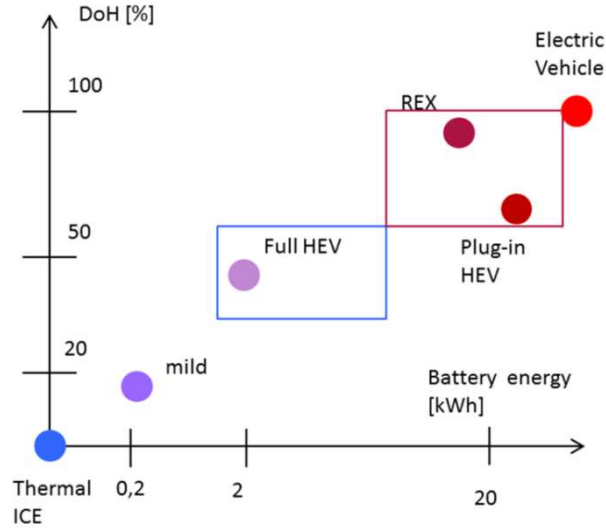
The model is based on a commercial D class diesel hybrid electric vehicle [116]. Some adaptations due to the optimization predisposal and the non-normalized driving cycle's evaluations are done.

Figure\_B-4 illustrates the generic units that are modeled in the vehicle powertrain and the backwards approach to estimate the energy consumption.



Figure\_B-4: Quasi- static model of the parallel thermal electric hybrid

The simulation model is based on parallel hybrid architecture. Hybrid- electric vehicles differ also according to the degree of hybridization of the powertrain and the battery capacity. In the optimization part the battery capacity is one of the decision variables, thus the solutions are classified according to the functional classification in Figure\_ B-5.



Figure\_ B-5: Functional classification of HEVs in term of degree of hybridization and battery capacity [140]

**Driving cycle:** the input of the model is a predefined discrete time and speed profile. The profiles used in this study are described in the study cases.

**The vehicle model** uses the traction force on the wheels, in order to find the power demand. It takes into account the rolling and aerodynamic resistance, the vehicle mass and the uphill force if driving on a slope.

**A transmission model** is used between the wheels and the energy converter to adapt the speed and the torque levels. The model has a manual gear box used for the simulations on harmonized driving cycles, with imposed gear ratios. For the usage driving cycles, when the gear ratio are unknown a CVT is used for the estimation of the optimal gear ratio for each point of the drive cycle.

The energy converter transforms the energy (chemical or electrical) from the energy storage into the mechanical power. The dynamics of such converters can be complex. Their modeling is simplified using efficiency maps, obtained from measurements from test benches.

The electric motor is considered in the model is a synchronous AC motor. The electromagnetic equations are not modeled, a black box approach based on motor efficiency being preferred. The inputs of the electric motor are its shaft's rotation speed  $\omega_{EM}$  in rpm and torque  $T_{EM}$  in Nm and the output is the power demand  $P_{EM}$  in kW (Figure\_ B-6). Thus one can write for the positive and negative traction cases.

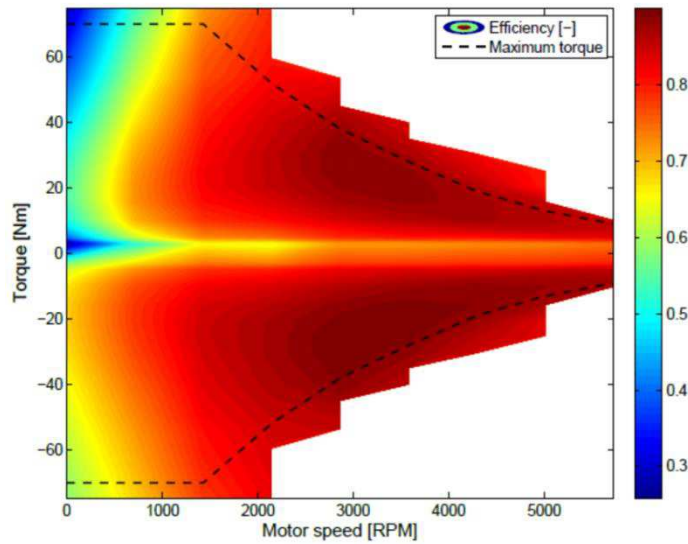
$$P_{EM}(t) = \frac{\omega_{EM}(t) * T_{EM}(t)}{\eta_{EM}(\omega_{EM}(t), T_{EM}(t))} \text{ for } T_{EM} \geq 0 \quad (B-6)$$

$$P_{EM}(t) = \omega_{EM}(t) * T_{EM}(t) * \eta_{EM}(\omega_{EM}(t), T_{EM}(t)) \text{ for } T_{EM} \leq 0 \quad (B-7)$$

The efficiency values  $\eta_{EM}(\omega_{EM}(t), T_{EM}(t))$  for  $T_{EM} \geq 0$  are obtained from the electric motor efficiency map of the QSS toolbox [141]. As the efficiency of the electric motors is usually not measured in generator mode, it is proposed in [140] to approximate it by mirroring the power losses.

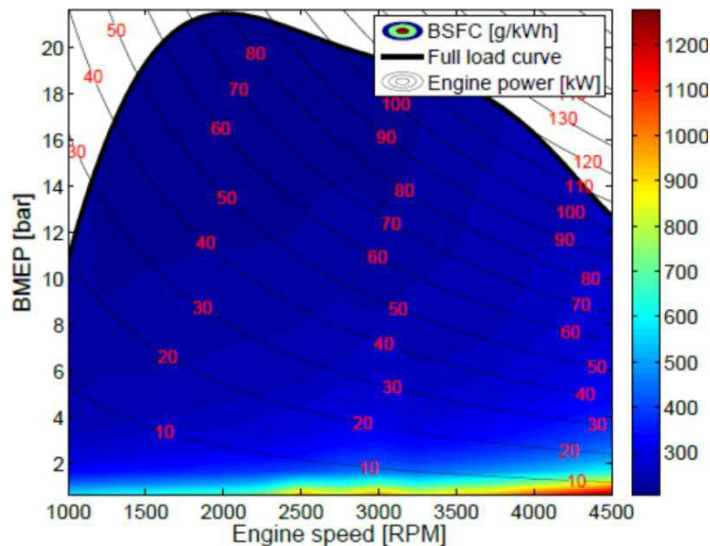
$$\eta_{EM}(\omega_{EM}, |T_{EM}|) = 2 - \frac{1}{\eta_{EM}(\omega_{EM}, T_{EM})} \tag{B-8}$$

The efficiency map is illustrated in Figure\_B-6:



Figure\_B-6: Two- quadrant electric motor efficiency map

The model of the combustion engine is based on the fuel consumption map. The inputs of the model are the engine shaft speed  $\omega_{ICE}$  and torque  $T_{ICE}$  and the output is the break specific fuel consumption BSFC . An example of a fuel consumption map is given in Figure\_B-7:



Figure\_B-7: Fuel consumption map of a 2.2 liters Diesel engine

The engine fuel consumption map is not scaled numerically. A new map is imported for each displacement volume.

Hybrid electric vehicle contains an electric motor powered from the high voltage battery, which may be assisted by supercapacitors when short power boosts for accelerations are demanded. In order to increase the vehicle autonomy, a thermal internal combustion engine is added. In this study a parallel hybrid electric powertrain is modeled. Its operating modes are the following:

- The internal combustion engine can drive the vehicle at high speed or when the battery charge is low.
- The electric motor can drive the vehicle when the battery is sufficiently charged to meet the power demand.
- The vehicle is driven by both simultaneously. The electrical motor and the ICE are connected to the drive shaft using a power split device.
- During deceleration phases the electric machine acts as generator and the electricity is stored in the high voltage battery. This mode is called regenerative braking.

The developed model is a parallel hybrid with diesel engine, electric motor and high voltage battery. The choice of diesel hybrid electric vehicles is done because of available data and models on commercial hybrid electric vehicles. The model can choose engines map for different displacements. The electric motor map and the battery are adapted from the QSS Tool Box [141]. Since in the quasi static model, the efficiency is interpolated in the electric machine map using  $\omega_{EM}$  and  $T_{EM}$ , the electric motor is scaled, by multiplying the rotation speed and torque vectors of the map with the appropriate scaling factor:

$$f_{scaling} = \frac{P_{EM}}{P_{ref}} \quad (B-9)$$

where  $P_{ref}$  is the rated power of the electric motor for the original efficiency data.

In parallel hybrid vehicles, the power split device connects the combustion engine and the electric machine to the drive shaft. These devices can be generally torque or speed couplers. The torque sent towards the transmission is expressed as a weighted sum of electric motor torque and the combustion engine torque.

$$T_s = k_1 T_{EM} + k_2 T_{ICE} \quad (B-10)$$

$$\omega_s = \frac{\omega_{EM}}{k_1} = \frac{\omega_{ICE}}{k_2} \quad (B-11)$$

$k_1$  and  $k_2$  are the structural parameters of the torque coupler

Respectively for the speed coupler, the rotational speed of the shaft, connected to the transmission is as the weighted sum of the electric motor and the combustion engine shaft speeds.

$$\omega_s = k_1 \omega_{EM} + k_2 \omega_{ICE} \quad (B-12)$$

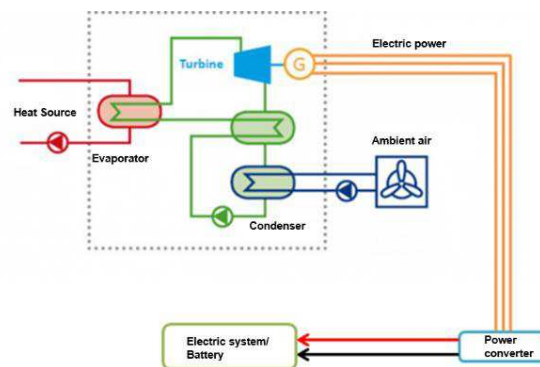
$$T_s = \frac{T_{EM}}{k_1} = \frac{T_{ICE}}{k_2} \quad (B-13)$$

The design of the coupler is not the focus of this study, therefore the simplest solution is chosen with the following assumption shown in equation (B-14).

$$k_1 = k_2 = 1 \quad (B-14)$$

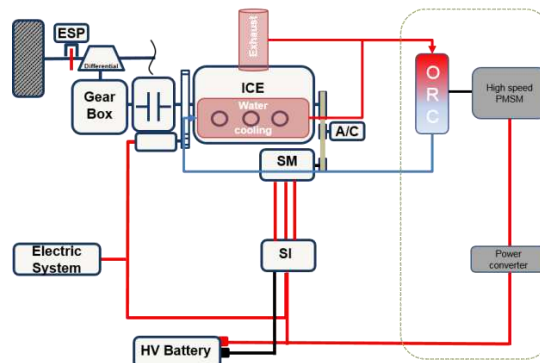
### B.1.3. Waste heat recovery model :

Hybrid electric vehicles have two or more prime movers as energy converters (internal combustion engine (ICE) or fuel cell and electric machine) and power sources (fuel tank, hydrogen tank and electrochemical battery) on their board. The main motivation for hybrid electric vehicles (HEV) development is the efficiency increase of the powertrain in comparison to the thermal (gasoline or Diesel) engines powertrain. HEV offer as well long ranges of autonomy, comparable to thermal vehicles. HEV vehicles recover the kinetic energy during braking. However, the ICE still has thermal losses due to the waste heat when is operating. In this case, the recovery of the waste heat is possible by using an external cycle- the Rankine cycle. The ICE energy balance is showing that there are two main sources of heat: the water jacket and the exhaust gases [7], [8]. The levels of the temperature between the water jacket and exhaust gases are different from 80°C to 900°C. To value the low heat temperature, an organic fluid is proposed to be used as working fluid.



Figure\_ B-8: ORC system to recover the waste heat of the ICE.

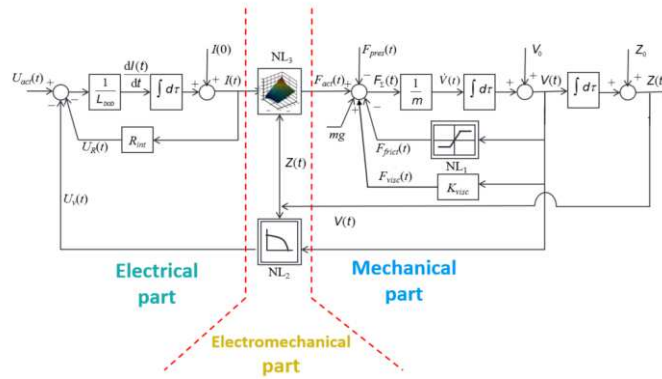
An ORC presented in Figure\_ B-8 will be investigated as principal utility for the energy integration. Its operation will be optimized for the operation points of the ICE, adapted for HEV. As shown in Figure\_ B-8 the turbine is linked to an electric generator and so electricity is produced from the waste heat of the engine. The electricity can be then used for the battery filling or to be sent the electrical network of the system, driving different accessories, devices around the engine or the consumers on the vehicle board (Figure\_ B-9). The ORC receives the heat from the water circuit and the gases of the exhaust of the engine. The turbine out is related to the high-speed generator which produces electricity. The electricity is converted into DC and to the adapted voltage level and enters into the high voltage battery. The functional architecture is presented in a Mild hybrid electric vehicle is presented in Figure\_ B-9.



Figure\_ B-9: Functional architecture of the ORC integration in a Mild HEV Architecture.

### B.1.4. Actuator Nonlinear Model

The model determination of the actuator requires the study of its mechanical part and its electrical part. Thus, the nonlinear model of the actuator consists of 3 interconnected sub-parts (Figure\_ B-10), one relating to the electrical part of the system, one of its electromechanical part and one relative of its mechanical part.



Figure\_ B-10: Block diagram of the nonlinear model of the actuator

The electrical part takes into account the electric circuit of the actuator. From the voltage across the actuator ( $U_{act}$ ) and the electromotive force of the actuator (voltage  $U_V$ ), it is possible to express the current  $I$  passing through the actuator.

The Electromechanical Part models the connection between the electrical and mechanical part of the actuator. By considering the limited operating domain of the valve, the model of the force produced by the electromagnetic actuator defined by (1) can be reduced to a fifth order polynomial. The Mechanical Part allows a simplified modelling of the mechanical part of the actuator (Figure\_ B-11).



Figure\_ B-11: Mechanical part of the actuator and lift profile Zref to be ensured for a mechanical valve train and an engine speed of 6000 rpm

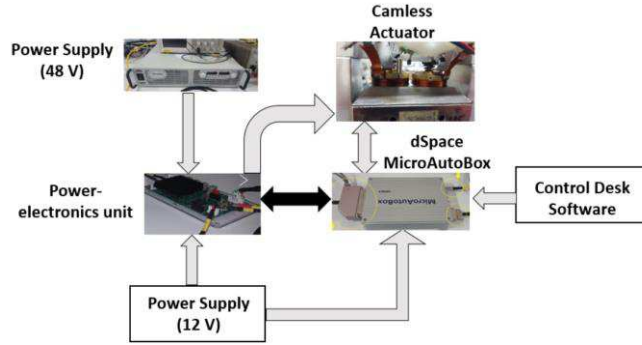
Newton's second law allows taking the balance of the forces having an influence on the movement of the valve:

$$F_{act}(t) - F_{frict}(t) - F_{pres}(t) - F_{visc}(t) + mg = m \frac{d^2Z(t)}{dt^2} \tag{B-15}$$

where  $m$  is the total mass of the moving part of the actuator,  $mg$  is its weight,  $F_{frict}$  is the friction force at the valve guide,  $F_{visc}$  is viscous force and  $F_{pres}$  is the force exerted by the pressure difference between the gases in the cylinder and the exhaust or intake gases. The direction of the current defines the sign of the force of the actuator. When the current is positive, the actuator force opens the valve, the negative current closes the valve.

## Experimental testing bench

For an easy study of the actuator and rapid implementation and validation of the control law, which is to be designed, a dSpace prototyping electronic unit has been chosen. Figure\_B-12 presents the block diagram of the actuator control set-up that is implemented. Taking into account several aspects which affect the experimental set-up, a sampling time  $T_s = 50\mu\text{s}$  is chosen. The control software receives the position sensor voltage through and generates current commands for the power-electronic unit which converts the requested current to the control voltage  $U_{\text{act}}$  which is applied to the actuator by means of a PWM technique with 20 kHz frequency. Due the new vehicle battery specification limit, the magnitude of the control voltage is limited to 48 V and the current to 90 A.



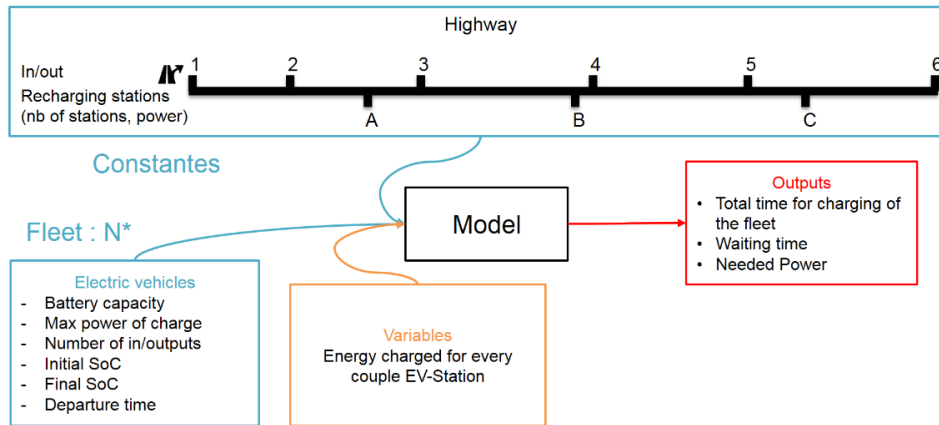
Figure\_B-12: Block diagram of the actuator control implementation set-up

### B.1.5. Recharging model for batteries:

Figure\_B-13 presents the study case that considers the modelisation. A fleet of electric vehicles enters on the highway. The vehicles have different levels of charging of the batteries and different capacities, all vehicles want to perform long drives ( $> 500$  km). The road has different gates with numbers (1 to 6) (Figure\_B-13), which allow the vehicles to leave the highway. Charging stations are located along the highway – A, B, C (Figure\_B-13). The vehicles can stop on the charging stations and charge fully or partially their batteries. The following simulation is applied.

The inputs in the described model are:

- the battery capacity of the electric vehicles:  $Q_{bat}$  in kWh
- the maximal power of the charging:  $P_{charging}$  in kW
- the number of the In-/ Outcomes from the highway:  $N_{in}$ ,  $N_{out}$  in [-]
- the SoC of every electric vehicle on the Income:  $SoC_{in}$ , in [-]
- the SoC of every electric vehicle on the Outcome:  $SoC_{out}$ , in [-]
- the departure time of every vehicle,  $t_{departure}$   $t_{departure}$  in [h]



Figure\_B-13: Charging on the highway: use case for long way drives.

The variable is the quantity of the charged energy for every vehicle and for every station. The charging energy is different for every couple electric vehicle- charging station, and depends on the quantity of the compensation of the SoC difference between the initial and final state of the vehicle.

The outputs are:

- the total time of charging of every vehicle to run the distance,  $Time_{charging\_i}$  [h]
- the total time of charging for the fleet,  $Time_{charging\_fleet}$  [h]
- the waiting time for every vehicle,  $Time_{waiting\_i}$  [h]
- the needed power for every station and for the highway  $P_{charging\_i}$  in [kW]

The objective is to evaluate the power that is needed to be delivered by the charging stations, the waiting time and the total time of charging as a function of the vehicles numbers in the fleet and the distance to run. The optimization is performed according to the following criteria:

- minimize the energy quantity of the charge,  $E_{charging}$  in kWh
- minimize the number of stops,  $N_{stops}$  in [-]
- minimize the waiting time,  $Time_{waiting\_i}$  [h]
- minimize the investment cost of the infrastructure,  $Cost_{investment}$  in [€]

The flow is considered optimal if the vehicles charge:

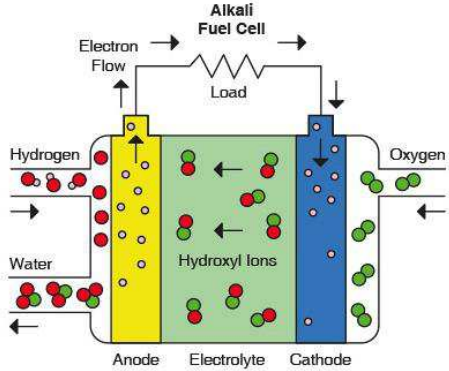
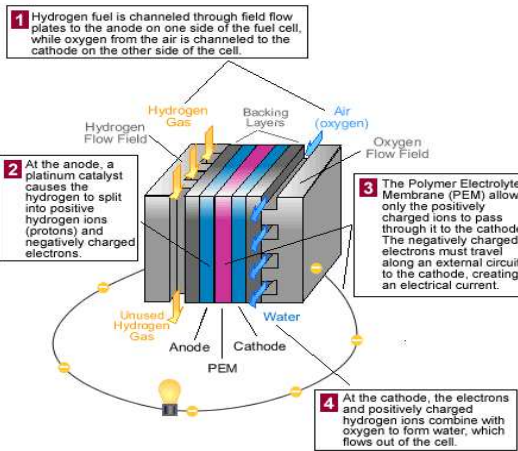
- the minimal quantity of charged energy,  $E_{charging}$  in kWh
- with the minimal number of stops,  $N_{stops}$  in [-]
- minimizing the waiting lines,  $Time_{waiting\_i}$  [h]
- Thus, the optimization problem is defined in (B-16) as:

$$\min(Time_{waiting}(x)), x \in X_{decision\_variables} \quad (B-16)$$



# Appendix C Energy efficiency, storage and conversion

Table\_C-1: Fuel cells types and their advantages and disadvantages to power electric vehicles

 <p style="text-align: center;"><b>Alkali Fuel Cell</b></p> <p style="text-align: center;"><math>\text{CO}_2 + 2\text{KOH} \rightarrow \text{K}_2\text{CO}_3 + \text{H}_2\text{O}</math></p>	
<p><b>Advantages of using AFC</b></p> <ul style="list-style-type: none"> <li>Low operating temperature</li> <li>High efficiency</li> <li>Quick start-up</li> </ul>	<p><b>Advantages of using PEMFC</b></p> <ul style="list-style-type: none"> <li>Low operating temperature</li> <li>Practical efficiency 50-60%</li> </ul>
<p><b>Disadvantages of using AFC</b></p> <ul style="list-style-type: none"> <li>carbonate formation during operation of the fuel cell which block the electrodes material</li> <li>the need to use pure oxygen and hydrogen</li> <li>corrosive solution of e.g. KOH</li> <li>Application of high purity reagents generates additional technological steps in order to produce electricity to power Fuel cells (high operating costs)</li> </ul>	<p><b>Disadvantages of using PEMFC</b></p> <ul style="list-style-type: none"> <li>Material of the cathodes</li> <li>High purity hydrogen and oxygen (less than 10 ppm of carbon monoxide used in the feed gases)</li> </ul>

## C.1. Optimal designs for efficient mobility service for hybrid electric vehicles

The improvement of the efficiency of vehicle energy systems promotes an active search to find innovative solutions during the design process. Engineers can use computer-aided processes to find automatically the best design solutions. This kind of approach named “multi-objective optimization” is based on genetic algorithms. The idea is to obtain simultaneously a population of possible design solutions corresponding to the most efficient energy system definition for a vehicle. These solutions will be optimal from technical, economic and environmental point of view. The “genetic intelligence” is tested for the holistic design of the environomic vehicle powertrain solutions. The environomic methodology for design is applied on D-class hybrid electric vehicles, in order to explore the techno-economic and environmental trade-off for different hybridization level of the vehicles powertrains. For powertrain efficiencies between 0.25 and 0.35 the electrification of the powertrain reduces the global CO<sub>2</sub> emissions. Hybrid electric and plug-in hybrid electric vehicles are reaching these levels. The break point of the electrification effect on the GWP occurs on 0.35 % of powertrain efficiency. For battery capacity value higher than 13 kWh the global reduction of the CO<sub>2</sub> emissions is not obvious. The method gives also an overview of the evolution of environmental categories indicators as a function of the cost of the vehicles. A direct relation links the economic and the environmental performances of the solutions.

Environmental model and economic model are described in Appendix A.

Commercial vehicles are characterized on the normalized driving cycle – New European Driving Cycle (NEDC). Table\_ C-2 summarizes the characteristics of the NEDC, which is well known and well referenced.

Table\_ C-2: Drive cycles characteristics.

Cycle	Distance (km)	Duration (s)	Average speed (km/h)
NEDC	11.023	1180	32.26

### C.1.1. Results - multi-objective environomic optimization

#### Definition of the optimization problem:

A hybrid vehicle characterized with multiple propulsion systems can operate them independently or together. The model contents are the electric machine, battery, supercapacitors, thermal engine and fuel tank, with diesel fuel. The thermal electric hybrid powertrain model characteristics are given in Table\_ B-2. The model represents a commercial D-class vehicle with a parallel thermal (diesel) and electric powertrain (Figure\_ C-1). The target is to size the components of the hybrid powertrain: the converters and the storage tanks and to evaluate on a simultaneous way, the environmental and the economic impacts of the solutions.

A multi objective optimization with three objectives is considered to define design solutions optimal from efficiency, economic and environmental point of view.

For every iteration of the model, the mean powertrain efficiency in traction mode is calculated according equation (C-1):

$$\eta_{powertrain} = \text{mean}\left(\frac{P_{wheel}}{P_{fuel} + P_{BT} + P_{SC}}\right) \quad (C-1)$$

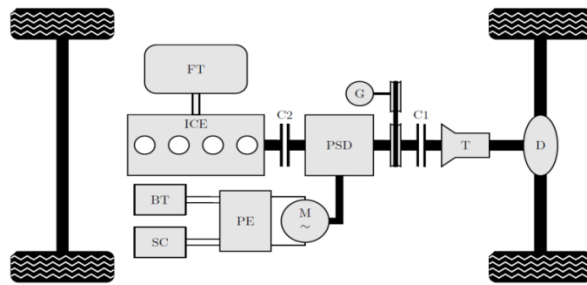
Where PBT and PSC are respectively the battery and the super capacitors powers in kW and  $P_{wheel}$  is the power on the wheels in kW.

The vehicle cost is computed for each set of the decision variables, according equation (A-1). The GWP is the category considered as environmental objective. The GWP has to be minimized. The GWP objective function for the environomic optimization considers the equivalent CO2 emissions during the vehicle life cycle (production, use phase). It is defined over the life cycle functional unit of 150000 km. The end of life is neglected, because of the high recycling ratio in the automotive industry and the consideration that the high voltage battery has a second life as storage device in the electricity distribution grid.

The equation (C-2) defines the GWP objective function:

$$GWP_{total} = GWP_{production} + GWP_{use\_phase} \text{ in kg. CO}_2 \text{ eq.} \quad (C-2)$$

In the case of hybrid electric vehicles, the use phase includes the GWP due of the CO2 tank-to-wheels emissions emitted by the ICE during the vehicle operation over 150000 km.



Figure\_ C-1: Parallel hybrid electric architecture: FT – fuel tank, ICE – internal combustion engine, BT – high voltage battery, SC – super capacitor, PE – power electronics, M- electric motor, PSD – power split device, G – electric generator, C1- clutch 1, C2- clutch 2, T- Transmission, D- Differential.

The use phase contains also the GWP impact of the production of the energy vectors for charging the vehicles storage tanks – the diesel for the fuel tank and the electricity for the charging of the high voltage battery, over 150000 km. This is adding the well-to-wheels aspect of the study. The impact of electricity is considered only for the plug-in hybrid electric vehicles and the range extender vehicles. This means for vehicles equipped with high voltage battery capacity superior to 3 kWh. On that way, equation (C-2) is detailed in equation (C-3).

$$GWP_{weel-to-wheel} = GWP_{total} = GWP_{vehicle\_production} + GWP_{tank-to-wheel\_CO2} + GWP_{diesel\_production} + GWP_{electricity\_production}, \text{kg.CO}_2 \text{ eq.} \quad (C-3)$$

The environomic optimization is defined in equation (C-4):

$$\min(-\eta_{powertrain}(x)) Investment\_cost(x), GWP_{total}(x), x \in X_{\text{decision variables}} \quad (C-4)$$

The other three categories of the impact are introduced as well, as environmental objectives to be minimized. Equations (C-2) to (C-4) are valid also for the other categories.

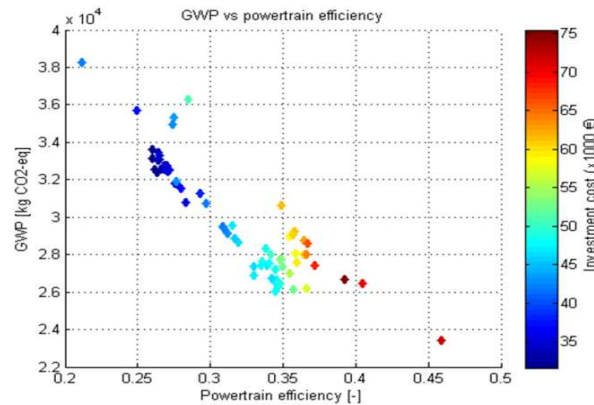
The decision variables for the powertrain design are defined in Table\_ C-3:

Table\_ C-3: Decision variables for powertrain design

Decision variables for design	Range
ICE displacement volume [l]	[0.8-1-1.4-1.6-2.2]
Electric motor rated power [kW]	[1-150]
Battery energy [kWh]	[5-50]
Number of super capacitors [-]	[1-10]

### Multi objective environomic optimization

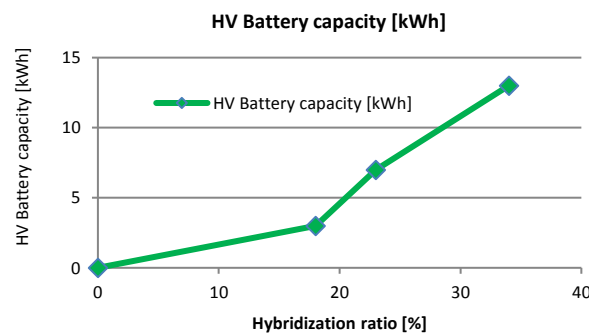
The solutions of the three objective environomic optimization converged on a Pareto Frontier optimal curve. They are projected in the 2D total GWP –powertrain efficiency vision (Figure\_ C-2). This represents the trade-off between the energy consumption and the total GWP impact of the vehicles. From this representation, it is visible that the GWP decreases with the powertrain efficiency. This is due to the reduction of the CO<sub>2</sub> emissions during the driving.



Figure\_ C-2: Pareto curve – total GWP to powertrain efficiency, investment cost in color bar, NEDC.

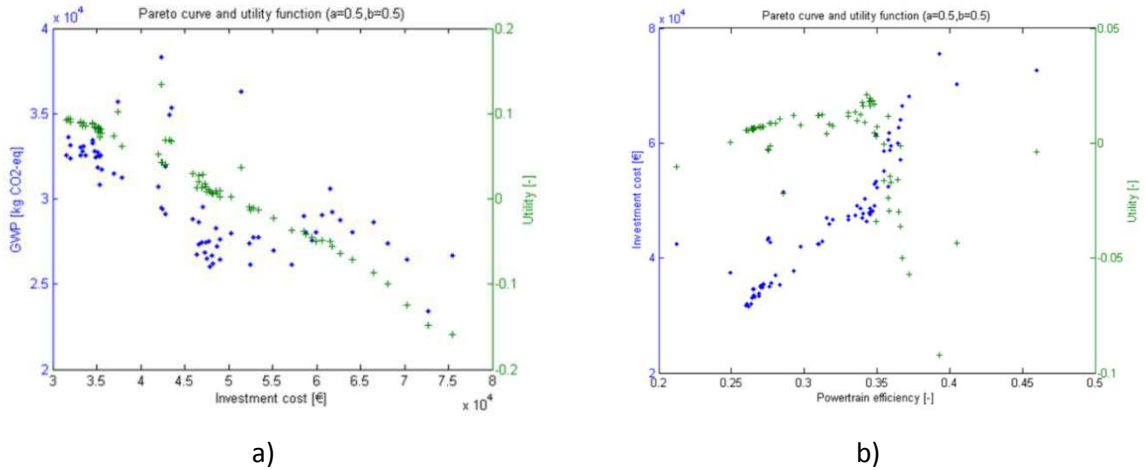
For powertrain efficiencies between 0.25 and 0.35 the electrification of the powertrain reduces the global CO<sub>2</sub> emissions. This corresponds on the families of hybrid electric and plug-in hybrid electric vehicles. The break point of the electrification effect on the GWP occurs on 0.35 % of powertrain efficiency. This corresponds on a battery capacity higher than 13 kWh. From this battery, capacity value the global reduction of the CO<sub>2</sub> emissions is not obvious.

Figure\_ C-3 illustrates the correspondence between the high voltage battery capacity and the hybridization ratio of the vehicle. The hybridization ratio is defined as the as the ratio between the electric power and the total power and represents the power contribution of the electric side of the powertrain.



Figure\_ C-3: Correspondence between the high voltage battery capacity and the hybridization ratio.

The linear fit between the GWP and the powertrain efficiency is illustrated in Figure\_ C-4.

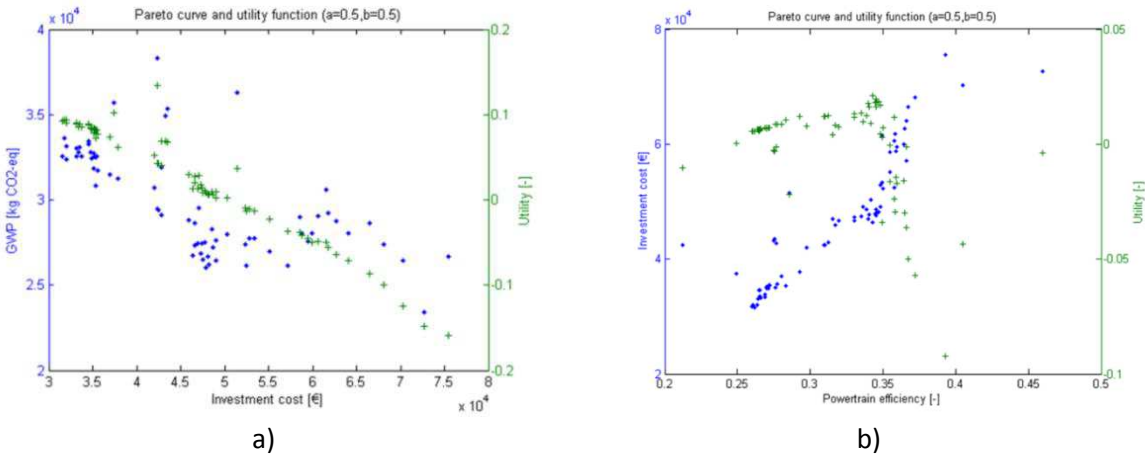


Figure\_C-4 is defined according to the linear equation (C-5). This equation is valid for the domain 25% -50% of powertrain efficiency. A quadratic utility function with balanced weight of the coefficients a and b between the cost and the powertrain efficiency is applied on the Pareto solution from Figure\_C-2. The maximum of the utility function is obtained for points concentrated around values of powertrain efficiency of 35% and investment cost of 45000 € (Figure\_C-4 a and Figure\_C-4 b).

The positive quadratic utility function with balanced techno-economic coefficients shows that utility maximums are in the PHEV zone, between 30% and 35% of powertrain efficiency (Figure\_C-4).

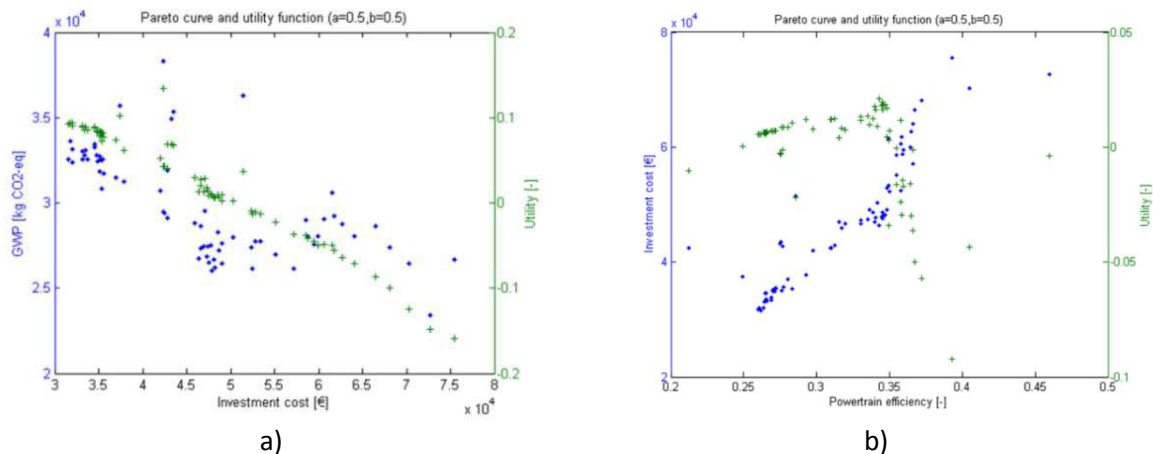
$$GWP = 48749 - 59592 * \eta_{powertrain} \text{ in [kg CO}_2 \text{ eq.]} \quad (C-5)$$

The total GWP is also related to the investment cost.



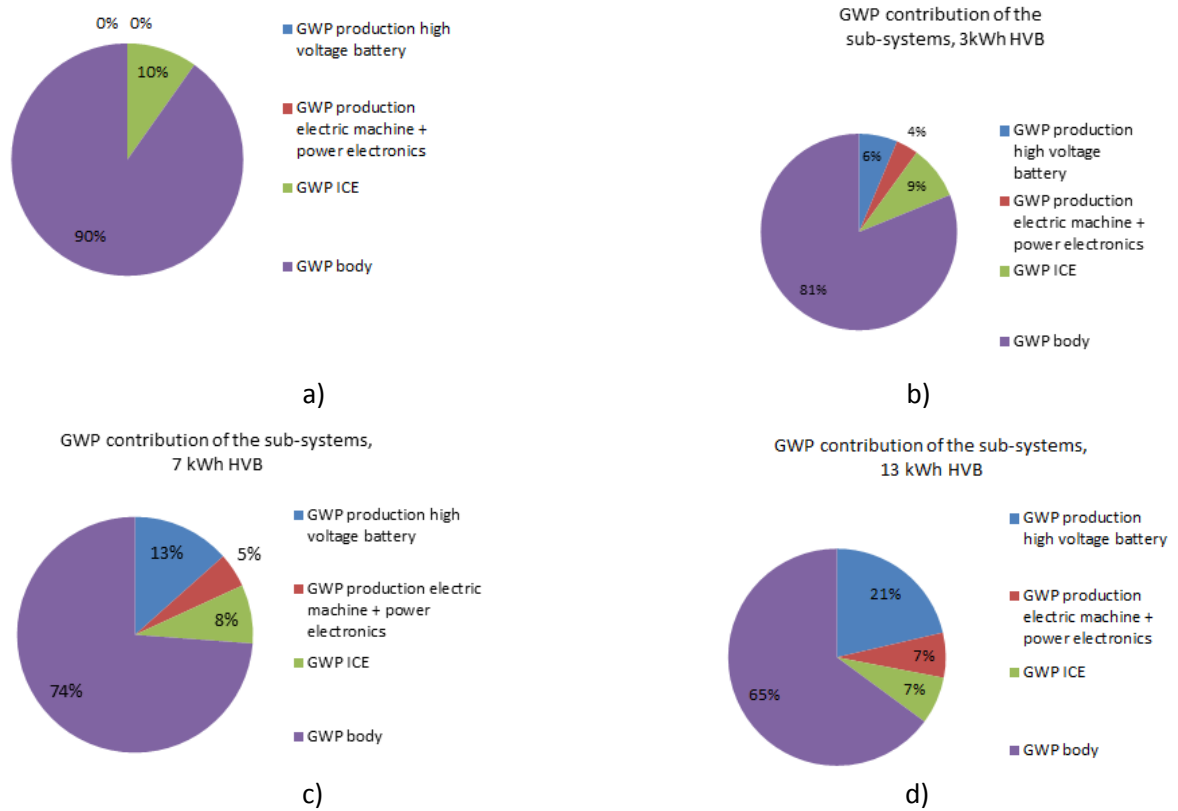
Figure\_C-4Figure\_C-4 proposes a macroscopic linear fit of the relation between the total GWP and the vehicle investment cost. The relation is given in equation (C-6). The relation is valid in the domain of 25%-50% of powertrain efficiency.

$$GWP = 38428 - 0.18267 * Investment\_cost_{vehicle} \text{ in [kg CO}_2 \text{ eq.]} \quad (C-6)$$



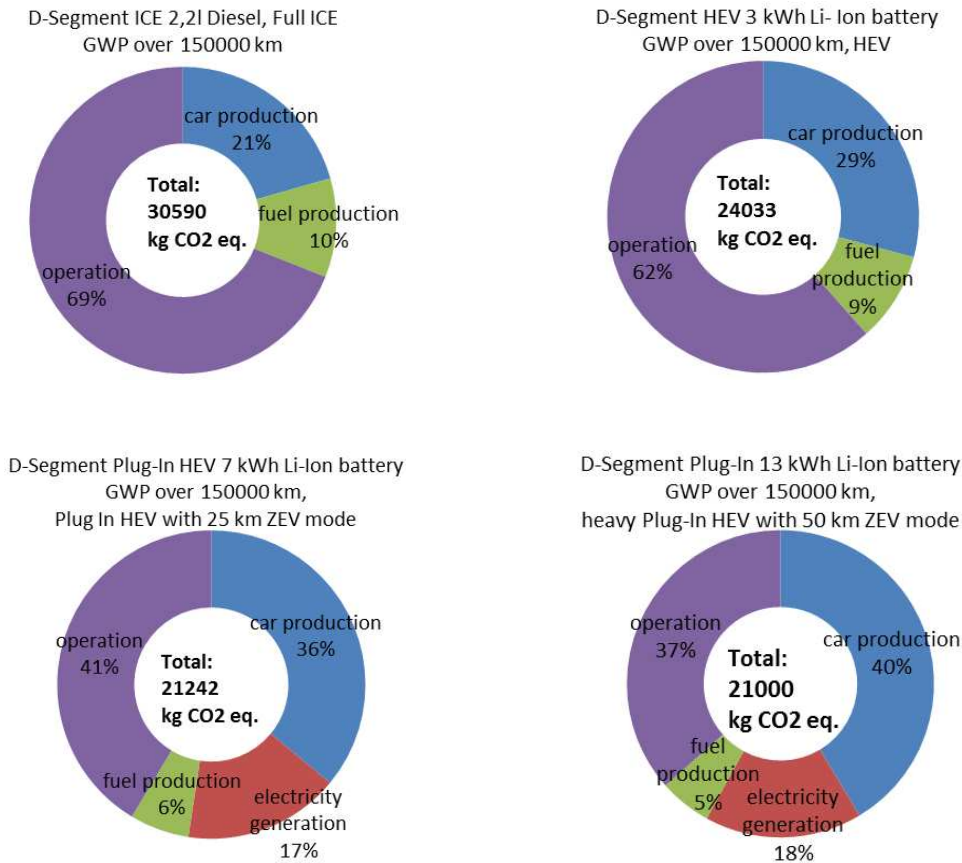
Figure\_C-4: Evolution of a) the total GWP as a function of the vehicle investment cost b) the investment cost as a function of the powertrain efficiency.

The total GWP decreases with the increasing of the total investment cost. Vehicles with higher powertrain efficiency require higher investment cost. Thus they are less fuel consuming in the operation phase and emit less CO<sub>2</sub> emissions. One can consider that if one maximizes the powertrain efficiency one minimizes the total GWP. The GWP can be considered as an indicator related to the other 2 objectives. This allows simplifying the optimization problem from 3 dimensional to 2 dimensional. The techno-economic optimization brings also optimal environmental solutions in the defined range of decisions variables for hybrid electric vehicles and so defines environomic solutions. The main interest of this conclusion is to simplify the optimization from 3D to 2D techno-economic with activated environmental model, which allows evaluating the environmental impacts of each solution of the techno-economic Pareto curve. The vehicle use phase (including the operation CO<sub>2</sub> emissions and the emissions due to the energy vectors production) is clearly the major contributor to the total equivalent CO<sub>2</sub> emissions, in comparison of the equivalent CO<sub>2</sub> emissions for the vehicle production phase, for powertrain efficiencies between 25% and 35%. The design choices are visible on the impacts of the production phase. With the increasing of the powertrain efficiency over 35% and respectively the hybridization ratio (heavy plug-in hybrid electric vehicles and range extenders) and the size of the electric part of the powertrain, the impact of the vehicles production phase increases. This is due to the increasing of the mass of the materials needed for production of the high voltage battery and the electric machine. Orders of magnitude for the total GWP evolution and the repartition of the impact for the different subsystems and for the production phase are given in Figure\_C-5 for different sizes of high voltage battery –this means for different hybridization ratio. The major impact is due to the body production. The second contributor to the GWP is the production of the high voltage battery and its part increases with the increasing of the on board battery capacity. With the increasing of the electrification of the powertrain, the vehicle mass increases and so the power range of the machine and the associated power electronics also increases. Thus the part production impact of the electric machine and the power electronics increases. As the thermal engine is downsized, its impact decreases with the increasing of the hybridization ratio. The environmental model uses the CML short impact as explained Appendix A.



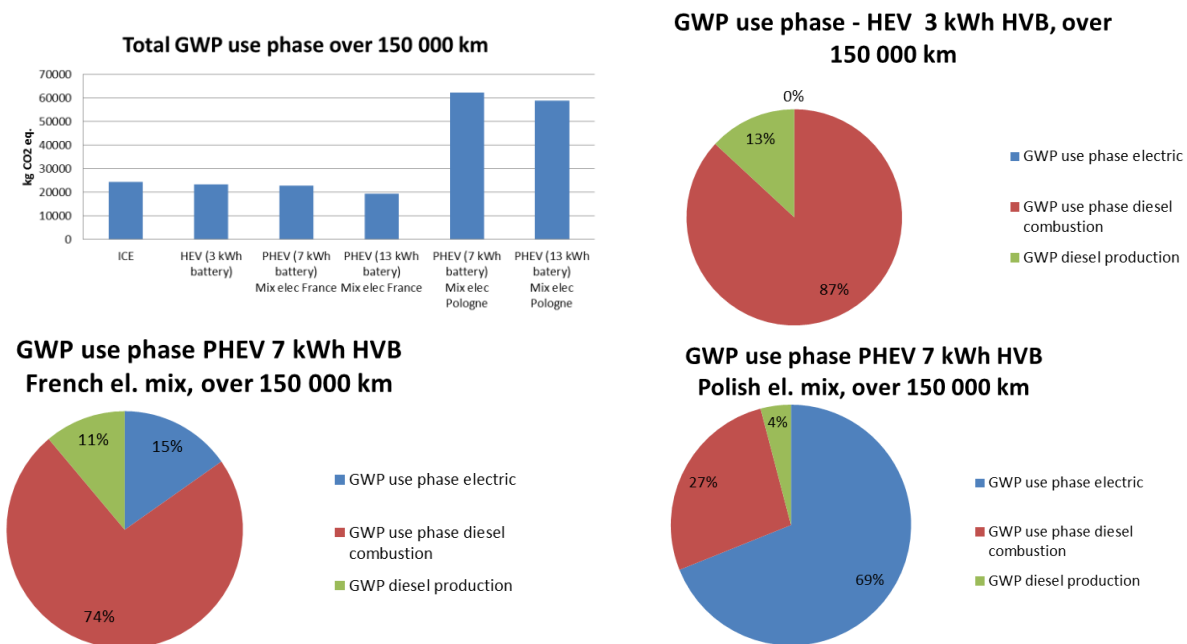
Figure\_C-5: GWP contribution for the production phase of the vehicles sub-systems a) Full ICE, b) 3 kWh of HVB, c) 7 kWh of HVB, d) 13 kWh of HEV

Orders of magnitude for the total GWP evolution and the repartition of the impact of the different life cycles phases are given in Figure\_C-6 for different sizes of high voltage battery –this means for different hybridization ratio. The vehicles are considered to be operated in France with European diesel and French electricity mix production. This means that the emissions due to the energy vectors are thus estimated for an optimistic scenario.



Figure\_C-6: Evolution of the total GWP and repartition of the contribution of reach phase as a function of the hybridization ratio, D –Class vehicles

The operation of the Plug –In vehicles in countries with high carbon percentage use in the electricity generation (Germany, Poland, and China) will increase the contribution of the equivalent CO<sub>2</sub> emissions, coming from the electricity generation (Figure\_C-7). The functional unit is 150000 km.

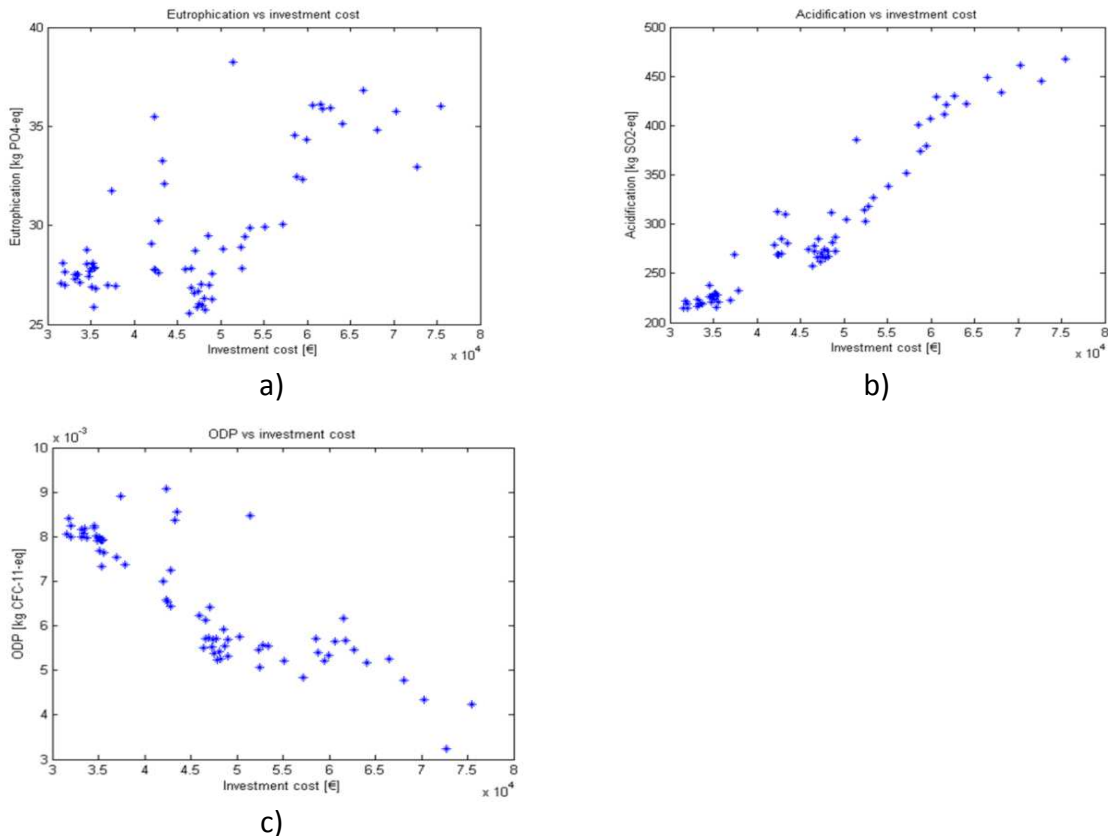


Figure\_C-7: Use phase: GWP evolution as a function of the hybridization ration and contribution of the energy vectors (diesel and electricity production)

### Life cycle impact categories and relations

The environmental model of the computational superstructure uses the CML\_01 short impact as explained in section 2. The GWP is one of the categories of this impact but there are also three other categories – the acidification, the eutrophication and the ODP. Figure\_ C-8 illustrates the evolution of these categories as a function of the investment cost, thus the powertrain efficiency.

The eutrophication is following the same tendency and increases with increasing hybridization ratio. These two categories are influenced from the vehicles production phase (Figure\_ C-8). On the opposite the ODP category decreases with the investment cost, thus the hybridization ratio (Figure\_ C-8).



Figure\_ C-8: Evolution of the CML impact categories a) eutrophication, b) acidification c) ODP as a function of the investment cost.

The acidification is increasing with the powertrain efficiency (hybridization ratio). The main contributors are the increasing material extraction need for bigger size of the high voltage battery and the electric machine. The materials used in the high hybridization ratio vehicles definitions increase and their impact on the acidification impact is visible. The eutrophication is following the same tendency and increases with increasing hybridization ratio. These two categories are influenced from the vehicles production phase. On the opposite the ODP category decreases with the investment cost, thus the hybridization ratio. The ODP is related exactly as the GWP with the vehicle use phase and the use of fossil fuels and prime energy for the energy vectors production.

Thus, when the GWP is minimized, the ODP is also minimized. In the environmental model for hybrid electric vehicles, one can consider that the GWP 100 years is the main impact category and thus simplifies the environmental impact evaluation of the environmental Pareto frontier curve.

The GWP is one of the categories of this impact but there are also three other categories – the acidification, the eutrophication and the ODP. Figure\_ C-8 illustrates the evolution of these categories as a function of the investment cost, thus the powertrain efficiency. The acidification is increasing with the powertrain efficiency (hybridization ratio). The main contributors are the increasing material extraction need for bigger size of the high voltage battery and the electric machine. The materials used

in the high hybridization ratio vehicles definitions increase and their impact on the acidification impact is visible.

The GWP can be considered as an indicator related to the other 2 objectives. This allows simplifying the optimization problem from 3 dimensional to 2 dimensional. The techno-economic optimization brings also optimal environmental solutions in the defined range of decisions variables for hybrid electric vehicles and so defines environomic solutions. The main interest of this conclusion is to simplify the optimization from 3D to 2D techno-economic with activated environmental model, which allows evaluating the environmental impacts of each solution of the techno-economic Pareto curve. This simplified optimization approach is applied for the definition of environomic designs of hybrid electric vehicles on the customers driving cycles – urban and holiday. The main interest is the reduced computation time.

The relation between the economic investment and the environmental performance was demonstrated through the multi-objective optimization. The investment in the technology improves the efficiency and reduces the CO<sub>2</sub> emissions. The correlation confirms the link between the economy and the environment. The effort done for the development of efficient energy storage and conversion technologies is sustainable from environmental point of view.

## Conclusion

This research presents a powertrain design study on hybrid electric vehicles, considering different vehicle usages through adapted driving profile – normalized cycle. The optimal environomic configurations are researched by using multi objective optimization techniques. The optimization methodology is based on a genetic algorithm and is applied for defining the optimal set of decision variables for powertrain design. The analysis of the environomic Pareto curves on NEDC illustrates the relation between the economic and the environmental performances of the solutions. The life cycle inventory allows calculating the environmental performance of the optimal techno-economic solutions. The environmental and the economic trades-off are defined for the different impact categories. Their impact for the production phase and the use phase of the vehicle is studied. The sensitivity of the impacts categories on the electricity production mix is as well studied.

In a second step the optimization is extended to a three objective optimization, integrating the environmental impacts as objective. The analysis of the evolution of the four impacts categories allows choosing one main environmental category, the GWP, to be minimized.

The analysis of the environomic Pareto curves on NEDC illustrates the relation between the economic and the environmental performances of the solutions. The optimization problem is then simplified from 3 objectives to 2 objectives optimization. The life cycle inventory allows calculating the environmental performance of the optimal techno-economic solutions.

The solutions in the lowest emissions zone show that the maximal powertrain efficiency on NEDC is limited on 45.2% and the minimal tank-to-wheel CO<sub>2</sub> emissions are 30 g CO<sub>2</sub> / km. They have the maximal cost – 75000 Euros.

The increase of the electric part of the powertrain increases all environmental categories, because of the materials and the processes to produce the electric components. The parameters and the performances bands for the optimal designs on NEDC cycle are summarized in Table\_ C-4.

Table\_ C-4: Parameters and performances bands for the optimal designs on NEDC cycle.

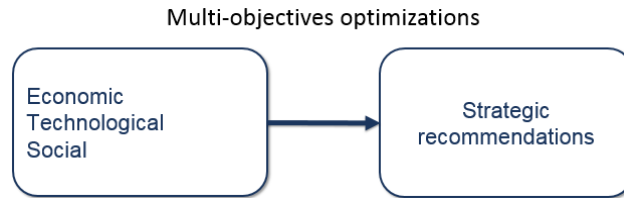
Parameters& indicators	NEDC
CO <sub>2</sub> emissions [g/km]	[140-30]
Powertrain efficiency [-]	[0.25-0.45]
Battery capacity [kWh]	[5-50]
EM Power [kW]	[20-50]
ICE displacement [l]	[2.2-0.8]
GWP [kg CO <sub>2</sub> eq]	[3.6 104-2.3 104]
Investment cost [€]	[30000-70000]

## C.2. Optimal designs of electric vehicles for a long-range mobility

The optimization considers optimal vehicles energy systems designs, considering technical, economic and environmental criteria. This three objectives optimization is also called environomic optimization. Methods, techniques to analyze, improvement and optimizations of energy systems have to deal not only with the energy consumption and economics, but also with the environmental impacts. The multi-objective environomic optimization includes all this activity.

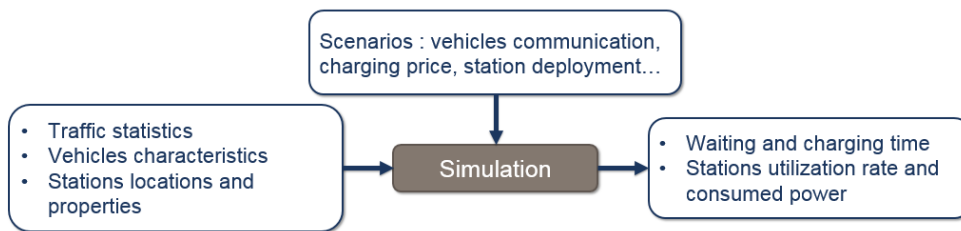
The developed prospective method serves to evaluate different options for the vehicles and the recharging technologies related to the density of the recharging installation and the investment capacities. A technical evaluation is given for considered vehicles and recharging technologies. The method includes the mapping of the charging stations on the driving ways and the information management of the charging grid, considering the need of the vehicles.

Figure\_ C-9 illustrates the generic computational framework for optimization of the extended and integrated vehicle energy system. The superstructure contains the simulation models and the optimizer. The optimizer is based on a genetic algorithm. The set of decision variables includes the types and the size of the equipment.



Figure\_ C-9: Multi-objective optimization framework.

The optimization is solved by an algorithm with the objectives of the minimization of the energy consumption from the grid during the charging, the minimization of the waiting time and the recharging time on the charging stations (Figure\_ C-9). The optimization results converges to solutions represented in Pareto curves.



Figure\_ C-10: Computational framework of technical simulation for vehicle energy integrated system

The current normalized driving cycle for characterization of the commercial vehicles is the New European Driving Cycle (NEDC). Table\_ C-5 presents the characteristics of the driving cycles used in this study.

Table\_ C-5: Drive cycles characteristics.

Cycle	Distance, km	Duration, s	Average speed, km/h
NEDC	11,023	1180	32,26

## C.2.1. Results – Multi Objective Optimization

### Problem definition

A multi-objective optimization is defined for electric vehicles. The environmental category is chosen as optimization function, in addition to the cost and the efficiency. The environmental optimization is researched and evaluated for electric vehicles. Based on the Pareto curves obtained with results from the multi-objective optimization, optimal vehicle configurations of the cars are discussed and decided.

The environmental impact category (GWP), coming from the LCA model as performance indicator in the superstructure, is used as an objective function. The variables for decision are defined in Table\_C-6.

Table\_C-6: Decisions variables for design – multi-objective optimization problem.

<b>Electric propulsion system components</b>	<b>Range</b>	<b>Unit</b>
Electric machine	15-50	kW
High voltage battery	10-100	kWh
Number of super capacitors in a parallel structure	0-5	-
Max Power of supercapacitors	87,5	kW

### Multi objective techno-economic optimization

The vehicle range is the main technical performance for the electric vehicle. The range depends on the battery capacity on board, and on the energy density of the battery cells.

The cost of the battery is also related on these two parameters and especially on the energy density. The battery specific energy which depends on the technology (cathode material, conductivity, etc.) takes considerable time and resources to evolve. The battery capacity can be more easily increased for a given battery type.

In this section a conceptual point-of-view design is adopted by varying the battery specific energy during the two-objective-techno-economic optimization.

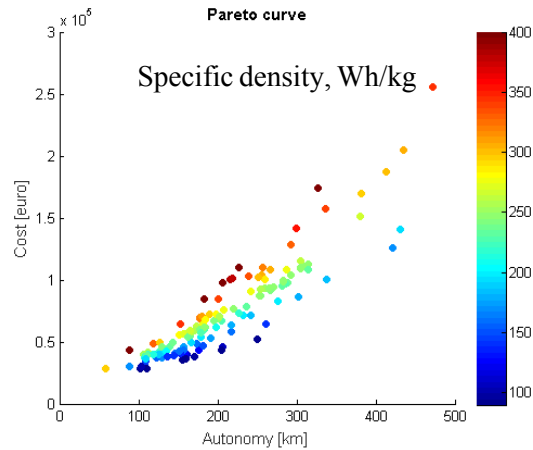
The optimization problem is defined in Table\_C-7.

The techno-economic optimization converges on the Pareto curve represented in Figure\_C-11. The results indicate the effect of the battery specific energy on the autonomy and cost, for current and future battery technologies. The cost and the ranges of the electric vehicle are related to the battery capacity and to the battery density.

The autonomy ranges vary between 100 km and 500 km. The vehicle cost increases also with the autonomy and the high specific energy. The minimal cost is obtained for batteries with lowest specific energy of 90 Wh/kg. The maximal autonomy of 500 km is obtained for batteries with 90 kWh of capacity and 400 Wh/kg of specific energy of the battery cells. The battery cost varies between 8000 € and 42000 €.

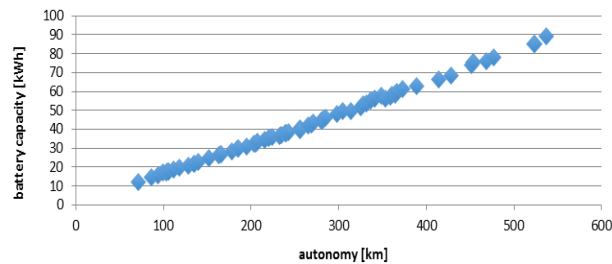
Table\_C-7: Multi objective optimization objectives and decision variables

<b>Techno-economic optimization – Objectives</b>		
Autonomy	km	Max
Cost	€	Min
Electric propulsion system components	Range	Unit
Electric machine	15-50	kW
High voltage battery capacity	10-100	kWh
High voltage battery specific energy	90-400	Wh/kg
Number of super capacitors in a parallel structure	0-5	-
Max Power of supercapacitors	87,5	kW



Figure\_C-11: Pareto for techno-economic optimization, battery specific density in colorbar

The energy capacity of 20 kWh is a reference for the serial electric vehicles and allows at least 150 km of autonomy. The autonomy of the electric vehicles needs to be increased and for that the battery capacity on board needs to be increased. Figure\_C-12 represents a simulation of the vehicle range as a function of the battery capacity. The simulation is done for the maximal considered in the study specific energy density of 400 Wh/kg. One can notice that a range of 550 km could be reached with a 100 kWh of battery capacity of the energy board, which is 5 times more than the state of the art of the today's on board capacities.



Figure\_C-12: Evolution of the vehicle autonomy as a function of the battery capacity, specific energy of 400 Wh/kg.

The ranges superior of 300 km are important for the development of the electric vehicles as a solution for the long ways mobility. Thus the electric vehicles can be used for holiday's drives and not just for home to work urban and peri-urban home to work commuting. In addition the important capacity of 100 kWh set the question of the vehicle recharging systems and imposes the development of the fast charging systems and their availability on the high ways.

The time of the recharging of the batteries depends of the battery capacity and also from the power that the recharging infrastructure is able to deliver (Table\_C-8). To insure long durability of the battery, the battery optimal use is considered to be for states of the charge between 20% and 80% of the maximal capacity. The computation of the time is considered for these boundaries. Table\_C-8 presents the times in minutes for the charging of the batteries with different powers for the chargers. For example to charge an electric vehicle with 100 kWh of battery with a charger of 50 kW, it will take 96 minutes. If the charging is operated on the high way, this time is considered too long. The charger of 50 kW can be used in the city parking or in the shopping centres. Acceptable time for the high way stop is considered to be 15 minutes. To reach this time performances a charger of 350 kW is needed. Thus the vehicle with 100 kWh of battery capacity can be charged in 14 minutes.

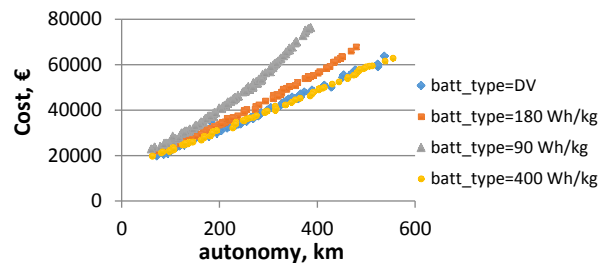
Table\_C-8: Times of charging of the batteries for different powers of the chargers

Power (kW)	Battery capacity		
	50 kWh	100 kWh	150 kWh
50	48	96	144
100	24	48	72
150	17	32	51
350	7	14	21

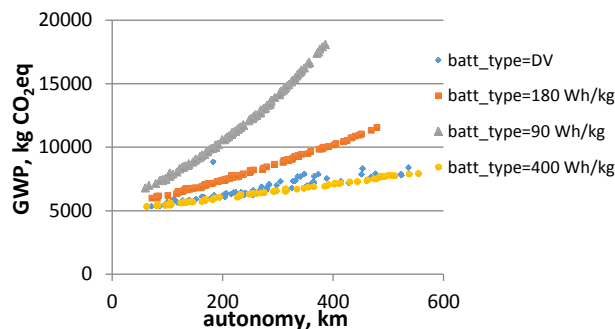
One can conclude that the long way electric mobility with ranges superior to 500 km, will develop with the increasing of the batteries capacities ( $> 100$  kWh) and with the deployment of the fast charging infrastructure on the high ways with chargers able to deliver at least 350 kW.

### Multi objective environomic optimization

In the environmental model, one can consider that the GWP 100 years is the main impact category and the GWP is considered as environmental objective to be minimized. The multi-objective problem is defined with 3 objective functions: the autonomy to be maximized, the cost and the GWP impact of the electric vehicles to be minimized. The decision variables are the same defined in Table\_C-6.



Figure\_C-13: Pareto of the environomic optimization, 2D plan cost/ autonomy.



Figure\_C-14: Pareto of the environomic optimization, 2D plan GWP/ autonomy.

The optimal environomic solutions converge on the Pareto frontiers presented in Figure\_C-13 and Figure\_C-14, as projections in the plans cost/autonomy and GWP/autonomy.

One can see that for the battery types with specific efficiency of 90 Wh/kg the maximal range is estimated on 380 km. For this point the vehicle cost is estimated to 76000 € and the GWP is estimated to 18000 kg CO<sub>2</sub> eq. For the battery with specific energy of 180 Wh/kg, the maximal range is 480 km, for a vehicle cost of 68000 € and GWP of 12000 kg CO<sub>2</sub> eq. For the battery with specific energy of 400 Wh/kg, the maximal range is 550 km, for a vehicle cost of 63000 € and GWP of 8000 kg CO<sub>2</sub> eq. The first conclusion is that the increase of the specific energy increases the autonomy, but also decreases the battery capacity that is needed to be stored on board. For the value of range, for example 300 km, the cost of the vehicles with 90 Wh/kg of battery is 58000 €, the GWP is 14400 kg CO<sub>2</sub> eq. For the same range of 300 km the cost of the vehicles with 180 Wh/kg of battery is 44000 €, the GWP is 8600 kg CO<sub>2</sub> eq. For the range of 300 km the cost of the vehicles with 400 Wh/kg of battery is 40000 €, the GWP is 6500 kg CO<sub>2</sub> eq. The optimizer chooses the highest specific energy (defined by the upper bound of the

variation range). With the cost model, the slope of the Pareto curve decreases with increasing specific energy, which explains the choice of the optimizer.

The environomic designs are presented in Table\_ C-9 for autonomies of 300 and 550 km.

Table\_ C-9: Environomic designs for long range electric vehicles, specific energy of 400 Wh/kg.

	<b>Units</b>	<b>ID = 17</b>	<b>ID = 78</b>
Autonomy	km	300	550
Cost	€	40000	63000
GWP impact	kg CO <sub>2</sub> eq.	6500	8000
Power EM	kW	40	47
Battery capacity	kWh	50	90
Specific energy	Wh/kg	400	400
Number of supercapacitors	-	1	2

The relations between the battery capacity, the battery energy density and the range of the electric vehicles are investigated. The designs for different mobility services (urban and long ways distance electric mobility) of the electric vehicles are defined and the time interaction with the charging infrastructure is analyzed. Information and connectivity solutions that inform in real time the drivers for the availability and the location of the charging infrastructure, including the possibility to book and pay for charge points in different places is an important part of the solution. Combined with fast, i.e. high power charging capacities, pure electric vehicles would be able to serve long range needs. The analysis of the environomic Pareto curves on NEDC illustrates as well the relation between the economic and the environmental performances of the solutions. Electric vehicles can be used for long way mobility (>400 km), if they have a consequent quantity of battery on board (between 100 and 150 kWh). The density of the battery is also important for the autonomy of the electric vehicles. The important capacity of the batteries induces the need of the high power chargers to allow the fast charging of the batteries. The pick power demands induce to investigate adequate links for such electric vehicles with the electricity grid. The multi-objective optimization can be used in an enlarged energy system, including the electric vehicles and the electric grid.



# ***Appendix D Mobile Robotics***

## **D.1. Perception**

Establish an efficient and accurate robot position system is the central pillar of a navigation system because its aim to find the robot in its environment. Different sensors, technique and technologies are used to build such system and can perform either a relative position measurement (called dead-reckoning) or an absolute position measurement. In addition to detect targets and obstacles, sensors are fundamental in the positioning system. Thus, sensors must be accurate and reliable to minimize errors. The tracking of mobile robots is a difficult task because mobile robots are a nonlinear system. If the robot suffers a small disturbance or visual input instabilities, it will degrade the tracking performance. Recently there is no good method; mobile robots usually combine both types of measurements. Dead-reckoning sensors are accurate in the short terms, but the position estimation can drift, an absolute position measurement sensor is less accurate and need more computation but it can correct the drift of dead-reckoning sensors and gives more information. Each positioning system can be realized with different technology of sensors. For example, rotary encoders, accelerometers or mouse optical sensors are used for odometer-positioning system, and Map Matching uses infrared sensors or ultrasonic sensors. Thus, mobile robots generally can be equipped with a multitude of sensors of the same type or different type, and which are complementary or redundant in order to get the best performance. Today, the vision-based technology become widely used because it acquires a lot of information and requires equipment that is cheaper recently. This technology offers precision and accuracy to the robot to do its tasks. Vision sensors are the best source of information compared to any other sensors which makes at the same time more difficult relevant information to be sorted and extract such as the positioning information. In our case, the mobile robot is equipped with a Light Detection And Ranging (LiDAR) sensor, it gives a 360° view of the robot's environment and thus creates a 2D top view map that will be used for the localization and the path planning.

## **D.2. Localization: SLAM**

The Mapping and the Localization are inherent attributes of mobile robot and the fundamental key to provide mobile robots with autonomous capabilities. Their quality determines the performance of the mobile robot. The Simultaneous Localization and Mapping (SLAM) is central to a range of indoor, outdoor, underwater or in-air autonomous vehicles and robots. SLAM is a method, that was proposed by Smith and Cheeseman in 1988, introducing a framework of statistical theory and aim to solve localization and mapping problems for mobile robots [142]. A mobile robot is equipped with sensors and evolving in an unknown environment and gradually builds a map while using the map to estimate its localization. After the map building process, the navigation system must be able to guide the robot from any initial position to any final position in the map [143]. The method consists of a map building process and a localization process. The localization refers to the estimation of time-dependent state of a robot where the robot state such as its position, orientation or velocity affects the future of the robot [144]. Using the relative localization with a kinematics model, a relative position is calculated that is based on angular and linear velocity. Then the global position is calculated using a matching method applied between the built map and the measured optical sensor information based on the relative position [143]. The map consists of features such as lines, arcs and other forms that have been measured in the environment based on the global position. One of the main drawback of this method is the lack of

accuracy in the localization process due to the inaccuracy and error of sensors, an incorrect matching result or a disturbance especially during a rotation [143]. In order to solve the problem, researches have been conducted on different matching methods and probabilistic approaches. In SLAM, matching methods calculate the global position. Iterative Closest Point (ICP) and Singular Value Decomposition (SVD) are the most studied methods. Their efficiency are similar because they directly depend on the accuracy of the calculated position [144].

### **D.3. Cognition: Mobile Robot Navigation Algorithms**

After perception and localization, the mobile robot must decide how to act in order to achieve its goal. The aim of navigation is to search an optimal and safe path from the initial point to the goal, while avoiding obstacles [145]. In addition, the algorithms for navigation must not be computationally expensive to allow fluid and real-time responses.

Navigation includes two different layers: the Global Navigation that uses available knowledge of the environment and the Local navigation that corresponds to the autonomous control of the robot using its equipped sensors. In the case of global navigation, optimization algorithms are used to minimize the cost of the search (in time and therefore in energy) in a static environment only [145]. For local navigation, there are reactive approaches to recognize the environment owning to sensors data and to plan a path online. Most famous reactive approaches algorithms are artificial neural network, fuzzy logic network or neuro-fuzzy strategies, called deterministic algorithms. Currently, new type of algorithm called the nondeterministic algorithms are used, their outputs are not only dependent on their input but also related to the time, etc. These approaches are biologically inspired such as Ant Colony Optimization or Particle Swarm Optimization and gain the attention of researcher owing to their social and cooperative behavior resulting in a faster computation. Finally, the evolutionary algorithms are a hybridization of both. In the literature review, the authors focused only on deterministic algorithms such as Fuzzy logic algorithms and Neural Network algorithms. Large numbers of methods and techniques in SLAM as well as path planning have been and are being developed today. For the SLAM, the challenge is to have a good balance between computational time and resources needed compare to the quality of mapping and the localization. Indeed, real-time is important for mobile robot it is why computational time must be lower as possible for designed applications.

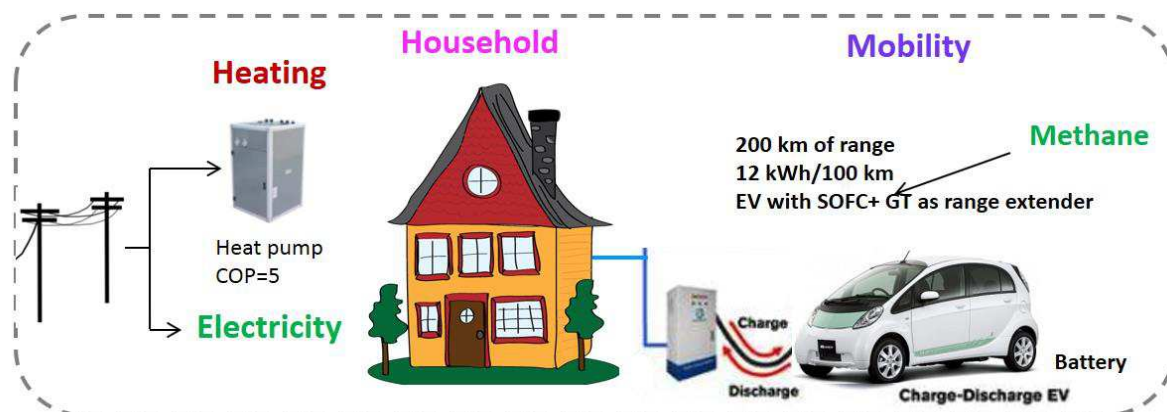
## Appendix E Extended energy systems

### E.1. Integration of the environomic energy services for mobility and household using electric vehicle with a range extender of solid oxide fuel cell

This research studies an innovative concept for vehicle propulsion, considered to deliver mobility services and integrated energy services for a household. An innovative converter – a Solid Oxide Fuel Cell with gas turbines system (SOFC- GT) is powering an electric vehicle. The vehicle architecture is as a serial range extender used to charge the high voltage battery. The range extender vehicle is optimized according to techno-economic and environmental criteria. It is researched to deliver optimal mobility and is integrated to the extended energy system, including the household needs. When the vehicle is unused is considered to be connected to the household and to deliver part of the energy services. In this configuration, the services of extended energy system are optimized. The environomic optimization concerns the extended energy system – vehicle and household and optimal designs for the integrated system are researched. The vehicle integrates energy services for mobility and household and becomes part of the large-scale energy grid for integrated services. The vehicle is sized for both uses. The major advantage of the energy integrated dual system is the reduction of the total global warming potential (GWP) impact with around 30000 kg CO<sub>2</sub> eq. (60%). – from 50590 kg CO<sub>2</sub> eq. to 20338 kg CO<sub>2</sub> in comparison to separate energy services for mobility and household needs.

This research presents the application of the environomic design method for an extended energy system, where the vehicle is connected to the household and delivers as well the part of energy services of the household. This is the so called Vehicle-to-house configuration, part of the Vehicle-to-grid concepts are described in the literature. The idea to use that electric vehicles to supply power to the grid for stabilization and peak time supply is interesting for region where traditional forms of storage

This research considers the vehicle as an extended energy system (Figure\_ E-1) related to the household and proposes optimal design for the energy services for mobility and for the household that the vehicle has to deliver. The optimization of the designs is done by using multi-objective environomic techniques.



Figure\_ E-1: Definition of the extended energy system for the vehicle and the energy services.

## Methodology for environomic design of integrated series for the vehicle energy systems

In the environomic methods and techniques to design, the improvement and the optimizations of energy systems deal simultaneously on the energy consumption, the economics and the environmental impacts.

The modelling of the SOFC GT module and the vehicle simulation models are explained in details in [4]. This research studies the environomic optimization of the extended energy system.

### E.1.1. Study definition

The study researches the dual mode of utilization of the system. This means that the driving and the residential modes are combined. In this mode, the SOFC-GT can be plugged into the house for electricity and heat co-generation.

#### Definition of the mobility and the residential needs

The mobility needs are estimated at 15000 km per year – 150000 km during 10 years. For the residential needs it is considered a household composed of 4 persons. The estimation of the needs of electricity consumption of this household is estimated using the average electricity consumption per capita in France in 2012. The mobility and the residential modes are summarized in the Table\_ E-1.

Table\_ E-1: Definition of mobility and residential needs.

<b>Mobility</b>	
Annual distance, km/year	15 000
Total distance during lifetime, km	150000
Household with 4 persons and 120 m <sup>2</sup> heated surface	
Annual electricity needs, kWh	10000
Annual heat needs, kWh	7200
Annual operating hours for heating, h/year	2000

The vehicle mass characteristics are given in Table\_ E-2:

Table\_ E-2: Vehicle characteristics.

Nominal mass, kg	1000
Mass of the methane tank, kg	25
Specific mass of the SOFC-GT, kg/kW	7.3

#### Strategy of the SOFC-GT use in dual mode

The optimization study targets the lowest possible investment cost by designing the SOFC-GT power for the vehicle. Due to its lower power, the SOFC-GT when used in residential mode will only provide a small part of the house electricity and heat needs. The rest of this needs are supplied by other energy sources (electricity for light and heat pump powering for heating). The part of the residential electricity provided by the SOFC-GT should be a design variable with the range from 0 to 1. This variable influences the operating cost and the CO<sub>2</sub> emissions during the usage.

#### Economic model and life cycle assessment (LCA) model.

The economic and the LCA models of the SOFC-GT technology and the vehicle cost models are explained and presented in details in [4]. The study applies the economic model for SOFC-GT presented in [146].

The annualized investment cost is remained in equation (E-1).

$$AIC = IC \frac{i(1+i)^n}{(1+i)^n - 1} \quad (E-1)$$

The methane used in the SOFC-GT installation is considered produced from bio mass. We use GWP as indicator for equivalent CO<sub>2</sub> emissions and electricity produced in France.

## E.1.2. Results: Multi-objective optimization for residential needs

### Residential needs –base case scenario

In the base case scenario, electricity is provided from the grid (French electricity mix). Heating is satisfied with a gas boiler using natural gas as fuel.

#### Economic evaluation of the base case scenario.

The investment cost of the energy technologies are annualized using the equation (E-1). The operating costs are calculated for the vehicle and the residential needs. The results are listed in Table\_ E-3.

Table\_ E-3: Economic evaluation for the base mobility and residential scenario.

<b>Driving</b>	
Operating cost, €/year	901.5
Annualized investment cost, €/year	2328
Total driving yearly cost, €/year	3229.5
<b>Residential</b>	
Heating cost, €/year	492
Electricity cost, €/year	1505
Annualized boiler cost, €/year	828
Total residential cost, €/year	2825
Total operating cost, €/year	2898.5
Total annualized investment cost, €/year	3156
Total yearly cost, €/year	6054.5

### Residential mode and environmental evaluation of the base case scenario

There are three sources of CO<sub>2</sub> emission in residential mode: methane combustion at boiler during the whole lifetime, eq. CO<sub>2</sub> emission of the fuel production for the total amount of fuel used in the whole lifetime and eq. CO<sub>2</sub> emission for the electricity production phase consumed in the house for 10 years. The CO<sub>2</sub> emission by combustion of methane in the boiler is computed using the CO<sub>2</sub> emission factor and the boiler efficiency. The results are summarized in Table\_ E-4.

Table\_ E-4: Equivalent CO<sub>2</sub> emission for the base case scenario.

<b>Mobility</b>	
Car production GWP, kg eq. CO <sub>2</sub>	3740
Gasoline production GWP, kg eq. CO <sub>2</sub>	3775
Tank-to-Wheels CO <sub>2</sub> emission, kg eq. CO <sub>2</sub>	17250
Total GWP / mobility, kg eq. CO <sub>2</sub>	24765
<b>Residential</b>	
CO <sub>2</sub> emission by NG boiler, kg eq. CO <sub>2</sub>	13640
GWP NG production, kg eq. CO <sub>2</sub>	3265
GWP electric production, kg eq. CO <sub>2</sub>	8920
Total GWP residential, kg eq. CO <sub>2</sub>	25825
Total GWP, kg eq. CO <sub>2</sub>	50590

The total GWP impact for the base scenario for mobility and residential is 50590 kg eq. CO<sub>2</sub> for the whole life duration (10 years exploitation and 150000 km). The mobility with internal combustion engine vehicle (ICEV) vehicle contributes to the half of the GWP impact. The tank-to-wheels CO<sub>2</sub> emission obtained by gasoline combustion represents 70% of the mobility with 17250 kg eq. CO<sub>2</sub>.

In the residential mode the contribution of the different parts is more equilibrated. The electricity contribution based on the French mix is representing around 9000 kg eq. CO<sub>2</sub>. This is a favourable case because the French mix is mostly based on nuclear energy. The introduction of other energy mixes majority based on coal will increase the contribution of the GWP impact of the electricity.

### Vehicle as grid related system – mobility and residential mode optimization – optimal scenario

In the dual mode, the SOFC-GT is used for mobility and residential energy needs. The calculation for mobility is done on NEDC and the simulation starts with a fully charged battery. The energy for the battery charge is provided by the house charger and is produced from the solar panels that equip the house. Part of the electricity needs in residential mode is provided by the SOFC-GT module and the remaining part is supplied by the grid (French electricity mix is considered). The complement of heat is supplied by a heat pump with a coefficient of performance (COP) of 5. The annual saving resulting from the use of SOFC-GT has to be enough to be able to amortize the total investment cost within the lifetime of the system defined at 10 years.

Parameters of the optimization. Two decision variables are added compared to previous optimizations – the SOFC-GT power in residential mode and the part of electricity provided by the SOFC-GT,  $\beta_{el,sofcgt}$ . The optimizer can decide the size of the SOFC-GT for driving or residential mode.

The yearly cost is an effective way to account the cost of both modes. The yearly cost includes:

- The annualized investment cost of the vehicle;
- The operating cost of methane used in driving mode for 150000 km;
- The operating cost of methane used in residential mode for electricity production during 10 years;
- The operating cost of heat production in the house via the heat pump during 10 years;
- Operating cost of pure oxygen needed for the driving and residential mode during 10 years;
- The computed GWP includes:
- GWP of the vehicle production phase;
- GWP of the production of methane (wood gasification) needed for mobility and residential mode during 150000 km (driving) and 10 years (residential);
- GWP of the production of the amount of electricity used by the household during 10 years;
- CO<sub>2</sub> emission in both driving and residential mode during 150000 km and 10 years.

The amount of CO<sub>2</sub> emitted during driving and residential mode is counted in the total GWP to be minimized. The decisions variables are summarized in Table\_ E-5. The 3 dimensional multi- objective optimization function is defined in equation (E-2):

$$\min( -autonomy(x), \quad yearly\ cost(x), total\ GWP(x) ), \quad (E-2)$$

$$x \in (Decisions\ variables)$$

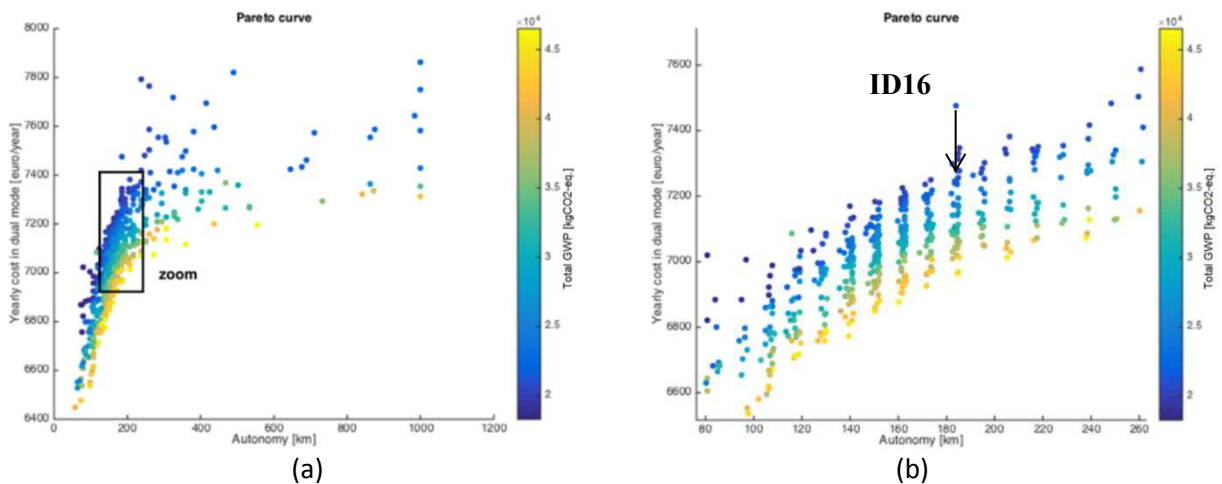
Table\_ E-5: Definition of the decision variables for a dual application of the range extender module.

Decision variables	
Electric machine power, kW	[15-50]
Battery capacity Q <sub>batt</sub> , kWh	[5-80]
Power of the SOFC-GT module for driving, kW	[1-10]
Power of the SOFC-GT module for residential, kW	[1-10]
Mass of methane, kg	[5-15]
$\beta_{el,sofcgt}$ , –	[0-1]

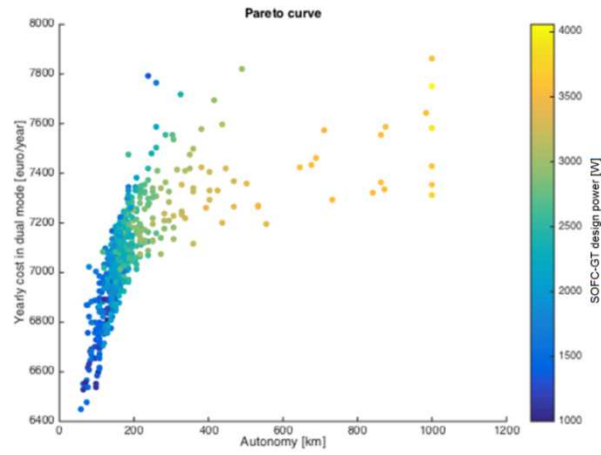
The resulting Pareto curve is shown in Figure\_ E-2. The solutions converge between 6400 €/year and 7800 €/year regarding the yearly cost and between 20000 and 45000 kg CO<sub>2</sub> eq. regarding the total GWP during the lifetime. The yearly cost and the total GWP of the base case scenario are 6055 €/year and 50590 kg eq. CO<sub>2</sub>. The studied integrated system cost more (from 400 to 1800 €/year) than the base case but the GWP impact for all solutions is improved. The families of solutions in the transient autonomy zone, already discussed in the previous section, are also present in this Pareto. They are represented on the Figure\_ E-2 (b). The variation of the solutions is large. For example, for the autonomy of 200 km, the solutions vary between the 6900 €/year and 7300 €/year. The solutions with less cost and bigger GWP give the lower scatter band. The solutions with bigger cost and lower GWP give the high scatter band. The width of the Pareto curve increases as the autonomy increases.

The evolution of the SOFC-GT designs is plotted on the Figure\_ E-3. It shows that the autonomy increases when the design power of the range extender increases, as observed in the previous optimizations. In this multi- objective optimization (MOO) the use phase is considered also, and as it contributes to the major impacts and cost, one can observed that the battery design capacity doesn't influence a lot the solutions. Figure\_ E-4 shows that the battery size between 5 and 15 kWh is selected in most of the solutions. The efficiency of the converter and the methane production way influence on an important way the use phase CO<sub>2</sub> emission.

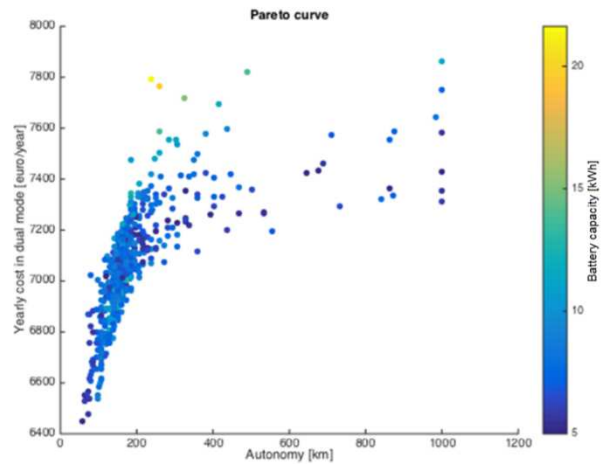
In order to identify for which application the SOFC-GT is optimally designed, a Boolean variable is created (Table\_ E-5). This variable is equal to 1 when the range extender is designed for the residential needs and is equal to 0 when the range extender is designed for the mobility needs. Figure\_ E-5 shows that in most of the cases the SOFC-GT is optimized to satisfy the mobility needs and to extend the vehicle autonomy. Figure\_ E-6 shows that the repartition coefficient  $\beta_{el,sofcgt}$  between the part of electricity provided by the SOFC-GT and the part provided by the electrical grid is related to the cost and the GWP.



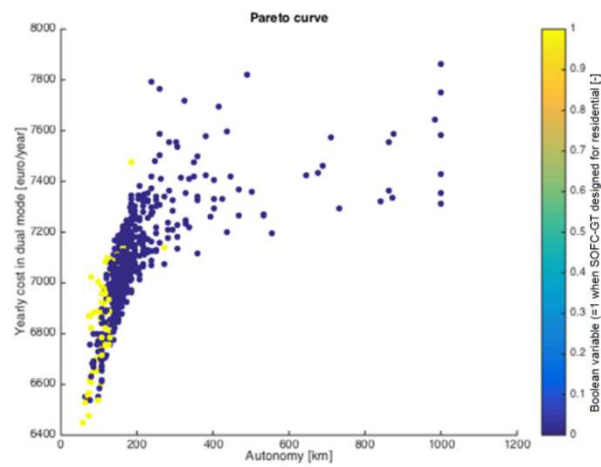
Figure\_ E-2 : Yearly cost/ autonomy Pareto curve in dual mode, GWP in color bar.



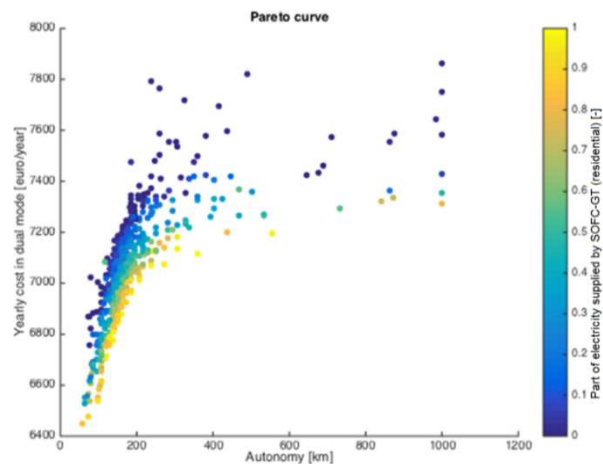
Figure\_ E-3: 3D MOO Pareto curve, SOFC-GT design in colorbar



Figure\_ E-4 : 3D MOO Pareto curve, battery design in color bar.



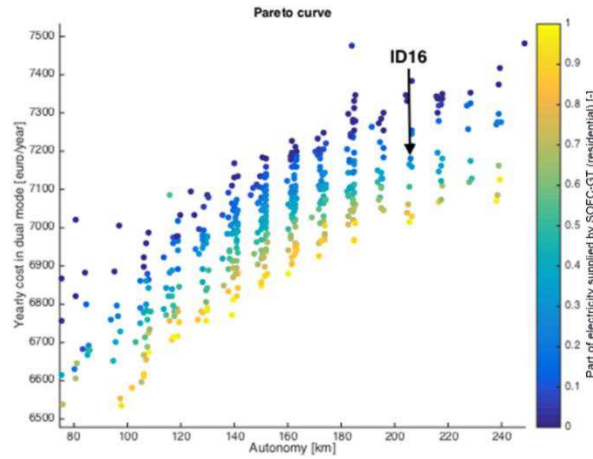
Figure\_ E-5 : Boolean variable=1 when the SOFC is designed for residential use, in color bar



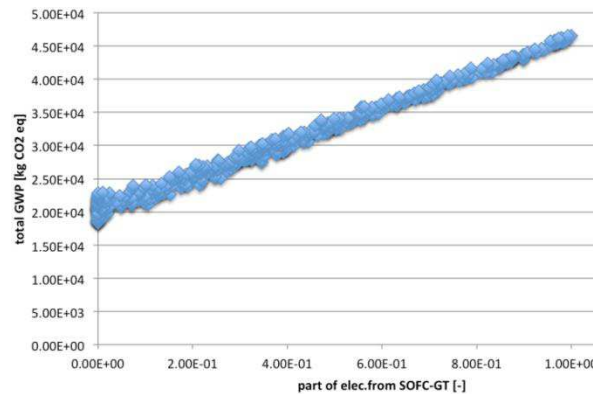
Figure\_ E-6: 3D MOO Pareto curve, with the part of the residential electricity from SOFC-GT in color bar.

If a low cost is targeted (meaning a high GWP impact), the optimizer choice is that 100% of the energy needs for the household are provided by the SOFC-GT (Figure\_ E-7). The total GWP is strongly dependent on the variable  $\beta_{el,sofcgt}$  and this is logical because most of the GWP comes from the use phase (the electricity use in the residential mode). The electricity needs per year is 10000 kWh and this means 100000 kWh for 10 years. Compared to that and considering a consumption of 11.8 kWh/100 km for the range extender vehicle, as observed in previous optimizations, the amount of energy needed for 150000 km is 17700 kWh. This value represents 18% of the consumption of electricity in residential mode.

Table\_ E-6. The CO<sub>2</sub> contribution for the production of 1kWh of electricity with the SOFC and biomethane is also illustrated. One can see that the electricity produced from SOFC-GT and biomethane has more CO<sub>2</sub> contribution than electricity produced in France. For the case of a house supplied with electricity supplied from France, the optimal GWP will be found for solutions supplying the total electricity needs from the grid, the SOFC-GT is used at the minimum. This is the case illustrated on the Figure\_ E-8.



Figure\_ E-7 :3D MOO Pareto curve, with the part of the residential electricity from SOFC-GT in color bar (zoom in the autonomy transition zone).



Figure\_ E-8: The total GWP as a function of the part of residential electricity from the SOFC-GT (French electricity mix).

Table\_ E-6: Specific GWP for different sources of electricity.

Source of electricity	Specific GWP of electrical production, eq. kg CO <sub>2</sub> /kWh
Mix France	0.0892
SOFC-GT	0.2805
Mix Germany	0.638
Mix Poland	1.1

If the German or the Polish electricity production mixes were chosen then the optimizer to minimize the GWP, would surely privilege the use of SOFC-GT for the total providing of the residential electricity needs by the SOFC-GT module.

The optimal solution for a system with integrated energy services is chosen in ID 16 (Figure\_ E-7). ID 16 presents autonomy of 200 km, which is the targeted autonomy for current electric vehicles. Globally, all integrated solutions present higher yearly cost than the base case. This is due to the high investment cost for the SOFC-GT installation. But all obtained solutions for the integrated services have lower total GWP impact than the base case separated house and mobility energy services. Therefore choosing a high autonomy vehicle for competitiveness with the ICEV would end up not economically competitive at all considering the high yearly cost. The vehicle with 200 km of autonomy integrated to the house energy services gives a balanced solution between cost and GWP. This solution is with integrated energy services for residential and driving mode. The details of the ID16 are presented in Table\_ E-7. The comparison with the base energy scenario is also done.

The detailed contribution of the cost and the GWP of the ID 16 are compared to the base scenario. One can observe that with the chosen solution, the main outcomes are: the yearly cost 1000 € higher for the integrated solution and the GWP is with around 30000 kg CO<sub>2</sub> eq. smaller than in the base case.

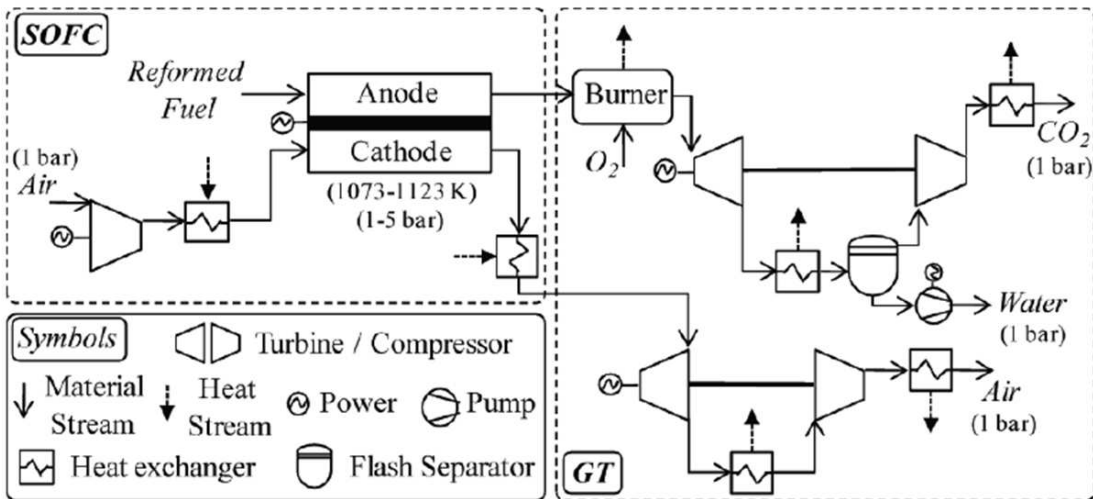
Table\_ E-7: Comparison between ID16 at 200 km of autonomy and the base case scenario.

	ID 16	Base case
Power Electric machine, kW	32.28	
Capacity of the battery, kWh	6.28	
SOFC-GT power for driving, kW	2.80	
SOFC-GT power for residential, kW	1.60	
Mass of methane, kg	10.2	
$\beta_{el,sofcgt}$ , -	0.33	
Range/Autonomy, km	206	1000
Vehicle cost, €	28430	20900
<b>Mobility</b>		
Operating costs, €/year	127	900
Annualized investment costs, €/year	3681	2328
Total driving yearly costs, €/year	3808	3229
Car production GWP, kg eq. CO <sub>2</sub>	6596	3740
Fuel production GWP, kg eq. CO <sub>2</sub>	768	3775
T-t-W CO <sub>2</sub> emission, kg eq. CO <sub>2</sub>	3594	17250
Total GWP driving, kg eq. CO <sub>2</sub>	10958	24765
<b>Residential</b>		
Total residential yearly costs, €/year	3258	2825
Total GWP residential, kg eq. CO <sub>2</sub>	9380	25825
Total operating costs, €/year	1660	2898.5
Total annualized investment costs, €/year	5406	3156
Total yearly costs, €/year	7066	6054.5
Total GWP, kg eq. CO <sub>2</sub>	20338	50590

The total GWP impact of the base case scenario is estimated to 50590 kg CO<sub>2</sub> eq. The multi-objective optimization for environomic design of the new vehicle- house system is performed for the definition of the environomic design of the driving and the residential mode. In the case of the energy supplied in France the optimization sizes the SOFC-GT module for the mobility needs. The rest of the energy needs of the house are covered by the grid supply. Optimal design of the range extender vehicle in dual mode is proposed for 200 km of autonomy, investment cost of 28430 € and 3808 €/year of total driving yearly cost. The base case scenario has lower investment (20900 €) and total driving yearly cost (3229 €/year).

The total yearly cost for the integrated system in dual mode stays still higher (1000 €/year) than the base case separately delivered energy services. This is due to the high investment cost of the equipment in the vehicle and the house. The major advantage of the energy integrated dual system is the reduction of the total GWP impact with around 30000 kg CO<sub>2</sub> eq. (60%). – from 50590 kg CO<sub>2</sub> eq. to 20338 kg CO<sub>2</sub> eq. This study illustrates large scale economic and environmental benefits opportunities by integration of the energy services for mobility and household.

The SOFC model used in this work integrates a methane reformer. The hydrogen is produced on the vehicle board and the efficiency of the reformer is integrated in the global system efficiency. The SOFC systems contains also gas turbines for heat recovery and combined power cycle which produce electricity from heat and increase the efficiency of the system. The system is illustrated in the Figure\_ E-9 and presented in [4].



Figure\_ E-9SOFC- GT integrated system [4]

## References

- [1] ERTRAC, « European road map, electrification of road transport, 3rd edition ». 2017.
- [2] Z. Dimitrova et F. Maréchal, « Environomic design of vehicle energy systems for optimal mobility service », *Energy*, vol. 76, p. 1019-1028, nov. 2014, doi: 10.1016/j.energy.2014.09.019.
- [3] Z. Dimitrova et F. Maréchal, « Techno-economic design of hybrid electric vehicles using multi objective optimization techniques », *Energy*, vol. 91, p. 630-644, nov. 2015, doi: 10.1016/j.energy.2015.08.073.
- [4] Z. Dimitrova et F. Maréchal, « Environomic design for electric vehicles with an integrated solid oxide fuel cell (SOFC) unit as a range extender », *Renewable Energy*, vol. 112, p. 124-142, nov. 2017, doi: 10.1016/j.renene.2017.05.031.
- [5] J. Van herle *et al.*, « Concept and technology of SOFC for electric vehicles », *Solid State Ionics*, vol. 132, n° 3, p. 333-342, juill. 2000, doi: 10.1016/S0167-2738(00)00649-4.
- [6] Y. Bessekon, P. Zielke, A. C. Wulff, et A. Hagen, « Simulation of a SOFC/Battery powered vehicle », *International Journal of Hydrogen Energy*, vol. 44, n° 3, p. 1905-1918, janv. 2019, doi: 10.1016/j.ijhydene.2018.11.126.
- [7] Z. Dimitrova et F. Maréchal, « Energy integration on multi-periods and multi-usages for hybrid electric and thermal powertrains », *Energy*, vol. 83, p. 539-550, avr. 2015, doi: 10.1016/j.energy.2015.02.060.
- [8] Z. Dimitrova et F. Maréchal, « Energy integration study on a hybrid electric vehicle energy system, using process integration techniques », *Applied Thermal Engineering*, vol. 91, p. 834-847, déc. 2015, doi: 10.1016/j.applthermaleng.2015.08.094.
- [9] N. Lümmen, E. Nygård, P. E. Koch, et L. M. Nerheim, « Comparison of organic Rankine cycle concepts for recovering waste heat in a hybrid powertrain on a fast passenger ferry », *Energy Conversion and Management*, vol. 163, p. 371-383, mai 2018, doi: 10.1016/j.enconman.2018.02.063.
- [10] R. Capata et C. Toro, « Feasibility analysis of a small-scale ORC energy recovery system for vehicular application », *Energy Conversion and Management*, vol. 86, p. 1078-1090, oct. 2014, doi: 10.1016/j.enconman.2014.06.024.
- [11] I. Briggs, G. McCullough, S. Spence, et R. Douglas, « Whole-vehicle modelling of exhaust energy recovery on a diesel-electric hybrid bus », *Energy*, vol. 65, p. 172-181, févr. 2014, doi: 10.1016/j.energy.2013.11.075.
- [12] P. Leduc, P. Smague, A. Leroux, et G. Henry, « Low temperature heat recovery in engine coolant for stationary and road transport applications », *Energy Procedia*, vol. 129, p. 834-842, sept. 2017, doi: 10.1016/j.egypro.2017.09.197.
- [13] M. F. Ezzat et I. Dincer, « Development and exergetic assessment of a new hybrid vehicle incorporating gas turbine as powering option », *Energy*, vol. 170, p. 112-119, mars 2019, doi: 10.1016/j.energy.2018.12.141.
- [14] S. Glover, R. Douglas, M. De Rosa, X. Zhang, et L. Glover, « Simulation of a multiple heat source supercritical ORC (Organic Rankine Cycle) for vehicle waste heat recovery », *Energy*, vol. 93, p. 1568-1580, déc. 2015, doi: 10.1016/j.energy.2015.10.004.
- [15] C. Yue et P. Wang, « Thermal analysis on vehicle energy supplying system based on waste heat recovery ORC », *Energy Procedia*, vol. 158, p. 5587-5595, févr. 2019, doi: 10.1016/j.egypro.2019.01.582.
- [16] N. Muralidhar, M. Himabindu, et R. V. Ravikrishna, « Modeling of a hybrid electric heavy duty vehicle to assess energy recovery using a thermoelectric generator », *Energy*, vol. 148, p. 1046-1059, avr. 2018, doi: 10.1016/j.energy.2018.02.023.
- [17] C. A. Frangopoulos, « Thermoeconomic Functional Analysis: A Method for Optimal Design or Improvement of Complex Thermal Systems. », p. 1, 1984.
- [18] Y. M. El-Sayed et R. B. Evans, « Thermoeconomics and the Design of Heat Systems », *J. Eng. Power*, vol. 92, n° 1, p. 27-35, janv. 1970, doi: 10.1115/1.3445296.
- [19] Dimitrova Z. et Marechal F., « Environomic design of vehicle integrated energy system application on a hybrid electric vehicle energy system », *Chemical Engineering Transactions*, vol. 39, p. 475-480, août 2014, doi: 10.3303/CET1439080.

- [20] J. Garcia, D. Millet, P. Tonnelier, S. Richet, et R. Chenouard, « A novel approach for global environmental performance evaluation of electric batteries for hybrid vehicles », *Journal of Cleaner Production*, vol. 156, p. 406-417, juill. 2017, doi: 10.1016/j.jclepro.2017.04.035.
- [21] M. Delogu, L. Zanchi, C. A. Dattilo, et M. Pierini, « Innovative composites and hybrid materials for electric vehicles lightweight design in a sustainability perspective », *Materials Today Communications*, vol. 13, p. 192-209, déc. 2017, doi: 10.1016/j.mtcomm.2017.09.012.
- [22] S. Alegre, J. V. Míguez, et J. Carpio, « Modelling of electric and parallel-hybrid electric vehicle using Matlab/Simulink environment and planning of charging stations through a geographic information system and genetic algorithms », *Renewable and Sustainable Energy Reviews*, vol. 74, p. 1020-1027, juill. 2017, doi: 10.1016/j.rser.2017.03.041.
- [23] J. C. González Palencia, Y. Otsuka, M. Araki, et S. Shiga, « Scenario analysis of lightweight and electric-drive vehicle market penetration in the long-term and impact on the light-duty vehicle fleet », *Applied Energy*, vol. 204, p. 1444-1462, oct. 2017, doi: 10.1016/j.apenergy.2017.05.054.
- [24] N. Juul, G. Pantuso, J. E. B. Iversen, et T. K. Boomsma, « Strategies for Charging Electric Vehicles in the Electricity Market », *International Journal of Sustainable Energy Planning and Management*, vol. 7, p. 67-74, nov. 2015, doi: 10.5278/ijsepm.2015.7.6.
- [25] P. A. Østergaard, F. M. Andersen, et P. S. Kwon, « Energy Systems Scenario Modelling and Long Term Forecasting of Hourly Electricity Demand », *International Journal of Sustainable Energy Planning and Management*, vol. 7, p. 99-116, 2015, doi: 10.5278/ijsepm.2015.7.8.
- [26] L. Setiartiti et R. A. A. Hasibi, « Low carbon-based energy strategy for transportation sector development », *International Journal of Sustainable Energy Planning and Management*, vol. 19, p. 29-44, janv. 2019, doi: 10.5278/ijsepm.2019.19.4.
- [27] J.-J. Liu, Y.-P. Yang, et J.-H. Xu, « Electromechanical Valve Actuator with Hybrid MMF for Camless Engine », *IFAC Proceedings Volumes*, vol. 41, n° 2, p. 10698-10703, janv. 2008, doi: 10.3182/20080706-5-KR-1001.01813.
- [28] P. Mercorelli, « A Lyapunov-based Adaptive Control Law for an Electromagnetic Actuator », *AASRI Procedia*, vol. 4, p. 96-103, 2013, doi: 10.1016/j.aasri.2013.10.016.
- [29] W. Hoffmann et A. G. Stefanopoulou, « Valve Position Tracking for Soft Landing of Electromechanical Camless Valvetrain », *IFAC Proceedings Volumes*, vol. 34, n° 1, p. 295-300, mars 2001, doi: 10.1016/S1474-6670(17)34413-0.
- [30] K. Peterson, A. Stefanopoulou, Yan Wang, et Mohammad Haghgoeie, « Nonlinear Self-Tuning Control for Soft Landing of an Electromechanical Valve Actuator », *IFAC Proceedings Volumes*, vol. 35, n° 2, p. 191-196, déc. 2002, doi: 10.1016/S1474-6670(17)33940-X.
- [31] I. Zenginlis, J. S. Vardakas, N. Zorba, et C. V. Verikoukis, « Analysis and quality of service evaluation of a fast charging station for electric vehicles », *Energy*, vol. 112, p. 669-678, oct. 2016, doi: 10.1016/j.energy.2016.06.066.
- [32] I. Karakitsios, E. Karfopoulos, et N. Hatziargyriou, « Impact of dynamic and static fast inductive charging of electric vehicles on the distribution network », *Electric Power Systems Research*, vol. 140, p. 107-115, nov. 2016, doi: 10.1016/j.epsr.2016.06.034.
- [33] R. S. Levinson et T. H. West, « Impact of public electric vehicle charging infrastructure », *Transportation Research Part D: Transport and Environment*, vol. 64, p. 158-177, oct. 2018, doi: 10.1016/j.trd.2017.10.006.
- [34] A. Zhang, J. E. Kang, et C. Kwon, « Incorporating demand dynamics in multi-period capacitated fast-charging location planning for electric vehicles », *Transportation Research Part B: Methodological*, vol. 103, p. 5-29, sept. 2017, doi: 10.1016/j.trb.2017.04.016.
- [35] X.-H. Sun, T. Yamamoto, et T. Morikawa, « Fast-charging station choice behavior among battery electric vehicle users », *Transportation Research Part D: Transport and Environment*, vol. 46, p. 26-39, juill. 2016, doi: 10.1016/j.trd.2016.03.008.
- [36] F. Wu et R. Sioshansi, « A stochastic flow-capturing model to optimize the location of fast-charging stations with uncertain electric vehicle flows », *Transportation Research Part D: Transport and Environment*, vol. 53, p. 354-376, juin 2017, doi: 10.1016/j.trd.2017.04.035.
- [37] A. Schroeder et T. Traber, « The economics of fast charging infrastructure for electric vehicles », *Energy Policy*, vol. 43, p. 136-144, avr. 2012, doi: 10.1016/j.enpol.2011.12.041.

- [38] N. Javani, I. Dincer, G. F. Naterer, et B. S. Yilbas, « Exergy analysis and optimization of a thermal management system with phase change material for hybrid electric vehicles », *Applied Thermal Engineering*, vol. 64, n° 1, p. 471-482, mars 2014, doi: 10.1016/j.applthermaleng.2013.11.053.
- [39] J. Cen, Z. Li, et F. Jiang, « Experimental investigation on using the electric vehicle air conditioning system for lithium-ion battery thermal management », *Energy for Sustainable Development*, vol. 45, p. 88-95, août 2018, doi: 10.1016/j.esd.2018.05.005.
- [40] M. Malik, I. Dincer, M. A. Rosen, M. Mathew, et M. Fowler, « Thermal and electrical performance evaluations of series connected Li-ion batteries in a pack with liquid cooling », *Applied Thermal Engineering*, vol. 129, p. 472-481, janv. 2018, doi: 10.1016/j.applthermaleng.2017.10.029.
- [41] T. Taner, « Energy and exergy analyze of PEM fuel cell: A case study of modeling and simulations », *Energy*, vol. 143, p. 284-294, janv. 2018, doi: 10.1016/j.energy.2017.10.102.
- [42] G. Liu, M. Ouyang, L. Lu, J. Li, et X. Han, « Analysis of the heat generation of lithium-ion battery during charging and discharging considering different influencing factors », *J Therm Anal Calorim*, vol. 116, n° 2, p. 1001-1010, mai 2014, doi: 10.1007/s10973-013-3599-9.
- [43] K. Darcovich, D. D. MacNeil, S. Recoskie, et B. Kenney, « Coupled electrochemical and thermal battery models for thermal management of prismatic automotive cells », *Applied Thermal Engineering*, vol. 133, p. 566-575, mars 2018, doi: 10.1016/j.applthermaleng.2018.01.094.
- [44] M. Jafari, K. Khan, et L. Gauchia, « Deterministic models of Li-ion battery aging: It is a matter of scale », *Journal of Energy Storage*, vol. 20, p. 67-77, déc. 2018, doi: 10.1016/j.est.2018.09.002.
- [45] X. Zhang *et al.*, « Evaluation of convective heat transfer coefficient and specific heat capacity of a lithium-ion battery using infrared camera and lumped capacitance method », *Journal of Power Sources*, vol. 412, p. 552-558, févr. 2019, doi: 10.1016/j.jpowsour.2018.11.064.
- [46] L. Sheng, L. Su, et H. Zhang, « Experimental determination on thermal parameters of prismatic lithium ion battery cells », *International Journal of Heat and Mass Transfer*, vol. 139, p. 231-239, août 2019, doi: 10.1016/j.ijheatmasstransfer.2019.04.143.
- [47] K. Smith et C.-Y. Wang, « Power and thermal characterization of a lithium-ion battery pack for hybrid-electric vehicles », *Journal of Power Sources*, vol. 160, n° 1, p. 662-673, sept. 2006, doi: 10.1016/j.jpowsour.2006.01.038.
- [48] M. Shen et Q. Gao, « System simulation on refrigerant-based battery thermal management technology for electric vehicles », *Energy Conversion and Management*, vol. 203, p. 112176, janv. 2020, doi: 10.1016/j.enconman.2019.112176.
- [49] K. Onda, T. Ohshima, M. Nakayama, K. Fukuda, et T. Araki, « Thermal behavior of small lithium-ion battery during rapid charge and discharge cycles », *Journal of Power Sources*, vol. 158, n° 1, p. 535-542, juill. 2006, doi: 10.1016/j.jpowsour.2005.08.049.
- [50] T. Ohshima, M. Nakayama, K. Fukuda, T. Araki, et K. Onda, « Thermal behavior of small lithium-ion secondary battery during rapid charge and discharge cycles », *Electrical Engineering in Japan*, vol. 157, n° 3, p. 17-25, 2006, doi: 10.1002/ej.20249.
- [51] H. J. Khasawneh et M. S. Illindala, « Battery cycle life balancing in a microgrid through flexible distribution of energy and storage resources », *Journal of Power Sources*, vol. 261, p. 378-388, sept. 2014, doi: 10.1016/j.jpowsour.2014.02.043.
- [52] Y.-H. Chiang, W.-Y. Sean, C.-H. Wu, et C.-Y. Huang, « Development of a converterless energy management system for reusing automotive lithium-ion battery applied in smart-grid balancing », *Journal of Cleaner Production*, vol. 156, p. 750-756, juill. 2017, doi: 10.1016/j.jclepro.2017.04.028.
- [53] B. Hollweck, T. Korb, G. Kolls, T. Neuner, et J. Wind, « Analyses of the holistic energy balance of different fuel cell powertrains under realistic boundary conditions and user behaviors », *International Journal of Hydrogen Energy*, vol. 44, n° 35, p. 19412-19425, juill. 2019, doi: 10.1016/j.ijhydene.2019.02.009.
- [54] S. Davidov et M. Pantoš, « Optimization model for charging infrastructure planning with electric power system reliability check », *Energy*, vol. 166, p. 886-894, janv. 2019, doi: 10.1016/j.energy.2018.10.150.

- [55] C. Madina, I. Zamora, et E. Zabala, « Methodology for assessing electric vehicle charging infrastructure business models », *Energy Policy*, vol. 89, p. 284-293, févr. 2016, doi: 10.1016/j.enpol.2015.12.007.
- [56] B. Csonka et C. Csiszár, « Determination of charging infrastructure location for electric vehicles », *Transportation Research Procedia*, vol. 27, p. 768-775, janv. 2017, doi: 10.1016/j.trpro.2017.12.115.
- [57] F. Xie, C. Liu, S. Li, Z. Lin, et Y. Huang, « Long-term strategic planning of inter-city fast charging infrastructure for battery electric vehicles », *Transportation Research Part E: Logistics and Transportation Review*, vol. 109, p. 261-276, janv. 2018, doi: 10.1016/j.tre.2017.11.014.
- [58] Y. Tao, M. Huang, et L. Yang, « Data-driven optimized layout of battery electric vehicle charging infrastructure », *Energy*, vol. 150, p. 735-744, mai 2018, doi: 10.1016/j.energy.2018.03.018.
- [59] J. Rominger et C. Farkas, « Public charging infrastructure in Japan – A stochastic modelling analysis », *International Journal of Electrical Power & Energy Systems*, vol. 90, p. 134-146, sept. 2017, doi: 10.1016/j.ijepes.2017.01.022.
- [60] V. Salapić, M. Gržanić, et T. Capuder, « Optimal sizing of battery storage units integrated into fast charging EV stations », in *2018 IEEE International Energy Conference (ENERGYCON)*, 2018, p. 1-6, doi: 10.1109/ENERGYCON.2018.8398789.
- [61] A. Gusrialdi, Z. Qu, et M. A. Simaan, « Distributed Scheduling and Cooperative Control for Charging of Electric Vehicles at Highway Service Stations », *IEEE Transactions on Intelligent Transportation Systems*, vol. 18, n° 10, p. 2713-2727, oct. 2017, doi: 10.1109/TITS.2017.2661958.
- [62] H. Qin et W. Zhang, « Charging scheduling with minimal waiting in a network of electric vehicles and charging stations », in *Proceedings of the Eighth ACM international workshop on Vehicular inter-networking*, Las Vegas, Nevada, USA, 2011, p. 51-60, doi: 10.1145/2030698.2030706.
- [63] J. Tan et L. Wang, « Real-Time Charging Navigation of Electric Vehicles to Fast Charging Stations: A Hierarchical Game Approach », *IEEE Transactions on Smart Grid*, vol. 8, n° 2, p. 846-856, mars 2017, doi: 10.1109/TSG.2015.2458863.
- [64] Y. Yang, E. Yao, Z. Yang, et R. Zhang, « Modeling the charging and route choice behavior of BEV drivers », *Transportation Research Part C: Emerging Technologies*, vol. 65, p. 190-204, avr. 2016, doi: 10.1016/j.trc.2015.09.008.
- [65] « Global EV Outlook 2018 – Analysis », *IEA*, 01-févr-2020. [En ligne]. Disponible sur: <https://www.iea.org/reports/global-ev-outlook-2018>. [Consulté le: 01-févr-2020].
- [66] H. Hou *et al.*, « Electrical Vehicle Wireless Charging Technology Based on Energy Internet Application in China », *Procedia Computer Science*, vol. 83, p. 1332-1337, janv. 2016, doi: 10.1016/j.procs.2016.04.278.
- [67] « Charge Points », *UK EVSE*, 01-févr-2020. [En ligne]. Disponible sur: <http://ukevse.org.uk/charge-points-chargers/>. [Consulté le: 01-févr-2020].
- [68] « DC Fast Charging Explained », *EV Safe Charge*, 01-févr-2020. [En ligne]. Disponible sur: <https://evsafecharge.com/dc-fast-charging-explained/>. [Consulté le: 01-févr-2020].
- [69] L. Sun, D. Ma, et H. Tang, « A review of recent trends in wireless power transfer technology and its applications in electric vehicle wireless charging », *Renewable and Sustainable Energy Reviews*, vol. 91, p. 490-503, août 2018, doi: 10.1016/j.rser.2018.04.016.
- [70] C. Panchal, S. Stegen, et J. Lu, « Review of static and dynamic wireless electric vehicle charging system », *Engineering Science and Technology, an International Journal*, vol. 21, n° 5, p. 922-937, oct. 2018, doi: 10.1016/j.jestch.2018.06.015.
- [71] K. A. Kalwar, M. Aamir, et S. Mekhilef, « Inductively coupled power transfer (ICPT) for electric vehicle charging – A review », *Renewable and Sustainable Energy Reviews*, vol. 47, p. 462-475, juill. 2015, doi: 10.1016/j.rser.2015.03.040.
- [72] Evatran, « Tech Specs - Gen 2 », *Plugless Power*, 01-févr-2020. [En ligne]. Disponible sur: <https://www.pluglesspower.com/gen2-tech-specs/>. [Consulté le: 01-févr-2020].
- [73] R. W. Carlson et B. Normann, « Test Results of the PLUGLESS™ Inductive Charging System from Evatran Group, Inc. », *SAE International Journal of Alternative Powertrains*, vol. 3, n° 1, p. 64-71, 2014.

- [74] « Automotive Solutions • WiTricity », *WiTricity*, 01-févr-2020. [En ligne]. Disponible sur: <https://witricity.com/products/automotive/>. [Consulté le: 01-févr-2020].
- [75] S. A. Birrell, D. Wilson, C. P. Yang, G. Dhadyalla, et P. Jennings, « How driver behaviour and parking alignment affects inductive charging systems for electric vehicles », *Transportation Research Part C: Emerging Technologies*, vol. 58, p. 721-731, sept. 2015, doi: 10.1016/j.trc.2015.04.011.
- [76] « BMW announce wireless charging is coming soon », 01-févr-2020. [En ligne]. Disponible sur: <https://www.sytner.co.uk/news/bmw-wireless-charging/>. [Consulté le: 02-févr-2020].
- [77] A. M. Zaki, O. Arafa, et S. I. Amer, « Microcontroller-based mobile robot positioning and obstacle avoidance », *Journal of Electrical Systems and Information Technology*, vol. 1, n° 1, p. 58-71, mai 2014, doi: 10.1016/j.jesit.2014.03.009.
- [78] J. Mullan, D. Harries, T. Bräunl, et S. Whitely, « The technical, economic and commercial viability of the vehicle-to-grid concept », *Energy Policy*, vol. 48, p. 394-406, sept. 2012, doi: 10.1016/j.enpol.2012.05.042.
- [79] P. Nunes et M. C. Brito, « Displacing natural gas with electric vehicles for grid stabilization », *Energy*, vol. 141, p. 87-96, déc. 2017, doi: 10.1016/j.energy.2017.09.064.
- [80] Y. Zhao, M. Noori, et O. Tatari, « Boosting the adoption and the reliability of renewable energy sources: Mitigating the large-scale wind power intermittency through vehicle to grid technology », *Energy*, vol. 120, p. 608-618, févr. 2017, doi: 10.1016/j.energy.2016.11.112.
- [81] K. M. Tan, V. K. Ramachandaramurthy, et J. Y. Yong, « Optimal vehicle to grid planning and scheduling using double layer multi-objective algorithm », *Energy*, vol. 112, p. 1060-1073, oct. 2016, doi: 10.1016/j.energy.2016.07.008.
- [82] J. Geske et D. Schumann, « Willing to participate in vehicle-to-grid (V2G)? Why not! », *Energy Policy*, vol. 120, p. 392-401, sept. 2018, doi: 10.1016/j.enpol.2018.05.004.
- [83] S. Ogo et Y. Sekine, « Recent progress in ethanol steam reforming using non-noble transition metal catalysts: A review », *Fuel Processing Technology*, vol. 199, p. 106238, mars 2020, doi: 10.1016/j.fuproc.2019.106238.
- [84] G. de Souza, V. C. Ávila, N. R. Marcílio, et O. W. Perez-Lopez, « Synthesis Gas Production by Steam Reforming of Ethanol over M-Ni-Al Hydrotalcite-type Catalysts; M=Mg, Zn, Mo, Co », *Procedia Engineering*, vol. 42, p. 1805-1815, janv. 2012, doi: 10.1016/j.proeng.2012.07.575.
- [85] E. van der Roest, L. Snip, T. Fens, et A. van Wijk, « Introducing Power-to-H<sub>3</sub>: Combining renewable electricity with heat, water and hydrogen production and storage in a neighbourhood », *Applied Energy*, vol. 257, p. 114024, janv. 2020, doi: 10.1016/j.apenergy.2019.114024.
- [86] S. Shiva Kumar et V. Himabindu, « Hydrogen production by PEM water electrolysis – A review », *Materials Science for Energy Technologies*, vol. 2, n° 3, p. 442-454, déc. 2019, doi: 10.1016/j.mset.2019.03.002.
- [87] P. Mishra, S. Krishnan, S. Rana, L. Singh, M. Sakinah, et Z. Ab Wahid, « Outlook of fermentative hydrogen production techniques: An overview of dark, photo and integrated dark-photo fermentative approach to biomass », *Energy Strategy Reviews*, vol. 24, p. 27-37, avr. 2019, doi: 10.1016/j.esr.2019.01.001.
- [88] Ø. Ulleberg et R. Hancke, « Techno-economic calculations of small-scale hydrogen supply systems for zero emission transport in Norway », *International Journal of Hydrogen Energy*, vol. 45, n° 2, p. 1201-1211, janv. 2020, doi: 10.1016/j.ijhydene.2019.05.170.
- [89] Z. Navas-Anguita, D. García-Gusano, J. Dufour, et D. Iribarren, « Prospective techno-economic and environmental assessment of a national hydrogen production mix for road transport », *Applied Energy*, vol. 259, p. 114121, févr. 2020, doi: 10.1016/j.apenergy.2019.114121.
- [90] J. Bellosta von Colbe *et al.*, « Application of hydrides in hydrogen storage and compression: Achievements, outlook and perspectives », *International Journal of Hydrogen Energy*, vol. 44, n° 15, p. 7780-7808, mars 2019, doi: 10.1016/j.ijhydene.2019.01.104.
- [91] R. Okuda, K. Komatsu, A. Nakamura, O. Ito, K. Nambu, et H. Saitoh, « Evaluation of released amount of hydrogen after high pressure hydrogen loading in carbonate », *Results in Engineering*, vol. 4, p. 100047, déc. 2019, doi: 10.1016/j.rineng.2019.100047.

- [92] Y. Zhang *et al.*, « Balancing wind-power fluctuation via onsite storage under uncertainty: Power-to-hydrogen-to-power versus lithium battery », *Renewable and Sustainable Energy Reviews*, vol. 116, p. 109465, déc. 2019, doi: 10.1016/j.rser.2019.109465.
- [93] M. Aziz, T. Oda, et T. Kashiwagi, « Comparison of liquid hydrogen, methylcyclohexane and ammonia on energy efficiency and economy », *Energy Procedia*, vol. 158, p. 4086-4091, févr. 2019, doi: 10.1016/j.egypro.2019.01.827.
- [94] A. Murugan *et al.*, « Measurement challenges for hydrogen vehicles », *International Journal of Hydrogen Energy*, vol. 44, n° 35, p. 19326-19333, juill. 2019, doi: 10.1016/j.ijhydene.2019.03.190.
- [95] Y. Ligen, H. Vrabel, et H. H. Girault, « Mobility from Renewable Electricity: Infrastructure Comparison for Battery and Hydrogen Fuel Cell Vehicles », *World Electric Vehicle Journal*, vol. 9, n° 1, p. 3, juin 2018, doi: 10.3390/wevj9010003.
- [96] S. Almeida Neves, A. Cardoso Marques, et J. Alberto Fuinhas, « Technological progress and other factors behind the adoption of electric vehicles: Empirical evidence for EU countries », *Research in Transportation Economics*, vol. 74, p. 28-39, mai 2019, doi: 10.1016/j.retrec.2018.12.001.
- [97] J. Liu et C. Zhong, « An economic evaluation of the coordination between electric vehicle storage and distributed renewable energy », *Energy*, vol. 186, p. 115821, nov. 2019, doi: 10.1016/j.energy.2019.07.151.
- [98] C. Münzel, P. Plötz, F. Sprei, et T. Gnann, « How large is the effect of financial incentives on electric vehicle sales? – A global review and European analysis », *Energy Economics*, vol. 84, p. 104493, oct. 2019, doi: 10.1016/j.eneco.2019.104493.
- [99] B. Ballinger *et al.*, « The vulnerability of electric vehicle deployment to critical mineral supply », *Applied Energy*, vol. 255, p. 113844, déc. 2019, doi: 10.1016/j.apenergy.2019.113844.
- [100] M. Pagani, W. Korosec, N. Chokani, et R. S. Abhari, « User behaviour and electric vehicle charging infrastructure: An agent-based model assessment », *Applied Energy*, vol. 254, p. 113680, nov. 2019, doi: 10.1016/j.apenergy.2019.113680.
- [101] S. Bellocchi, K. Klöckner, M. Manno, M. Noussan, et M. Vellini, « On the role of electric vehicles towards low-carbon energy systems: Italy and Germany in comparison », *Applied Energy*, vol. 255, p. 113848, déc. 2019, doi: 10.1016/j.apenergy.2019.113848.
- [102] Z. DIMITROVA, L. G. P. MENDES, et Z. KOSSOWSKI, « Actionneur électromagnétique pour soupape de moteur à combustion interne », WO2016051041A1, 07-avr-2016.
- [103] Chun Tai et Tsu-Chin Tsao, « Control of an electromechanical actuator for camless engines », in *Proceedings of the 2003 American Control Conference, 2003.*, 2003, vol. 4, p. 3113-3118 vol.4, doi: 10.1109/ACC.2003.1244007.
- [104] Ī. Haskara, V. V. Kokotovic, et L. A. Mianzo, « Control of an electro-mechanical valve actuator for a camless engine », *International Journal of Robust and Nonlinear Control*, vol. 14, n° 6, p. 561-579, 2004, doi: 10.1002/rnc.903.
- [105] K. S. Peterson, J. W. Grizzle, et A. G. Stefanopoulou, « Nonlinear control for magnetic levitation of automotive engine valves », *IEEE Transactions on Control Systems Technology*, vol. 14, n° 2, p. 346-354, mars 2006, doi: 10.1109/TCST.2005.863669.
- [106] M. Montanari, F. Ronchi, C. Rossi, et A. Tonielli, « Control of a camless engine electromechanical actuator: position reconstruction and dynamic performance analysis », *IEEE Transactions on Industrial Electronics*, vol. 51, n° 2, p. 299-311, avr. 2004, doi: 10.1109/TIE.2004.825230.
- [107] K. S. Peterson et A. G. Stefanopoulou, « Extremum seeking control for soft landing of an electromechanical valve actuator », *Automatica*, vol. 40, n° 6, p. 1063-1069, juin 2004, doi: 10.1016/j.automatica.2004.01.027.
- [108] R. Seethaler et K. Duerr, « Electromagnetic Valve Actuation System With Two Configurations », présenté à ASME 2009 International Design Engineering Technical Conferences and Computers and Information in Engineering Conference, 2010, p. 391-398, doi: 10.1115/DETC2009-87131.
- [109] A. Oustaloup et P. Coiffet, *Systèmes asservis linéaires d'ordre fractionnaire: théorie et pratique*. Paris, France, 1983.
- [110] A. Oustaloup, *La commande CRONE: Commande robuste d'ordre non entier*. Paris: Hermès, 1991.

- [111] P. Lanusse, « De la commande CRONE de première génération à la commande CRONE de troisième génération », thesis, Bordeaux 1, 1994.
- [112] A. Oustaloup, B. Mathieu, et P. Lanusse, « The CRONE Control of Resonant Plants: Application to a Flexible Transmission », *European Journal of Control*, vol. 2, n° 1, p. 113-121, 1995, doi: 10.1016/S0947-3580(95)70014-0.
- [113] P. Lanusse, « CRONE control system design, a CRONE toolbox for Matlab », *CRONE Group, University of Bordeaux, France*, 2010.
- [114] J. Sabatier, P. Lanusse, P. Melchior, et A. Oustaloup, *Fractional Order Differentiation and Robust Control Design: CRONE, H-infinity and Motion Control*. Springer Netherlands, 2015.
- [115] I. D. Landau, D. Rey, A. Karimi, A. Voda, et A. Franco, « A Flexible Transmission System as a Benchmark for Robust Digital Control\* », *European Journal of Control*, vol. 1, n° 2, p. 77-96, janv. 1995, doi: 10.1016/S0947-3580(95)70011-5.
- [116] Z. K. Dimitrova, « Environomic design of vehicle integrated energy systems », *Infoscience*, 2015. [En ligne]. Disponible sur: <https://infoscience.epfl.ch/record/213648>. [Consulté le: 01-févr-2020].
- [117] D. Bernardi, E. Pawlikowski, et J. Newman, « A General Energy Balance for Battery Systems », *J. Electrochem. Soc.*, vol. 132, n° 1, p. 5-12, janv. 1985, doi: 10.1149/1.2113792.
- [118] T. M. Bandhauer, S. Garimella, et T. F. Fuller, « A Critical Review of Thermal Issues in Lithium-Ion Batteries », *J. Electrochem. Soc.*, vol. 158, n° 3, p. R1-R25, janv. 2011, doi: 10.1149/1.3515880.
- [119] G. Karimi et X. Li, « Thermal management of lithium-ion batteries for electric vehicles », *International Journal of Energy Research*, vol. 37, n° 1, p. 13-24, 2013, doi: 10.1002/er.1956.
- [120] Y. Inui, Y. Kobayashi, Y. Watanabe, Y. Watase, et Y. Kitamura, « Simulation of temperature distribution in cylindrical and prismatic lithium ion secondary batteries », *Energy Conversion and Management*, vol. 48, n° 7, p. 2103-2109, juill. 2007, doi: 10.1016/j.enconman.2006.12.012.
- [121] E. Hosseinzadeh, R. Genieser, D. Worwood, A. Barai, J. Marco, et P. Jennings, « A systematic approach for electrochemical-thermal modelling of a large format lithium-ion battery for electric vehicle application », *Journal of Power Sources*, vol. 382, p. 77-94, avr. 2018, doi: 10.1016/j.jpowsour.2018.02.027.
- [122] Y. Chung et M. S. Kim, « Thermal analysis and pack level design of battery thermal management system with liquid cooling for electric vehicles », *Energy Conversion and Management*, vol. 196, p. 105-116, sept. 2019, doi: 10.1016/j.enconman.2019.05.083.
- [123] H. Liu, Z. Wei, W. He, et J. Zhao, « Thermal issues about Li-ion batteries and recent progress in battery thermal management systems: A review », *Energy Conversion and Management*, vol. 150, p. 304-330, oct. 2017, doi: 10.1016/j.enconman.2017.08.016.
- [124] Y. Bai *et al.*, « Reversible and irreversible heat generation of NCA/Si-C pouch cell during electrochemical energy-storage process », *Journal of Energy Chemistry*, vol. 29, p. 95-102, févr. 2019, doi: 10.1016/j.jechem.2018.02.016.
- [125] D. H. Jeon et S. M. Baek, « Thermal modeling of cylindrical lithium ion battery during discharge cycle », *Energy Conversion and Management*, vol. 52, n° 8, p. 2973-2981, août 2011, doi: 10.1016/j.enconman.2011.04.013.
- [126] G.-H. Kim, A. Pesaran, et R. Spotnitz, « A three-dimensional thermal abuse model for lithium-ion cells », *Journal of Power Sources*, vol. 170, n° 2, p. 476-489, juill. 2007, doi: 10.1016/j.jpowsour.2007.04.018.
- [127] R. Kantharaj et A. M. Marconnet, « Heat Generation and Thermal Transport in Lithium-Ion Batteries: A Scale-Bridging Perspective », *Nanoscale and Microscale Thermophysical Engineering*, vol. 23, n° 2, p. 128-156, avr. 2019, doi: 10.1080/15567265.2019.1572679.
- [128] H. Maleki, S. A. Hallaj, J. R. Selman, R. B. Dinwiddie, et H. Wang, « Thermal Properties of Lithium-Ion Battery and Components », *J. Electrochem. Soc.*, vol. 146, n° 3, p. 947, mars 1999, doi: 10.1149/1.1391704.
- [129] T. L. Bergman, F. P. Incropera, D. P. DeWitt, et A. S. Lavine, *Fundamentals of Heat and Mass Transfer*. John Wiley & Sons, 2011.

- [130] P. Elayiaraja, S. Harish, L. Wilson, A. Bensely, et D. M. Lal, « Experimental Investigation on Pressure Drop and Heat Transfer Characteristics of Copper Metal Foam Heat Sink », *Experimental Heat Transfer*, vol. 23, n° 3, p. 185-195, juin 2010, doi: 10.1080/08916150903399722.
- [131] A. Plesca, « Thermal Analysis of Busbars from a High Current Power Supply System », *Energies*, vol. 12, n° 12, p. 2288, janv. 2019, doi: 10.3390/en12122288.
- [132] D. (direction des routes Île-de-France), « Les comptages », 14-janv-2016. [En ligne]. Disponible sur: <http://www.dir.ile-de-france.developpement-durable.gouv.fr/les-comptages-a174.html>. [Consulté le: 02-févr-2020].
- [133] « Paper: J.L. Blanco's Phd Thesis – MRPT », 02-févr-2020. [En ligne]. Disponible sur: <https://www.mrpt.org/contributions-to-localization-mapping-and-navigation-in-mobile-robotics/>. [Consulté le: 02-févr-2020].
- [134] A. I. Eliazar et R. Parr, « DP-SLAM 2.0 », in *IEEE International Conference on Robotics and Automation, 2004. Proceedings. ICRA '04. 2004*, 2004, vol. 2, p. 1314-1320 Vol.2, doi: 10.1109/ROBOT.2004.1308006.
- [135] B. Steux et O. E. Hamzaoui, « CoreSLAM : a SLAM Algorithm in less than 200 lines of C code », 2009.
- [136] « Nissan unveils world's first Solid-Oxide Fuel Cell vehicle », *Nissan News USA*, 04-août-2016. [En ligne]. Disponible sur: <https://usa.nissannews.com/en-US/releases/nissan-unveils-world-s-first-solid-oxide-fuel-cell-vehicle>. [Consulté le: 02-févr-2020].
- [137] H. Song, X. Bao, C. M. Hadad, et U. S. Ozkan, « Adsorption/Desorption Behavior of Ethanol Steam Reforming Reactants and Intermediates over Supported Cobalt Catalysts », *Catal Lett*, vol. 141, n° 1, p. 43-54, janv. 2011, doi: 10.1007/s10562-010-0476-z.
- [138] O. Jolliet, M. Saadé, et P. Crettaz, *Analyse du cycle de vie: Comprendre et réaliser un écobilan*. PPUR Presses polytechniques, 2010.
- [139] S. Richet et P. Tonnelier, « 2013, PSA Peugeot Citroën, internal unpublished report ». PSA Peugeot Citroën, 2013.
- [140] L. Guzzella et A. Sciarretta, *Vehicle Propulsion Systems: Introduction to Modeling and Optimization*, 3<sup>e</sup> éd. Berlin Heidelberg: Springer-Verlag, 2013.
- [141] « L. Guzzella QSS Tool Box », 01-févr-2020. [En ligne]. Disponible sur: <https://idsc.ethz.ch/research-guzzella-onder/downloads.html>. [Consulté le: 02-févr-2020].
- [142] L. Yuan, S. Qin, Z. Yi, et Z. Xiaofeng, « Improved Rao-Blackwellized  $H_{\infty}$  filter based mobile robot SLAM », *The Journal of China Universities of Posts and Telecommunications*, vol. 23, n° 5, p. 47-55, oct. 2016, doi: 10.1016/S1005-8885(16)60057-2.
- [143] H. Cho, E. K. Kim, et S. Kim, « Indoor SLAM application using geometric and ICP matching methods based on line features », *Robotics and Autonomous Systems*, vol. 100, p. 206-224, févr. 2018, doi: 10.1016/j.robot.2017.11.011.
- [144] H. Peel, S. Luo, A. G. Cohn, et R. Fuentes, « Localisation of a mobile robot for bridge bearing inspection », *Automation in Construction*, vol. 94, p. 244-256, oct. 2018, doi: 10.1016/j.autcon.2018.07.003.
- [145] A. Pandey, « Mobile Robot Navigation and Obstacle Avoidance Techniques: A Review », *IRATJ*, vol. 2, n° 3, mai 2017, doi: 10.15406/iratj.2017.02.00023.
- [146] R. K. Akikur, R. Saidur, H. W. Ping, et K. R. Ullah, « Performance analysis of a co-generation system using solar energy and SOFC technology », *Energy Conversion and Management*, vol. 79, p. 415-430, mars 2014, doi: 10.1016/j.enconman.2013.12.036.

## Nomenclature

Abbreviation	Unit (if applicable)	Description
AFC		Alkaline fuel cell
B	[T]	Magnetic field
b		number of batteries in a battery pack
batspecifmass	[kg]	Specific mass of the battery
BEV		Battery electric vehicle
BMEP	[bar]	Brake main effective pressure
BSFC	[g/kWh]	Brake specific fuel consumption
BET		Brunauer–Emmett–Teller theory
BT		High voltage battery
C	Ah	capacity of the cell,
CC	A	Constant current
CV	V	Constant voltage
CML_01_short		Impact method
CAFE		Corporate Average Fuel Economy
CAPEX	[€]	Investment cost
CNG		Compressed natural gas
CO <sub>2</sub> – eq.		Equivalent CO <sub>2</sub>
CRONE		French acronym which means fractional order robust control
CSL		Control System law
CTL		Coal to liquid

CVT		Continuous variable transmission
$C_F$ :	( $s$ )	fractional controller
$C_R$ :	( $s$ )	rational controller
DoH		Degree of hybridization
EI		Energy integration
EM		Electric motor
EMOO		Evolutionary Multi Objective Optimization
Environomic design		Environmental, economic and efficiency design
EGR		Exhaust gas recirculation
el. machine		Electric machine
EU		European Union
EUDC		Extra Urban Driving Cycle
ESR		Ethanol Steam Reforming
ENR		Renewable energy
eq.		Equivalent
EtOH		Ethanol
<b>F. U.</b>		Functional unit
FCV		Fuel Cell Vehicle
GB		Gear Box
$G$	( $s$ )	uncertain plant of the actuator
$G_0$	( $s$ )	nominal plant of the actuator
GDP		Gross domestic product

---

GLPK, Cplex		Solvers
GT		Gas turbine
GWP	[kg CO <sub>2</sub> equivalent]	Global warming potential
GWP 100y	[kg CO <sub>2</sub> equivalent]	Global Warming Potential for 100 years
GHG		Greenhouse gas
HEV		Hybrid Electric Vehicle
HT/ LT battery		High voltage/ low voltage battery
I	[A]	Current amperage
ICE		Internal Combustion Engine
ICEV		Internal Combustion Engine Vehicle
IEA		International energy agency
IVC		Intake Valve Closing
IVO		Intake Valve Opening
IVT		Infinitely Variable Transmission
L	[m]	Length of the wire
LCA		Life Cycle Assessment
LCI		Life cycle inventory
LCIA		Life Cycle Impact Assessment
LHV	[kJ/kg]	Low Heating Value
Li- Ion		Lithium- Ion
LVB		Low voltage battery
MER	[kW]	Minimum energy requirement

MILP		Mixed Integer Linear Programming
MGB		Manuel Gear Box
MINLP		Mixed Integer Non Linear Programming
MOO		Multi Objective Optimization
LPG		Liquefied petroleum gas
NA		Natural Aspirated
NEDC		New European Drive Cycle
NiMH		Nickel Metal hydride
OPD	[kg CFC-11 equivalent]	Ozone Deplation
ORC		Organic Rankine Cycle
OPEX	[€]	Operating cost
PA		Power amplifier
PB		Power link
Peugeot 3008 HY4		Peugeot vehicle with hybrid electric powertrain
PHEV		Plug-in Hybrid Electric Vehicle
PI		Process Integration
PEM FC		Proton exchange membrane fuel cell
PV		Photo voltaic
REX		Range Extender Vehicle
RPM	[s <sup>-1</sup> ]	Rotation per minute
SNG		Synthetic natural gas
SoC	[%]	State of Charge

SOFC		Solid oxide fuel cell
SOFC- GT		Solid oxide fuel cell with gas turbine module
TEE		Thermo Economic Evaluation
TES		Thermo- economic Simulation
th engine		Thermal engine
TTC		“Toutes Taxes Comprises” – VAT(Value Added Tax)
T-t-W		Tank to Wheel
$U_{act}$ :	[V]	voltage across the actuator
UDC		Urban Driving Cycle
YAC		Yearly annualized cost in Euros
ZEV		Zero emissions vehicles
$Z(t)$ :	[mm]	position of the valve
$Z_{mes}(t)$	[mm]	measured position of the valve
$Z_{ref}(t)$	[mm]	reference position of the valve
2D		2 dimensions
3D		3 dimensions
<b>Greek letters</b>		
$\beta_0$	[s]	nominal open-loop
$\Delta T_a$	[°C]	Temperature of stream a
$\Delta T_b$	[°C]	Temperature of stream b
$\Delta T_{min}$	[°C]	Minimum approach temperature
$\varepsilon$	[-]	Exergetic efficiency

$\gamma$	[-]	Gear ratio
$\gamma_{i,j}$	[-]	activity coefficient of species $i$ in phase $j$
$\eta$	[-]	Thermal efficiency
$\eta_{engine}$	[-]	Engine efficiency
$\eta_{orc\_cycle}$	[-]	Efficiency of the ORC cycle
$\eta_{powertrain}$	[-]	Powertrain efficiency
$\omega_s$	[rpm]	Rotation speed of the driving shaft
$\omega_w$	[rpm]	Rotation speed of the wheels
$v_j$	[cm <sup>3</sup> ]	volume element of phase $j$

**Roman letters**

$A_{ex}$	[m <sup>2</sup> ]	Heat exchange area
c11, c22, c3, c4		High voltage battery coefficients
$c_{i,j}$	[J/(kg K)]	specific heat,
$c_{pb}$	[J/(kg K)]	specific heat of a busbar,
$c_{i,j}$	[mol/m <sup>3</sup> ]	concentration of species $i$ in phase $j$
$cp_{b\_Al}$	[J/(kg K)]	specific heat of Al busbar,
$cp_{b\_Cu}$	[ J/(kg K)]	specific heat of Cu busbar
$c_{pc}$	[J/(kg K)]	specific heat of a cell
$\dot{E}_C$	[kW]	Compressor power
$E_L$	[kJ]	energy delivered on the load
$E_{tot}$	[kJ]	total energy
$\dot{E}_{pump}$	[kW]	Pump power

$\dot{E}_{turbine}$	[kW]	Power on the turbine shaft
$\dot{E}_{shaft}$	[kW]	Power on the engine shaft
$F$	[N]	Force
$F$	96.485 C/mol	Faraday constant
$F_{act} :$	[N]	Electromagnetic force delivered by the actuator
$F_{frict}$	[N]	friction force at the valve guide
$F_{pres} :$	[N]	pressure force exerted by the exhaust or intake gases
$f_{scaling}$	[-]	Scaling factor for the electric motor
$f_1$	[-]	Function 1
$f_2$	[-]	Function 2
$h_c$	[W/(m <sup>2</sup> K)]	heat transfer coefficient of a cell,
$h_b$	[W/(m <sup>2</sup> K)]	heat transfer coefficient of a busbar,
$\Delta H_{i,j \rightarrow m}^0$	[J/mol]	molar enthalpy phase change of species $i$ from phase $j$ to $m$
$H_r$	[-]	Hybridation ratio
$i_{BP}$	[A]	discharge (or charge) current from a single battery package,
$i_{cell}$	[A]	discharge (or charge) current from a cell,
$k_1, k_2$	[-]	Structural parameters of the torque coupler
$m$	[kg]	Vehicle mass
$m :$	[kg]	total mass of the moving part of the actuator
$m_{fuel}$	[kg/s]	Fuel flow rate
$\dot{m}$	[kg/h]	Working fluid mass flow
$M_b$	[kg]	mass of a busbar

$M_c$	kg	mass of a cell
$\dot{M}_p$	[kg/h]	Mass flow of the sink source
$\dot{M}_s$	[kg/h]	Mass flow of the heat source
$n_e$	[-]	number of electrons participating in the reaction
$n_{i,j}$	[mol]	moles of species $i$ in phase $j$
$P_{BT}$	[kW]	Power of the battery
$P_{eff}$	[kW]	Effective power
$P_{EM}$	[kW]	Power of the electric motor
$P_{fuel}$	[kW]	Power in the fuel
$P_{hybrid}$	[kW]	Hybrid power
$P_m$	[kW]	Power of the electric motor
$P_{meca\_out}$	[kW]	Engine output mechanical power
$P_s$	[kW]	Power of the drive shaft
$P_{SC}$	[kW]	Power of the supercapacitors
$P_{th\_engine}$	[kW]	Power of the thermal engine
$P$	[kN]	Weight of the actuator
$P_1, P_2, P_3, P_4$	[bar]	Pressures in the ORC loop
SOFC		Solid oxide fuel cell
$T$	[Nm]	Torque
$T_{ICE}$	[Nm]	Torque of the internal combustion engine
$T_{EM}$	[Nm]	Torque of the electric motor
$T_{p,in}$	[°C]	Sink source in temperature

---

$T_{p,out}$	[°C]	Sink source out temperature
$T_s$	[Nm]	Torque on the drive shaft
$T_{s,in}$	[°C]	Heat source inlet temperature
$T_{s,out}$	[°C]	Heat source out temperature
$\dot{Q}$	[W]	heat transfer of a battery package
$Q_{Acell}$	[kJ]	heat accumulated in a cell
$Q_{batt}$	[kWh]	Energy of the battery
$Q_{Abus}$	[kJ]	heat accumulated in a busbar
$Q_{dis}$	[kJ]	heat dissipated to the ambient
$Q_{bus}$	[kJ]	heat generated in the busbar
$Q_c$	[kJ]	heat generated in the cables,
$Q_{cab}$	[kJ]	sum of $Q_c$ and $Q_{con}$ ,
$Q_{cell}$	[kJ]	heat generated in the cell,
$Q_{con}$	[kJ]	heat generated in the battery package due to resistance of metallic connections between cell and busbar
$Q_{GEN}$	[kJ]	heat generated in the whole battery package
$Q_{irr}$	[kJ]	irreversible heat
$Q_{Ncell}$	[kJ]	heat from adjacent cells
$Q_{ohmic}$	[kJ]	Ohmic heat,
$Q_{rev}$	[kJ]	reversible heat of the electrodes
$Q_r$	[kJ]	heat from electrochemical reaction
$\dot{Q}_A$	[kW]	Condensation heat power

$\dot{Q}_E$	[kW]	Evaporating heat power
$Q_{\text{heating/cooling}}$	[kJ]	Thermal energy for heating or cooling
$\dot{Q}_{in}$	[kW]	Heat power delivered to the cycle
$Q_{\text{supercap}}$	[kW]	Power of supercapacitor
$R$	8.314 J/(mol K)	universal gas constant
$R_{\text{bus}}$	[ $\Omega$ ]	resistance of a busbar
$R_c$	[ $\Omega$ ]	sum of $R_{\text{cab}}$ and $R_{\text{con}}$ ,
$R_{\text{cab}}$ ,	[ $\Omega$ ]	resistance of the cables connected to battery pack
$R_{\text{con}}$	[ $\Omega$ ]	resistance of all metallic connections in a battery pack
$R_{\text{load}}$	[ $\Omega$ ]	resistance of load
$R_{\text{wc}}$	[ $\Omega$ ]	internal resistance of cell,
$\Delta S$	[J/(mol K)]	entropy change
$S_b$	[m <sup>2</sup> ]	surface of a busbar
$S_{\text{BP}}$	[m <sup>2</sup> ]	surface of a battery package
$S_c$	[m <sup>2</sup> ]	surface of a cell
$t_{\text{off}}$	[s]	time of discharge process of the battery package
$T$	[K]	temperature
$T_A$	[C]	temperature of the ambient
$T_b$	[C]	temperature of a busbar
$T_c$	[C]	temperature of a cell
$U_{\text{ocv}}$	[V]	open voltage circuit
$V$	[V]	terminal voltage of a cell

---

$V_{\text{cutoff}}$	[V]	cut-off voltage of a cell,
$V_{\text{BP}}$	[V]	voltage of a battery pack
$V_n$	[V]	nominal voltage
$\dot{V}$	[m/s <sup>2</sup> ]	Vehicle acceleration or deceleration
$V$	[m/s]	Vehicle speed
WEVC		Wireless electric vehicles charger
WtW		Well-to-Wheels
$X_{\text{wc}}$	[ $\Omega$ ]	internal reactance of a cell

**Subscripts**

A	Condensation
E	Evaporation
P	Pump
T	Turbine
ext	External

**Superscripts**

+	Materials/ energy streams entering the system
-	Materials/ energy streams leaving the system



# List of Figures

Figure 1-1: CO<sub>2</sub> emissions regulatory forecast per regions ..... 1

Figure 2-1: Static Wireless Electric Vehicles Charging System. .... 15

Figure 2-2: Hydrogen production methods ..... 17

Figure 3-1: ORC Pareto curves: techno-economic trade-off, exergy efficiency in [-], in the colorbar ..... 23

Figure 3-2: Map of the ORC power output, design after multi-objective optimization, ORC net power in [kW], in the colorbar ..... 23

Figure 3-3: Schematic of the actuator ..... 27

Figure 3-4: Electromagnetic modelling of the actuator..... 28

Figure 3-5: Structure of the control system architecture ..... 29

Figure 3-6: Bode diagram of nominal plant frequency response (—) and set of frequency responses of G(s) (—) ..... 30

Figure 3-7: Experimental time responses (—) and nonlinear model time responses (—): position; voltage; current..... 31

Figure 3-8: Nichols plot G: nominal frequency response (—); uncertainty domains (—)..... 31

Figure 3-9: Nichols plot of  $\beta_0$  nominal frequency response (—); uncertainty domains (—); 1 dB M-contour (—) ..... 32

Figure 3-10: Pressure force (—) and force generated by the exhaust valve actuator (—) at 6000 rpm ..... 34

Figure 3-11: Opening and closing of the exhaust valve at 6000 rpm: reference signal (—); simulation response (—) ..... 34

Figure 3-12: Control voltage at 6000 rpm (exhaust simulation) ..... 34

Figure 3-13: Opening and closing of the intake valve at 6000 rpm: reference signal (—); experimental response (—). ..... 34

Figure 3-14: Control voltage at 6000 rpm..... 35

Figure 3-15: Battery cell components and principle ..... 36

Figure 3-16: Discharging and charging phases of a Li-Ion cell ..... 36

Figure 3-17: Cells technologies – evolutions of the technologies and their maturity [116] .. 37

Figure 3-18: Evolution of the batteries technology: opportunities for compactness..... 37

Figure 3-19: Comparison of the dimensions for different battery types ..... 38

Figure 3-20: Fundamentals issues of the solid-state batteries ..... 38

Figure 3-21: Classification of the solid electrolyte types..... 39

Figure 3-22: Energy distribution in the energy storage system..... 41

Figure 3-23: Energy flow in a battery pack..... 41

Figure 3-24: Temperature inside the battery package, in °C..... 44

Figure 3-25: Heat flow in a battery package ..... 45

Figure 3-26: Symmetry of the busbar ..... 45

Figure 3-27: Temperature gradient in battery pack with Al busbar a), Cu busbar b).....	46
Figure 3-28: The electrical circuit of the battery module with the parasitic resistances in steady-state operation conditions .....	47
Figure 3-29: Front view of the Cu busbar with 16 welding spots .....	47
Figure 3-30: Distribution of temperature measurement points on the battery package.....	48
Figure 3-31: Characteristics T(t) measured for the battery pack with Al busbar a), with Cu busbar b).....	49
Figure 4-1: Definition of the recharging systems .....	52
Figure 4-2: Highway with charging stations installations .....	52
Figure 4-3: Results from the optimization: flow of 10 vehicles, minimization of the waiting time.....	55
Figure 4-4: Results from the optimization: flow of 30 vehicles, minimization of the waiting time.....	56
Figure 4-5: Overview of possible communication flow and related constraints .....	58
Figure 4-6: Communication flow chart .....	60
Figure 4-7: Average daily incoming vehicle flow .....	61
Figure 4-8: Generated vehicles trip characteristics .....	61
Figure 4-9: Average waiting time comparison .....	62
Figure 4-10: Waiting times at charging station, 3 charging points per station.....	63
Figure 4-11: Waiting times at charging station, 2 charging points.....	63
Figure 4-12: Numerical model of the mobile robot.....	64
Figure 4-13: Structure and communication of the mobile robot with SLAM .....	66
Figure 4-14: Representation of the different steps of the algorithm.....	67
Figure 4-15: Mapping of the mechanical labotary. a) Quality: 50 / Size: 15 b) Quality: 1 / Size: 20 .....	69
Figure 4-16: Reference map of the robot.....	71
Figure 5-1: Vehicle propulsion system with an innovative range extender system [136].....	74
Figure 5-2: Reactions involved in the ethanol steam reforming.....	74
Figure 5-3: Carbon neutral cycle of the e-Bio Fuel Cell vehicle.....	75
Figure 5-4: Working principle of the e-Bio Fuel Cell system .....	75
Figure 5-5: Schematic diagram of the various type of fuel cell powered by various feedstocks .....	76
Figure 5-6: Mechanism of ethanol steam reforming [137].....	79
Figure 5-7: Main performances of the catalysts (bimetallic catalyst) .....	81
Figure 5-8: Photo of 1900 Sorptomatic apparatus 51 .....	82
Figure 5-9: Catalyst support preparation scheme .....	82
Figure 5-10: Monometallic supported catalysts preparation scheme .....	83
Figure 5-11: BET measurements .....	84
Figure 5-12: Activity test of 20%Ni/Al <sub>2</sub> O <sub>3</sub> , configuration 1 .....	85

Figure 5-13: Activity test of 20%Ni/Al <sub>2</sub> O <sub>3</sub> , configuration 2.....	85
Figure 5-14: Ethanol conversion ratio.....	85
Figure 5-15: Hydrogen selectivity for the catalyst.....	85
Figure 5-16: influence of the reaction temperature and Ni concentration in ethanol steam reforming (ESR) process.....	86
Figure 5-17: Influence of the Ni concentration and Zn addition in ethanol steam reforming (ESR) process.....	86
Figure 5-18: The influence of the Ni concentration and Zn addition on the H <sub>2</sub> selectivity in ethanol steam reforming (ESR) process.....	87
Figure 5-19: Influence of the Ni concentration and Ce addition in SRE process in ethanol steam reforming (ESR) process.....	87
Figure 5-20: H <sub>2</sub> selectivity for monometallic Ni catalyst for ESR process.....	88
Figure 5-21: influence of the catalyst composition on the H <sub>2</sub> selectivity in ESR process – monometallic and bimetallic catalysts .....	88
Figure 5-22: Stability test in ESR process, p = 1Bar, C <sub>2</sub> H <sub>5</sub> OH: H <sub>2</sub> O = 1:4.5, T = 600°C, after red. 500°C, m <sub>kat</sub> = 0.2 g 5%Ni/Al <sub>2</sub> O <sub>3</sub> -20%Ce.....	89
Figure 5-23: Stability test in ESR process, p = 1Bar, C <sub>2</sub> H <sub>5</sub> OH: H <sub>2</sub> O = 1:4.5, T = 600°C, after red. 500°C, m <sub>kat</sub> = 0.2 g, 0,1%-Pd-5%Ni/Al <sub>2</sub> O <sub>3</sub> -20%Ce.....	89
Figure 5-24: CO selectivity of 5%Ni/Al <sub>2</sub> O <sub>3</sub> -20%Ce and 0,1%-Pd-5%Ni/Al <sub>2</sub> O <sub>3</sub> -20%Ce catalysts.....	89
Figure 5-25: W-t-W total CO <sub>2</sub> emissions for different powertrain solutions for vehicles.....	91
Figure 5-26: Energy mix of France for LCA analysis.....	91
Figure 5-27: W-t-W total CO <sub>2</sub> emissions for different powertrain solutions for vehicles .....	92
Figure 5-28: Energy mix of Europe for LCA analysis.....	92
Figure 6-1: method for environomic design of vehicle grid related energy systems .....	98
Figure 7-1: Technologies for storage and conversion of hydrogen between energy grids. Integration of energy grids and services.....	100
Figure_ A-1: Computational framework of environomic optimization. ....	103
Figure_ A-2: Structure for multi-objective optimization .....	105
Figure_ A-3: Architecture of the multi-objective optimization tool for vehicle applications .....	106
Figure_ A-4: Energy integration and multi-periods model.....	106
Figure_ A-5: Steps of the life cycle analysis, selection of the environmental impacts and categories.....	110
Figure_ A-6: Vehicle unitary processes flow chart – system definition .....	110
Figure_ B-1: Generic backwards simulation model.....	111
Figure_ B-2: Efficiency map of a diesel engine.....	112
Figure_ B-3: Electric vehicle quasi-static model – BT- battery, PB – power link, EM- electric machine, GB- gear box, V- vehicle.....	113
Figure_ B-4: Quasi- static model of the parallel thermal electric hybrid.....	114

Figure_ B-5: Functional classification of HEVs in term of degree of hybridization and battery capacity [140] .....	115
Figure_ B-6: Two- quadrant electric motor efficiency map .....	116
Figure_ B-7: Fuel consumption map of a 2.2 liters Diesel engine .....	116
Figure_ B-8: ORC system to recover the waste heat of the ICE. ....	118
Figure_ B-9: Functional architecture of the ORC integration in a Mild HEV Architecture. ....	118
Figure_ B-10: Block diagram of the nonlinear model of the actuator .....	119
Figure_ B-11: Mechanical part of the actuator and lift profile Zref to be ensured for a mechanical valve train and an engine speed of 6000 rpm .....	119
Figure_ B-12: Block diagram of the actuator control implementation set-up .....	120
Figure_ B-13: Charging on the highway: use case for long way drives. ....	121
Figure_ C-1: Parallel hybrid electric architecture: FT – fuel tank, ICE – internal combustion engine, BT – high voltage battery, SC – super capacitor, PE – power electronics, M- electric motor, PSD – power split device, G – electric generator, C1- clutch 1, C2- clutch 2, T- Transmission, D- Differential. ....	125
Figure_ C-2: Pareto curve – total GWP to powertrain efficiency, investment cost in color bar, NEDC. ....	126
Figure_ C-3: Correspondence between the high voltage battery capacity and the hybridization ratio. ....	126
Figure_ C-4: Evolution of a) the total GWP as a function of the vehicle investment cost b) the investment cost as a function of the powertrain efficiency. ....	128
Figure_ C-5: GWP contribution for the production phase of the vehicles sub-systems a) Full ICE, b) 3 kWh of HVB, c) 7 kWh of HVB, d) 13 kWh of HEV .....	129
Figure_ C-6: Evolution of the total GWP and repartition of the contribution of reach phase as a function of the hybridization ratio, D –Class vehicles .....	130
Figure_ C-7: Use phase: GWP evolution as a function of the hybridization ration and contribution of the energy vectors (diesel and electricity production) .....	130
Figure_ C-8: Evolution of the CML impact categories a) eutrophication, b) acidification c) ODP as a function of the investment cost. ....	131
Figure_ C-9: Multi-objective optimization framework. ....	133
Figure_ C-10: Computational framework of technical simulation for vehicle energy integrated system .....	133
Figure_ C-11: Pareto for techno-economic optimization, battery specific density in colorbar .....	135
Figure_ C-12: Evolution of the vehicle autonomy as a function of the battery capacity, specific energy of 400 Wh/kg. ....	135
Figure_ C-13: Pareto of the environomic optimization, 2D plan cost/ autonomy. ....	136
Figure_ C-14: Pareto of the environomic optimization, 2D plan GWP/ autonomy. ....	136
Figure_ E-1: Definition of the extended energy system for the vehicle and the energy services. ....	141
Figure_ E-2 : Yearly cost/ autonomy Pareto curve in dual mode, GWP in color bar. ....	145
Figure_ E-3: 3D MOO Pareto curve, SOFC-GT design in colorbar .....	146
Figure_ E-4 : 3D MOO Pareto curve, battery design in color bar .....	146

---

Figure_ E-5 : Boolean variable=1 when the SOFC is designed for residential use, in color bar.....	146
Figure_ E-6: 3D MOO Pareto curve, with the part of the residential electricity from SOFC-GT in color bar. ....	147
Figure_ E-7 :3D MOO Pareto curve, with the part of the residential electricity from SOFC-GT in color bar (zoom in the autonomy transition zone). ....	148
Figure_ E-8: The total GWP as a function of the part of residential electricity from the SOFC-GT (French electricity mix).....	148
Figure_ E-9SOFC- GT integrated system [4] .....	150



## List of Tables

Table 2-1: Properties of stationary WEVCS on the market. ....	15
Table 3-1: Drive cycles characteristics .....	24
Table 3-2: Driving cycles and fuel consumption results on C-Segment Vehicle.....	25
Table 3-3: Seating valve velocity (m/s) at various engine speeds.....	33
Table 3-4: Energy balance calculation for the battery pack .....	46
Table 3-5: Parameters of busbars applied for the tests.....	48
Table 3-6: Balance of energy in battery system .....	49
Table 3-7: Balance of energy in battery system .....	49
Table 4-1: Initial charging stations characteristics.....	52
Table 4-2: Vehicles types for the flows constitution.....	53
Table 4-3: Decision variables for powertrain design .....	53
Table 4-4: Electric vehicles flow on the high way – 10 vehicles .....	54
Table 4-5: Studied vehicles characteristics .....	60
Table 4-6: Average charging and waiting time for the three scenarios.....	63
Table 4-7: Tracking of the robot .....	69
Table 4-8: Localization errors .....	70
Table 5-1: Comparison of the values of the energy balance for the different configurations	77
Table 5-2: Advantages and disadvantages of the different configurations (variants) .....	77
Table 5-3: Characterization of the samples (supports and catalysts) with BET analysis .....	83
Table_ A-1: Equations for the economic model [116].....	107
Table_ A-2: Listing of impact categories implemented in cml01_short .....	109
Table_ B-1: Electric vehicle main characteristics [116] .....	113
Table_ B-2: D- Class hybrid electric vehicle characteristics [116].....	114
Table_ C-1: Fuel cells types and their advantages and disadvantages to power electric vehicles .....	123
Table_ C-2: Drive cycles characteristics .....	124
Table_ C-3: Decision variables for powertrain design.....	125
Table_ C-4: Parameters and performances bands for the optimal designs on NEDC cycle.	132
Table_ C-5: Drive cycles characteristics .....	133
Table_ C-6: Decisions variables for design – multi-objective optimization problem.....	134
Table_ C-7: Multi objective optimization objectives and decision variables .....	134
Table_ C-8: Times of charging of the batteries for different powers of the chargers .....	136
Table_ C-9: Environomic designs for long range electric vehicles, specific energy of 400 Wh/kg.....	137
Table_ E-1: Definition of mobility and residential needs. ....	142
Table_ E-2: Vehicle characteristics.....	142
Table_ E-3: Economic evaluation for the base mobility and residential scenario. ....	143

Table\_ E-4: Equivalent CO<sub>2</sub> emission for the base case scenario. .... 143

Table\_ E-5: Definition of the decision variables for a dual application of the range extender module. .... 144

Table\_ E-6: Specific GWP for different sources of electricity..... 149

Table\_ E-7: Comparison between ID16 at 200 km of autonomy and the base case scenario..... 149

# Curriculum Vitae

# Table des matières du CV

Table des matières du CV.....	1
1. Curriculum Vitae.....	2
2. Liste des publications et des brevets.....	5
3. Activités de recherche et indices de reconnaissance .....	11
4. Activités d'enseignement .....	22



# 1. Curriculum Vitae

## Zlatina DIMITROVA

39 ans, Chercheur, Chef de projet en Recherche et Innovation à PSA Groupe (Entreprise Industrielle)  
Direction de la Recherche et de l'Innovation  
Département scientifique, unité « stockage et transformation de l'énergie »  
Centre Technique Vélizy-Villacoublay, France

## Diplômes

---

- 2015 **Thèse de doctotat (Docteur ès Sciences) en Energétique et Mécanique** : Environomic design of vehicles integrated energy systems au Laboratoire « Industrial process and energy system engineering (IPESE) » de l'Institut de Génie Mécanique de l'Ecole Polytechnique Fédérale (**EPFL**) de Lausanne, Ecole Doctorale « **Energie** », **Suisse**  
Directeurs de thèses : Professeur François Maréchal (EPFL), Dr. Erwann Samson (co-directeur, PSA)  
Rapporteurs : Prof. Panos Seferlis, Prof. Christopher Onder, Prof. Sylvain Allano, Dr. Peter Ott
- 2006 **Diplôme d'ingénieur** de l'Institut National des Sciences Appliquées (**INSA**) de Lyon, **France**  
Spécialité Génie Mécanique et Conception
- 2006 Diplôme de Master de l'Université Technique (**TU**) de Karlsruhe, **Allemagne**  
Spécialité Moteurs à combustion internes et turbomachines
- 1998 Diplôme du Baccalauréat du Lycée français Rakovski de Burgas, **Bulgarie**  
Mention excellente

## Expériences professionnelles

---

- Depuis 2019 Guest-lecturer, Programmes de Master, Transport et Logistique, Académie militaire nationale de la Bulgarie, Sofia, Bulgarie
- Depuis 2016 Chef de Projet en Recherche, Direction de la Recherche et l'Innovation, PSA Groupe, Vélizy-Villacoublay, France
- 2012-2016 Ingénieur de recherche, Direction de la Recherche et de l'Innovation, PSA Groupe, Vélizy-Villacoublay, France
- 2010-2012 Ingénieur de développement, Direction des Projets véhicules, PSA Groupe, Vélizy-Villacoublay, France
- 2006-2009 Ingénieur Combustion, Direction de la Recherche et de l'Innovation, PSA Groupe, La Garenne Colombes, France

## Enseignement

---

- 2019 Académie Militaire Nationale de la Bulgarie « Rakovski », Sofia, 58h de cours données dans les Programmes de Master
- 2012-2015 Doctorante-Assistante de Prof. François Maréchal, 150 h dans le cadre de ma thèse, cours de master, EPFL, Suisse

## Recherche

---

- Depuis 2016 Chef de Projet Recherche, Direction de la Recherche et l'Innovation, PSA Groupe, Vélizy-Villacoublay, France
- 2012-2016 Ingénieur de recherche, Direction de la Recherche et de l'Innovation, PSA Groupe, Vélizy-Villacoublay, France
- 2012-2015 Doctorante à l'Ecole Polytechnique Fédérale de Lausanne, Lausanne, Suisse

Mots Clés : Vehicules propulsion systems, energy storage, energy conversion, multi-objective optimization, Life Cycle Analysis

Encadrement :

Nbre de thèses soutenues : 2 en cours :2 thèses CIFRE (2 bourses CIFRE obtenues de l'ANRT, avec CentralSupelec Paris)

Nbre Master : 10, Projet de semestre :7 ; Projet de semestre de groupe :4, Post-doctorats :8

Participation projets et réseaux de recherche :

Stel Lab de PSA (Réseau de recherche de PSA) avec les laboratoires de recherche en France et à l'étranger. Pilotage et évaluation de deux laboratoires :

- Mechanics: Applied Mechanics Laboratory Lodz University of Technology, Lodz, Poland – PSA Groupe France
- Mechatronics : IMS de Bordeaux, UNP Bordeaux, France – PSA Groupe, France

Erasmus2025+ avec l'Université Technique de Sofia

Partenariats Industriels :

- Industrie Automobile : responsable du partenariat entre PSA et des fournisseurs pour le « Robot Chargeur »
- Industrie Aéronautique : responsable du partenariat entre PSA et Airbus

Nombre Publications et Productions :

- Publications dans des journaux scientifiques internationaux, avec comité de relecture (ACL): 20
- Articles publiés dans des actes de colloques / congrès, avec comité de relecture (ACTI): 15
- Brevets (BRE) : 41

Autres publications :

Journées thématiques / Séminaires : 3 Posters de recherche présentés

Rapports de contrat : 10 rapports de livrables sur les projets de recherche et innovation à PSA

Rapports internes : >10 rapports techniques internes à PSA.

## Responsabilités collectives et/ou administratives

---

- 2019 Membre de la commission scientifique de sélection des thèses CIFRE, PSA Groupe, Vélizy-Villacoublay, France

## Eléments remarquables du dossier et Rayonnement

---

- Depuis 2012
- Membre de 43 Jurys de soutenances académiques (PhD, Master Thesis, Projets de semestre)
  - 51 évaluations d'articles scientifiques pour la période 2015-2020 : International Journal of Energy, Applied Energy, Energy and Buildings, Transportation research part ,Transport and Environment, Energy Conversion and management journal, Environment, Development and Sustainability, Journal of the Brazilian Society of Mechanical Sciences and Engineering , IEEE open access, IEEE Transactions on Intelligent Transportation Systems
  - Organisation d'une journée thématique à PSA en octobre 2018.
  - H-index Scopus = 10 avec 380 citations
  - Prix: Palmarès des Inventeurs du Groupe PSA : 1er Prix en 2016 et 1er Prix en 2017
  - 2004 : Bourses d'études de la Région Baden- Württemberg, Allemagne
- Langues étrangères : Français, Anglais, Allemand, Bulgare, Russe, Espagnol, Portugais

## Motivation

Mon employeur « PSA Peugeot Citroën Groupe » est une entreprise industrielle qui est l'un des acteurs majeurs de l'industrie automobile. Je travaille à la direction de l'Innovation et de la Recherche et je suis chercheuse dans le secteur privé.

La stratégie scientifique et technologique du groupe PSA est basée sur de multiples champs scientifiques et technologiques essentiels pour préparer **la mobilité et le véhicule du futur**. Pour adresser ces champs scientifiques, PSA Groupe a construit son réseau de recherche « StelLab », composé d'Open Labs inspiré des meilleures pratiques mondiales en matière de structure commune de recherche avec les milieux académiques en France et à l'étranger.

Je dirige des projets de recherche et d'innovation et j'ai la responsabilité des activités de recherche et d'innovation dans le domaine « Energies et groupes motopropulseurs » pour les véhicules. Ma nomination à ce poste est effective depuis janvier 2016. Je dirige des activités de recherche appliquées en automobile. J'ai une codirection de thèses CIFRE, avec des chercheurs HDR des laboratoires partenaires de PSA. Je dirige également des partenariats avec les institutions de recherche académiques (universités ou instituts de recherche).

Mon projet professionnel est de préparer mon habilitation à diriger des recherches (HDR) et de continuer à diriger les activités de recherche dans l'industrie, par exemple chez PSA, avec un diplôme reconnu dans le monde académique. Dans l'industrie, nous avons des ressources de recherche considérables, par exemple, 80 doctorants au total et environ 30 nouvelles thèses de doctorat (CIFRE) sont discutées chaque année pour approbation, au sein de la commission des thèses de PSA, dans laquelle je siége.

Après mon HDR, j'ai l'ambition de motiver, de diriger et d'animer les activités de recherche du Groupe PSA avec les partenaires académiques selon les axes stratégiques d'innovation et de développement du Groupe PSA. Cette démarche d'habilitation est soutenue par ma hiérarchie dans l'entreprise.

## 2. Liste des publications et des brevets

### 2.1 Article dans des Journaux / revues

#### 2.1.1 Articles scientifiques, avec comité de relecture (ACL) : 20

1. Z. Dimitrova, F. Maréchal, Optimal designs for efficient mobility service for hybrid electric vehicles, *International Journal of Sustainable Energy Planning and Management* 22 **2019** 121-132.
2. Z. Dimitrova, M. Tari, P. Lanusse, F. Aioun, X. Moreau, Robust control for an electromagnetic actuator for a camless engine, *International Journal of Mechatronics* 57 **2019** 109-128.
3. Z. Dimitrova, M. Tari, P. Lanusse, F. Aioun, X. Moreau, Development and Control of a Camless Engine Valvetrain, *IFAC-PapersOnLine*, 52 **2019** 399-404.
4. G. Mitukiewicz, M. Głogowski, J. Stelmach, J. Leyko, Z. Dimitrova, D. Batory, Strengthening of cruciform sample arms for large strains during biaxial stretching, *Materials Today Communications* 21 **2019** 100692.
5. Z. Dimitrova, Integration of the environomic energy services for mobility and household using electric vehicle with a range extender of solid oxide fuel cell, *IOP Conference Series: Materials Science and Engineering* 664 (1) **2019** 012008.
6. Z. Dimitrova, Performance and economic analysis of an organic Rankine Cycle for hybrid electric vehicles, *IOP Conference Series: Materials Science and Engineering* 664 (1) **2019** 012009.
7. R. Gozdur, B. Guzowski, Z. Dimitrova, A. Noury, D. Batory, G Mitukiewicz, An energy balance evaluation in lithium-ion battery modules under high temperature operation, *Energy conversion and management journal*, **2020**.
8. Z. Dimitrova, F. Maréchal, Environomic design for electric vehicles with an integrated solid oxide fuel cell (SOFC) unit as a range extender, *Renewable Energy Journal* **2017** 112 124-142.
9. Z. Dimitrova, F. Maréchal, Energy integration on multi-periods for vehicle thermal powertrains, *Canadian Journal of Chemical Engineering* 95 (2) **2017** 253-264.
10. Z. Dimitrova, F. Maréchal, Energy integration on a gasoline engine for efficiency improvement, *International Journal of Thermodynamics* 20 **2017** 70-79.
11. Z. Dimitrova, F. Maréchal, Efficiency improvement for vehicle powertrains using energy integration techniques, *International Journal of Thermodynamics*, 20 **2016** 70-79.
12. Z. Dimitrova, F. Maréchal, Techno-economic design of hybrid electric vehicles and possibilities of the multi-objective optimization structure, *Applied Energy Journal* 161 **2015** 746-759.
13. Z. Dimitrova, F. Maréchal, Energy integration study on a hybrid electric vehicle energy system, using process integration techniques, *Applied Thermal Engineering Journal* 91 **2015** 834-847.
14. Z. Dimitrova, F. Maréchal, Techno-economic design of hybrid electric vehicles, *Energy Journal* 91 **2015** 630-644.

15. Z. Dimitrova, F. Maréchal, Performance and economic optimization of an organic Rankine cycle for a gasoline hybrid pneumatic powertrain, *Energy Journal* 86 **2015** 574-588.
16. Z. Dimitrova, F. Maréchal, Gasoline hybrid pneumatic engine for efficient vehicle powertrain hybridization, *Applied Energy Journal*, 151 **2015** 168-177.
17. Z. Dimitrova, F. Maréchal, Energy integration on multi-periods and multi-usages for hybrid electric and thermal powertrains, *Energy Journal* 83 **2015** 539-550.
18. Z. Dimitrova, F. Maréchal, Environomic design of vehicle energy systems for optimal mobility service, *Energy Journal*, 76 **2014** 1019-1028.
19. Z. Dimitrova, F. Maréchal, Environomic design of vehicle integrated energy systems-application on a hybrid electric vehicle energy system, *CET* 39 **2014** 475-480.
20. Z. Dimitrova, T. Alger, T. Chauvet, Synergies between high EGR operation and GDI Systems – SAE Paper, 01-0134 **2008** 101-114.

## 2.2 Articles dans des colloques / congrès, séminaires de recherche

### 2.2.1 Articles publiés dans des actes de colloques / congrès, avec comité de relecture (ACTI): 15

1. Z. Dimitrova, ENERGY PLANNING FOR SUSTAINABLE MOBILITY FOR 2030: ENERGY STORAGE AND CONVERSION OPTIONS FOR THE AUTOMOTIVE SECTOR, Long-term security environment challenges and armed forces capabilities development, Proceeding of the International Scientific Conference 12 – 14 November **2019**, Sofia, Part I, © Военна академия „Георги Стойков Раковски“, издател, 2019, ISBN 978-619-7478-34-1
2. P. Lanusse, M. Tari, Z. Dimitrova, Fr. Aioun, Fractional Order Design of a Digital Controller for a High-Speed Electromagnetic Actuator, 7th International Conference on Control, Mechatronics and Automation (ICCMA), **2019**, 44-48, IEEE
3. Z. Dimitrova, J. Hassler, P. Dessante, M. Petit, Design of electric vehicles grid related energy systems for optimal mobility service. Efficiency Cost and Optimization of Energy systems conference, ECOS 2019, Wroclaw, Poland
4. Z. Dimitrova B. Guzowski, Z. Dimitrova, A. Noury, D. Batory, G Mitukiewicz, An energy balance evaluation in lithium-ion battery modules under high temperature operation. Efficiency Cost and Optimization of Energy systems conference, ECOS **2019**, Wroclaw, Poland
5. J. Hassler, Z. Dimitrova, M. Petit, P. Dessante, Coordination interest in electric vehicles long distance trips. EVS 32 International Battery, Hybrid and Fuel Cell Electric Vehicle Symposium, **2019**, Lyon France
6. Z. Dimitrova, F. Maréchal, Optimal designs for efficient mobility service for hybrid electric vehicles. ECOS – efficiency, cost, optimization of the energy systems, conference, **2018** Guemaraes, Portugal
7. J. Hassler, Z. Dimitrova, M. Petit, P. Dessante, Service for optimization of charging stations selection for electric vehicles users during long distances drives. ECOS – efficiency, cost, optimization of the energy systems, conference, **2019**, Wroclaw, Poland
8. Z. Dimitrova, Electro mobility and fast charging, environomic design for efficient mobility service. *Revue MATEC Web of Conferences* (2018), *Bultrans* **2018**, Sozopol, Bulgaria
9. Z. Dimitrova, A. L. Alarcon Oliveira, Automated driving and charging of electric vehicles. *Revue MATEC Web of Conferences* (2018) *Bultrans* **2018**, Sozopol, Bulgaria
10. Z. Dimitrova, Predictive and holistic energy distribution for hybrid electric vehicles. *Revue MATEC Web of Conferences* (**2017**), Volume133, Pages 02002, *Bultrans* 2017, Sozopol, Bulgaria

11. Z. Dimitrova, Vehicle propulsion systems design methods. Revue MATEC Web of Conferences (2017), Volume 133, Pages, 02001, Bultrans 2017, Sozopol, Bulgaria
12. Z. Dimitrova, Energy integration on a gasoline engine for a vehicular application. ECOS – efficiency, cost, optimization of the energy systems, conference, 2017 San Diego, USA
13. Z. Dimitrova, F. Maréchal, Environomic design of hybrid electric vehicles. ECOS – efficiency, cost, optimization of the energy systems, conference, 2016 Portoroz, Slovenia,
14. Z. Dimitrova, F. Maréchal, Efficiency improvement for vehicle powertrains using energy integration techniques. ECOS – efficiency, cost, optimization of the energy systems, conference, 2015, Pau, France
15. Z. Dimitrova, F. Maréchal Environomic design of a vehicle integrated energy system – application on an electric vehicle. ECOS – efficiency, cost, optimization of the energy systems, conference, 2014, Turku, Finland

### 2.2.2 Autres produits présentés dans des colloques / congrès et des séminaires de recherche : 3 posters

Trois posters présentés aux journées de doctorants, organisées deux fois par an chez PSA Groupe et un poster présenté à un colloque international.

1. Study and design of an Electric mobility high level service for long distance trips, Jean Hassler, **Zlatina Dimitrova**, Marc Petit Philippe Dessante, PSA Posters Days, Vélizy, 18/12/2018
2. Coordination interest in electric vehicles long distance trips, Jean Hassler, **Zlatina Dimitrova**, Marc Petit Philippe Dessante, PSA Posters Days, Vélizy, 29/06/2019
3. Coordination interest in electric vehicles long distance trips, Jean Hassler, **Zlatina Dimitrova**, Marc Petit Philippe Dessante, EVS 32 International Conference, Lyon, 19/05/2020 - 22/05/2020

Les journées des posters sont visitées par les collaborateurs et les membres du Directoire du Groupe PSA. Le poster est le support pour les communications scientifiques.

Nous expliquons l'objectif de notre recherche, la manière dont elle s'intègre sur les axes stratégiques du Groupe PSA et les résultats obtenus.

## 2.3 Brevets, licences et déclarations d'invention : 41 brevets

1. (2019P01560 FR - N° de dépôt de la demande: 2000305 du **2020-Jan-14** ) Heatsinks with holes and busbar for cooling and conductivity of a battery pack, **DIMITROVA ZLATINA**, ROMAN GODZUR, BARTOLOMEJ GUZOWSKI, Dariusz BOGDANSKI, ANTONIN VINATIER
2. (2019P01270 FR - N° de dépôt de la demande: 2000279 du **2020-Jan-14**) Architecture programme du robot chargeur, GIRIN ALEX, **DIMITROVA ZLATINA**
3. (2019P01074 FR - N° de dépôt de la demande: 1909809 du **2019-Sep-06**) Heatsinks as busbar for cooling of a battery pack, **DIMITROVA ZLATINA**, ROMAN GODZUR, BARTOLOMEJ GUZOWSKI, Dariusz BOGDANSKI, ANTONIN VINATIER
4. (2019P00931 FR - N° de dépôt de la demande: 1907633 du **2019-Jul-08**), Module d'appel eCALL intégré (à l'antenne radio) et à alimentation autonome (capteur solaire) déclenchant appel des secours, après choc GAIN PRF, Applicable tous Projets, MARC PERU, PATRICIA LEMBERT, RICHARD ZEITOUNI, **DIMITROVA ZLATINA**
5. (2019P00975 FR - N° de dépôt de la demande: 1907485 du **2019-Jul-04**) Prédire une position de sécurité d'un conducteur dans un véhicule autonome suite à un danger détecté, MARC PERU, PATRICIA LEMBERT, **DIMITROVA ZLATINA**

6. (2019P00798 FR - N° de dépôt de la demande: 1906409 du **2019-Jun-14**) Procédé de détermination de stations de recharge d'un véhicule électrique sur son parcours, JEAN HASSLER, Marc PETIT, Philippe Dessante, **DIMITROVA ZLATINA**
7. (2019P00797 FR - N° de dépôt de la demande: 1906408 du **2019-Jun-14**) Combinaisons de réservations possibles sur stations de recharge électriques, JEAN HASSLER, Marc PETIT, Philippe Dessante, **DIMITROVA ZLATINA**
8. (2019P00621 FR - N° de dépôt de la demande: 1905528 du **2019-May-24**) Procédé de communication pour la gestion de la recharge des véhicules électriques sur autoroute pour effectuer des trajets de longue distance en véhicules électriques, **DIMITROVA ZLATINA**, JEAN HASSLER, Marc PETIT, Philippe Dessante, Zahra SEKKAT, Soufiane Achmaoui
9. (2019P00065 FR - N° de dépôt de la demande: 1904468 du **2019-Apr-26**) Procédé d'un service de gestion de la recharge des véhicules électriques sur autoroute pour effectuer des trajets de longue distance en véhicules électriques, **DIMITROVA ZLATINA**, JEAN HASSER, PRINCE LADIMIR
10. (2018P01170 FR - N° de dépôt de la demande: 1871811 du **2018-Nov-26**), Procédés et programme principal du robot chargeur. Recharge par induction des batteries des véhicules électriques et hybrides par robot. **DIMITROVA ZLATINA**, ANNA LUARA ALARCON OLIVEIRA
11. (2018P01548 FR - N° de dépôt de la demande: 1859282 du **2018-Oct-08**) Service de recharge par robot chargeur pour des clients particuliers, **DIMITROVA ZLATINA**, ANNA LUARA ALARCON OLIVEIRA
12. (2018P01128 FR - N° de dépôt de la demande: 1858962 du **2018-Sep-28**) Système de communication du robot chargeur pour la recharge par induction des batteries des véhicules électriques et hybrides par robot. **DIMITROVA ZLATINA**, ANNA LUARA ALARCON OLIVEIRA
13. (2018P01127 FR - N° de dépôt de la demande: 1858937 du **2018-Sep-28**) Service de recharge par robot chargeur pour des clients particuliers ou des opérateurs de parkings. Recharge par induction des batteries des véhicules électriques et hybrides par robot, **DIMITROVA ZLATINA**, ANNA LUARA ALARCON OLIVEIRA
14. (FR3084025), Boîtier mobile autonome à éclairage de son environnement, pour recharger par induction une batterie de véhicule, **DIMITROVA ZLATINA**, SIN YONG WOOK
15. (FR3052184) SYSTEM FOR ACTUATION OF A VALVE OF AN INTERNAL COMBUSTION ENGINE, **DIMITROVA ZLATINA**, AIOUN FRANCOIS, ONFRAY FREDERIC
16. (FR3077844) METHOD FOR CONTROL OF AN ELECTROMAGNETIC ACTUATOR OF THE THERMAL ENGINE VALVE, AIOUN FRANCOIS, **DIMITROVA ZLATINA**, MASSINISSA TARI, LANUSSE PATRICK
17. (**WO201973133**) Recharge by induction of electrical vehicles by means of a robot, **DIMITROVA ZLATINA**, FROEDE GONCALVES RAFAEL, GONCALVES WHILK MARCELINO
18. (FR3070329) ASSISTANCE METHOD FOR THE INDUCTIVE CHARGING OF A BATTERY OF A VEHICLE PARKED ON A LOCATION, **DIMITROVA ZLATINA**, FROEDE GONCALVES RAFAEL
19. (FR3069813) AUTONOMOUS MOVING BODY HOUSING FOR SUPPLY CABLE BY ITS ROTATIONS, FOR RECHARGING A BATTERY OF A VEHICLE INDUCTION, **DIMITROVA ZLATINA**, FROEDE GONCALVES RAFAEL, PRINCE LADIMIR
20. (FR3068728) METHOD FOR ELECTRONIC CONTROL OF ACTUATORS OF VALVES OF A COMBUSTION ENGINE, **DIMITROVA ZLATINA**, FROEDE GONCALVES RAFAEL
21. (FR3068960) DEVICE FOR MONITORING THE VOLTAGE OF A POWER SUPPLY LINK OF A MOVABLE AUTONOMOUS BOX, FOR AN AUTOMATIC WINDER,

- BONVALOT PATRICK, **DIMITROVA ZLATINA**, RASCOL JULIAN, BOUCHE THOMAS, JUTEAU MATTHIEU, MONNIER CLEMENT, NIKOLAYENKOV ANDREW
22. (FR3066052) DEVICE FOR RECHARGING BY INDUCTION OF BATTERY (S) OF A VEHICLE, HAS MULTIPLE POWER OUTLETS FOR A MOVABLE BOX, **DIMITROVA ZLATINA**, FROEDE GONCALVES RAFAEL, GONCALVES WHILK MARCELINO
  23. (FR3062607) MOBILE DEVICE BATTERY RECHARGING BY INDUCTION OF A VEHICLE, FOR AUTONOMOUS MOVEMENTS, **DIMITROVA ZLATINA**, BONVALOT PATRICK
  24. (FR3058750) CONTROL SYSTEM FOR OPENING AND CLOSING OF A DOOR OF A VEHICLE, IN A PARTICULAR MOTOR VEHICLE, **DIMITROVA ZLATINA**, MESARIC STEPHANE, FIGOLI DAVID
  25. (FR3057813) ANTI-CAMBERING SYSTEM FOR VARIABLE STIFFNESS COMPRISING THE SERIES OF BARS WHICH MOVE APART BETWEEN THEM, **DIMITROVA ZLATINA**, KASZUBA STANISLAW, MACIKOWSKI KRZYSZTOF
  26. (FR3055389) ASSEMBLY COMPRISING AN ELECTROMAGNETIC ACTUATOR AND AN ELEMENT TO ACTUATE, DUFOUR FREDERIC, **DIMITROVA ZLATINA**
  27. (FR3055364) APPARATUS FOR THE RECOVERY OF THERMAL ENERGY OF AN ENGINE OF A MOTOR VEHICLE, **DIMITROVA ZLATINA**
  28. (FR3051569) METHOD AND SYSTEM FOR CONTROL OF AN ELECTROMAGNETIC ACTUATOR OF VALVE OF AN ENGINE HAS DOCKING LAW OPTIMISED, AOUN FRANCOIS, **DIMITROVA ZLATINA**
  29. (FR3051567) METHOD AND SYSTEM FOR CONTROL OF AN ELECTROMAGNETIC ACTUATOR OF VALVE OF AN INTERNAL COMBUSTION ENGINE OPTIMIZING THE ENERGY CONSUMPTION, AOUN FRANCOIS, **DIMITROVA ZLATINA**
  30. (**WO2017198923**) Method and system for controlling an electromagnetic valve actuator of a combustion engine AOUN FRANCOIS, **DIMITROVA ZLATINA**, FADIGA LAMINE, LANUSSE PATRICK, MOREAU XAVIER
  31. (FR3047513) ELECTROMAGNETIC ACTUATOR FOR VALVE OF INTERNAL COMBUSTION ENGINE, **DIMITROVA ZLATINA**, ROY FRANCIS
  32. (FR3046629) METHODS AND SYSTEMS OF ELECTRICAL CURRENT SUPPLY IN A MOTOR VEHICLE, **DIMITROVA ZLATINA**, PORTO MENDES LUIZ GUSTAVO, PRINCE LADIMIR
  33. (FR3040431) COOLING SYSTEM OF AN ELECTROMAGNETIC ACTUATOR FOR A VALVE OF AN INTERNAL COMBUSTION ENGINE, **DIMITROVA ZLATINA**, PORTO MENDES LUIZ GUSTAVO, KOSSOWSKI ZBIGNIEW
  34. (EP3135872) Method for mounting a valve electromagnetic actuator and a cooling oil circuit **DIMITROVA ZLATINA**, PORTO MENDES LUIZ GUSTAVO, RADZIMINSKI BARTEK, KOSSOWSKI ZBIGNIEW
  35. (**WO2017/032930**) Electrical connector for electromagnetic valve actuator, **DIMITROVA ZLATINA**, PORTO MENDES LUIZ GUSTAVO, KOSSOWSKI ZBIGNIEW
  36. (**WO2016/071597**) System for electromagnetic actuation of valves for an internal combustion engine, PORTO MENDES LUIZ GUSTAVO, **DIMITROVA ZLATINA**
  37. (**WO2016/066912**) System for electromagnetic actuation of a valve of an internal combustion engine, **DIMITROVA ZLATINA**, PORTO MENDES LUIZ GUSTAVO
  38. (FR3026777) Electromagnetic actuator as cooling for an internal combustion engine valve, **DIMITROVA ZLATINA**, PORTO MENDES LUIZ GUSTAVO, KOSSOWSKI ZBIGNIEW
  39. (**WO2016051041**) Electromagnetic actuator for a valve of an internal combustion engine, **DIMITROVA ZLATINA**, PORTO MENDES LUIZ GUSTAVO, KOSSOWSKI ZBIGNIEW
  40. (**WO201651040**) Electromagnetic actuator comprising three coils, **DIMITROVA ZLATINA**, PORTO MENDES LUIZ GUSTAVO, KOSSOWSKI ZBIGNIEW

41. (FR3007155) PROCESS OF ORDERING OF POSITION OF A MOBILE BODY BY MEANS OF A BODY OF DEFORMABLE OPERATION , RUIZ TONY, GOHLKE MARC, SZMYTKA FABIEN, **DIMITROVA ZLATINA**

## **2.4 Rapports d'expertises techniques, produits des instances de normalisation : supérieur à 10**

Rédaction de rapports d'expertise pour le Groupe PSA, pour les multiples instances de l'entreprise, dans le cadre de ma mission en tant que chercheur à la Direction Scientifique du Groupe.

Je suis la représentante pour la filière de l'expertise du Groupe PSA dans le domaine du stockage et la conversion de l'énergie et de la robotisation des services énergétiques.

## **2.5 Produits des activités didactiques**

### **2.5.1 E-learning, moocs, cours multimedia, etc.: 1 conference grand public diffusée on-line**

1 conférence grand public réalisée au CNAM de Paris en Juin 2017.

C'était le 18<sup>ème</sup> cycle des conférences CNAM/ SIA intitulé : « Utilisation rationnelle des énergies et l'environnement »

## **2.6 Ouvrages**

### **2.6.1 Monographies et ouvrages scientifiques, éditions critiques, traductions : 2 traductions, 1 monographie (en cours)**

Traductions réalisées:

1. Lecture of Technology Transfer and Technology Foresight - translation from English to Bulgarian language
2. Lecture Energy storage and conversion and product life cycle management – translation from English to Bulgarian Language

Dans le cadre de l'enseignement dans les programmes de master de l'Académie Militaire Nationale Rakovski de Sofia, Bulgarie, **un projet d'édition de monographie est en cours**. La publication est attendue pour la fin de l'année 2020. La monographie contient les méthodes théoriques et les revues des systèmes énergétiques diverses, enseignées pendant les cours et s'appuie sur les articles scientifiques écrits par les élèves pour leur examen dans mes deux matières enseignées. Les articles sont intégrés comme des cas pratiques développés sur la base des méthodes théoriques enseignées dans les cours, mentionnés ci-dessus (point 1 et 2).

### **2.6.2 Thèses publiées / éditées: 1**

1. Z. Dimitrova, Environomic design of vehicles integrated energy systems, PhD thesis, Ecole Polytechnique Fédérale de Lausanne, **2015**, Lausanne, Suisse.

## **3. Activités de recherche et indices de reconnaissance**

### **3.1 Activités de recherche**

Le fil conducteur des recherches présentées dans ce dossier est l'amélioration de l'efficacité des systèmes énergétiques des véhicules et la réduction de leurs émissions, au travers de solutions compétitives et rentables de technologies de stockage et de conversion d'énergie. Les activités de recherche sont présentées dans trois domaines principaux :

- Efficacité énergétique, stockage et conversion à bord des véhicules
- Extension des systèmes énergétiques des véhicules, les véhicules en tant que systèmes liés au réseau électrique
- Systèmes de stockage et de conversion d'énergie pour les différents vecteurs énergétiques; véhicules électriques à pile à combustible, hydrogène et leur écosystème

La majeure partie de mon travail de recherche est conduite au sein de la direction de la Recherche et Innovation de PSA, où j'ai passé 12 de mes 14 années d'expérience professionnelle depuis 2006. J'ai commencé ma carrière en tant que jeune embauchée au sein du département « Moteurs » comme ingénieur combustion. De 2010 à 2012, j'ai été employée au département de développement de véhicules de PSA et engagée dans le développement et l'industrialisation de véhicules commerciaux. Il s'agissait pour moi d'un projet industriel de grande envergure, où j'ai expérimenté la gestion de projet: ressources, budget, planification, ingénierie et gestion de la qualité, contraintes industrielles et délais de commercialisation. J'ai géré le budget R&D et les investissements industriels de l'usine de production.

Par la suite, en 2012, j'ai réintégré le Département Recherche et Innovation et j'ai été nommée dans le domaine de recherche des systèmes de propulsion des véhicules. J'ai commencé ma thèse de doctorat à l'Ecole Polytechnique Fédérale de Lausanne (EPFL), Suisse en 2012 au Laboratoire des Systèmes d'Energie Industrielle et Ingénierie des Procédés (IPESE). La durée de mon doctorat la thèse était de 3 ans et 3 mois. J'étais affiliée à l'école doctorale de l'Energie de l'EPFL où j'ai suivi et validé 12 crédits ECTS. Ma thèse était basée sur des techniques de simulation et d'optimisation pour rechercher des meilleures configurations de chaînes de traction pour les véhicules. En 2016, j'ai été nommé Chef de Projet en recherche et innovation et jusqu'à aujourd'hui, j'ai la responsabilité de conduire, de diriger et d'administrer des projets de recherche liés au domaine de l'énergie et des systèmes de propulsion des véhicules.

#### **3.1.1 Efficacité énergétique, stockage et conversion à bord des véhicules**

La modélisation et l'optimisation des différents systèmes énergétiques (principalement la propulsion, mais aussi les systèmes de confort thermique (chauffage / refroidissement)) ont été l'objet de mes recherches de 2006 à 2015. Principalement les systèmes énergétiques des systèmes de propulsion des véhicules ont été considérés.

Un autre aspect du système énergétique est la récupération de la chaleur perdue et la satisfaction du service de confort thermique du véhicule (chauffage et refroidissement de l'habitacle). Des cycles de récupération de la chaleur ont été étudiés et les configurations optimales des systèmes énergétiques définies. Ces travaux ont fait objet à des publications et sont inclus dans le chapitre 3 du manuscrit.

La récupération de la chaleur dans les véhicules hybrides électriques est également étudiée pour différentes configurations. La récupération de l'énergie thermique des moteurs à combustion interne par des cycles thermodynamiques externes (cycle de Rankine à fluide organique) et l'hybridation électrique des chaînes de traction qui présente une source de récupération d'énergie cinétique est brevetée et les résultats sont présentés en dans le chapitre 3 du manuscrit. Il apparaît que différentes configurations de groupes motopropulseurs sont en concurrence pour un service de mobilité optimal en fonction des critères environnementaux sélectionnés.

La conversion d'énergie est traitée dans la période 2013-2018 où, je me suis occupée d'un projet de recherche « Actionneur électromagnétique » pour un moteur Camless. Cette technologie permet l'augmentation de l'efficacité des moteurs, grâce à un système de distribution variable. La première contribution scientifique significative est l'étude et la réalisation d'un actionneur électromagnétique et son contrôle/commande innovant pour un moteur Camless.

L'application a été faite sur un moteur 3 cylindres essence. Le projet a été mené jusqu'à une maturité technologique TRL4. J'ai eu le rôle de chef de projet en tant que responsable technique et scientifique de l'innovation.

La synthèse des bénéfices de la nouvelle technologie d'actionneur électromagnétique est présentée ci-dessous :

- Attractivité: Gain en compacité - 100 mm en hauteur culasse
  - Impact favorable sur le bloc avant du véhicule
  - Impact favorable sur le style de la silhouette du véhicule
- Gain en émissions de CO<sub>2</sub> – 3-5 % sur cycle d'homologation WLTP
- Originalité: « Carpet bombing » + de 10 brevets autour de la technologie
- Modularité:
  - Modules transversaux applicables aux moteurs à essence, à diesel et aux chaînes de traction hybridées (électrifiées)

Les activités scientifiques les plus marquantes sont :

- L'étude théorique de l'électromagnétisme, suivie de la conception, la réalisation et de la validation et l'évaluation économique d'un moteur Full Camless.
- L'étude théorique de la mécatronique, suivie par la mise en place d'un banc d'essais pour la mise au point du contrôle/commande de l'actionneur électromagnétique.

En 2018, j'ai également débuté les recherches sur les bilans énergétiques des batteries haute tension, utilisées dans les véhicules électriques. La recharge à forte puissance provoque de l'échauffement de batteries Li-Ion et il est nécessaire de gérer la dissipation de chaleur. Les techniques passives de dissipation thermique sont étudiées et les connexions des batteries à travers le pack sont utilisées avec une double fonction: conduction électrique et dissipation thermique. La recherche a conçu des connecteurs de chaleur et d'électricité, appelés « busbars ». Ces connecteurs ont été brevetés. Des analyses de sensibilité sur les matériaux des barres omnibus sont effectuées, en utilisant du cuivre et de l'aluminium. Ce travail de recherche est basé sur des expériences. Cette recherche est toujours active en 2020.

### **3.1.2 Extension des systèmes énergétiques des véhicules, les véhicules en tant que systèmes liés au réseau électrique**

La recharge électrique des véhicules et leur connexion au réseau énergétique est devenue une question importante. La définition du système énergétique est étendue et comprend le stockage et la conversion d'énergie des véhicules et leur connexion au réseau électrique. Le système énergétique étendu est modélisé par les flux de véhicules sur l'autoroute et une optimisation est réalisée pour définir la capacité optimale de stockage d'énergie des batteries des véhicules et le nombre optimal de recharges sur les trajets (Thèse J. Hassler 2017-2020). Le temps de recharge et les taux d'occupation, la localisation des chargeurs sont également évalués. L'optimalité est recherchée pour de longs trajets (>500 km), en mode tout électrique.

La stratégie de coordination entre les véhicules et l'infrastructure de recharge via la communication entre les véhicules (V2V) ou entre les véhicules et l'infrastructure (V2X) est également étudiée et brevetée. Cette stratégie a été présentée dans les articles scientifiques et fait également partie du chapitre 4 du rapport HDR. La principale contribution est le travail de mon doctorant Jean Hassler. Ces travaux ont donné des résultats prometteurs et se poursuivront en tant que nouvelle thèse de doctorat (CIFRE) pour la période 2020-2023.

La deuxième contribution scientifique significative est l'étude et la réalisation d'un prototype de robot-chargeur. Ce robot chargeur a été développé et présenté dans le cadre d'un projet d'innovation au sein de la Direction de la Recherche et de l'Innovation de PSA. Ce projet a démarré en 2017 et continue toujours aujourd'hui. Mon rôle est d'être chef de projet. Cela inclut la supervision et la contribution scientifique et technique.

La technologie est dédiée aux recharges de faible puissance (3,6 – 22 kW). Le concept est présenté dans le brevet (FR3062607) et consiste à proposer une recharge robotisée des véhicules. Pour les véhicules électrifiés, l'opération de recharge des batteries devient une opération quotidienne. Le but du robot est de rendre l'opération de recharge autonome pour les clients et de déléguer l'opération à un robot mobile. Le robot mobile est équipé d'une plaque inductive primaire. Le véhicule est équipé d'une plaque inductive secondaire. Le robot localise la plaque secondaire sous le véhicule, se positionne de manière très précise sous la plaque. Le transfert inductif de puissance s'opère au contact des deux plaques (primaire - située sur le robot, et secondaire - située sur le véhicule). Un module d'élévation permet à la plaque inductive primaire d'entrer en contact avec la plaque secondaire et le processus de charge commence.

La technologie « Robot chargeur » représente un intérêt majeur. Elle propose des services de mobilité aux opérateurs professionnels (parkings, flottes). Elle peut être également déployée chez les particuliers pour un usage domestique. Cette recherche technologique a conduit à 12 dépôts de brevets à ce stade.

La recherche est intéressante par la proposition de services énergétiques intégrés entre la mobilité et l'habitat. Le principal avantage de ce système en mode dual (mobilité/ habitat) à énergie intégrée est la réduction des émissions à effet de serre, à grande échelle.

### **3.1.3 Systèmes de stockage et de conversion d'énergie pour les différents vecteurs énergétiques; véhicules électriques à pile à combustible, hydrogène et leur écosystème**

L'hydrogène est considéré comme une énergie propre, mais plusieurs questions liées à sa production son stockage et sa distribution à grande échelle demeurent. L'état de l'art actuel d'un véhicule à pile à combustible est l'utilisation d'hydrogène gazeux sous pression à 700 bar, stocké au bord du véhicule et converti par une pile à combustible à membrane (PEM). Le stockage et la distribution sous 700 bar de pression de l'hydrogène présentent des problèmes techniques, économiques et environnementaux. L'idée de la recherche dans ce domaine est de proposer un concept de stockage de l'énergie sous

forme de bioéthanol et de convertir le bioéthanol en hydrogène à bord du véhicule par une pile à combustible à oxyde solide (SOFC).

En 2017 et 2018, la production d'hydrogène issue du reformage à la vapeur de bioéthanol et sa conversion en électricité pour un concept de véhicule à pile à combustible SOFC a été étudiée avec le Laboratoire de génie chimique de l'Université de Technologie de Lodz (Pologne). Une étude du bilan énergétique de la conversion du bioéthanol en électricité a été effectuée. La sélection du catalyseur pour une conversion optimale du bio-éthanol en hydrogène, dans des conditions de fonctionnement optimales a également été étudiée. Ce travail de recherche est basé sur des expériences.

Ce projet de recherche propose l'utilisation d'un système SOFC alimenté par l'hydrogène produit par le reformage de carburant liquide à partir de ressources renouvelables telles que le bioéthanol. L'installation SOFC dispose d'un reformeur de carburant intégré. Ce type de pile à combustible peut utiliser une variété de carburants au lieu de l'hydrogène traditionnellement utilisé dans piles à combustible à membrane (PEM). Ainsi le véhicule peut être alimenté par éthanol ou d'autres combustibles liquides ce qui est très avantageux du point de vue de l'application de telles piles à combustible à bord des automobiles. La conversion totale du bio éthanol est essentielle du point de vue économique. Le catalyseur qui est utilisé pendant le processus a un rôle important pour atteindre une conversion de 100% car il augmente la vitesse de réaction de telle manière que le système tend vers l'équilibre thermodynamique.

L'objectif principal de cette recherche est de sélectionner le système catalytique le plus actif et sélectif pouvant être directement utilisé dans le microréacteur avant la pile à combustible SOFC. Le bioéthanol est l'un des meilleurs candidats comme stockeur liquide d'hydrogène pour les piles à combustible. L'éthanol et en particulier le bioéthanol est pratique pour le reformage dans le réacteur monté en avant de la pile à combustible et a l'avantage d'être un carburant renouvelable, produit à partir de la biomasse.

## 3.2 Activités d'évaluation

### 3.2.1 Responsabilités au sein d'instances d'évaluation : 43 jurys de soutenance

**Depuis 2018**, membre de jury de deux **thèses de doctorat**:

1. Bartek Radziminski, Design and tests of mechanical energy recovery system for hybrid electric vehicles, AML Laboratory, Politechnika Lodzka, Lodz (Poland), PSA Groupe Vélizy (France), 2013-2018.
2. Jaroslaw Jarowski, Design of the control and energy management strategies for a mechanical energy recovery system for hybrid electric vehicles, AML Laboratory, Politechnika Lodzka, Lodz (Poland), PSA Groupe Vélizy (France), 2013-2018.

Encadrement à 25%, les sujets de recherches sont donnés par PSA Groupe et l'encadrement académique s'est fait au laboratoire AML de l'Université Polytechnique de Lodz, en Pologne.

**Depuis 2011** : Membre de **11 jurys d'évaluation de Master Thesis** des étudiants qui sont en Projet de Master : 11 participations dans des jurys de Master Thesis

1. Ignaas Detavernier, Development d'un nouveau véhicule pour le marché russe, Master Thesis, INSA Rennes, Département of Mechanics and Automatics, Rennes (France), PSA Groupe Vélizy (France), 02/2012-07/2012, grade 14,5/20
2. Julien Marquant, Multi-objective design and optimization of vehicle energy systems, coupled with a life cycle analysis, Institute of Mechanical Engineering, EPFL, (Switzerland)/ PSA Groupe Vélizy (France), 02/2013- 07/2013, grade 5/6

3. John Ingram, Energy integration study of hybrid vehicles energy systems, Institute of Mechanical Engineering, EPFL, (Switzerland)/ PSA Groupe Vélizy (France), 02/2014-07/2014, grade 5,5/6
4. Quoc Nhat Nam Pham, Environomic design of electric vehicles, coupled with a solid oxide fuel cell – gas turbine system as a range extender, Institute of Mechanical Engineering, EPFL, (Switzerland), 10/2014- 02/2015, grade 5/6
5. Charles-Thomas Stern, Design and optimization of vehicle energy systems, using an energy integration methodology for hybrid vehicles energy systems, 01/2015- 06/2015, Institute of Mechanical Engineering, EPFL, (Switzerland), 10/2014- 02/2015, grade 5/6
6. Eduard-Gabriel Turturica, Moteur Camless, le contrôle et la commande d'un actionneur électromagnétique, Département de Mechanical Engineering, ENSAM Paris (France), PSA Vélizy (France), 02/2015 – 07/2015, grade 14/20
7. Hugo Raynal, Etude de conception et de contrôlabilité d'un actionneur pour distribution variable, UTC Compiègne (France), PSA Groupe Vélizy (France), 02/2016- 07/2016, grade 15/20.
8. Luiz Gustavo Porto Mendes, Evaluation et optimisation d'un système innovant de distribution pour les moteurs à combustion interne, Ecole Centrale de Lille (France) ; PSA Groupe Vélizy (France), 05/2014 – 11/2014, grade 15/20.
9. Rafael Froede Gonçalves, Etude électronique d'un actionneur électromagnétique pour un système de distribution variable, ENSMM Besançon (France), PSA Groupe Vélizy (France), 02/2017- 07/2017, grade 19/20.
10. Anna Luara Alarcon Oliveira, Etude d'un robot mobile pour la recharge des batteries pour les véhicules hybrides et électriques, ENSMM Besançon (France), PSA Groupe Vélizy (France), 02/2018- 07/2018, grade 18/20.
11. Alex Guérin : Etude du système de navigation d'un robot mobile pour la recharge des batteries pour les véhicules hybrides et électriques, ENSAM Lille, PSA Groupe Vélizy (France), 11/02/2019 au 08/08/2019, grade 16/20.

**Depuis 2012** : Membre de 7 jurys d'évaluation de Projets de Semestre des étudiants qui ont été en Projet de Semestre : 7 participations dans des jurys d'évaluation de projet de Semestre

1. Julien Marquant, Study of the models for the multi-objective design and optimization of a vehicle energy systems, including alternative energy sources and sectors, Institute of Mechanical Engineering, EPFL, (Switzerland), 10/2012- 01/2013, grade 5/6.
2. Frédéric Tschirhart, Multi-objective design and optimization of a vehicle energy system, using a life cycle assessment methodology, Institute of Mechanical Engineering, EPFL, (Switzerland), 10/2013 – 01/2014, grade 5/6.
3. John Ingram, Energy integration study of a parallel hybrid electric vehicle, Institute of Mechanical Engineering, EPFL, (Switzerland), 10/2013 – 01/2014, grade 5, 5/ 6.
4. Quoc Nhat Nam Pham, Environomic design of vehicle integrated energy systems, LCA modelling, Institute of Mechanical Engineering, EPFL, (Switzerland), 10/2013 – 01/2014, grade 5, 5/6.
5. Pierre Lourdais, Performance and economic optimization of an Organic Rankine Cycle for hybrid vehicles, Institute of Mechanical Engineering, EPFL, (Switzerland), 10/2014 – 01/2015, grade 5, 5/6.
6. Charles-Thomas Stern, Energy integration and heat exchange network for vehicle energy system, Institute of Mechanical Engineering, EPFL, (Switzerland), 10/2014 – 01/2015, grade 5, 5/6.
7. Zeyu Huang, Modelling of Solid Oxide Fuel Cell – gas turbine system as a range extender for electric vehicles, Institute of Mechanical Engineering, EPFL, (Switzerland), 10/2014 – 10/2014, grade 5, 5/6.

**Depuis 2016** : évaluation de projet de Semestre de groupes d'étudiants: 4 jurys de projets de groupe

PSA collabore avec des écoles d'ingénieurs en France. Le but de la collaboration est de proposer des sujets industriels qui sont travaillés par des groupes d'étudiants. Il y a un défi qui promeut les meilleurs projets livrés par les étudiants. Je suis responsable du challenge avec l'Ecole d'Ingénieurs ICAM Toulouse en France. La durée du projet est d'un semestre. Je suis responsable de la direction académique et industrielle des étudiants. Les 15 étudiants travaillent dans 3 groupes pendant 250 heures. Mes étudiants ont reçu le prix des meilleurs projets en 2017 et 2018.

1. Mechanical design of a robot for charging the batteries of the vehicles, 15 students, 250 hours of work, ICAM Toulouse (France), fall semester 2016
2. Suspended system for charging for private usage, 15 students, 250 hours of work, ICAM Toulouse (France), fall semester 2017
3. Conception des interfaces de recharge pour entre les véhicules et les systèmes de recharge, 15 students, 250 hours of work, ICAM Toulouse (France), fall semester 2018
4. Conception des mécanismes mobile de recharge par induction des véhicules particuliers, 15 students, 250 hours of work, ICAM Toulouse (France), fall semester 2018

**Evaluation des projets de Semestres des étudiants** à qui j'ai enseigné les 60 heures de cours à l'académie militaire nationale « Rakovski » de la Bulgarie : **Evaluation principale de 20 étudiants.** Les devoirs ont consisté à écrire un article scientifique par étudiant. Les étudiants ont appliqué les méthodes théoriques enseignés dans les cours.

Les étudiants se présentent devant un jury académique, pour présenter et défendre leur articles scientifiques, composé de deux professeurs externes à ma discipline de cours. Je participe à ce jury.

### **3.2.2 Évaluation d'articles et d'ouvrages scientifiques : 51 évaluations d'articles pour la période 2015-2020**

**Depuis 2015** - Reviewer pour la conférence international ECOS (Efficiency, Cost, Optimization of Energy Systems), 2015 – 2020

La conférence ECOS a lieu tous les ans, en 2020 c'est sa 34ème édition, je suis membre du comité de relectures depuis 2016 et je participe en tant que présentateur tous les ans, depuis 2014.

**Depuis 2016** - Reviewer pour la conférence international BulTrans (International Conference of Aeronautics, Automotive and Railways Transportation and Technologies).

### **3.2.3 Activités d'évaluation d'articles pour des journaux scientifiques internationaux :**

**Depuis 2015** - Reviewer pour les journaux scientifiques internationaux (Editions **Elsevier** et **Springer**) et des journaux « Open Source »: **51 évaluations d'articles pour la période 2015-2020**

- International Journal of Energy (Edition Elsevier): **33 évaluations** d'articles
- Applied Energy (Edition Elsevier): 4 évaluations d'articles
- Energy and Buildings (Edition Elsevier): 2 évaluations d'articles
- Transportation research part D (Edition Elsevier): Transport and Environment: 2 évaluations d'articles
- Energy Conversion and management journal (Edition Elsevier) : 3 évaluations d'articles
- Environment, Development and Sustainability (Edition Springer) : 1 évaluation d'articles
- Journal of the Brazilian Society of Mechanical Sciences and Engineering (Edition Springer): 2 évaluations d'articles
- IEEE: 4 évaluations d'articles

### 3.2.4 Évaluation de laboratoires (Open Labs) : 2

Évaluation des activités des **Open Labs** (les laboratoires partenaires privilégiés entre PSA et les Universités de France et à l'étranger). Un Open Lab a un contrat de 3 ans renouvelable. Le budget est pluriannuel. Les conditions de recherche, de publication et de propriété intellectuelle sont précisées dans le contrat.

En tant que membre des Open Lab et responsable de projets de recherche PSA, menés dans les Open Lab, je participe dans l'évaluation de deux laboratoires :

1. Applied Mechanics Laboratory – entre PSA et Lodz Technical University, Lodz, Pologne
2. Open Lab Mechatronics entre PSA et UNP de BORDEAUX (IMS de Bordeaux)

### 3.2.5 Évaluation de projets de recherche : 3

Je participe à l'évaluation des projets de recherche proposés pour les Open Labs de PSA

1. Applied Mechanics Laboratory – Lodz Technical University, Lodz, Poland
2. Open Lab Mechatronics entre PSA et UNP de BORDEAUX (IMS de Bordeaux)
3. Laboratoire Geeps, à CentralSupélec, Paris Saclay

Je suis membre à la commission d'évaluation des propositions des thèses CIFRE, proposées par PSA. C'est une instance qui se réunit tous les ans pour valider le caractère scientifique et innovant des sujets de recherche, proposés par toutes les directions du Groupe PSA. Mon rôle est d'être examinateur et rapporteur au sein de cette instance. Tous les ans, PSA propose environ 30 sujets de thèses CIFRE. Les doctorants travaillent sur des sujets de recherche qui sont conformes aux axes stratégiques du Groupe PSA.

## 3.3 Organisation de colloques / congrès : 1

**En 2018 : 10/10/2018** : Organisateur d'une journée thématique chez PSA pour la visite d'une délégation de l'académie militaire nationale de Bulgarie « Rakovski ». La délégation a été composée de 4 membres : le commandant le Général Majeur Grudi Angelov et 3 professeurs (Prof. DSc Colonel Dimitar Nedialkov, Prof. Associé Colonel Miroslav Dimitrov et Prof. Associé Vikenti Spassov. La journée portait sur la thématique National power : diachronic approach to concept definition.

## 3.4 Direction des projets de recherche

Dans les cadres des Open Labs, **depuis 2015**, j'ai accueilli sur mes activités de recherches 8 post-doctorants. Ils ont été engagés sur le projet de l'actionneur électromagnétique, sur les activités de recherche de catalyseur pour la production d'hydrogène par le vapo- reformage de bioéthanol et sur les activités d'intelligence économique pour identification de la structuration de l'écosystème de la recharge électrique pour les véhicules électriques et hybrides. Une étude est en cours pour l'écosystème de l'hydrogène.

1. Lamine Fadiga, Inversed design method for the control model of an active electromagnetic actuator, IMS Laboratory, University of Bordeaux (France), PSA Groupe Vélizy (France), 2015-2016.  
Bugdet: 85 k€, durée 1 an, 1 brevet:
  - (WO2017198923) Method and system for controlling an electromagnetic valve actuator of a combustion engine AOUN FRANCOIS, DIMITROVA ZLATINA, FADIGA LAMINE, LANUSSE PATRICK
2. Florian Monsallier, Design and operation of an experimental set up for the control model validation of an innovative electromagnetic actuator, IMS Laboratory, University of Bordeaux

- (France), PSA Groupe Vélizy (France), 2017.  
Budget: 45 k€, durée 6 mois.
3. Tari Massinissa, Robust control law and correlation of the control model with experimental data for an innovative active electromagnetic actuator, IMS Laboratory, University of Bordeaux (France), PSA Groupe Vélizy (France), 03/2017- 04/2018.  
Budget **85 k€**, durée 1 an, **2 publications scientifiques**:
    - Z. Dimitrova, M. Tari, P. Lanusse, F. Aioun, X. Moreau, Robust control for an electromagnetic actuator for a camless engine, International Journal of Mechatronics 57, 2019 109-128.
    - Z. Dimitrova, M. Tari, P. Lanusse, F. Aioun, X. Moreau, Development and Control of a Camless Engine Valvetrain, IFAC-PapersOnLine, 52 2019 399-404.
  4. Pawel Mierczynski, Tomasz Maniecki, Catalyst selection for ethanol reforming for Alkaline and Solid Oxide Fuel Cells, Chemistry Department, Politechnika Lodzka, Lodz (Poland), PSA Groupe Vélizy (France), 2017.  
Budget: 20 k€ (en Pologne), durée 1 an, Rapports internes, une publication est en cours de rédaction
  5. Stephane Miollan, Economic Intelligence study for the recharging systems for electrified vehicles, patents portfolio, GRETHA Laboratory, University of Bordeaux (France), 2018  
Budget: 40 k€ (dans le cadre de l'Open Lab PSA – GRETHA), durée 1 an, Rapports internes
  6. Sonia Siah, Economic Intelligence for the ecosystem of recharging systems for electrified vehicles, financial transactions portfolio, GRETHA Laboratory, University of Bordeaux, PSA Groupe Vélizy (France), 2018.  
40 k€ (dans le cadre de l'Open Lab PSA – GRETHA), durée 1 an, Rapports internes Rapports internes
  7. Gzegorz Mitukiewicz, Applied Mechanics Laboratory, Lodz University of Technology, Lodz, Poland. Budget 20 k€, durée 1 an, **1 publication scientifique**:
    - G. Mitukiewicz, M. Głogowski, J. Stelmach, J. Leyko, Z. Dimitrova, D. Batory, Strengthening of cruciform sample arms for large strains during biaxial stretching, Materials Today Communications 21 2019 100692
  8. Roman Gudzur, Busbars for high voltage batteries, Electrical engineering laboratory, Lodz University of Technology, Lodz, Poland.  
Budget 20 k€, durée : 1 an, **2 publications scientifiques et 2 brevets**:
    - Z. Dimitrova B. Guzowski, Z. Dimitrova, A. Noury, D. Batory, G Mitukiewicz, An energy balance evaluation in lithium-ion battery modules under high temperature operation. Efficiency Cost and Optimization of Energy systems conference, ECOS 2019, Wroclaw, Poland
    - R. Gozdur, B. Guzowski, Z. Dimitrova, A. Noury, D. Batory, G Mitukiewicz, An energy balance evaluation in lithium-ion battery modules under high temperature operation, Energy conversion and management journal, 2020.
    - (2019P01560 FR - N° de dépôt de la demande: 2000305 du 2020-Jan-14 ) Heatsinks with holes and busbar for cooling and conductivity of a battery pack, DIMITROVA ZLATINA, ROMAN GODZUR, BARTOLOMEJ GUZOWSKI, Dariusz BOGDANSKI, ANTONIN VINATIER
    - (2019P01074 FR - N° de dépôt de la demande: 1909809 du 2019-Sep-06) Heatsinks as busbar for cooling of a battery pack, DIMITROVA ZLATINA, ROMAN GODZUR, BARTOLOMEJ GUZOWSKI, Dariusz BOGDANSKI, ANTONIN VINATIER

## 3.5 Interactions avec les acteurs socio-économiques :

Mon employeur est une entreprise industrielle qui est l'un des acteurs majeurs de l'industrie automobile. Je suis ingénieur docteur de formation et chercheur pour cette entreprise. Je gère des projets de recherche scientifique et d'innovation technologique pour le domaine « **Energy and vehicle's powertrains** ». Ma nomination à ce poste est effective depuis janvier 2016. Je participe à la direction des activités de recherche, à la direction de thèses et aux partenariats avec les institutions de recherche académique (universités ou instituts de recherche).

J'ai deux types d'interactions majeures avec des acteurs socio-économiques :

- Interactions avec des laboratoires de recherche, des instituts de recherche, des universités
- Interactions avec des entreprises industrielles de différents types dans le domaine automobile (des fournisseurs majeurs, des PME, des start-up) ou dans les autres secteurs industriels (l'aéronautique).

Chaque interaction est règlementée par des accords de confidentialités et par des contrats de recherches.

### 3.5.1 Contrats de R&D avec des industriels : 3 contrats majeurs

#### Industrie Automobile :

Direction de **Projets d'Innovation** – contrats d'innovation avec des fournisseurs

- Projet « Robot chargeur »
  - Contrat d'innovation avec des fournisseurs de rang 1 et de rang 2 de PSA
  - Contrat d'innovation avec une PME (Mag Tech)

Contribution aux **Projets de développement et industriels du Groupe PSA**– Développement et industrialisation d'un véhicule dans une usine nouvelle : investissements industriels 500 M€, ressources 850 hommes/an, durée 2 ans.

#### Autres industries :

**Depuis 2017** à aujourd'hui 2020, je contribue également grâce à mon expertise et à mes connaissances à définir des concepts de systèmes de propulsion hautement efficaces pour les objets volants, tels que les hélicoptères, les taxis volants (VTOL) et les avions. La mobilité 3D est considérée comme la future révolution du secteur des transports.

Sur ce sujet, je travaille en collaboration avec Airbus. Le secteur industriel aérospatial a pu bénéficier de mon expertise acquise dans les systèmes de propulsion pour. Mon implication et mon expertise ont été très appréciées par les responsables de la recherche d'Airbus. Aujourd'hui, je dirige des workshops liés aux technologies de l'énergie et de la conversion développées dans l'industrie automobile et qui sont intéressantes à étudier et à évaluer pour le secteur de l'aviation. Ces échanges sont couverts par un accord de confidentialité et reposent sur des contrats entre les deux entreprises. Nous avons 3 workshops par an qui mobilisent 15 personnes des deux entreprises et nous nous rencontrons dans les événements majeurs des deux industries, tels que le Salon International de l'Aéronautique du Bourget.

## 3.6 Bourses de thèses Cifre : 2

- Direction de la Thèse de Jean Hassler 2017- 2020, PSA Groupe, Laboratoire Geeps de CentralSupélec, Paris- Saclay.
- Direction de Thèse à pourvoir 2020- 2023, PSA Groupe, Laboratoire Geeps de CentralSupélec, Paris- Saclay.
- Directions à 50%, les autres 50 % se font par les chercheurs HDR de CentralSupélec.

### **3.6.1 Créations de laboratoires communs avec une / des entreprise(s) laboratoires de recherche : 2**

#### **Open Labs:**

- Mechanics: Applied Mechanics Laboratory Lodz University of Technology, Lodz, Poland – PSA Groupe France
- Mechatronics : IMS de Bordeaux, UNP Bordeaux, France – PSA Groupe, France

### **3.6.2 Création de réseaux ou d'unités mixtes technologiques : 1**

#### **2018-2020 : Projet d'innovation « Robot chargeur » :**

Intégration d'acteurs de différents niveaux (fournisseurs de rang 1, rang 2, des PME, des académiques). Construction et contrôle de la chaîne de valeur totale de l'Innovation pour le Groupe PSA.

### **3.7 Contrats de recherche financés par des institutions publiques ou caritatives**

De fait de mon profil de chercheur dans l'industrie les activités de recherches pour lesquelles je suis responsable sont pris en charge par le budget propre de R&D de PSA Groupe. Les activités s'intègrent dans l'axe stratégique « Clean Technologies » de PSA. PSA Groupe investit 9% de son chiffre d'affaires tous les ans pour financer la recherche, l'innovation et le développement afin d'assurer son avenir technologique et de proposer aux clients des produits et des services propres, attractifs et respectueux de l'environnement.

J'ai connaissance des leviers de financements publics de recherches (projets européens, projets ANR). Le Groupe PSA est actif et est un partenaire dans les deux premières catégories : Contrats européens H2020 et les contrats nationaux, comme co-déposant de projets ANR.

### **3.8 Indices de reconnaissance**

#### **H-Index Scopus:10, Nombre de citations 380**

**Le premier prix de l'Inventeur de l'année du Groupe PSA** m'a été décerné à deux reprises, en 2016 et 2017, pour des brevets déposés. On m'a distingué en 2018 Inventeur du mois. Le Groupe PSA emploie 200 000 collaborateurs dans le monde entier.

#### **Prix : 2**

- 1<sup>er</sup> Prix : Grand Prix du Palmarès des Inventeurs de PSA Groupe (200 000 employés, en 2016 (Figure 16).
- 1<sup>er</sup> Prix : Grand Prix du Public du Palmarès des Inventeurs de PSA Groupe (200 000 employés), en 2017 (Figure 17).

#### **Distinctions : 4**

Inventeur du mois et finaliste au Palmarès des Inventeurs de PSA Groupe, en 2018

Nomination pour le prix de la recherche délivrée par le groupe italien ENI

Certificat de récompenses pour la contribution à l'élévation du niveau scientifique des Journaux Scientifiques Internationaux de l'éditeur Elsevier :

- International Journal of Energy
- Applied Energy Journal
- Transportation research part D: Transport and Environment

### **Invitations à des colloques / congrès à l'étranger, séjours dans des laboratoires étrangers : 15**

Participations depuis 2014 à au moins deux conférences scientifiques par an, 15 Conférences Internationale au total.

En 2018 et en 2019, j'ai eu l'honneur de faire la plénière de la conférence internationale BulTrans.

La liste des conférences internationales se trouve ci-dessous, avec présentation d'articles avec comité de relecture :

1. ECOS **2020**, « Efficiency cost and optimization of energy systems », Osaka, **Japan**
2. Long-term security environment challenges and armed forces capabilities development, 12 - 14 November **2019**, Sofia, **Bulgaria**
3. ECOS **2019**, « Efficiency cost and optimization of energy systems », Wroclaw, **Poland**
4. Bultrans **2019**, Sozopol, **Bulgaria**
5. Bultrans **2018**, Sozopol, **Bulgaria**
6. ECOS **2018**, Guemaraes, **Portugal**
7. Bultrans **2017**, Sozopol, **Bulgaria**
8. ECOS **2017**, San Diego, **USA**
9. ECOS **2016**, Portoroz, **Slovenia**
10. ECCE10 **2015**, Nice, **France**
11. ECOS **2015**, Pau, **France**
12. 15. Automotive Day **2014**, Biel, **Switzerland**, SAE CH, FISITA
13. PRES **2014**, Prague, **Czech Republic**
14. ECOS **2014**, Turku, **Finland**
15. Jahrestagung 2013 E'Mobile Nachhaltigkeit im Straßenverkehr –Herausforderung für Forschung und Markt“ – EPFL, **2013**, Lausanne, **Switzerland**

Je suis régulièrement invitée et je participe en présentant ma recherche à :

- ECOS (Efficiency, Cost, Optimization of Energy Systems) que je connais depuis ma thèse au sein du laboratoire IPESE de l'Ecole Polytechnique Fédérale de Lausanne (EPFL), Suisse. La conférence ECOS est à chaque fois organisée par des universités hôtes différentes. Elle reste très largement visitée par le milieu académique mondiale.
- Bultrans (International Scientific Conference on Aeronautics, Automotive and Railway Engineering and Technologies) est une conférence scientifique organisée tous les ans par l'Université technique de Sofia (Bulgarie).
- Long-term security environment challenges and armed forces capabilities development, 12 - 14 November 2019, Sofia, (Bulgarie)

## 4. Activités d'enseignement

En 2019, j'ai été invitée en tant que maître de conférence invité à enseigner deux disciplines de 58 heures de cours dans les programmes de master de l'Académie militaire nationale « Rakovski » de la Bulgarie. L'Académie a contribué de manière unique à la fondation du Corps des officiers bulgares, ainsi qu'à la création du nouvel État bulgare et à la diffusion des valeurs européennes à travers la nation bulgare. Aujourd'hui, c'est une institution nationale d'enseignement supérieur, de qualification et de recherche scientifique sur les questions de sécurité et de défense nationales. L'Académie de défense et d'état-major de Rakovski a pour mission de préparer les chefs militaires et le personnel civil dans tous les domaines. L'Académie est accréditée en tant que haute institution d'enseignement par les autorités de l'état bulgare. Les unités académiques et de recherche de l'Académie de défense et d'état-major Rakovski sont les suivantes: Faculté de sécurité nationale et de défense, Faculté de commandement et d'état-major, Faculté de logistique et de transport, Faculté d'interopérabilité et de défense, Institut de recherche avancée. L'éducation des étudiants civils augmente de plus en plus ces 5 dernières années avec une tendance stable à la croissance. La reconnaissance des anciens élèves de l'Académie est très élevée. Ils occupent des positions de leaders dans leur carrière professionnelle. Le président de la Bulgarie, Général Dr. Rumen Radev, est un ancien élève de l'Académie militaire nationale « Rakovski » de Bulgarie.

J'ai proposé deux nouvelles disciplines liées au secteur des transports. Ces propositions ont été acceptées pour les programmes de master spécialisés de la chaire de logistique et transport. Les titres des cours sont les suivants:

- Stockage et conversion d'énergie et gestion du cycle de vie des produits - durée de 38 heures
- Transfert de technologie et prospective technologique - durée de 20 heures

L'intérêt de l'introduction de mes cours est l'enseignement des méthodes scientifiques et d'ingénierie structurées, déployées dans le secteur Recherche et Développement de l'industrie automobile. Ils assurent une gestion structurée et systématique des technologies. L'objectif est que les étudiants diplômés de ces programmes de master spécialisé obtiennent une qualification solide et systématique qu'ils puissent appliquer au cours de leur carrière professionnelle dans l'administration d'État et en particulier dans le secteur des transports ou pour les besoins de l'armée. Mon obligation est également de proposer les sujets d'examen et de participer au jury d'examen. Les cours sont en anglais et en bulgare.

## **4.1 Contenu et objectifs des cours: 2 disciplines de cours (58 heures) en programme de Master :**

### **4.1.1 Stockage et conversion d'énergie, gestion du cycle de vie des produits (Energy storage and conversion, product life cycle management)**

Le contenu est le suivant:

- Présentation de la gestion du cycle de vie des produits (PLM)
- Le cycle de vie complet d'un produit
- Méthode d'analyse du cycle de vie (ACV)
- Technologies émergentes pour le PLM en boucle fermée
- Décisions: comment gérer et soutenir les décisions:
- Modèles technico-économiques
- Modèles environnementaux et économie circulaire
- Début de vie (BOL) et phase de conception: importance des spécifications techniques pour la valeur ajoutée finale
- Problèmes de milieu de vie (MOL) et de phase d'utilisation: importance de la maintenance et efficacité de la conversion
- Problèmes de fin de vie (EOL) et de recyclage: comment valoriser la seconde vie du produit
- Outils de modélisation et d'analyse pour PLM / LCA
- Logistique: vecteurs énergétiques et leur distribution pour un service de mobilité efficace
- Applications des méthodes PLM / LCA dans l'industrie automobile

Les objectifs pédagogiques sont:

- Comprendre en quoi consiste la gestion du cycle de vie du produit (PLM) et comment elle devrait être envisagée aujourd'hui.
- Comprendre ce que c'est l'analyse du cycle de vie et comment la prendre en compte.
- Comprendre les différentes phases du cycle de vie d'un produit - Début de vie (BOL), Milieu de vie (MOL), Fin de vie (EOL)) et les opérations commerciales impliquées et les flux d'informations associés.
- Connaître les technologies et les méthodes et outils de modélisation et d'analyse qui peuvent être utilisés dans les opérations PLM dans le secteur des transports.
- Définir le service énergétique pour la mobilité
- Appliquer et discuter d'exemples d'études de cas liés à la logistique et à la distribution des différents vecteurs énergétiques utilisés dans le secteur des transports.
- Montrer et discuter d'exemples d'études de cas dans l'industrie automobile.

### **4.1.2 Transfert de technologie et prospective technologique (Technology transfer and Technology foresight):**

Le contenu est le suivant:

- Aperçu des innovations dans la technologie
- Valeur des innovations
  - Définir la valeur ajoutée des Innovations
  - Comment imaginer, créer, développer et vendre des Innovations
  - Protéger les innovations:
    - Propriété intellectuelle: processus, gestion, avantages, licences
    - Valoriser les innovations: valeur des produits et des services
    - Gérer la phase de conception
- Intelligence économique: définition, processus, outils et méthodes, comment l'utiliser
- Connaissances et sciences appliquées comme base des Innovations
  - Créativité et design
- Publications et communications scientifiques et techniques: valeur ajoutée, classement des organisations
- Aperçu de la prospective technologique
- Méthodes de prévision technologique
- Politique technologique: une présentation d'exercices réels - la tendance à l'électrification dans l'industrie automobile
- Discuter des options futures: analyse des signaux faibles
- Construire un scénario technologique
  - Recherche ou élaboration de stratégies
  - Networking et prévoyance
  - Technologies de rupture
  - Décisions et actions
- Des exercices
- Discussion finale

Les objectifs pédagogiques sont:

#### **Fournir aux étudiants:**

- Références clés tirées d'études du futur mettant cause des cas et des questions sur lesquels réfléchir.
- Compréhension de la valeur ajoutée des innovations et comment les protéger et comment les valoriser:
  - Propriété intellectuelle (PI) - brevets, licences, marques
  - Intelligence économique (IE)
  - Publications et communications scientifiques et techniques
- Acquérir des connaissances de pointe dans le domaine (faire face à des avenir incertains) et développer des capacités analytiques concrètes.

**Objectif du cours:**

- Développer une compréhension systématique de la façon dont les entreprises et les organisations fonctionnent. Anticiper, maintenir leurs atouts de performance (optimiser leur sens de la résilience et de la sérendipité), Gérer pour rester proactif en termes d'initiatives technologiques innovantes et toujours, se conformer aux exigences réglementaires ou aux changements sociétaux si besoin
- Représentant une opportunité de formation majeure dans le domaine de la prospective et de la détection précoce
- Implication des caractéristiques technologiques émergentes et la résolution de ses défis et options avec une méthodologie appropriée

Lors de ma thèse à l'EPFL (**2013-2015**), en tant que membre du Laboratoire IPSE de l'EPFL, j'ai assisté Prof. Maréchal pour le Cours de Master « Modeling and Optimization of energy systems ». J'étais en charge de la partie « Cycles thermodynamiques et moteurs à combustion interne ». J'ai supervisé des étudiants en Master de l'EPFL, à l'Institut de génie mécanique de l'EPFL. Certains de mes étudiants sont venus pour des projets de semestre et des projets de thèse de Master, que j'ai définis avec le professeur Maréchal. Ces travaux sont listés au paragraphe des activités évaluations.

**4.2 Résumé des activités d'enseignement:**

La Table 1 résume mes activités d'enseignement:

Table 4-1: Activités d'enseignement

Année	Matière	Type				Niveau	Université
		Lecture (h)	Exercices (h)	Practice (h)	Evaluation		
2013-2015	Modelling and optimization of energy systems		50	100	Yes	Master Students, Institute of Mechanical engineering	EPFL (Switzerland)
2019	Energy storage and conversion/ Product lifecycle management	38			Yes	Specialized Master Students, Logistics and road transportation	Military Academy "Rakovski" Sofia, Bulgaria
2020	Technology transfer and technology foresight	20			Yes	Specialized Master Students, Logistics and road transportation	Military Academy "Rakovski" Sofia, Bulgaria